ÉVOLUTION DES CONDITIONS OCÉANIQUES DE SURFACE DURANT LA FIN DE L'HOLOCÈNE À L'AIDE DE PROXIES BIOGÉNIQUES ET SÉDIMENTAIRES DANS LE NORD-OUEST DE LA BAIE DE BAFFIN

Thèse présentée

dans le cadre du programme de doctorat en océanographie

en vue de l'obtention du grade de Philosophiae doctor (Ph.D)

PAR

© KELSEY KOERNER

Avril 2026

Composition du jury :

Michel Gosselin, président du jury, Université du Québec à Rimouski

André Rochon, directeur de recherche, Université du Québec à Rimouski

Audrey Limoges, codirectrice de recherche, University of New Brunswick

El Mahdi Bendif, examinateur interne, Université du Québec à Rimouski

Fabienne Marret-Davies, examinatrice externe, University of Liverpool

Dépôt initial le 11 décembre 2025 Dépôt final le 20 avril 2026

REMERCIEMENTS

I would like to thank my supervisors, Dr. André Rochon and Dr. Audrey Limoges, who provided me with invaluable scientific, professional, and personal guidance over the last 5 years. I would also like to thank Dr. Jean-Carlos Montero-Serrano for his input on this project and Dr. Anne de Vernal for her input and the opportunity to work as the coordinator of ArcTrain during my PhD. Thank you to my evaluation committee, Dr. Michel Gosselin, Dr. El Mahdi Bendif, and Dr. Fabienne Marret-Davies for taking the time to read this thesis and provide your feedback.

This project would not have been possible without the help of the incredible administrative team at ISMER, UNB, and onboard the CCGS Amundsen. Thank you to Dominique, Mélanie, Éricka, Martine, and Nancy at ISMER and to Tammy and Nicolas at UNB for your help over the years. Thank you to the scientific and coast guard crew onboard the CCGS Amundsen for four incredible trips at sea, and the recovery of the samples used in this project in 2019. Finally, thank you to ArcTrain, Geotop, and ArcticNet for the conferences and networking activities that kept me motivated throughout my time in grad school.

Thank you to my officemates at ISMER: Élodie, Camille, Juliette, Daniel F, Daniel R, Florian, Naomi, Morgane, Quentin B, Quentin D, Arthur, Stefano and at UNB: Hannah, Margaret, Brayden, Jenny, Tazeen for all the great memories I hold close. Thank you to my friends outside of the university who were everything to me these last 5 years: Julia, Regan, Joel, Kalen, Brian, Hannah, Tommy, Melissa, Justin, Megan, and Srdjan. To my mom Michele Koerner and my stepdad Allan Miurhead for always believing in me and encouraging me every step of the way. To my dad, Allan Dietrich for instilling in me the importance of hard work and my stepmom Cindy Dietrich for keeping my spirits high during the difficult moments. To my brothers Mitchell, Jeremy, Hunter, and Cash, for always

providing comedic relief. Thank you to my two cats Merlin and Daisy for spending countless hours watching me write this thesis.

Lastly to the two people who have been with me since the start of grad school: Josh Evans and Rosalie Shink. Thank you for being there every step of the way. I am forever grateful that we were able to go on these journeys together.

RÉSUMÉ

La baie de Baffin septentrionale se situe à l'embouchure des détroits de Nares, de Jones et de Lancaster via lesquels l'eau douce (solide et liquide) en provenance de l'océan Arctique est exportée. Le nord de la baie de Baffin est caractérisé par la polynie des eaux du Nord, une zone d'eau libre très productive. Les eaux libres de la polynie des eaux du Nord sont en partie dues à la formation de ponts de glace dans le détroit de Nares, qui limitent l'export de la glace vers la baie de Baffin. Depuis du XXIe siècle, la formation de ces ponts de glace est devenue plus irrégulière, voire parfois inexistante, créant ainsi un passage ouvert entre l'océan Arctique et la baie de Baffin. L'objectif de cette thèse est de comprendre comment l'affaiblissement des ponts de glace du détroit de Nares et le flux subséquent d'eau douce (solide et liquide) vers le nord de la baie de Baffin influencent les conditions de surface de la mer dans cette région, comparativement aux changements survenus au cours des 400 à 1200 dernières années.

Le premier chapitre analyse les assemblages de kystes de dinoflagellés (dinokystes) présents dans des échantillons de sédiments de surface de la baie de Baffin et de la polynie des eaux du Nord afin de déterminer s'ils reflètent des conditions hydrologiques distinctes. Nous avons ensuite analysé les assemblages de dinokystes et la géochimie (carbone organique total, azote total et les signatures $\delta^{15}N$, $\delta^{13}C$ de la matière organique) sur deux carottes sédimentaires couvrant les quelques 400 dernières années. Nos résultats révèlent des compositions d'assemblages de dinokystes différentes entre les zones plus froides et plus riches en glace de mer de l'ouest de la baie de Baffin et les eaux relativement plus chaudes et plus salées de l'est. Les deux carottes sédimentaires montrent une évolution de la composition des assemblages vers une plus grande présence de taxons mixotrophes et une augmentation des flux de dinokystes au début du XXe siècle, indiquant une réponse à l'amplification arctique plus précoce que celle documenté jusqu'à présent.

Le deuxième chapitre analyse les assemblages de diatomées présents dans des sédiments de surface de la polynie des eaux du Nord et dans deux carottes de sédiment. Les diatomées présentent une relation distincte de part et d'autre de la polynie des eaux du Nord, avec une plus grande abondance de diatomées typiquement associés à la floraison printanière dans la partie ouest de la polynie des eaux du Nord que dans la partie est. Les carottes de sédiment ont révélé des différences spatio-temporelles entre les deux carottes. Les variations d'abondance des diatomées étant principalement dues à de petits taxons pennés, caractéristiques des floraisons printanières précoces et de la zone marginale de la banquise. Les concentrations de diatomées suivent une tendance similaire, suggérant que la bordure de glace dynamique de la polynie des eaux du Nord ouest joue un rôle important dans la localisation et l'intensité de la production de diatomées.

Le dernier chapitre examine un enregistrement sédimentaire composite, utilisant les kystes de dinoflagellés, l'analyse granulométrique et la minéralogie pour mieux comprendre les variations des conditions de surface de la mer au cours des quelque 1200 dernières années. Nos résultats montrent des variations dans les indicateurs sédimentaires qui peuvent être associées à des apports provenant de sources plus proches (par exemple, la calotte glaciaire de Devon) et de sources plus éloignées (ouest du détroit de Jones/nord du détroit de Nares), ce qui renseigne sur le type d'apports d'eau douce dans le nord de la baie de Baffin. L'évolution des indicateurs sédimentaires est également concomitante aux variations des assemblages de dinokystes, fournissant des informations supplémentaires sur les variations des conditions de surface de la mer au cours du temps.

Cette thèse montre que la polynie des eaux du Nord est particulièrement sensible aux changements climatiques, le réchauffement actuel ayant des répercussions plus précoces qu'on ne le pensait. Il est important de poursuivre la surveillance de l'influence des apports d'eau douce via le détroit de Nares et les glaciers locaux, ainsi que des eaux provenant de l'Atlantique, sur la polynie des eaux du Nord afin de comprendre comment le système continuera de réagir au réchauffement climatique actuel.

Mots clés : Baie de Baffin, changement climatique, sédiments marins, microfossiles, géochimie, Arctique

ABSTRACT

Northern Baffin Bay lies at the confluence of Nares Strait, Jones Sound, and Lancaster Sound, through which freshwater (both solid and liquid) is exported out of the Arctic Ocean. Northern Baffin Bay is also host to the North Water Polynya (NOW), a highly productive area of open water. The open water in the NOW is due in part to the consolidation of ice bridges upstream in Nares Strait, limiting the transport of sea ice to Baffin Bay. Since the 21st century, the formation of these ice bridges has become more irregular, and sometimes even non-existent, creating an open passage between the Arctic Ocean and Baffin Bay. The objective of this thesis is to understand how the weakening of the Nares Strait ice bridges and the subsequent flow of freshwater (solid and liquid) to northern Baffin Bay influences sea surface conditions in this region, compared to changes that have occurred over the last 400 to 1200 years.

The first chapter analyzes assemblages of dinoflagellate cysts (dinocysts) present in surface sediment samples from Baffin Bay and the NOW to determine whether they reflect distinct hydrological conditions. We then analyzed dinocyst assemblages and geochemistry (total organic carbon, total nitrogen, and $\delta^{15}N$ and $\delta^{13}C$ signatures of organic matter) in two sediment cores covering the last 400 years. Our results reveal different dinocyst assemblage compositions between the colder, sea ice-rich areas of western Baffin Bay and the relatively warmer, saltier waters of the east. Both sediment cores show a change in assemblage composition towards a greater contribution of mixotrophic taxa, complimented by an increase in dinocyst fluxes at the beginning of the 20th century, indicating an earlier response to Arctic amplification than previously documented.

The second chapter analyzes the diatom assemblages present in surface sediments across the NOW and in two sediment cores covering the last 400 years. Diatoms show a distinct relationship across the NOW, with a greater abundance of diatoms typically associated with spring blooms in the western part of the NOW than in the east. Downcore diatom assemblage composition revealed spatio-temporal differences between the two sediment cores. The variations in diatom abundance were mainly due to small pennate taxa, characteristic of early spring blooms and the marginal zone of the ice pack. Diatom concentrations followed a similar trend, suggesting that the dynamic ice edge of the western NOW plays an important role in the location and intensity of diatom production.

The final chapter examines a composite sediment record, using dinoflagellate cysts, grain size analysis, and mineralogy to better understand variations in sea surface conditions over the past 1,200 years. Our results show changes in sedimentary indicators can be associated with inputs from more proximal sources (e.g., the Devon Ice Cap) and more distal

sources (e.g., west of Jones Sound/north of Nares Strait), providing insight into the type of freshwater inputs into northern Baffin Bay. The evolution of these sedimentary indicators also coincides with variations in dinocyst assemblages, providing additional information on variations in sea surface conditions over time.

This thesis shows that the NOW is particularly sensitive to climate change, with current warming having earlier impacts than previously thought. It will be important to continue monitoring the influence of freshwater outflow via Nares Strait, as well as the input Atlantic-derived waters into the NOW to understand how the system will continue to respond to current global warming.

Keywords: Baffin Bay, climate change, marine sediment, microfossils, geochemistry, Arctic

TABLE DES MATIÈRES

LISTE DES TABLEAUX

LISTE DES FIGURES

LISTE DES ABRÉVIATIONS, DES SIGLES ET DES ACRONYMES

AMD	Abbreviation for cores collected onboard the Amundsen
AIC	Agassiz Ice Cap
BIC	Baffin Island Current
BC	Box Core
BCE	Before Common Era
BP	Before Present
CAA	Canadian Arctic Archipelago
CCGS	Canadian Coast Guard Ship
CE	Common Era
CS	Composite Sequence
DIC	Devon Ice Cap
GC	Gravity Core
GIS	Greenland Ice Sheet
GAMs	Generalized Additive Models
H	Heterotrophic dinoflagellate cyst
HCl	Hydrochloric Acid
IRD	Ice-Rafted Debris

ISMER	Institut des sciences de la mer
LIA	Little Ice Age
M	Mixotrophic dinoflagellate cyst
MCA	Medieval Climate Anomaly
MIF	Manson Ice Field
MoW	Modern Warming
MSCL	Multi-Sensor Core Logger
NOW	North Water Polynya
NPP	Non-pollen palynomorph
PC	Principal Component
PCA	Principal Component Analysis
PoW	Prince of Wales Ice Field
SE	Standard Error
TN	Total nitrogen
TOC	Total organic carbon
UNB	University of New Brunswick
WGC	West Greenland Current
qXRD	Quantitative X-ray Diffraction
X-CT	X-ray Computed Tomography

LISTE DES SYMBOLES

ΔR	Local age-reservoir correction for radiocarbon
^{210}Pb	Lead 210 (radiogenic lead that is used in dating sediments)
^{14}C	Carbon 14 (radiogenic carbon that is used in carbon dating)
δ^{15}N	Delta N-15: Measurement of the ratio between ^{15}N and ^{14}N, provides information on nutrient utilization in the water column
δ^{13}C	Delta C-13: Measurement of the ratio between ^{13}C and ^{12}C, provides information on organic matter provenance

INTRODUCTION GÉNÉRALE

INTRODUCTION OF THE PROBLEM

Arctic air temperatures are warming at nearly four times the global average rate; a phenomenon referred to as Arctic amplification (Serreze & Barry, 2011; Rantanen et al., 2022). One of its most visible consequences is the rapid decline of the Arctic cryosphere, encompassing regions where water remains frozen. Since the 1980's, the extent of Arctic sea ice sets record lows (Parkinson & DiGirolamo, 2021; Fig. 1) with losses now occurring across all seasons rather than being restricted to summer months (Stroeve & Notz, 2018). The state of Arctic sea ice is also changing with younger, thinner sea ice replacing older, thicker sea ice (Babb et al., 2023; Fig. 1). Climate models from the Intergovernmental Panel on Climate Change project continued Arctic warming, with some scenarios predicting an ice-free Arctic Ocean as early as 2050 (Notz et al., 2020).

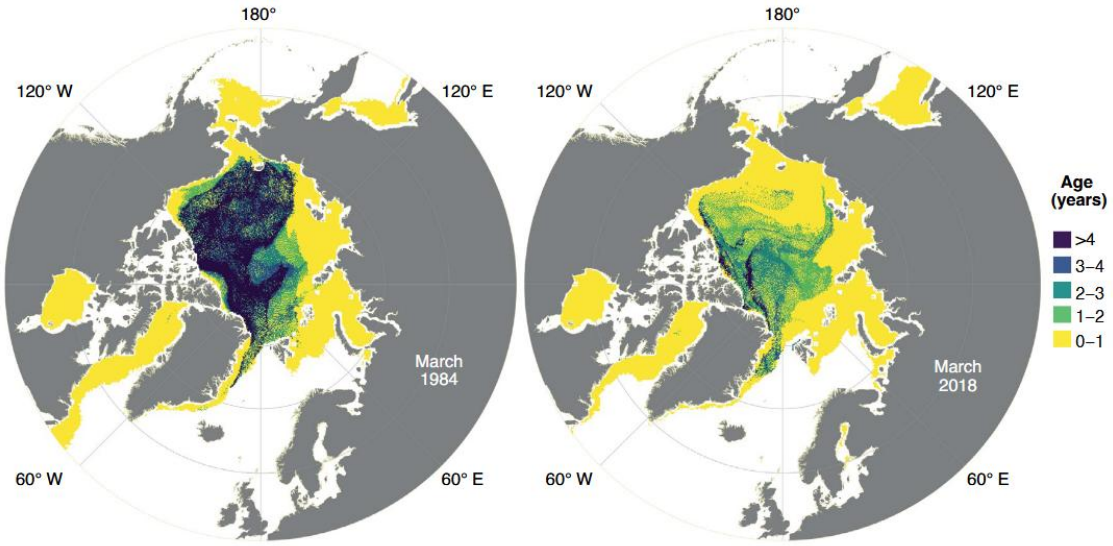

Figure 1. Map of the Arctic Ocean showing sea ice extent and age, in 1984 (left) and 2018 (right) (from Ardyna et al., 2020).

Glaciers in the Canadian Arctic Archipelago (CAA) and the Greenland Ice Sheet (GIS) also show continued retreat since the 1980's (Otosaka et al., 2023), with accelerated mass loss observed over the last 20 years (Carr et al., 2017). Ice caps in the CAA make up over 14% of the global cryosphere and have undergone significant decline over the last 60 years (Noël et al., 2018). High latitude glacier retreat is predominately driven by atmospheric forcing, as warmer air temperatures enhance surface melt and ablation rates (Cook et al., 2019; Slater & Straneo, 2022). Ablation of these glaciers contributes large amounts of freshwater to adjacent marine environments, typically from spring through summer, with peak discharge in September (Wouters & Sasgen, 2022), a process that has also intensified over the last 30 years due to Arctic warming (Hanna et al., 2008).

These processes have contributed to the "freshening" of the Arctic Ocean (Carmack et al., 2016; Zhuang et al., 2021) that is, an increase in its freshwater content. For example, the reservoir of freshwater in the Beaufort Gyre has increased by 40% over the last 25 years (Proshutinsky et al., 2019). Simultaneously, freshwater export from the Arctic Ocean has also intensified (Carmack et al., 2016). Fram Strait, the main route for freshwater export has shown an increase in the proportion of sea ice meltwater in the 21st century (Dodd et al., 2012). Additional export routes such as Nares Strait and Mc'Clure (MC) Strait have similarly showed increasing fluxes of both liquid and solid freshwater (Vincent., 2019). This increased freshwater discharge ultimately reaches the North Atlantic where it can influence large-scale ocean circulation patterns such as the Atlantic Meridional Overturning Circulation (Wang et al., 2018).

Changes in both salinity and sea ice dynamics have important implications for primary production. The earlier break up and later formation of sea ice increases light availability in surface waters (Nicolaus et al., 2012), extending the growing season for phytoplankton and enhancing primary production (Arrigo et al., 2008; Bélanger et al., 2013). Satellite observations have shown that the thinning and decrease in the extent of Arctic sea ice has resulted in a pan-Arctic increase in primary production (Arrigo & van Dijken, 2015), with some regions now experiencing two phytoplankton blooms per year (Ardyna et al., 2014).

This change in the timing and magnitude of primary production can alter grazing dynamics among primary and secondary consumers, causing cascading effects on upper trophic levels (Tremblay et al., 2012). Increased stratification can also modify nutrient inventories in the upper portions of the water column (Tremblay et al., 2015; López-Blanco et al., 2020). While freshwater inputs can deliver nutrients that stimulate primary production, a strongly stratified layer can simultaneously limit the upward mixing of nutrient-rich deep waters, limiting productivity in some regions (Varela et al., 2013). However, understanding the response of primary producers to changes in salinity and sea ice dynamics is complicated, as localized effects also play an important role in modulating nutrient availability through vertical mixing and input of important nutrients via riverine and glacial outflow (Arrigo and van Dijken, 2015).

The Arctic Ocean is typically characterized by a 5-10 m layer of freshwater derived from riverine input from the western Canadian Arctic and Russia, along with cryospheric melt (Rudels et al., 1996; Fig. 2). Beneath this layer lies Pacific-derived waters that enter through Bering Strait at depths of approximately 50 to 150 m carrying nutrient-rich (N, P, Si) and relatively fresh (<33) waters (Torres-Valdes et al., 2013). Relatively warm (> 0 °C) and saline (>34) Atlantic waters lie below the Pacific waters at depths of 200 to 400 m (Swift et al., 1997; Rudels et al., 2012; Fig. 2). These Atlantic-derived waters are typically capped by the overlying Pacific and freshwater layers, which act as an insulating barrier, limiting the upward heat flux and thereby reducing sea ice melt (Jones, 2001). Circulation in the Arctic Ocean follows a counterclockwise pattern with important inputs from: 1) the northward flowing Atlantic waters that enter the eastern Arctic via Fram Strait and the Barents Sea (Fig. 2), 2) Pacific waters that enter the Arctic from the Bering Strait into the Chukchi Sea that flow eastward over the CAA, where a portion becomes entrained in the Beaufort Gyre (Fig. 2), and 3) Freshwater in the western Canadian Arctic and Russia that enter the Arctic via river runoff and are entrained in the upper portions of the water column (Fig. 2).

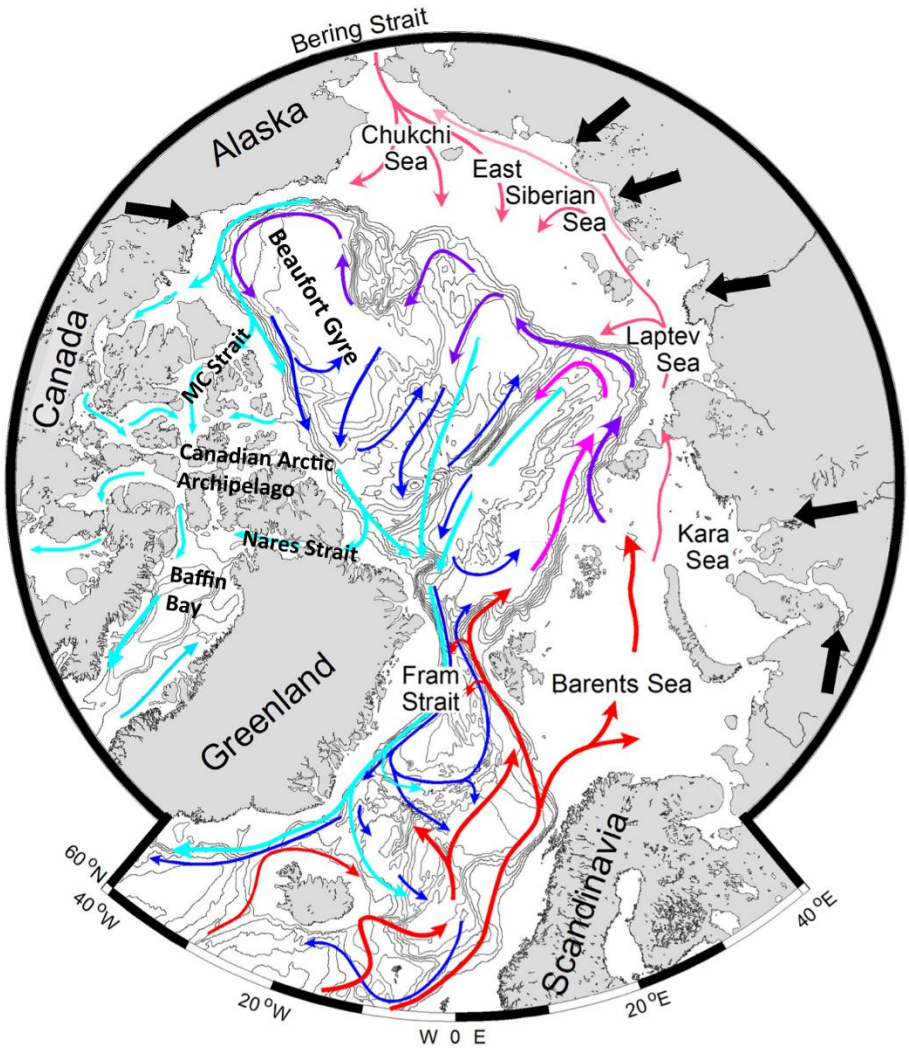

Figure 2. Arctic Ocean circulation showing warm Atlantic-derived waters (red), cold surface currents (light blue), intermediate modified waters (purple and dark blue), and riverine input (black) (modified from Anderson & MacDonald, 2015).

Water from the Arctic Ocean is exported via three main gateways: MC, Nares, and Fram Straits where it then flows southward either through Baffin Bay or along the eastern Greenland margin before entering the North Atlantic (Jones, 2001). These freshwater outflow routes are important regions of rapid change in the Arctic and thus can serve as barometers of oceanographic and biological shifts. In recent years, freshwater export has increased via Nares Strait and more broadly, the CAA (Moore et al., 2021), a trend that has been linked to

Arctic amplification (Vincent, 2019). This increased export into northern Baffin Bay has resulted in more freshwater and sea ice input into the region changing the hydrology of the surrounding marine environment. The interplay of this increased freshwater export on the sea-surface conditions its subsequent impact on primary production remains poorly understood.

REGIONAL SETTING

Baffin Bay is located along one of the main export routes of Arctic freshwater and sea ice, flowing through Nares Strait and the Canadian Arctic Archipelago, acting as an important connection between the Arctic Ocean and the North Atlantic. The oceanography of Baffin Bay is influenced by two major oceanic currents. The first is the Baffin Current (BIC), which originates in northern Baffin Bay and flows southward along the western margin, carrying fresh, cold (salinity <34, temperature >-1°C), and nutrient-rich (phosphorus and silicate) waters (Melling et al., 2001; Tremblay et al., 2002; Tang et al., 2004; Fig. 3). The BIC originates as a combination of modified nutrient-rich Pacific waters and Arctic meltwater from Nares Strait, Jones Sound, and Lancaster Sound (Jones, 2001; Münchow et al. 2007; Fig. 3). Freshwater flows in from west to east in Lancaster and Jones Sound into northern Baffin Bay (Tang et al., 2004) making up almost two-thirds of the surface waters and constituting the upper ~300 m of the water column in western Baffin Bay (Melling et al., 2001; Bâcle et al., 2002). The second current is the West Greenland Current (WGC), a subsurface, northward-flowing current characterized by warmer and more saline waters (salinity >34, temperature >2°C). It represents an important source of nitrate to northern Baffin Bay (Tremblay et al., 2002; Fig. 3). The WGC originates at the southern tip of Greenland and is a combination of the cold and fresh waters of the East Greenland Current, and relatively warm and saline Atlantic-sourced waters of the Irminger Current (Bâcle et al., 2002; Rysgaard et al., 2020). The depth of the WGC varies in the water column from 700 to 200 m, becoming shallower as it travels toward northern Baffin Bay (Bâcle et al., 2002; Tang et al., 2004). In deeper regions (>1800 m), the Baffin Bay Deep Water is also present, although its origin and formation processes remain poorly understood (Bourke & Paquette,

1991). Additionally, freshwater inputs from the GIS and glaciers of the eastern CAA further influence the hydrography of Baffin Bay. These meltwater inputs can occur both at the surface and at the glacier base, where subglacial discharge drives upwelling and entrainment of nutrient-rich deeper waters (Halbach et al., 2021).

Lithogenic sediment input in Baffin Bay is predominately influenced by terrestrial runoff such as the meltwater from the surrounding ice caps (Mortimer et al., 2018; Wychen et al, 2020; Fig. 3). As a result, modern sediments are derived from glacial erosion of the bedrock of the CAA and northwestern Greenland and are then transported laterally via the BIC and WGC. The bedrock geology of the northern CAA and Greenland is composed of seven distinct units (Fig. 3) that can be broadly described into 3 bedrock categories: 1) the Rae Craton and Ellesmere-Inglefield Mobile Belt: Precambrian gneisses with gabbroic intrusions, 2) the Ellesmere-North Greenland fold belt, Thule Supergroup, and the Canadian/Greenland Shield: Mesoproterozoic to Neoproterozoic sedimentary rocks and carbonate reefs, and 3) Sverdrup Basin and Foxe Basin: Paleozoic limestone and dolomites (Kravtiz et al., 1976; Andrews et al., 2018; Andrews, 2019; Jennings et al., 2019; Fig. 3). The sedimentary transport in northern Baffin Bay can be summarized into four main processes; 1) deposition via ice-rafted debris from glaciers, 2) submarine glacial plumes from marine-terminating glaciers, 3) turbidity currents, and 4) glacigenic debris flows (St-Onge & St-Onge, 2014; Andrews et al., 2018; Andrews, 2019; Caron et al., 2019). Due to the proximity to several glaciers, northern Baffin Bay generally has a high sedimentation rate as a result of these glacially influenced processes along with pelagic deposition.

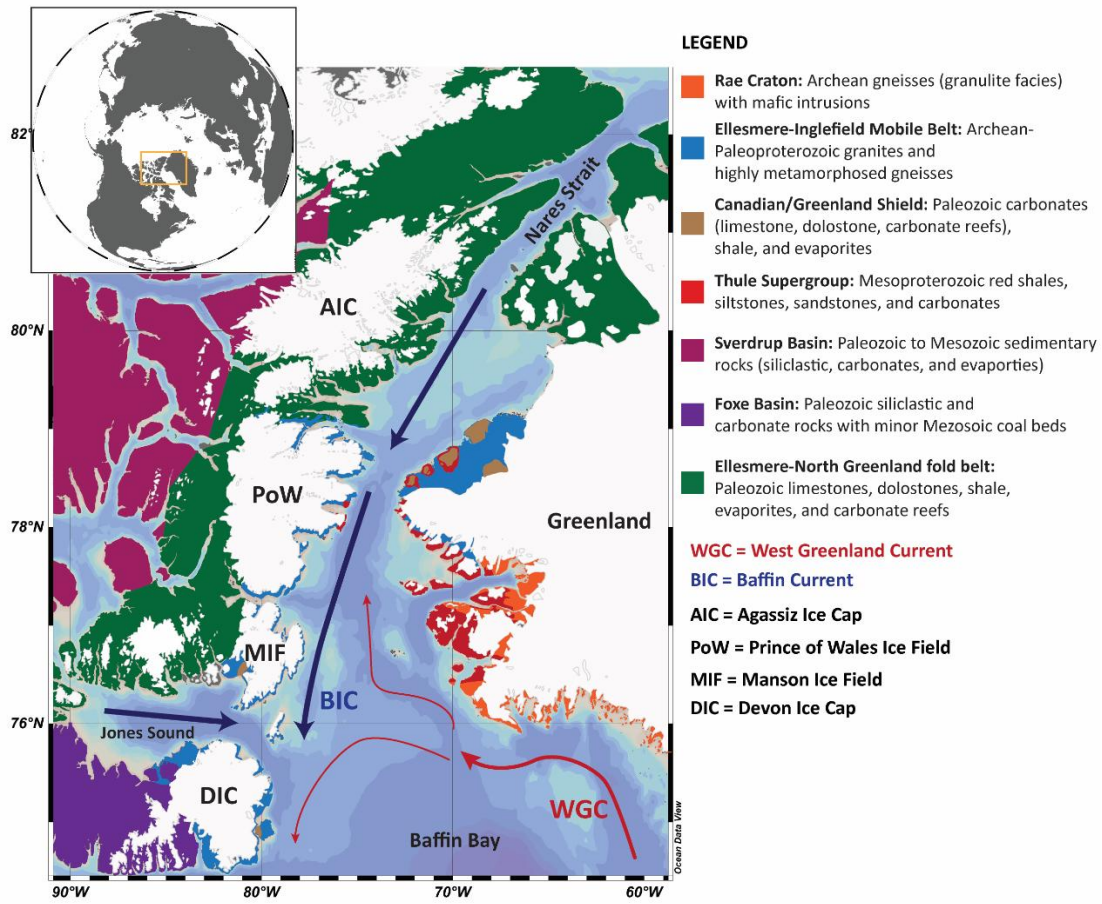

Figure 3. Map showing the regional geology of northern Baffin Bay and major ocean currents influencing the region (modified from Koerner et al., in prep., see chapter 3).

Northern Baffin Bay is an ecologically important region as it is host to the North Water (NOW) polynya - *Pikialasorsuaq* in Greenlandic (Eegeesiak et al., 2017) and *Sarvarjuaq* in Inuktitut (North Qikiqtaaluk). It is the largest recurrent polynya in the Arctic (Dunbar & Dunbar, 1972; Deming et al., 2002; Fig. 4). Polynyas are areas of open water in regions with high sea-ice concentrations that can influence the marine setting (e.g., ocean-atmospheric heat loss, sinking of brines due to new sea ice formation) and they provide multiple ecosystem services (e.g., enhanced primary production that helps in sustaining a large and diverse food web; Morales Maqueda et al., 2004). The modern NOW's open water season typically begins in March and continues until June, when the open waters join with the rest of Baffin Bay and stop being a polynya in the strict sense. The spring open-water conditions

of the NOW help foster an earlier phytoplankton bloom that is dominated by diatoms and to a lesser extent autotrophic flagellates (where dinoflagellates make up a significant portion; Lovejoy et al., 2002; Blais et al., 2017; Marchese et al., 2017) resulting in a highly productive region with high biogenic fluxes to the seafloor (Hargrave et al., 2002; Sampei et al., 2004). This elevated primary production helps sustain a large and diverse food web where large mammals such as narwhals and walruses are known to overwinter (Heide-Jørgensen et al., 2013; 2016). The formation and maintenance of the open water conditions in the NOW are tightly linked to both physical and oceanic parameters, making it sensitive to changes in the climate.

The open water conditions in the NOW rely on three main factors:

1. Ice bridge formation and consolidation in Nares Strait, Jones Sound, and Lancaster Sound, which restrict the inflow of sea ice into northern Baffin Bay (Dumont et al., 2009; Moore et al., 2021).

2. Strong northerly winds that drive newly formed sea ice southward out of the NOW region (Moore & McNeil, 2018) and promote the upwelling of the WGC.

3. Upwelling of the relatively warm and saline WGC in the eastern part of the NOW, which helps inhibit sea-ice formation in this region (Bâcle et al., 2002; Rysgaard et al., 2020) and enriches surface waters with nutrients that enhance primary production (Marchese et al., 2017).

During the 21st century, the NOW's formation has been impacted by Arctic warming. Most notable is the early collapse or failure of the Nares Strait ice bridges where the stability of the Nares Strait ice bridges has become more variable due to: 1) a decrease in thicker multi-year sea-ice in the Arctic Ocean which is essential to the cohesion of the ice bridges (Kwok et al., 2010; Moore et al. 2021; Fig. 4), 2) a decrease in land-fast ice on the eastern portion of Kane Basin, which is important to the structural integrity of the southern ice bridge (Vincent, 2019), 3) changes to atmospheric circulation patterns such as the Arctic Oscillation (Georgiadis et al., 2020), and 4) increasing presence of warmer Atlantic and Pacific-sourced

waters that reduce thermodynamic ice growth (Kirillov et al., 2022). In the 21st century (2007, 2009, 2010, 2017, 2019, and 2022) the ice bridge has collapsed in the early spring or failed to form, resulting in increased freshwater and multi-year sea-ice flow through Nares Strait into Baffin Bay (Vincent, 2019; Moore et al., 2021). With continued predicted Arctic warming (Notz et al., 2020), and subsequent failure of the Nares Strait ice bridges (Moore et al., 2021), how the NOW's open water conditions will persist into the future is unknown.

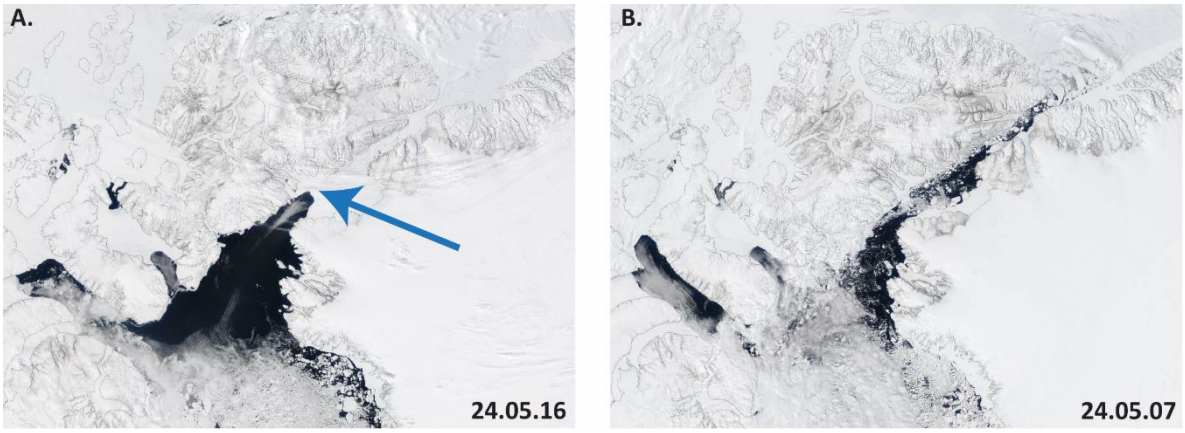

Figure 4. EOSDIS Images of the NOW with A) a stable ice bridge, indicated by the blue arrow and B) without a stable ice bridge.

These formation factors of the NOW are not only important in the functioning and maintenance of open water conditions, but they also impact the timing and type of primary production in the region (Lovejoy et al., 2002; Tremblay et al., 2002; Marchese et al., 2017; Joli et al., 2018). Earlier phytoplankton blooms have been observed in the eastern portion of the NOW attributed to the upwelling of the relatively warm WGC (Marchese et al., 2017), and the western portion of the NOW is dominated by diatom blooms due to the input of silicate-rich polar waters. Furthermore, there is also an observed seasonality in the functional groups of primary producers within the NOW. Earlier spring blooms are dominated by diatoms (Lovejoy et al., 2002), the summer months are distinguished by more diversity in primary producers, and the autumn blooms are generally dominated by dinoflagellates (Freyria et al., 2021). As such, the phytoplankton bloom dynamics are impacted by the formation factors of the NOW. Modern changes in the formation factors such as the ice

bridge failures in Nares Strait, are likely to have a direct impact on the phytoplankton communities.

PREVIOUS RESEARCH

Northern Baffin Bay is a dynamic region influenced by a combination of hydrologically distinct ocean currents (i.e., WGC and BIC), freshwater outflow from the Arctic Ocean, and localized meltwater from glaciers on the Canadian and Greenland side. Thus, the open water conditions in the NOW are tightly linked to environmental conditions and more broadly Arctic climate change. Modern observations in the NOW, such as oceanographic, biological, and physical measurements provide a robust baseline for current functioning of the ecosystem. However, understanding the full impact of current climate warming requires assessing the long-term natural variability of the system.

Previous research on sediment archives in Nares Strait and northern Baffin Bay have shown that the ice bridges in Nares Strait have undergone other periods of instability throughout the last ca. 11,700 years (Mudie et al., 2005; Georgiadis et al., 2020; Ribeiro et al., 2021), attributed to large-scale atmospheric changes such as differences in the Arctic Oscillation (Darby et al., 2012; Georgiadis et al., 2020), but also with periods of warming such as the Roman Warm Period (RWP; Jackson et al., 2021), and Medieval Climate Anomaly (MCA; Limoges et al., 2023). These periods of ice bridge instability have been shown to impact the sea-surface conditions in the eastern portion of the NOW (Koerner et al., 2021) and influence the size and communities of diatoms (Limoges et al., 2023). These changes in ice bridge stability have also been inferred to have cascading effects on both the marine and terrestrial ecosystem, where periods of NOW instability impact little auk colonies in Greenland (Davidson et al., 2018), and influence the migration and settlement patterns of pre-Inuit communities in the region (Davidson et al., 2018; Gotfredsen et al., 2018; Hastrup et al., 2018; Jeppesen et al., 2018; Ribeiro et al., 2021).

However, comparing the recent variability of ice bridge instability and subsequent freshwater flow to that of 21st century warming has only been done in the central portion of

the NOW, which is less influenced by these freshwater inputs than the western portion (Jackson et al., 2021; Koerner et al., 202; Ribeiro et al., 2021). Other records in northwestern Baffin Bay have analyzed changes in sea-surface conditions (Cormier et al., 2016) and primary productivity (Bailey et al., 2013), along with the spatial variability of the NOW over the Holocene (Harning et al., 2025) but do not capture the last ca. 30 years of climate change that encompass the most recent failures of ice bridges in Nares Strait. Another important avenue that has not been explored is the impact of Arctic freshwater flow versus glacial outflow and the impacts on primary production. Modern studies have explored the impact of glacial outflow in Jones Sound (Bhatia et al., 2021; Williams et al., 2021). However, this has been conducted in modern surface waters and understanding the long-term variability associated with the CAA glacial outflow remains relatively understudied and poorly constrained. By looking at long-term evolution of sea-surface conditions in the western sector of the NOW we can better understand how surface waters have evolved and responded to climatic variability, which can give us a better understanding on how the system will respond in the future.

RESEARCH OBJECTIVES AND METHODOLOGY

The overall aim of this thesis is to assess how 21st century ice-bridge failures in Nares Strait and other climate-driven cryosphere changes have affected sea-surface conditions in northwestern Baffin Bay during the Late Holocene. This project uses three sediment cores (two box cores and a corresponding gravity core; Fig. 5; Table 1) located in the western region of the NOW and 12 surface sediment samples collected onboard the Canadian Coast Guard Ship (CCGS) icebreaker Amundsen during the 2019 ArcticNet expedition under the project "Arctic Seafloor Mapping Data Processing and Dissemination" (Fig. 5; Table 1). The western portion of the NOW and northern Baffin Bay offers the ideal location to study the interactions between freshwater (solid and liquid) export and sea-surface conditions over long-time scales.

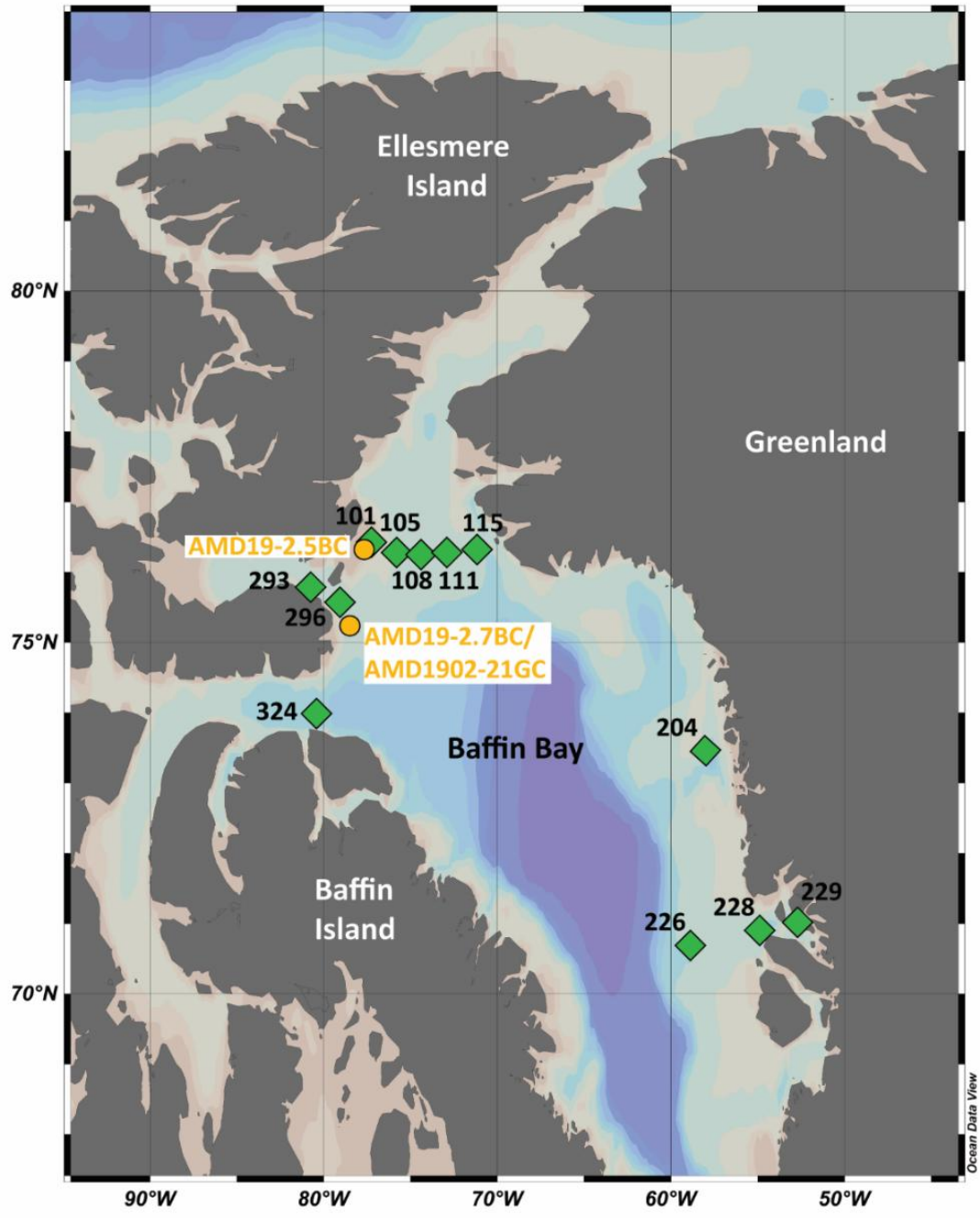

Figure 5. Map with the surface sediment (green diamonds) and sediment cores (yellow circles) used in this thesis.

Table 1. Information about the surface (0-1cm) sediment samples and short cores analyzed in this study.

Name	Latitude (N)	Longitude (W)	Water depth (m)	Length (cm)	Station #
AMD19-115BC	76.31460	-71.2370	663	surface (1)	115
AMD19-111BC	76.30856	-73.1941	607	surface (1)	111
AMD19-108BC	76.25988	-74.5926	443	surface (1)	108
AMD19-105BC	76.31967	-75.7756	334	surface (1)	105
AMD19-101BC	76.38236	-77.3909	351	surface (1)	101
AMD19-296BC	75.52303	-79.7538	556	surface (1)	296
AMD19-204BC	73.26541	-58.0081	961	surface (1)	204
AMD19-228BC	70.90592	-55.0128	574	surface (1)	228
AMD19-229BC	71.01072	-53.0451	431	surface (1)	229
AMD19-226BC	70.69894	-59.0045	594	surface (1)	226
AMD19-324BC	73.98845	-80.4738	774	surface (1)	324
AMD19-293BC	75.72819	-80.6897	627	surface (1)	293
AMD19-2.5BC	76.35642	-77.5054	379	43	2.5BC
AMD19-2.7BC	75.48239	-78.6753	521	40	2.7BC
AMD1902-21GC	75°28'56.6"N	78°40'33.7"W	522	223.5	21GC

This thesis is organized around three sub-objectives, each corresponding to a study that has been published or is intended for submission to peer-reviewed journals.

Sub-objective 1: Use dinoflagellate cysts and geochemistry (TOC, TN, $\delta^{15}N$, $\delta^{13}C$) as proxies for changes in sea-surface conditions and organic matter provenance, respectively, to assess changes in the NOW conditions and primary production

Hypothesis: The NOW is influenced by two main oceanic currents: the WGC and BIC that have different water mass properties. The WGC is relatively warm, saline, and rich in dissolved nitrogen compared to the BIC, which is relatively cool, fresh, and rich in dissolved silicon. Dinoflagellate cysts (dinocysts) which are sensitive to changes in sea-surface conditions can reflect these two distinct oceanic currents and provide information down-core about changes in sea-surface conditions. The geochemistry (TOC, TN, $\delta^{15}N$, $\delta^{13}C$) can also provide additional down-core information about changes in primary production and provenance of organic matter that can help understand NOW functioning.

The objective of this first chapter is twofold: 1) to assess whether modern organic-walled dinoflagellate cysts preserved in surface sediments across Baffin Bay and the NOW reflect distinct hydrological conditions, and 2) to investigate changes in sea-surface conditions and organic matter provenance over the past ~400 years using two sediment cores from northwestern Baffin Bay. Although this represents a relatively short temporal window, we specifically compared modern warming over the last 50 years with the system's natural variability.

Sub-objective 2: Use sub-fossil diatoms as an indicator of changes in sea-ice dynamics and sea-surface conditions to assess changes in the western NOW's marginal ice

Hypothesis: In addition to oceanographic forcing, the NOW is influenced by cryospheric variability, including sea-ice concentration and extent. This influence is particularly pronounced in the western NOW, which lies at the confluence of sea ice export through Nares Strait. This region features a prominent ice edge whose structure depends on the formation

and persistence of ice bridges in Nares Strait. Understanding the dynamics of the marginal ice zone is therefore important to understanding the earlier primary production in the NOW.

The objective of this second chapter is to use sub-fossil diatoms as a proxy to reconstruct past changes in the position and dynamics of the ice edge along the western NOW. Diatoms, the main primary producers in the NOW, inhabit a variety of environments, from landfast ice along the coast, the marginal ice zone to open waters, making them valuable indicators of sea-surface conditions and sea ice presence. Here we again start by analysing a surface sediment transect across the NOW to see if diatoms reflect distinct oceanic currents and sea-ice conditions. By using diatom assemblages preserved in sediment, the aim is to document changes in sea-ice dynamics and marginal ice zone variability over the last ca. 400 years.

Sub-objective 3: Assess the use of sediment provenance and grain size analysis as an additional tool to provide information on freshwater transport pathways into northern Baffin Bay

***Hypothesis*:** Western Baffin Bay is influenced by both freshwater export from Nares Strait, Jones Sound, and Lancaster Sound along with glacial outflow from surrounding ice masses in the CAA and Greenland. Glacial outflow provides an important source of micronutrients that can enhance phytoplankton productivity and stimulate blooms (Bhatia et al., 2013; Williams et al., 2021). However, disentangling the relative influence of polar outflow and glacial discharge through time remains difficult. Considering the impacts from polar outflow and glacial outflow could result in different implications for the marine system, understanding the difference over time is important to better understand the impact of Arctic amplification on oceanography and primary production.

This chapter investigates the influence of different freshwater transport pathways into northern Baffin Bay, with a focus on differentiating the impacts of localized glacier input from freshwater Arctic outflow. To achieve this, we apply a multi-proxy approach combining sedimentological data (grain size analysis, qXRD) and dinocyst data from a box core and

gravity core covering the last ca. 1200 years. The qXRD and grain size data are used to determine sediment provenance and depositional energy respectively, providing insights into variations in sediment source and, by extension, past oceanic circulation patterns.

ORIGINAL ASPECTS OF WORK

Understanding how sea-surface conditions have changed over long timescales to put into context modern climate warming is essential to better understand how our system may respond to future change. These responses help better inform forecast models (i.e., Notz et al., 2020), that can in turn help shape climate policy. The aim of this thesis is to assess how modern freshwater export into northern Baffin Bay has affected the sea-surface conditions compared to the Late Holocene, providing important context to current climate warming. This thesis includes three publications either submitted to, or in preparation for peer-reviewed journals, that together aim to improve our understanding of changes to sea surface conditions over the late Holocene in the northwestern NOW.

The first chapter entitled "Early impacts of Arctic amplification in the western North Water Polynya: A 400-year perspective" has been published in the journal *Marine Micropaleontology* in May 2025. Our results indicate that: 1) dinoflagellate cysts can be used as indicators of differing hydrological conditions in the NOW and more broadly, in Baffin Bay and that; 2) down core changes over the last ca. 400 years show an earlier response to Arctic Amplification than in the eastern NOW, predating the documented instability of the Nares Strait ice bridges. Despite the relatively short timescale of the two sediment cores used, the changes in geochemistry and dinoflagellate cysts demonstrate the sensitivity of the NOW to climate-induced change and show that the system responds rapidly to climatic variability.

The second chapter entitled "Ice edge variability in the western North Water Polynya over the last 400 years based on diatom assemblages" is in preparation to be submitted to Paleogeography, Paleoclimatology, and Paleoecology. This paper investigates the distribution and composition of sub-fossil diatom assemblages from surface sediment samples collected across a longitudinal gradient in the NOW, and their relationship to sea-

ice conditions. This paper highlights that diatoms can be used as a tracer for changes in the ice edge in the NOW, a dynamic feature that has important implications for the early springtime bloom. The differences between the two box cores highlights the dynamic nature of sea ice in the western NOW, and the importance of understanding localized effects on the sea-surface conditions in the region.

The third chapter entitled "Differing freshwater outflow pathways into northwestern Baffin Bay over the last ca. 1200 years using sedimentary and biogenic proxies" is in preparation to be submitted to JGR Biogeosciences. This paper integrates sediment provenance and grain size analysis to distinguish between more proximal freshwater sources (i.e., Devon Island) and distal inputs (i.e. Ellesmere Island) into northern Baffin Bay. These data are compared with dinoflagellate cyst assemblages to understand how both proxies co-vary and provide complementary insights into changes in sea-surface conditions over time. This paper offers a new perspective by differentiating between freshwater export through Nares Strait and more localized inputs, assessing how glacial outflows have influenced sea-surface conditions in the western NOW.

CONFERENCES AND OTHER EXPERIENCES

During my PhD, I have participated in 5 international conferences, 2 national conferences, and 5 provincial conferences. I have also had the opportunity to participate in four oceanographic field missions onboard the CCGS Amundsen in 2021 (Leg 3), 2022 (Sea Trials + Leg 2), and 2023 (Leg 3) where my principal roles were to collect phytoplankton and sediment samples (surface sediment and sediment cores). This resulted in my co-authorship on three cruise reports, and a peer-reviewed paper in *Arctic Science*.

I also participated in two research stays at the Université du Québec à Montréal, for $^{210}Pb/^{137}Cs$ analyses, benthic foraminifera identification, and geochemistry laboratory preparation and analyses. In addition to my research stays in Montreal, I also participated in two others at the University of New Brunswick for diatom sample preparation and taxonomic

identification. Finally, I was the Canadian representative and the coordinator of the NSERC CREATE Program ArcTrain from October 2021 until the end of the program in July 2023.

Peer-Reviewed Articles

Geoffroy, M., Limoges, A., Ardyna, M., Matthes, L., Archambault, P., Barut, G., Bécu, G., Bélanger, S., Belko, A., Bertrand, E., Blais, G., Brice, C., Brunner, L., Burgers, T., Capelle, D., Charette, J., Combaz, T., Daase, M., Desmarais, A., …**Koerner, K**.,.. Michel, C. (2026). First characterization of the marine ecosystem of Archer Fiord in the Lasting Ice Area of the high Arctic: A productivity paradox. *Arctic Science* 12:1-31. https://doi.org/10.1139/as-2024-0073

Cruise Reports

Montero-Serrano, J.C, Belko, A., Brice C., Girard, J., Harker, B., **Koerner, K**., Limoges, A., Ribeiro, S., Stancu, C. (2023). ArcticNet Seafloor Mapping Data Processing and Dissemination and Rapidly changing ecosystem dynamics in the Arctic Ocean's Last Ice Area (RED-AO). ArcticNet Leg 3, Cruise Report – CCGS Amundsen (7 September to 5 October), 47 p.

Montero-Serrano, J.-C, Bracquart, E., Brice, C., & **Koerner, K**. (2022). ArcticNet seafloor mapping and marine geology project. ArcticNet Leg 2, Cruise Report – CCGS Amundsen (22 September to 19 October), 30 p.

Montero-Serrano, J.-C. & **Koerner, K**. (2021). Collecting sedimentary sequences and plankton samples in the continental margins from the eastern Canadian Arctic Archipelago. ArcticNet seafloor mapping and marine geology project. ArcticNet Leg 3, Cruise Report – CCGS Amundsen (12 August to 9 September), 45 p.

Conferences

Koerner, K., Rochon, A., Limoges, A. 2020. Evolution of sea-surface conditions and primary production during the last 2000 years of climatic variability in northern Baffin Bay. *ArcTrain Annual Meeting*, October 23-30, Online, Oral/Poster Communication.

Koerner, K., Rochon, A., Limoges, A. 2021. Évolution de l'océanographie et de la production primaire au cours des 2000 dernières années de variabilité climatique dans le nord de la baie de Baffin. *Geotop Annual Student Meeting*, March 16-18, Oral/Poster Communication.

Koerner, K., Rochon, A., Limoges, A. 2022. Évolution de l'océanographie et de la production primaire à la fin de l'Holocène dans le nord-ouest de la baie de Baffin. *Geotop Annual Student Meeting*, March 29-31, Oral/Poster Communication.

Koerner, K., Rochon, A., Limoges, A. 2022. Evolution of oceanography and primary production over the late Holocene in northwestern Baffin Bay. *ArcTrain Annual Meeting*, May 13-17, Oral/Poster Communication.

Koerner, K., Rochon, A., Limoges, A.2022. Late Holocene Changes in Oceanography and Regional Export Primary Production in Northwestern Baffin Bay. *12th International Conference on Modern and Fossil Dinoflagellates*, July 4-8, Oral Communication.

Koerner, K., Rochon, A., Limoges, A. 2022. Evolution of oceanography and primary production over the late Holocene in northwestern Baffin Bay, *ArcticNet Annual Meeting*, December 4-8, Oral Presentation.

Koerner, K., Rochon, A., Limoges, A. 2023. Evolution of oceanography and primary production over the late Holocene in northwestern Baffin Bay, *Geotop Annual Student Meeting*, March 10-12, Poster Presentation.

Koerner, K., Rochon, A., Limoges, A. 2023. Evolution of oceanography and primary production over the late Holocene in northwestern Baffin Bay, *ArcTrain Annual Meeting*, March 27-31, Poster/Oral Presentation.

Koerner, K., Rochon, A., Limoges, A. 2024. Changes in sea-surface conditions in northwestern Baffin Bay over the last 400 years inferred from organic-walled dinoflagellate cysts assemblages, *Geotop Annual Student Meeting*, March 22-24, Oral Presentation.

Koerner, K., Rochon, A., Limoges, A. 2024. Changes in sea-surface conditions in northwestern Baffin Bay over the last 400 years inferred from organic-walled dinoflagellate cyst assemblages, *XV International Palynological Congress/XI International Organization of Paleobotany Conference*, May 27-31, Oral Presentation.

Koerner, K., Rochon, A., Limoges, A. 2024. Changes in sea-surface conditions in northwestern Baffin Bay inferred from organic-walled dinocyst assemblages over the last ca. 400 years, *ArcticNet Annual Conference*, Dec 9-12, Poster Presentation.

Koerner, K., Rochon, A., Limoges, A. 2025. Understanding changes in early season primary production in the North Water (NOW) polynya from ca. 1620 to 2019 CE, *Geotop Annual Student Meeting*, March 14-16, Poster Presentation.

CHAPITRE 1
IMPACTS DE L'AMPLIFICATION ARCTIQUE DANS LA POLYNIE DES EAUX DU NORD : UNE PERSPECTIVE SUR 400 ANS

1.1 RESUME EN FRANÇAIS

La polynie des eaux du Nord, située au nord de la baie de Baffin, est connue pour ses eaux libres persistantes, attirant mammifères marins et oiseaux durant l'hiver. Les ponts de glace qui se forment au nord de la Polynie aux points de constriction du détroit de Nares, contribuent au maintien de ces conditions d'eaux libres. Cependant, l'amplification arctique a fragilisé ces ponts de glace, modifiant ainsi les flux d'eau et de glace de mer vers la Polynie. Nous avons examiné l'effet du réchauffement climatique et des ruptures récentes de ponts de glace sur 400 ans d'évolution dans la partie ouest de la Polynie. Nous avons analysé les assemblages de kystes de dinoflagellés (dinokystes) dans un transect de sédiments de surface traversant la Polynie afin d'évaluer leur distribution en tant qu'indicateurs des masses d'eau de surface. Nous avons ensuite analysé les dinokystes et les indicateurs géochimiques (signatures du carbone et de l'azote) de deux carottes de sédiments prélevées dans la partie ouest de la Polynie. Les résultats montrent que la partie orientale de la Polynie, influencée par le courant du Groenland occidental (WGC), présente des contributions plus importantes de taxons mixotrophes et des concentrations totales de dinoflagellés plus élevées que la partie occidentale, influencée par les eaux arctiques. Les carottes sédimentaires révèlent une période de stabilité de 300 ans dans la partie occidentale de la Polynie (1620-1920 CE), suivie d'une augmentation des taxons mixotrophes et des flux totaux de dinoflagellés, antérieure aux ruptures de ponts de glace observées. Vers 1980, l'abondance accrue d'*Operculodinium centrocarpum* et de kystes de *Polarella glacialis* et de *Pentapharsodinium dalei* suggère un recul précoce de la banquise, apparemment attribuable à une influence accrue du WGC. Ces résultats démontrent l'impact précoce de l'amplification arctique sur la polynie des eaux du

Nord, avec des changements significatifs dès la première moitié du XXIe siècle, contribuant ainsi à la compréhension de la chronologie et de la propagation des changements océanographiques dans la polynie.

Cet article, intitulé « I*mpacts de l'amplification arctique dans la polynie des Eaux du Nord: Une perspective sur 400 ans.* » a été accepté pour publication dans sa version finale par les éditeurs de la revue *Marine Micropaleontology* en mai 2025. En tant que première autrice, j'ai effectué la revue de la littérature, les analyses de tous les échantillons de carottes sédimentaires (analyses des dinokystes et du ^{210}Pb) et la rédaction de la première version du manuscrit. Audrey Limoges, deuxième autrice et André Rochon, dernier auteur, ont participés à la mise à disposition des ressources matérielles, à la supervision et à la révision du manuscrit. Emily Pike-Connolly, troisième autrice, a effectué le comptage des dinokystes sur les échantillons de sédiments de surface et à la révision du manuscrit. Nicolas Van Nieuwenhove, quatrième auteur, a aidé au traitement de certains échantillons de dinokystes et a également effectué l'analyse GAM et à la révision du manuscrit. Les résultats de ce chapitre ont été présentés lors des conférences annuelles ArcTrain (2020, 2022, 2023), Geotop (2021, 2022, 2023) et ArcticNet (2022, 2024), sous forme d'exposés oraux et de présentations par affiches.

1.2 ABSTRACT

The North Water (NOW) polynya in northern Baffin Bay is known for persistent open water, attracting marine mammals and birds during winter. Ice bridges forming north of the NOW at constriction points in Nares Strait aid in sustaining these open water conditions. However, Arctic Amplification has weakened these ice bridges, altering water and sea ice flow into the NOW. We examined the effect of climate warming and recent ice bridge failures through 400 years of changes in the western NOW. We analyzed dinoflagellate cyst (dinocyst) assemblages in a surface sediment transect across the NOW to assess their distribution as indicators of surface water masses. We then analysed dinocysts and geochemical proxies (carbon and nitrogen signatures) from two sediment cores in the western NOW. Results show the eastern NOW, influenced by the West Greenland Current (WGC), exhibits higher contributions of mixotrophic taxa and total dinocyst concentrations than the western region, influenced by Arctic water outflow. Sediment cores show a 300-year period of stability in the western NOW (1620–1920 CE), followed by an increase in mixotrophic taxa and total dinocyst fluxes, predating observed ice bridge failures. Around 1980 CE, higher abundances of *Operculodinium centrocarpum*, and cysts of *Polarella glacialis* and *Pentapharsodinium dalei*, suggest early sea ice retreat, seemingly attributable to increased WGC influence. These findings demonstrate the early impact of Arctic Amplification on the NOW, with significant changes starting in the first half of the 20th century, which contribute to understanding the timing and propagation of oceanographic changes in the polynya.

Keywords: Pikialasorsuaq, Marine sediment, Dinoflagellate cysts, Organic carbon and nitrogen, Stable isotopes, Northern Baffin Bay, Climate change, Arctic

1.3 EARLY IMPACTS OF ARCTIC AMPLIFICATION IN THE NORTH WATER (NOW) POLYNYA: A 400-YEAR PERSPECTIVE

Authors: Kelsey A. Koerner[1*], Audrey Limoges[2], Emily Pike-Connolly[2], Nicolas Van Nieuwenhove[2], André Rochon[1]

Institutions:

1. Institut des sciences de la mer, Université du Québec à Rimouski, Rimouski, Canada
2. Department of Earth Sciences, University of New Brunswick, Canada

1.4 INTRODUCTION

Over the past four decades, the Arctic has experienced a rapid decrease in sea-ice extent and thickness (e.g., Stroeve & Notz, 2018), with record lows consistently observed since 1986 (Parkinson & DiGirolamo, 2021). The resulting increased absorption of solar radiation by darker ocean water has intensified warming in the Arctic compared to other areas globally, a phenomenon referred to as Arctic Amplification. The decrease in sea-ice extent leads to southward sea ice export (Stroeve & Notz, 2018), impacting the Arctic regions' freshwater budget and resulting in more liquid freshwater stored in the Arctic (Haine et al., 2015). After Fram Strait, the Canadian Arctic Archipelago serves as the main export route for solid and liquid freshwater outflow through Nares Strait, Jones Sound, and Lancaster Sound (Fig. 6A). While liquid freshwater export through these channels remained relatively stable between 1980-2010 (Haine et al., 2015), models predict a future intensification in the export, especially via Nares Strait (Fig. 6A, B; Jahn & Laiho, 2020).

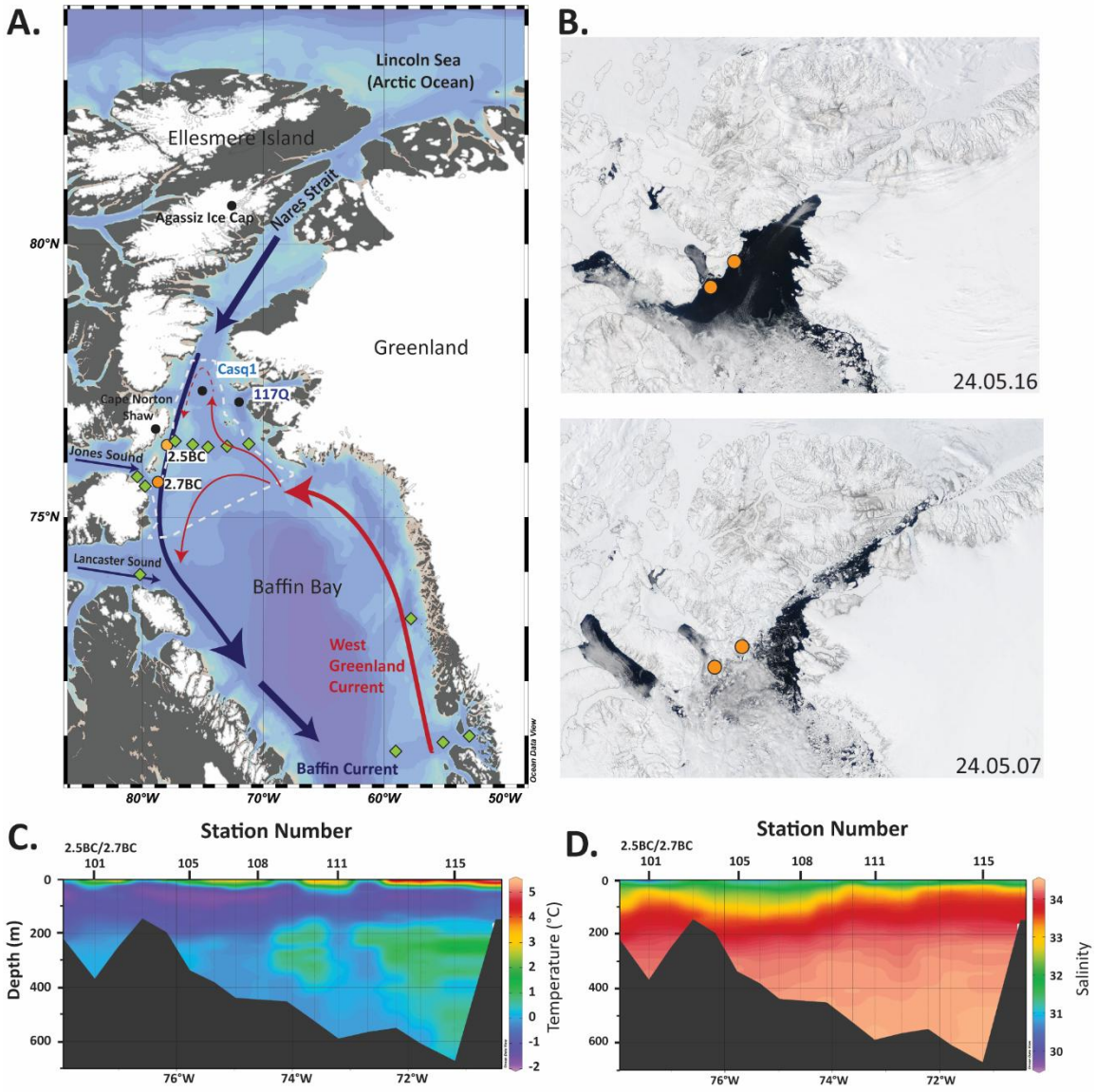

Figure 6. A) Map of northern Baffin Bay, showing the location of the surface sediment (green), AMD19-2.5BC/AMD19-2.7BC (orange), Casq1 (Jackson et al., 2021; Koerner et al., 2021; Limoges et al., 2023; Ribeiro et al., 2021), and 117Q (Jackson et al., 2021). The white dotted line represents the average spring-time extent of the NOW. B) EOSDIS images of northern Baffin Bay and Nares Strait showing sea-ice conditions in the NOW when the ice bridge forms (top) and when the ice bridge collapses (bottom). C) CTD profiles collected onboard the CCGS Amundsen in 2019 along the same profile as the transect of surface sediment samples, showing C) temperature and D) salinity (Amundsen Science Data Collection).

Nares Strait, a narrow channel between Ellesmere Island (Canada) and Greenland, is the only direct connection between the Arctic Ocean and northern Baffin Bay. It features ice bridges that typically form in February and persist until July when regional sea ice melts completely (Moore et al., 2021). These ice bridges play a crucial role in restricting sea-ice drift from the Lincoln Sea to northern Baffin Bay. However, increasing instability in the ice bridges has been observed in recent decades, with later formation and earlier breakup (Moore et al., 2021). In some cases, the ice bridges failed to form completely, creating a gateway between the Arctic Ocean and Baffin Bay. The first recent documented collapse of the ice bridges occurred in 2007 (Kwok et al., 2010), with subsequent failures in 2009, 2010, 2017, 2019 and 2022 (Vincent, 2019; Moore et al., 2021).

Instabilities in the Nares Strait ice bridges and resulting changes in the outflow of ice, freshwater, and nutrients have been identified as important mechanisms affecting biogeochemical processes and circulation patterns downstream in the North Water polynya (NOW; *Pikialasorsuaq* in Greenlandic and *Sarvarjuaq* in Inuktitut) (Joli et al., 2018; Moore et al., 2021; Fig. 6A). Polynyas are areas of ice-free waters in regions typically characterized by high sea-ice concentrations. The NOW is primarily classified as a latent heat polynya, owing its open waters to the ice bridges that form in Nares Strait, along with strong northerly winds that push newly formed sea ice southward. The NOW typically opens in late March and remains open until the rest of Baffin Bay becomes ice-free in summer. As a crucial mixing area for two main ocean currents, the West Greenland and Baffin currents, the NOW is characterized by high nutrient availability, which supports elevated primary production (Tremblay et al., 2002b; Michel et al., 2015). The high primary production in the region is important in sustaining the NOW ecosystem, which provides key provisioning and cultural services to communities of Inuit Nunangat and Kalaallit Nunaat (Greenland; Pikialasorsuaq Commission, 2017; Hastrup et al., 2018; Jeppesen et al., 2018). As such, the NOW is recognized as the Arctic's most productive ecosystem (e.g., Barber & Massom, 2007).

The western and eastern regions of the NOW exhibit contrasting hydrological conditions. The western region is primarily influenced by southward Arctic Ocean water flows, referred to as the Baffin Current, which consists of modified Pacific water and Arctic meltwater (Jones, 2001; Münchow et al., 2007), carrying cold (>-1°C), low salinity (<34), phosphate- and silicate-rich waters into Baffin Bay (Fig. 6A; Melling et al., 2001; Tremblay et al., 2002a; Tang et al., 2004). In contrast, the eastern sector is influenced by the northward-flowing West Greenland Current (WGC), which originates at the southern tip of Greenland. The WGC is a combination of the cold, fresh East Greenland Current waters and warm, saline Atlantic-sourced Irminger Current waters (Fig. 6A; Bâcle et al., 2002; Rysgaard et al., 2020). As the WGC flows toward northern Baffin Bay, its depth decreases from 700 to 200 m (Bâcle et al., 2002; Tang et al., 2004). It then upwells in the eastern portion of the NOW, circulates counterclockwise and flows southward along the Canadian coast (Fig. 6A). The WGC is relatively warm (>2°C) and saline (>34) and serves as an important nitrate source for northern Baffin Bay (Tremblay et al., 2002a). The eastern sector of the NOW typically opens first in early March due to the upwelling of the comparatively warm WGC (Marchese et al., 2017). Additionally, hydrological conditions in northern Baffin Bay are affected by meltwater input from marine-terminating glaciers, influencing water column stratification and nutrient inventories on both sides (Bhatia et al., 2013).

Studies conducted in northern Baffin Bay have emphasized the importance of the NOW ecosystem for Arctic top predators such as narwhals (*Monodon monoceros*), belugas (*Delphinapterus leucas*), and polar bears (*Ursus maritimus*), as well as maintaining high biodiversity in the polar regions (e.g., Heide-Jørgensen et al., 2013, 2016; Bryndum-Buchholz et al., 2024). Furthermore, investigations into the NOW's functioning over the Holocene indicate that the region is likely undergoing an environmental transition since the 21st century (e.g., Koerner et al. 2021; Limoges et al., 2023) with implications for the entire ecosystem (Ribeiro et al., 2021). This includes the timing and composition of phytoplankton blooms at the base of the marine food web (Freyria et al., 2021), which can impact the synchronization of prey-predator relationships. However, most of the long-term studies to date have focused on the central and eastern portions of the NOW (Jackson et al., 2021;

Koerner et al., 2021; Ribeiro et al, 2021; Limoges et al., 2023). In contrast, the western region, which is ideally located to capture the interplay between ice dynamics, ocean circulation, freshwater input and ecosystem productivity, has remained largely understudied with respect to recent climate change.

We tested the hypothesis that marine sediments from northwestern Baffin Bay can serve as a valuable record for studying historical and ongoing changes in the polynya dynamics that result from rising global temperature, including the recent Nares Strait ice bridge collapses. We used dinoflagellate cysts (dinocysts) as proxies for changes in sea-surface conditions along with geochemical proxies (total organic carbon (TOC), total nitrogen (TN), and the nitrogen and carbon isotopic signature of organic matter ($\delta^{15}N$ and $\delta^{13}C$)) as indicators of organic matter provenance and circulation patterns. Dinoflagellates, unicellular eukaryotes active in the upper water column, are typically an important component of the NOW's summer and autumn productivity (Freyria et al., 2021). Approximately 15-20% of dinoflagellate species produce highly resistant organic resting cyst that preserves well in sediment (Versteegh & Blokker, 2004; Jeong et al., 2010), where they constitute diverse assemblages whose abundances and composition are largely influenced by variations in temperature, salinity, sea ice conditions and the trophic state of the surface waters (e.g., de Vernal et al., 2020). While cyst-based studies traditionally interpreted cysts as being produced by either autotrophic or heterotrophic dinoflagellates, it is now clear that dinoflagellates exhibit diverse trophic strategies, functioning either as strict heterotrophs, constitutive mixotrophs (species with permanent chloroplasts that also consume other organisms), or non-constitutive phototrophs (species that acquire and temporarily retain chloroplasts from their prey; e.g., Mitra et al. 2016). Hence, the traditionally considered autotrophic species are here grouped under the "mixotroph" appellation.

In this paper we first analyzed the dinocyst content of five surface sediment samples collected along a west to east transect across the NOW. We then analyzed seven new surface sediment samples from Baffin Bay and combined them with 92 samples from a previously existing database from the region (de Vernal et al., 2020). The objective was to determine

whether the dinocyst distribution patterns reflected the influence of hydrologically distinct ocean currents within the NOW and more broadly in Baffin Bay. We then focused on two marine sediment cores collected from the western NOW region, spanning approximately the last ca. 400 years. In these archives, dinocysts and geochemical proxies provide information about decadal to multidecadal changes in sea-surface conditions, encompassing both long-term system variability and contemporary warming trends.

1.5 METHODS

Surface sediment samples (upper 1 cm of sediment) and two short cores (AMD19-2.5BC and AMD19-2.7BC, hereafter referred to as 2.5BC and 2.7BC respectively) were collected as part of the ArcticNet Leg 2a/b Expedition onboard the CCGS Amundsen in 2019 (Table 2), using a box corer. All samples were kept at 4°C until analyses. The cores were split, photographed and described for their sediment colour and general lithologic characteristics. The split cores were imaged using an X-ray Computer Tomography (XCT) scanner at the Institut des sciences de la mer for 2.7BC and the Geological Survey of Canada for 2.5BC. Cores were then sub-sampled at every 1 cm (2.7BC) and every 0.5 cm (2.5BC) for chronological and palynological analyses.

Table 2. Information about the surface (0-1cm) sediment samples and short cores analyzed in this study.

Name	Latitude (N)	Longitude (W)	Water depth (m)	Length (cm)	Identification
AMD19-115BC	76.31460	-71.2370	663	surface (1)	115
AMD19-111BC	76.30856	-73.1941	607	surface (1)	111
AMD19-108BC	76.25988	-74.5926	443	surface (1)	108
AMD19-105BC	76.31967	-75.7756	334	surface (1)	105
AMD19-101BC	76.38236	-77.3909	351	surface (1)	101
AMD19-296BC	75.52303	-79.7538	556	surface (1)	296
AMD19-204BC	73.26541	-58.0081	961	surface (1)	204
AMD19-228BC	70.90592	-55.0128	574	surface (1)	228
AMD19-229BC	71.01072	-53.0451	431	surface (1)	229
AMD19-226BC	70.69894	-59.0045	594	surface (1)	226
AMD19-324BC	73.98845	-80.4738	774	surface (1)	324
AMD19-293BC	75.72819	-80.6897	627	surface (1)	293
AMD19-2.5BC	76.35642	-77.5054	379	43	2.5BC
AMD19-2.7BC	75.48239	-78.6753	521	40	2.7BC

1.5.1 Core chronology

Sediment samples for ^{210}Pb activity analysis were freeze dried and a spike ^{209}Po was combined with sediments. Samples were then subjected to a series of acid digestions (nitric and hydrochloric acid (HNO_3 and HCl), hydrofluoric acid (HF), boric acid (H_3BO_4), and hydrogen peroxide (H_2O_2) to remove sedimentary material. Samples were treated with a final HCl solution and centrifuged to transfer the ^{210}Po to silver disks. The silver disks were counted for alpha particle emissions with the EGG-Ortec Type 576Atm alpha spectrometer at Geotop (Montreal, Canada). 2.5BC was analyzed at every 1 cm for the first 30 cm and then every 5 cm down to a depth of 40 cm. 2.7BC was analyzed at every 1 cm for the first 20 cm, and every 5 cm down to a depth of 40 cm. Sediment samples for ^{137}Cs activity analysis were sealed into small plastic containers and analyzed using the EGG-Ortec gamma well detector at Geotop. The R package "rPlum" (Version 0.5.0; Aquino-López et al., 2018), which uses a Bayesian approach that integrates both ^{210}Pb and ^{137}Cs activities, was used to develop an age model.

1.5.2 Organic carbon and nitrogen analyses (TOC, TN, δ^{15}N, δ^{13}C)

Sediment samples were acid-washed following the protocol described in Hélie (2009). Approximately 150 mg of wet sediment was dried for 2-5 days at room temperature. Samples were then ground and homogenized using a mortar and pestle, and ~50 mg was treated twice with HCl (2N), rinsed with distilled water, centrifuged and decanted until neutral pH was reached. Both cores were sampled at every 1 cm for the first five centimeters, and every 5 cm for the remainder of the cores.

The samples were then weighed into small tin capsules and measured for their %C and %N using the Carlo Erba NC2500 elemental analyzer at Geotop via combustion analysis. Both the δ^{15}N and δ^{13}C were analyzed using the Isoprime 100 MicroCube isotope ratio mass spectrometer. δ^{13}C values are expressed as ‰ vs. Vienna Pee Dee Belemnite (VPDB), and δ^{15}N values are expressed as ‰ vs. atmospheric values with analytical uncertainties of 1σ (or +/- 0.1‰) and 1σ (or +/- 0.2‰), respectively.

1.5.3 Dinoflagellate cyst preparation and identification

Dinocyst samples were analyzed every 1 cm for the first 16 cm and every 2 cm for the remainder of the cores. Prior to treatments, calibrated tablets of the marker grain *Lycopodium clavatum* were added to the sediment samples for later estimation of dinoflagellate cyst concentrations (Lund University batch #414831 with 12,100 ± 1,892 spores/tablet for 2.5BC and 2.7BC, batch #177745 with 18,584 ± 1,853 spores/tablet for the surface sediments). The sediments were then sieved through a 100 µm and 10 µm mesh to remove larger and smaller particles, respectively. The 10<x<100µm fraction was treated with room-temperature HCl (2N) for 24 hours to remove carbonate material, and room-temperature HF (49%) for 24 hours to 7 days to remove silicate material. Between acid treatments the samples were rinsed with distilled water to a neutral pH. The samples were then sonicated for < 30s and sieved again using the 100 µm and 10 µm nylon mesh to remove any remaining material finer than 10 µm. A drop of the residue was then mixed with glycerin jelly, mounted to permanent microscope slides, and analyzed on a transmitted light microscope (Nikon Eclipse 80i at ISMER and Olympus BX43 at UNB) at magnifications of 400–1000x. Dinocysts were counted following the taxonomy described in Rochon et al. (1999), Radi et al. (2013), Potvin et al., (2018), Van Nieuwenhove et al. (2020) and Limoges et al. (2020) to a minimum of 300 cysts, with the exception of one sample (2.7BC 5-6 cm), in which overall counts were low (n<150). When the preservation and orientation of dinocysts did not permit identification to the species level, smooth round brown cysts were counted as “round brown”, and process-bearing round brown cysts were counted as “spiny brown”. In addition, while routine light microscope observations do not allow to distinguish between the cyst produced by *Pentapharsodinium dalei* and *Pentapharsodinium imariense* (Li et al., 2020), numerous scanning electron microscope observations by AR of monadoid (vegetative) cells recovered from the Canadian (sub-)Arctic and Baffin Bay region have revealed the presence of only the former species in the region.

We present dinocyst relative abundances (%) and fluxes (cysts·cm-2·yr-1). The latter were calculated by multiplying the dinocyst concentrations (cysts·g-1) by the mass accumulation rates (g·cm-2·yr-1). Additionally, the ratio between presumed mixotrophic (M)

and heterotrophic (H) dinoflagellate cysts (M/H ratio), was calculated. The cyst of *Polarella glacialis*, found in sea ice (Montresor et al., 2003), was excluded from the M/H ratio calculation because of its unique ecological niche. This decision was made since the other mixotrophic taxa found in sediment are pelagic, inhabiting the open ocean waters. In addition to the new data from surface and core sediment sample analyses generated here, we used surface data from the modern dinocyst database presented in de Vernal et al. (2020). To capture the most recent and rapid environmental changes in the database, we restricted our selection to entries from sediment samples collected after 2010 (Fig. 9). Although numerous surface samples lack an associated age model, and this methodology does not preclude the inclusion of older samples, it effectively excludes samples that are unequivocally too old for the intended analysis.

1.5.4 Principal Component Analysis and Generalized Additive Models

To identify the dominant patterns of variability within the dinocyst assemblages, principal component analysis (PCA) was conducted. Prior to analysis, the dinocyst data were log-transformed to balance the influence of dominant and rare taxa. PCA was calculated using the program PAST4 (Version 4.09; Hammer et al., 2001).

Generalized Additive Models (GAMs) were also used to fit smooth trends to the downcore data (e.g., Wood, 2017; Simpson, 2018). The process used the mgcv package (version 1.8-41; Wood, 2017) in the R statistical programming environment (version 4.2.2; R Core Team, 2022), and R studio (version 2022.07.2; RStudio Team, 2022). GAMs are non-parametric statistical tools that utilize objective automatic smoothness selection methods to estimate non-linear data trends over time. To address heteroscedasticity in the data resulting from variations in sedimentation rates, observational weights were applied as recommended by Simpson (2018). The gratia package (version 0.7.3; Simpson, 2022) was used to compute the first derivative of the smooth terms from the fitted GAMs, along with their simultaneous confidence intervals. This approach enabled the identification of significant change in the datasets. A change is considered significant when the confidence interval of the first

derivative of the smooth fit does not include zero. The GAMs were applied to the total dinocyst fluxes (Fig.13).

1.6 RESULTS

1.6.1 Sedimentology and Age model

2.7BC and 2.5BC consist primarily of clay and silt, with dark organic material present throughout 2.7BC. The X-CT images show relatively undisturbed sediment structures in both cores, with only minor evidence of bioturbation (Fig. 7)

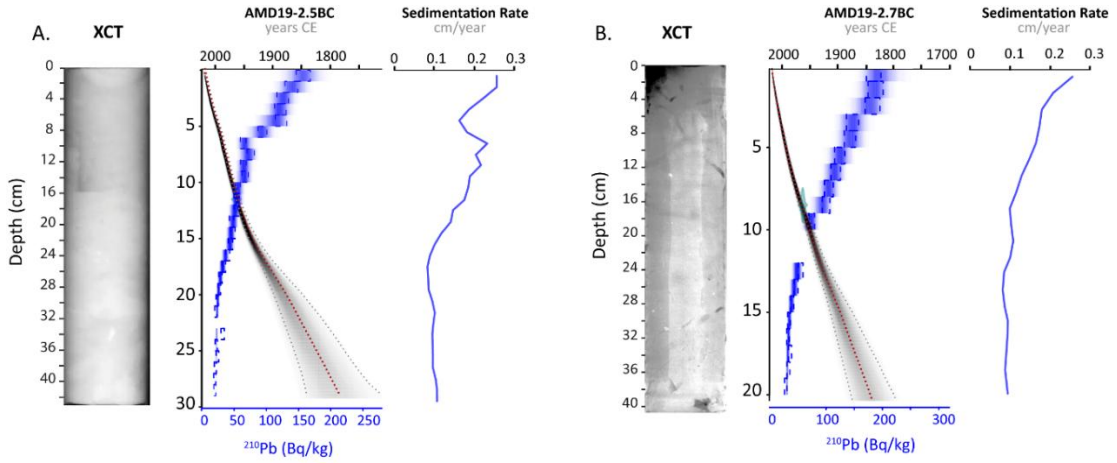

Figure 7. ^{210}Pb (blue) and ^{137}Cs (teal) measurements for 2.5BC (A) and 2.7BC (B). The red line represents the ages (cal year CE), the grey lines represent the upper and lower margins of 95% certainty, and the shaded black regions represent the margin of error. X-ray Computed Tomography (XCT) images of the cores are on the left of each age-model.

In both cores, the ^{210}Pb values show high activity in the surface sediment that exponentially decays to reach background ^{210}Pb values around 20 cm (Fig. 7). 2.5BC has two ^{137}Cs peaks at 0.5 and 11.5 cm, while 2.7BC has two ^{137}Cs peaks at 6.5 and 8.5 cm (Table 4). Considering the well-defined ^{210}Pb profiles and limited bioturbation in both cores (Fig. 7), combined with ages coherent with other cores in the region (Cormier et al., 2016), the ^{137}Cs peaks at 0.5 and 6.5 cm were not included in the age models and likely represent laboratory error (2.5BC) or an extended ^{137}Cs plateau (2.7BC). The ^{137}Cs peaks at 8.5 cm for 2.5BC and

11.5 cm for 2.7BC are attributed to the high point in atomic weapons testing in 1963 (Kansanen et al., 1991). Both cores show relatively high sedimentation rates, with values fluctuating between 0.1 and 0.3 cm of sediment per year (Fig. 7). As such, both cores cover the last ca. 360 years with a resolution of ~10 years per centimeter (Fig. 7).

1.6.2 Geochemical analyses

Carbon and nitrogen elemental and isotopic values remained relatively constant in both cores. In 2.5BC, $\delta^{13}C$ values ranged from -23.1 to -23.2‰, δ15N between 6.1 and 6.7‰, TOC between 2.2 and 3.0 wt%, and TN between 0.2 and 0.4% (Fig. 11). In 2.7BC, $\delta^{13}C$ values ranged between -22.7 and -23.5‰, $\delta^{15}N$ between 6.4 and 8.1‰, TOC between 1.4 and 3.5 wt%, and TN between 0.2 and 0.4% (Fig. 12).

To determine organic matter provenance, we used previously determined end-members to differentiate the marine vs. terrestrial signal of organic material (e.g., Meyers, 1997; Tremblay et al., 2006; Perdue & Koprivnjak, 2007; Kuzyk et al., 2010; Bailey et al., 2013; Fox & Walker, 2022). Both cores show relatively stable isotope values through time, with geochemical signals indicating organic matter of predominantly marine origin (Bailey et al., 2013), with a greater sympagic signature in a few samples (Figs. 11 & 12).

1.6.3 Dinoflagellate cyst assemblages

1.6.3.1 Modern distribution of dinocysts in the NOW and Baffin Bay

Along the NOW transect, total dinocyst concentrations ranged between ~5,700 and 44,000 cysts·g^{-1} (Fig. 10A). A total of twenty-nine taxa and groups of morpho-species were identified, with the dominant taxa being *Brigantedinium* spp. (including *B. simplex* and *B. cariacoense*), Round Brown cysts, *Islandinium minutum* subsp. *minutum*, *Echinidinium karaense*, cf. *Islandinium brevispinosum*, Round Brown process-bearing cysts (hereafter referred to as Spiny Brown cysts; Gurdebeke et al., 2019), cyst of *Pentapharsodinium dalei*, *Operculodinium centrocarpum* sensu Wall & Dale 1966 (hereafter referred to as *Operculodinium centrocarpum*), and the cyst of *Polarella glacialis* (Table 3, Fig. 8).

Table 3. The main >4% dinocyst taxa observed in this study, their trophic mode (mixotrophic (M) or heterotrophic (H)), and their groupings. The asterisk indicates taxa not included in the M/H ratio.

Dinoflagellate cyst taxa	Trophic mode	Grouped as
Brigantedinium simplex	H	
Brigantedinium cariacoense	H	*Brigantedinium* spp.
Brigantedinium spp.	H	
Round Brown	H	Round Brown
Islandinium minutum subsp. *minutum*	H	*Islandinium minutum* subsp. *minutum*
Echinidinium karaense	H	*Echinidinium karaense*
cf. *Islandinium brevispinosum*	H	cf. *Islandinium brevispinosum*
Round Brown process-bearing cysts (Gurdebeke et al. 2019)	H	Spiny Brown
Cyst of *Polarella glacialis*	M*	cyst of *Polarella glacialis*
Cyst of *Pentapharsodinium dalei*	M	cyst of *Pentapharsodinium dalei*
Operculodinium centrocarpum	M	
Operculodinium centrocarpum - short processes	M	*Operculodinium centrocarpum*
Operculodinium centrocarpum - cezare morphotype	M	
Operculodinium centrocarpum - Arctic morphotype	M	

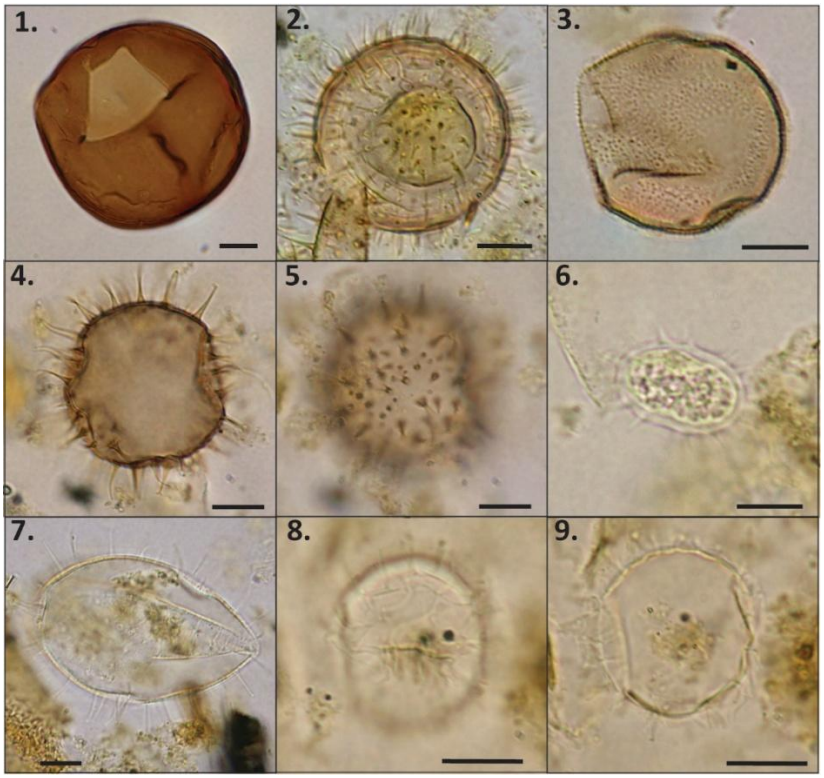

Figure 8. Selected microphotographs of the main dinocyst taxa observed in 2.5BC and 2.7BC. 1. *Brigantedinium simplex*. 2. *Islandinium minutum* subsp. *minutum*. 3. cf. *Islandinium brevispinosum.* 4-5. *Echinidinium karaense* (same specimen). 6. Cyst of *Polarella glacialis* 7. *Operculodinium centrocarpum* 8. High focus cyst of *Pentapharsodinium dalei*. 9. Mid focus cyst of *Pentapharsodinium dalei*. Scale bar represents 10 µm.

The lowest dinocyst concentrations were found in the western sector of the NOW (Fig. 10A). Assemblages are characterized by low M/H ratios, and comparatively higher proportions of cf. *Islandinium brevispinosum* and the cyst of *Polarella glacialis*. The central region of the NOW shows the maximum total dinocyst concentrations and is marked by the highest relative abundance of *Islandinium minutum* subsp. *minutum, Echinidinium karaense*, and *Brigantedinium* spp. Finally, the eastern region shows a high M/H ratio, and higher proportions of the mixotrophic species *Operculodinium centrocarpum* and the cyst of *Pentapharsodinium dalei* (Fig. 10B).

In Baffin Bay, total dinocyst concentrations follow a distinct pattern with the highest concentrations in the east and the lowest concentrations in the west (Fig. 9A-B). In terms of dinocyst assemblage composition, Baffin Bay can be broadly divided into two distinct regions. The western region exhibits the highest concentrations of "cold-water" heterotrophic taxa (*Islandinium minutum*, *Islandinium*? *cezare*, and *Echinidinium karaense*; Head et al., 2001) (Fig. 9C). Conversely, along the western Greenland margin, the highest abundances of the mixotrophic *Operculodinium centrocarpum* occur where the WGC is the shallowest (Rysgaard et al., 2020) (Fig. 9D).

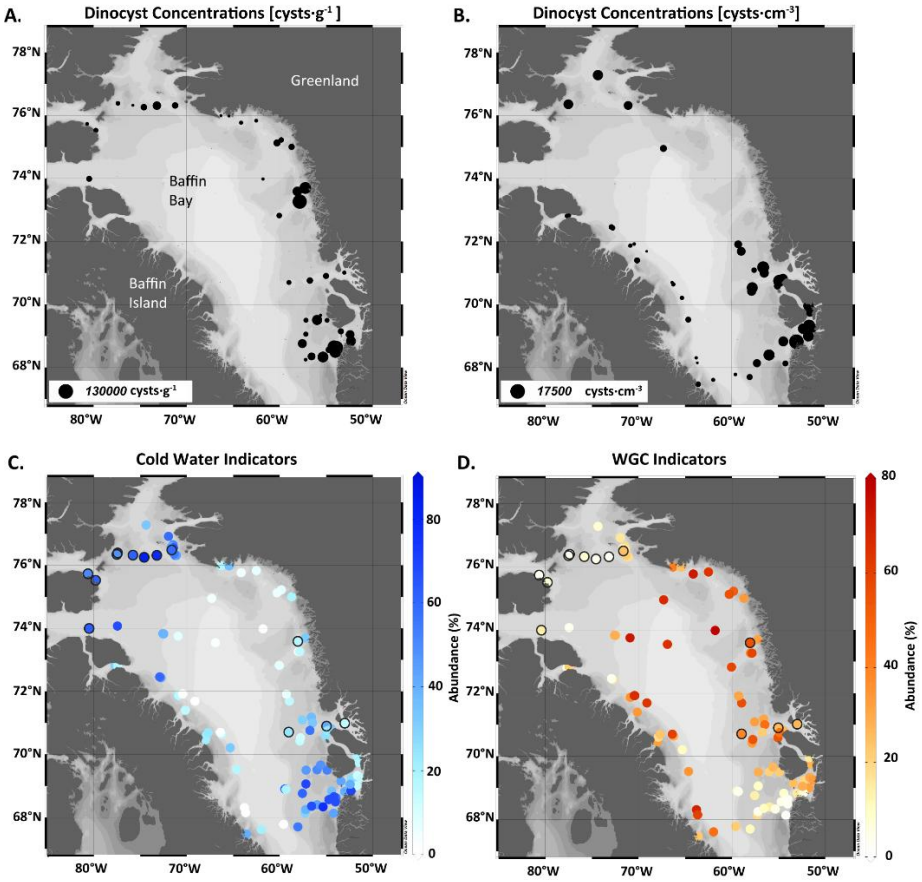

Figure 9. NOW and Baffin Bay surface sediment sample distribution from this study (black outlines) and de Vernal et al. (2020). A) Total dinocyst concentrations in cysts·g^{-1} B) Total dinocyst concentrations in cysts·cm^{-3} C) Relative abundances of cold-water indicators (*Islandinium minutum* subsp. *minutum*, *Echinidinium karaense*, and *Islandinium*? *cezare*; Head et al., 2001) D) Relative abundances of WGC indicator *Operculodinium centrocarpum.*

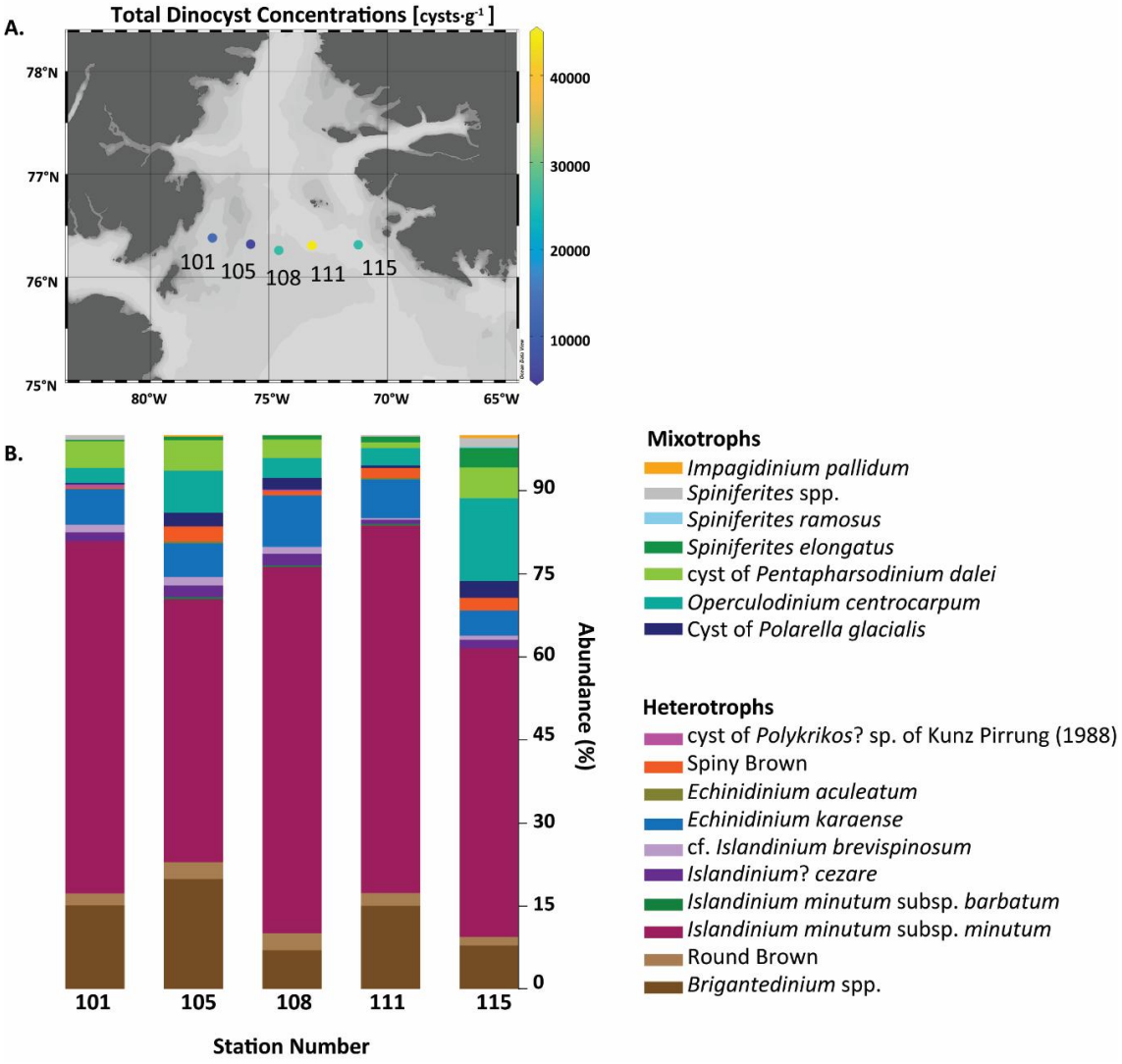

Figure 10. A) Locations of the transect of surface sediment samples in the NOW and total dinocyst concentrations (cysts·g^{-1}). F) Histogram of the relative abundances (%) of each taxon at each sampling location.

1.6.3.2 Box cores

Total dinocyst fluxes ranged between 900 and 1900 cysts·cm^{-2}·yr^{-1} and 700 and 2900 cysts·cm^{-2}·yr^{-1} for 2.5BC and 2.7BC, respectively. A total of thirty-six taxa and morpho-groups were observed in both cores (Table 5). The dominant (> 4% of assemblages) taxa were *Islandinium minutum* subsp. *minutum* (39 to 71%; 43 to 60.5%), *Brigantedinium* spp. (including *B. simplex* and *B. cariacoense*; 4.3 to 12.5%; 3.5 to 14.5%), Round Brown cysts

(3 to 9%; 2 to 11.8%), cf. *Islandinium brevispinosum* (0 to 2.3%; 2.5 to 11.5%), *Echinidinium karaense* (0.3 to 5%; 0.5 to 4.5%), Spiny Brown cysts (10 to 21%; 3.5 to 23%), cyst of *Polarella glacialis* (0 to 5%; 0 to 6.5%), *Operculodinium centrocarpum* (including short process, Arctic, and cezare morphotypes (de Vernal et al., 2001; 0 to 7.3%), and the cyst of *Pentapharsodinium dalei* (0 to 4.3%; 0 to 4.8%; Figs. 11 & 12). Both cores showed good preservation of dinocysts throughout, including taxa that are typically vulnerable to oxidative degradation, such as cysts from *Protoperidinium* and *Echinidinium* species (Zonneveld et al., 2008).

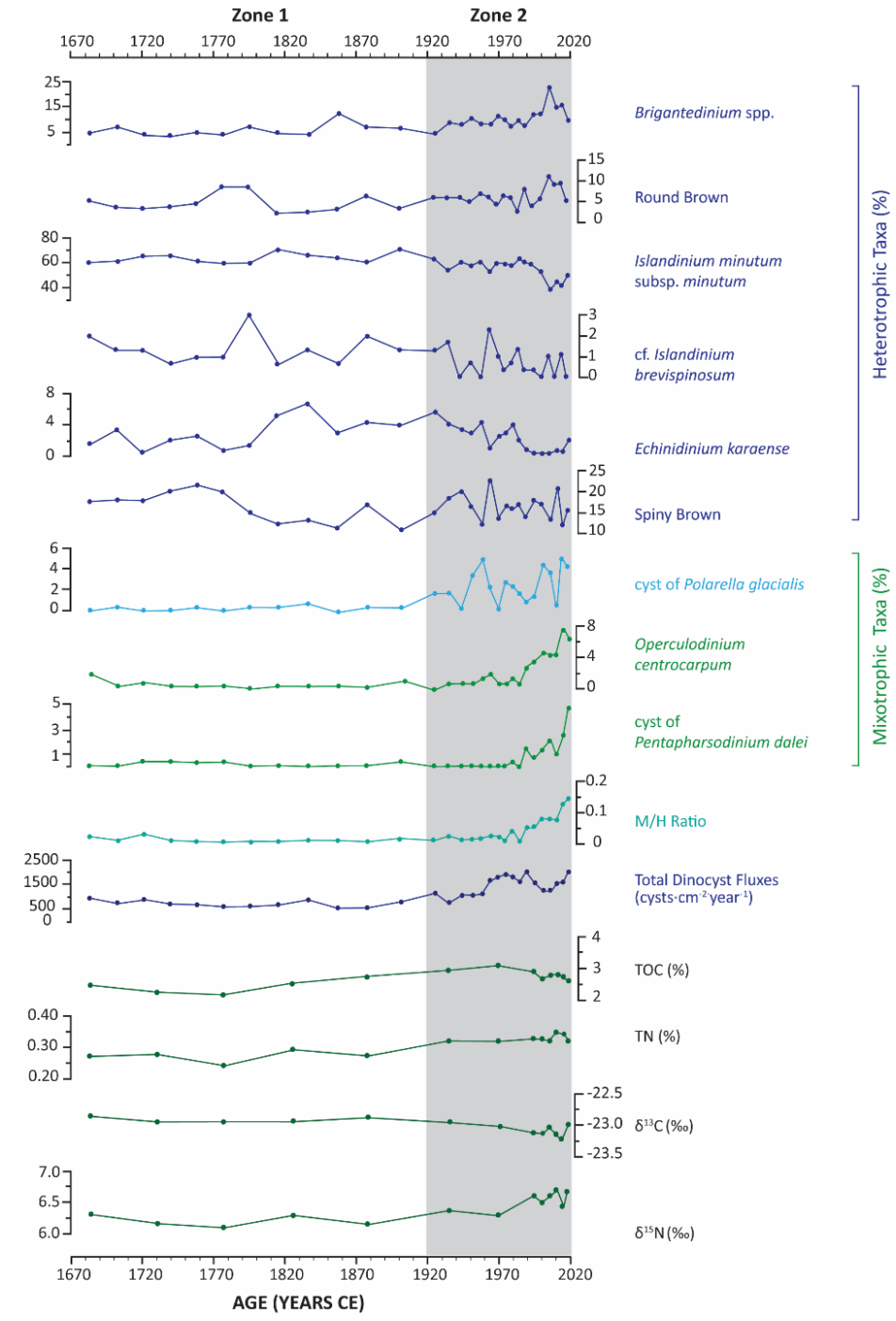

Figure 11. Relative abundances, M/H ratio, total dinocyst fluxes, and geochemical proxies (TOC, TN, $\delta^{13}C$, and $\delta^{15}N$) for 2.5BC. The grey box represents the start of significant change in dinocyst fluxes as identified by the first derivative of the GAM fit, and the start of changes from negative to positive PC1 values.

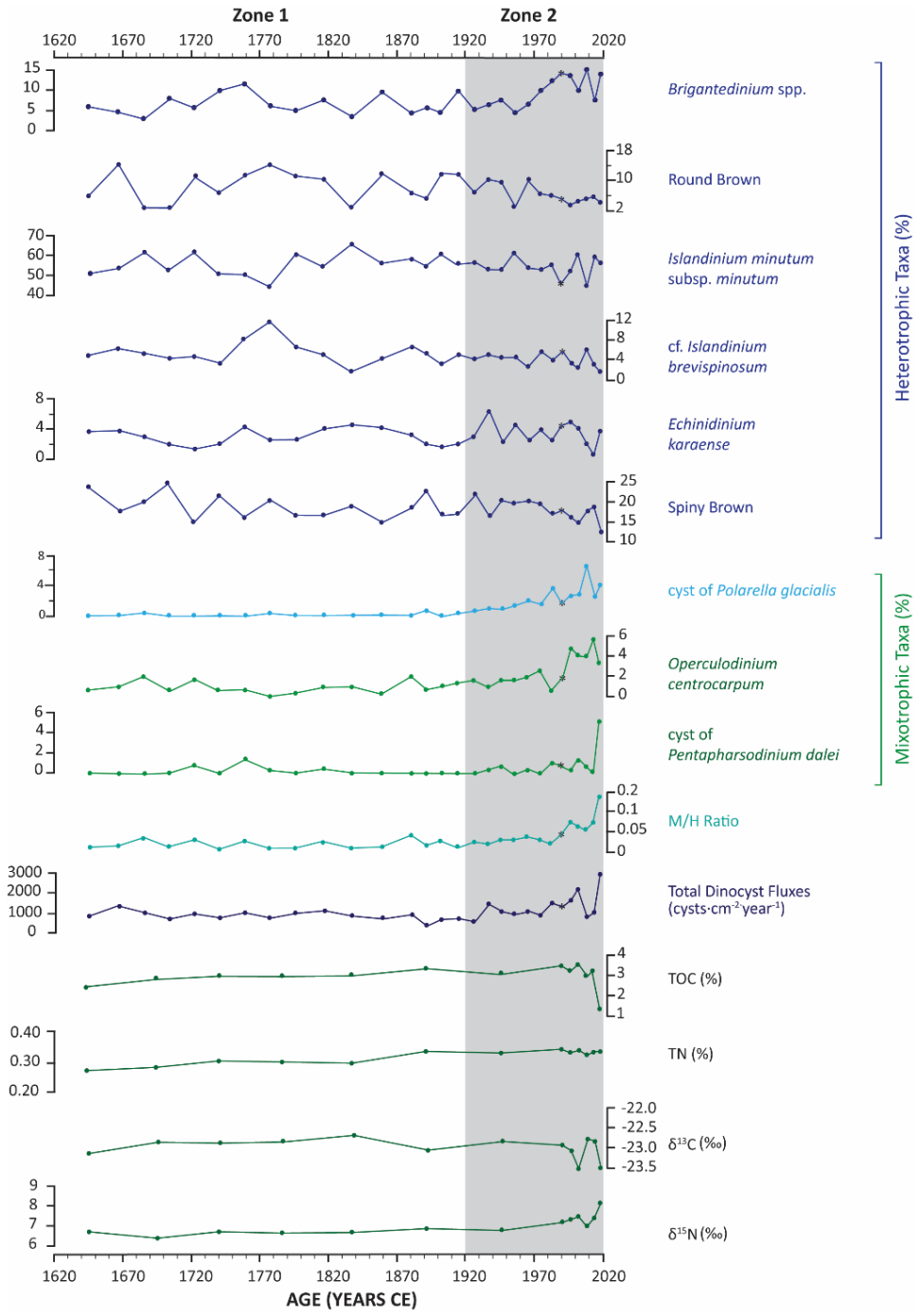

Figure 12. Relative abundances, M/H ratio, total dinocyst fluxes, and geochemical proxies (TOC, TN, $\delta^{13}C$, and $\delta^{15}N$) for 2.7BC. The dark grey box represents the start of changes from negative to positive PC1 values. An asterisk denotes the sample with fewer than 300 dinocysts counted.

Both cores are characterized by low contributions of mixotrophic taxa and a dominance of "cold water" indicators (Figs. 11 & 12). Dinocyst fluxes increase in 2.5BC and 2.7BC from less than 1000 cysts·cm^{-2}·yr^{-1} before 1900 CE to up to 2000 cysts·cm^{-2}·yr^{-1} around 1980 CE for 2.5BC and up to 3000 cysts·cm^{-2}·yr^{-1} around 2017 for 2.7BC (Figs. 11 & 12), accompanied by higher variability in the relative abundances of taxa. The composition of the dinocyst assemblages remained relatively constant until ca. 1940 CE, after which a transition from generally negative to positive PC1 values occurred for both cores (Figs. 11-13). This shift was driven by a notable increase in *Brigantedinium* spp. and mixotrophic taxa, particularly *Operculodinium centrocarpum* and the cyst of *Polarella glacialis*, coupled with a decrease in the relative abundance of process-bearing brown taxa (*Islandinium minutum* subsp. *minutum*, cf. *Islandinium brevispinosum*, Spiny Brown). We also note a rise in the cyst of *Pentapharsodinium dalei* from 1970 and 1920 CE for 2.5BC and 2.7BC, respectively (Figs. 11 & 12). Although percentages of mixotrophic taxa are low, *Operculodinium centrocarpum* accounted for 1-2% of the assemblages throughout 2.7BC and the overall mixotrophic contribution was higher than that of 2.5BC.

1.6.4 Principal Component Analysis and Generalized Additive Models

The first principal component (PC1) explains 39.5 and 30.6 % of the dinocyst assemblage variation in cores 2.5BC and 2.7BC, respectively. Both cores show a change from dominantly negative PC1 values to positive values around ca. 1940 CE (Fig. 13), suggesting a concomitant ecological transition at both sites. Mixotrophic taxa and *Brigantedinium* spp. exhibit positive scores on PC1. In contrast, species from the *Islandinium* and *Echinidinium* genera, as well as other spiny brown morphotypes, generally show negative correlations with the PC1 axis in both cores (Table 6). The GAMs applied to the total dinocyst fluxes identified the most significant changes in 2.5BC at ca. 1900, 1950, and 2010 CE, whereas the most significant change in 2.7BC occurred around 1920 CE (Fig. 13).

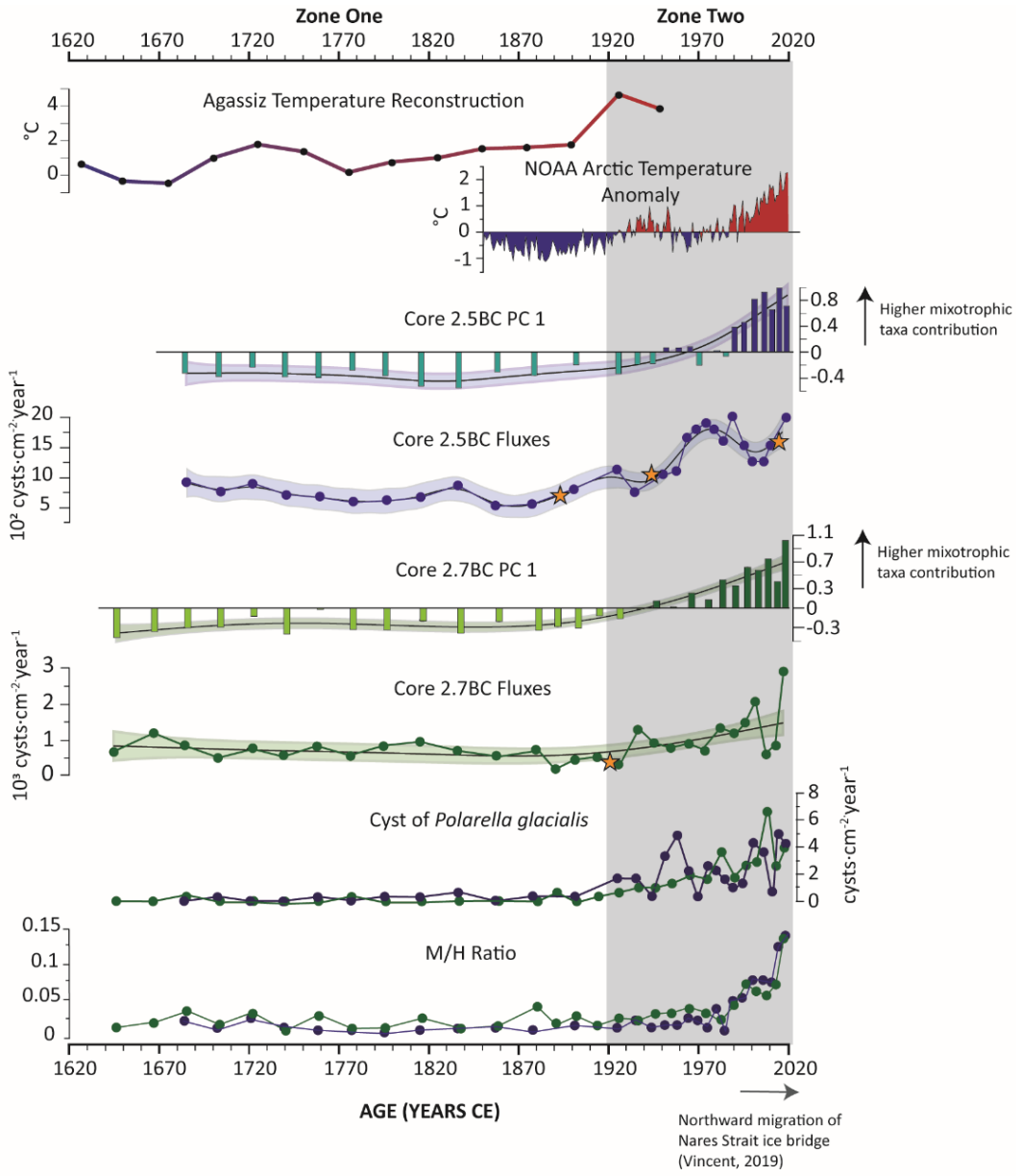

Figure 13. M/H ratio, cyst of *Polarella glacialis* fluxes, total dinocyst fluxes with associated GAM 95% confidence intervals, the PC1 axis for each core based on log-transformed assemblage data with the GAM 95% confidence intervals (2.5BC = dark blue, 2.7BC = dark green). Also shown are the Agassiz temperature reconstruction (Lecavalier et al., 2017) and the NOAA surface temperature anomaly for the Arctic. Stars represent significant changes as identified by the GAMs.

1.7 DISCUSSION

1.7.1 Distribution of dinocysts in modern Baffin Bay sediments

The significant variations in dinocyst concentrations and assemblage composition along the 300 km transect in the NOW are consistent with broader distribution patterns across Baffin Bay. Two key observations stand out: 1) the eastern sector exhibits higher percentages of mixotrophic species, particularly *Operculodinium centrocarpum* and *Spiniferites elongatus*, and 2) total dinocyst concentrations in the eastern region of the NOW are substantially higher than the west, reaching values up to three times those observed in the western sector.

The observed patterns align with the distinct hydrological conditions on each side of Baffin Bay (Fig. 9A-D). The eastern area, influenced by the Atlantic-derived WGC, typically exhibits warmer sea-surface waters and earlier ice-free conditions (Rysgaard et al., 2020). In Baffin Bay, WGC-like water signatures often correlate with a higher presence of *Operculodinium centrocarpum* (Rochon et al, 1999; Mudie and Rochon 2001; Zonneveld et al., 2013; de Vernal et al., 2020), a cosmopolitan species that seems to thrive in temperate and subpolar conditions with relatively high nutrient levels and light availability (Marret et al., 2020). Increased abundances of *Spiniferites elongatus* are also seen in cold water and seasonally sea-ice covered Arctic and subarctic environments (de Vernal et al., 2018; Pospelova et al., 2018). Additionally, Allan et al. (2019) noted higher abundances of *Operculodinium centrocarpum* and *Spiniferites elongatus* in areas with higher summer productivity.

In contrast, dinocyst assemblages from regions influenced by the cold freshwater Arctic outflow and in regions with extended seasonal sea-ice coverage consist almost exclusively of "cold water" heterotrophic taxa (>85%; *Islandinium minutum* subsp. *minutum, Echinidinium karaense, Islandinium*? *cezare;* Head et al., 2001; Fig 9C) with comparatively higher contributions of cysts of the sympagic species *Polarella glacialis*. Surface sediment data from the Northern Hemisphere also show that *Islandinium minutum* subsp. *minutum*, *Echinidinium karaense*, and *Islandinium*? *cezare* are most abundant in the polar regions

where sea ice typically persists for over 8 months annually (Rochon et al., 1999; de Vernal et al., 2013; 2020; Zonneveld et al., 2013). Overall, the prevalence of heterotrophic taxa in sedimentary assemblages within the western NOW aligns with the high diatom concentrations observed in this area (Lovejoy et al., 2002; Freyria et al., 2021), which thrive on the Si-rich waters flowing into northern Baffin Bay (Tang et al., 2004), and which represent important prey for dinoflagellates (Lovejoy et al., 2002; Sherr & Sherr, 2007). These data demonstrate that the dinocyst distribution patterns reflect the influence of hydrologically distinct ocean currents within the NOW and more broadly in Baffin Bay.

1.7.2 400-years of changes in sea-surface conditions in the western NOW

1.7.2.1 Relatively short open water season (~1670 to 1920 CE)

Between 1670 and 1920 CE, 2.5BC and 2.7BC show stable geochemical signals and stable but low total dinocyst fluxes. Assemblages in both cores are dominated (>60%) by *Islandinium minutum* subsp. *minutum*, *Echinidinium karaense* and cf. *Islandinium brevispinosum*. Sediment trap studies from Hudson Bay suggest that the typical cold-water indicators such as *Islandinium minutum* subsp. *minutum* dominate in open water during late summer-fall (Heikkilä et al, 2016), and that most so-called sea-ice indicator species are rather representative of summer-fall conditions (Luostarinen et al., 2023). The predominance of these taxa, coupled with the very low contribution of mixotrophic dinocysts, suggest an extended seasonal sea ice season. This indicates that ice likely remained present in the western NOW longer into the summer months, contrasting with current conditions where the NOW experiences sea-ice free summers.

In our records, relatively stable and cool conditions during the 17th to 19th centuries correspond with the late stages of the Little Ice Age (ca. 1300-1850 CE; Auger et al., 2019), a period of cooler temperatures that has been documented more regionally in the Canadian Arctic and Greenland (e.g., Briner et al., 2016). Other marine records in northern Baffin Bay have identified this period as a time of increased sea-ice presence inferred from high abundances of sea-ice diatoms (Knudsen et al., 2008) and cold-water indicator dinocysts

(Levac et al., 2001; Mudie et al., 2005; Cormier et al., 2016; Koerner et al., 2021). Furthermore, stable temperatures are suggested from an Agassiz ice cap record on Ellesmere Island (Lecavalier et al., 2017), with $\delta^{18}O$-based temperature anomalies hovering between approximately 0 to 2 °C between 1620 to 1900 CE (Fig. 13).

Additionally, Holocene glacial movement reconstructions suggest that neoglacial cooling facilitated glacier advance (Solomina et al., 2015). The Cape Norton Shaw glacier, located near the site where 2.5BC was retrieved (Fig. 6A), also exhibited signs of growth until approximately 1850 CE (Stevenard et al., 2021). Georgiadis et al. (2020) inferred a stable southern Nares Strait ice arch and reduced sea-ice export between roughly 750 to 1750 CE, based on high fluxes of the sea ice biomarker IP_{25}. Consequently, cool atmospheric conditions may have contributed conditions favourable for glacial advance and thus a more stable ice bridge and western ice edge. This situation may have resulted in a shorter open water season, especially at the polynya's western boundary.

1.7.2.2 Transition to longer open water season (~1920 to 2019 CE)

The timing of significant changes in both dinocyst composition and fluxes around the start of the 20th century, and increased instability in the sedimentary signal towards the second half of the 20th century, imply pervasive changes in environmental conditions from 1920 CE onward in the western NOW. We note that later sea-ice formation has also been documented from 1950 to 2021 CE in northern Baffin Bay, with an important breaking point in the timing of sea ice formation from 2001 considered as a characteristic signature of the Arctic Amplification (Ballinger et al., 2022).

The significant increase in the dinocyst fluxes by a factor of two in both cores around 1920 CE (Figs. 11 & 12) could be due to either increased production during single annual dinoflagellate blooms or the development of a second bloom in the fall, as observed by Ardyna et al. (2014) in the Arctic Ocean. In our record, this rise in total dinocyst fluxes is accompanied by an increase in the M/H ratio, with *Operculodinium centrocarpum* being the main contributor (~5-8%). This may point to a greater influence of Atlantic-sourced waters (i.e., WGC) and/or earlier open water conditions in the western NOW. Two other

mixotrophic taxa contributing to the assemblages are the cysts of *Pentapharsodinium dalei* and *Polarella glacialis*, both gradually increasing starting at ca. 1970 CE (Figs. 11 & 12). The cyst of *Pentapharsodinium dalei* has been associated with terrestrially-sourced, stratified, productive spring waters in Hudson Bay (Heikkilä et al., 2014). *Polarella glacialis* lives in sea-ice but cysts are released into the water column following break-up and melt, typically in the spring or early summer (Harðardóttir et al., 2024). The increase in both the abundances of the cyst of *Pentapharsodinium dalei* and the cyst of *Polarella glacialis* indicates more stratified springtime or early summer waters, likely linked to increasing atmospheric temperatures (Lecavalier et al., 2017) and glacial retreat (Sharp et al., 2014). An earlier melt-season and sea ice break up, accompanied by an extended open water season in the summer, may thus have allowed the increase of mixotrophic taxa from ca. 1920 CE onwards.

The geochemical proxies for both cores also show increased variability from ca. 1980 onwards, with TOC decreasing in 2.7BC and $\delta^{13}C$ values fluctuating but generally decreasing. This trend may suggest a change in sea-surface conditions toward more open-water production and a decline in sympagic taxa. In northern Baffin Bay, $\delta^{13}C$ values ranging from -20‰ to -23‰ indicate marine organic material (Fox & Walker, 2022), while higher $\delta^{13}C$ values up to -13‰ have been observed in sea-ice algae (Tremblay et al., 2006). Thus, the decreasing values of $\delta^{13}C$ could point to changes in sympagic primary production in the NOW as a result of the ice bridge failures.

The $\delta^{15}N$ values for both cores also show an increase from 6 to 8‰ between 2010 and 2020 CE, where Pacific water values are typically closer to 8‰ (Fox and Walker, 2022). Pacific water primarily enters the NOW through Nares Strait, having been modified as it flowed through the Arctic Ocean before being exported into Baffin Bay (Tang et al., 2004). The increase of $\delta^{15}N$ to values approaching 8‰ also points to an increased inflow of Pacific water from Nares Strait, suggesting increased inflow from the north. This is coherent with other sediment records in the central NOW, where typical $\delta^{15}N$ values range between 6-7‰

(Bailey et al., 2013) and more broadly in Baffin Bay, where similar $\delta^{15}N$ values of 8‰ are associated with increased Arctic outflow (Limoges et al., 2020).

1.7.3 Arctic Amplification and the NOW

In the northeastern part of Baffin Bay, the WGC upwells to the ocean surface before turning south alongside downwelling surface waters (Fig. 6A). This cyclonic circulation pattern helps promote the southward movement of water masses, including the Baffin Current (Melling et al., 2001). At our study sites, a gradual rise in the Atlantic-indicator species *Operculodinium centrocarpum* (Rochon et al., 1999) from 1920 CE onward and steeper increase after 2000 CE might suggest a change in WGC strength and/or enhanced heat transfer towards the western NOW. Ocean model simulations indicate that the rapid sea ice decline in northern Baffin Bay since 2001 CE is due to warming by Atlantic-origin water, facilitating tide-water glacial retreat and later sea-ice formation (Ballinger et al., 2018; 2022).

Our sediment records align with this interpretation, showing that changes in sea ice conditions and primary production in the western NOW region began as early as the first decades of the 20th century, with a signature seemingly reflecting increased WGC influence at both study sites. Given that the uncertainty on the ages of the sediments are approximately 17 years for 2.5BC and 2.7BC, the significant changes documented between ca. 1884-1940 CE (Fig. 13) occurred well before the start of the northward migration of the ice bridges in the 1990's (Vincent, 2019) and years of complete failure of the bridges in the 21st century.

Arctic air temperature data, including those from Ellesmere Island (Lecavalier et al., 2017; Fig. 13) and NOAA surface temperature data, indicate a transition from negative to positive temperature anomalies beginning around 1920 CE (NOAA, 2024; Fig. 13), followed by an increasingly rapid temperature rise into the 21st century. The mid-20th century marked the onset of extensive glacial retreat in the Canadian Arctic Archipelago (Sharp et al., 2014), with up to 94% of glaciers receding since the 1950s (Cook et al., 2019). Our marine records align well with these changes, indicating a regional transformation in northern Baffin Bay beginning in the mid-20th century.

While many studies have emphasized the reduction of multi-year ice as the primary factor in ice bridge migration and failures (Kwok et al., 2010; Vincent, 2019; Moore et al., 2021), thermodynamic modeling suggests that the northward movement of Atlantic-sourced waters also affects ice bridge formation (Kirillov et al., 2022). Notably, peak abundances of *Operculodinium centrocarpum* and cysts of *Pentapharsodinium dalei* from approximately 2000 to 2019 CE (Figs. 11 & 13) suggest further increased influence of the WGC in the western NOW, which could impact ice bridge formation. Given that GAMs have identified 2010 CE as a significant point of change in 2.5BC, the early 21st century likely represents the start of another transitional period.

Overall, our findings suggest that over the last 400 years, the western sector of the NOW polynya has been increasingly influenced by processes originating from the south, particularly the inflow of warm Atlantic-origin waters carried by the WGC. However, in the future, northern processes such as ice bridge failures and resulting increased Arctic sea-ice and freshwater export into northern Baffin Bay are expected to play a greater role in driving transformations in the NOW polynya due to climate change. Understanding the balance of southern and northern influences in the NOW is crucial for predicting how the polynya, a key ecological hotspot, will respond to future climate change.

1.8 CONCLUSIONS

Polynyas are often regarded as early indicators for climate change due to their reliance on sea ice and specific physical and oceanic parameters for maintaining open water conditions (Morales Maqueda, 2004). Our study shows that surface sediment and sediment archives from northwestern Baffin Bay can help us understand historical and modern changes in NOW dynamics. We first established baseline data on modern dinocyst assemblage composition from surface sediment samples across a longitudinal gradient in the NOW. Second, we investigated downcore changes in the assemblages from two sediment archives. The data suggest that the western NOW exhibited an early response to Arctic warming, preceding the observed Nares Strait ice bridge failures and associated increase in freshwater influx. Before the 20th century, the NOW experienced a period of relative stability of at least

300 years, as reflected by stable dinocyst fluxes and assemblage compositions, and TOC values. Around ca. 1940 CE, both 2.5BC and 2.7BC show a two-fold increase in total dinocyst fluxes, a marked increase in mixotrophic dinocyst contribution, and increased variability in TOC, TN, $\delta^{13}C$, and $\delta^{15}N$ values, indicating an early response to Arctic Amplification.

The NOW serves as a dynamic interface between contrasting physical and ecological systems and is influenced by the convergence of both the Arctic Water input from the north and the Atlantic Water inflow from the south. The balance of these influences shapes the polynya's oceanographic conditions, which in turn affect its ecological and biogeochemical processes. Our results highlight the early impacts of the Arctic Amplification on the NOW and the need for continued monitoring and integrative modeling efforts to capture the complex interplay of oceanic and cryospheric processes in this globally significant ecosystem.

1.9 ACKNOWLEDGEMENTS

We thank the two anonymous reviewers whose comments helped improve the quality of this paper. We thank Nicole Sanderson and Jean-François Hélie (UQAM) for meaningful discussions regarding the age-model and geochemistry, respectively. This study was funded by ArcticNet, a Network of Centres of Excellence in Canada (Arctic Seafloor Mapping Data Processing and Dissemination project). Financial support was received from the National Sciences and Engineering Research Council of Canada (NSERC) Discovery Grants to AR (RGPIN-2019-06564) and AL (2018-03984), and Bourse de doctorat pour la francophonie canadienne from the Fonds de recherche du Québec, ISMER bourse d'excellence, and the American Association of Palynologists Grant to KK. We thank Crown-Indigenous Relations and Northern Affairs Canada (CIRNAC). We thank Amundsen Science, which is supported by the Canada Foundation for Innovation and NSERC. Finally, we thank the officers, crew members, scientific personnel, and the chief scientists Alexandre Forest (Amundsen Science) and Jean-Carlos Montero-Serrano (UQAR) of the ArcticNet leg 2a/b expedition onboard the CCGS Amundsen for the collection of the material and data used in this project.

1.10 REFERENCES

Allan, E., de Vernal, A., Krawczyk, D., Moros, M., Radi, T., Rochon, A., Seidenkrantz, M.-S., & Zaragosi, S. (2019). Distribution of dinocyst assemblages in surface sediment samples from the West Greenland margin. *Marine Micropaleontology*, 101818. https://doi.org/10.1016/j.marmicro.2019.101818

Amundsen Science Data Collection. (2019). CTD data collected by the CCGS Amundsen in the Canadian Arctic. ArcticNet Inc., Québec, Canada. Processed data. Canadian Cryospheric Information Network. https://doi.org/10.5884/12713

Aquino-López, M. A., Blaauw, M., Christen, J. A., & Sanderson, N. K. (2018). Bayesian Analysis of ^{210}Pb Dating. *Journal of Agricultural, Biological and Environmental Statistics*, *23*(3), Article 3. https://doi.org/10.1007/s13253-018-0328-7

Ardyna, M., Babin, M., Gosselin, M., Devred, E., Rainville, L., & Tremblay, J.-É. (2014). Recent Arctic Ocean sea ice loss triggers novel fall phytoplankton blooms. *Geophysical Research Letters*, *41*(17). https://doi.org/10.1002/2014GL061047

Auger, J. D., Mayewski, P. A., Maasch, K. A., Schuenemann, K. C., Carleton, A. M., Birkel, S. D., & Saros, J. E. (2019). 2000 years of North Atlantic-Arctic climate. *Quaternary Science Reviews*, *216*, 1–17. https://doi.org/10.1016/j.quascirev.2019.05.020

Bâcle, J., Carmack, E. C., & Ingram, R. G. (2002). Water column structure and circulation under the North Water during spring transition: April–July 1998. *Deep Sea Research Part II: Topical Studies in Oceanography*, *49*(22), Article 22. https://doi.org/10.1016/S0967-0645(02)00170-4

Bailey, J. N.-L., Macdonald, R. W., Sanei, H., Outridge, P. M., Johannessen, S. C., Hochheim, K., Barber, D., & Stern, G. A. (2013). Change at the margin of the North Water Polynya, Baffin Bay, inferred from organic matter records in dated sediment cores. *Marine Geology*, *341*, 1–13. https://doi.org/10.1016/j.margeo.2013.04.017

Ballinger, T. J., Hanna, E., Hall, R. J., Miller, J., Ribergaard, M. H., & Høyer, J. L. (2018). Greenland coastal air temperatures linked to Baffin Bay and Greenland Sea ice conditions during autumn through regional blocking patterns. *Climate Dynamics*, *50*(1), 83–100. https://doi.org/10.1007/s00382-017-3583-3

Ballinger, T. J., Moore, G. W. K., Garcia-Quintana, Y., Myers, P. G., Imrit, A. A., Topál, D., & Meier, W. N. (2022). Abrupt Northern Baffin Bay Autumn Warming and Sea-Ice Loss Since the Turn of the Twenty-First Century. *Geophysical Research Letters*, *49*(21), Article 21. https://doi.org/10.1029/2022GL101472

Barber, D. G., & Massom, R. A. (2007). Chapter 1 The Role of Sea Ice in Arctic and Antarctic Polynyas. In W. O. Smith & D. G. Barber (Eds.), *Elsevier Oceanography Series* (Vol. 74, pp. 1–54). Elsevier. https://doi.org/10.1016/S0422-9894(06)74001-6

Bhatia, M. P., Kujawinski, E. B., Das, S. B., Breier, C. F., Henderson, P. B., & Charette, M. A. (2013). Greenland meltwater as a significant and potentially bioavailable source of iron to the ocean. *Nature Geoscience*, *6*(4), Article 4. https://doi.org/10.1038/ngeo1746

Briner, J. P., McKay, N. P., Axford, Y., Bennike, O., Bradley, R. S., de Vernal, A., Fisher, D., Francus, P., Fréchette, B., Gajewski, K., Jennings, A., Kaufman, D. S., Miller, G., Rouston, C., & Wagner, B. (2016). Holocene climate change in Arctic Canada and Greenland. *Quaternary Science Reviews*, *147*, 340–364. https://doi.org/10.1016/j.quascirev.2016.02.010

Bryndum-Buchholz, A., Herbig, J. L., Darnis, G., Geoffroy, M., & Eddy, T. D. (2024). Ecosystem structure and function of the North Water Polynya. *Arctic Science*, *10*(3), Article 3. https://doi.org/10.1139/as-2023-0050

Cook, A. J., Copland, L., Noël, B. P. Y., Stokes, C. R., Bentley, M. J., Sharp, M. J., Bingham, R. G., & Broeke, M. R. van den. (2019). Atmospheric forcing of rapid marine-terminating glacier retreat in the Canadian Arctic Archipelago. *Science Advances*, *5*(3), Article 3. https://doi.org/10.1126/sciadv.aau8507

Cormier, M.-A., Rochon, A., de Vernal, A., & Gélinas, Y. (2016). Multi-proxy study of primary production and paleoceanographical conditions in northern Baffin Bay during the last centuries. *Marine Micropaleontology*, *127*, 1–10. https://doi.org/10.1016/j.marmicro.2016.07.001

de Vernal, A., Hillaire-Marcel, C., Rochon, A., Fréchette, B., Henry, M., Solignac, S., & Bonnet, S. (2013). Dinocyst-based reconstructions of sea ice cover concentration during the Holocene in the Arctic Ocean, the northern North Atlantic Ocean and its adjacent seas. *Quaternary Science Reviews*, *79*, 111–121. https://doi.org/10.1016/j.quascirev.2013.07.006

de Vernal, A., Radi, T., Zaragosi, S., Van Nieuwenhove, N., Rochon, A., Allan, E., De Schepper, S., Eynaud, F., Head, M. J., Limoges, A., Londeix, L., Marret, F., Matthiessen, J., Penaud, A., Pospelova, V., Price, A., & Richerol, T. (2020). Distribution of common modern dinoflagellate cyst taxa in surface sediments of the Northern Hemisphere in relation to environmental parameters: The new n=1968 database. *Marine Micropaleontology*, *159*, 101796. https://doi.org/10.1016/j.marmicro.2019.101796

Eegeesiak, O., Aariak, E., & V. Kleist, K. (2017). *People of the Ice Bridge: The future of the Pikialasorsuaq* (Report of the Pikialasorsuaq Commission, p. 119). Inuit Circumpolar Council Canada.

Fox, A., & Walker, B. D. (2022). Sources and Cycling of Particulate Organic Matter in Baffin Bay: A Multi-Isotope δ13C, δ15N, and Δ14C Approach. *Frontiers in Marine Science*, *9*. https://doi.org/10.3389/fmars.2022.846025

Freyria, N. J., Joli, N., & Lovejoy, C. (2021). A decadal perspective on north water microbial eukaryotes as Arctic Ocean sentinels. *Scientific Reports*, *11*(1), Article 1. https://doi.org/10.1038/s41598-021-87906-4

Georgiadis, E., Giraudeau, J., Jennings, A., Limoges, A., Jackson, R., Ribeiro, S., & Massé, G. (2020). Local and regional controls on Holocene sea ice dynamics and oceanography in Nares Strait, Northwest Greenland. *Marine Geology*, *422*, 106115. https://doi.org/10.1016/j.margeo.2020.106115

Gurdebeke, P. R., Mertens, K. N., Pospelova, V., Nieuwenhove, N. V., & Louwye, S. (2019). Islandinium pacificum sp. Nov., a new dinoflagellate cyst from the upper Quaternary of the northeast Pacific. *Palynology*, *0*(0), Article 0. https://doi.org/10.1080/01916122.2018.1549118

Haine, T. W. N., Curry, B., Gerdes, R., Hansen, E., Karcher, M., Lee, C., Rudels, B., Spreen, G., de Steur, L., Stewart, K. D., & Woodgate, R. (2015). Arctic freshwater export: Status, mechanisms, and prospects. *Global and Planetary Change*, *125*, 13–35. https://doi.org/10.1016/j.gloplacha.2014.11.013

Hammer, Ø., Harper, D. A. T., & Ryan, P. D. (n.d.). *PAST: Paleontological Statistics Software Package for Education and Data Analysis. 9.*

Harðardóttir, S., Haile, J. S., Ray, J. L., Limoges, A., Van Nieuwenhove, N., Lalande, C., Grondin, P.-L., Jackson, R., Skaar, K. S., Heikkilä, M., Berge, J., Lundholm, N., Massé, G., Rysgaard, S., Seidenkrantz, M.-S., De Schepper, S., Lorenzen, E. D., Lovejoy, C., & Ribeiro, S. (2024). Millennial-scale variations in Arctic sea ice are recorded in sedimentary ancient DNA of the microalga Polarella glacialis. *Communications Earth & Environment*, *5*(1), Article 1. https://doi.org/10.1038/s43247-023-01179-5

Hastrup, K., Mosbech, A., & Grønnow, B. (2018). Introducing the North Water: Histories of exploration, ice dynamics, living resources, and human settlement in the Thule Region. *Ambio*, *47*(2), Article 2. https://doi.org/10.1007/s13280-018-1030-2

Head, M. J., Harland, R., & Matthiessen, J. (2001). Cold marine indicators of the late Quaternary: The new dinoflagellate cyst genus Islandinium and related morphotypes. *Journal of Quaternary Science*, *16*(7), Article 7. https://doi.org/mar

Heide-Jørgensen, M. P., Burt, L. M., Hansen, R. G., Nielsen, N. H., Rasmussen, M., Fossette, S., & Stern, H. (2013). The Significance of the North Water Polynya to Arctic Top Predators. *AMBIO*, *42*(5), Article 5. https://doi.org/10.1007/s13280-012-0357-3

Heide-Jørgensen, M. P., Sinding, M.-H. S., Nielsen, N. H., Rosing-Asvid, A., & Hansen, R. G. (2016). Large numbers of marine mammals winter in the North Water polynya. *Polar Biology*, *39*(9), Article 9. https://doi.org/10.1007/s00300-015-1885-7

Heikkilä, M., Pospelova, V., Forest, A., Stern, G. A., Fortier, L., & Macdonald, R. W. (2016). Dinoflagellate cyst production over an annual cycle in seasonally ice-covered Hudson Bay. *Marine Micropaleontology*, *125*, 1–24. https://doi.org/10.1016/j.marmicro.2016.02.005

Heikkilä, M., Pospelova, V., Hochheim, K. P., Kuzyk, Z. Z. A., Stern, G. A., Barber, D. G., & Macdonald, R. W. (2014). Surface sediment dinoflagellate cysts from the Hudson Bay system and their relation to freshwater and nutrient cycling. *Marine Micropaleontology*, *106*, 79–109. https://doi.org/10.1016/j.marmicro.2013.12.002

Hélie, J.-F. (2009). Elemental and stable isotopic approaches for studying the organic and inorganic carbon components in natural samples. *IOP Conference Series: Earth and Environmental Science*, *5*(1), 012005. https://doi.org/10.1088/1755-1307/5/1/012005

Jackson, R., Kvorning, A. B., Limoges, A., Georgiadis, E., Olsen, S. M., Tallberg, P., Andersen, T. J., Mikkelsen, N., Giraudeau, J., Massé, G., Wacker, L., & Ribeiro, S. (2021). Holocene polynya dynamics and their interaction with oceanic heat transport in northernmost Baffin Bay. *Scientific Reports*, *11*(1), 10095. https://doi.org/10.1038/s41598-021-88517-9

Jahn, A., & Laiho, R. (2020). Forced Changes in the Arctic Freshwater Budget Emerge in the Early 21st Century. *Geophysical Research Letters*, *47*(15), Article 15. https://doi.org/10.1029/2020GL088854

Jeong, H. J., Yoo, Y. D., Kim, J. S., Seong, K. A., Kang, N. S., & Kim, T. H. (2010). Growth, feeding and ecological roles of the mixotrophic and heterotrophic dinoflagellates in marine planktonic food webs. *Ocean Science Journal*, *45*(2), Article 2. https://doi.org/10.1007/s12601-010-0007-2

Jeppesen, E., Appelt, M., Hastrup, K., Grønnow, B., Mosbech, A., Smol, J. P., & Davidson, T. A. (2018). Living in an oasis: Rapid transformations, resilience, and resistance in the North Water Area societies and ecosystems. *Ambio*, *47*(2), Article 2. https://doi.org/10.1007/s13280-018-1034-y

Joli, N., Gosselin, M., Ardyna, M., Babin, M., Onda, D. F., Tremblay, J.-É., & Lovejoy, C. (2018). Need for focus on microbial species following ice melt and changing freshwater regimes in a Janus Arctic Gateway. *Scientific Reports*, *8*(1), Article 1. https://doi.org/10.1038/s41598-018-27705-6

Jones, E. P. (2001). Circulation in the Arctic Ocean. *Polar Research*, *20*(2), Article 2. https://doi.org/10.1111/j.1751-8369.2001.tb00049.x

Kansanen, P. H., Jaakkola, T., Kulmala, S., & Suutarinen, R. (1991). Sedimentation and distribution of gamma-emitting radionuclides in bottom sediments of southern Lake Päijänne, Finland, after the Chernobyl accident. *Hydrobiologia*, *222*(2), Article 2. https://doi.org/10.1007/BF00006100

Kirillov, S., Dmitrenko, I., Babb, D. G., Ehn, J. K., Koldunov, N., Rysgaard, S., Jensen, D., & Barber, D. G. (2022). The role of oceanic heat flux in reducing thermodynamic ice growth in Nares Strait and promoting earlier collapse of the ice bridge. *Ocean Science*, *18*(5), Article 5. https://doi.org/10.5194/os-18-1535-2022

Knudsen, K. L., Stabell, B., Seidenkrantz, M.-S., Eiríksson, J., & Blake, W. (2008). Deglacial and Holocene conditions in northernmost Baffin Bay: Sediments, foraminifera, diatoms and stable isotopes. *Boreas*, *37*(3), Article 3. https://doi.org/10.1111/j.1502-3885.2008.00035.x

Koerner, K., Limoges, A., Van Nieuwenhove, N., Richerol, T., Massé, G., & Ribeiro, S. (2021). Late Holocene sea-surface changes in the North Water polynya reveal freshening of northern Baffin Bay in the 21st century. *Global and Planetary Change*, 103642. https://doi.org/10.1016/j.gloplacha.2021.103642

Kunz-Pirrung, M. (1998). Rekonstruktion der Oberflächenwassermassen der östlichen Laptevsee im Holozän anhand von aquatischen Palynomorphen. Ber. Polarforsch. 281, 1–117.

Kuzyk, Z. Z. A., Macdonald, R. W., Tremblay, J.-É., & Stern, G. A. (2010). Elemental and stable isotopic constraints on river influence and patterns of nitrogen cycling and biological productivity in Hudson Bay. *Continental Shelf Research*, *30*(2), Article 2. https://doi.org/10.1016/j.csr.2009.10.014

Kwok, R., Pedersen, L. T., Gudmandsen, P., & Pang, S. S. (2010). Large sea ice outflow into the Nares Strait in 2007. *Geophysical Research Letters*, *37*(3), Article 3. https://doi.org/10.1029/2009GL041872

Lecavalier, B. S., Fisher, D. A., Milne, G. A., Vinther, B. M., Tarasov, L., Huybrechts, P., Lacelle, D., Main, B., Zheng, J., Bourgeois, J., & Dyke, A. S. (2017). High Arctic Holocene temperature record from the Agassiz ice cap and Greenland ice sheet

evolution. *Proceedings of the National Academy of Sciences*, *114*(23), Article 23. https://doi.org/10.1073/pnas.1616287114

Levac, E., Vernal, A. D., & Jr, W. B. (2001). Sea-surface conditions in northernmost Baffin Bay during the Holocene: Palynological evidence. *Journal of Quaternary Science*, *16*(4), Article 4. https://doi.org/10.1002/jqs.614

Li, Z., Mertens, K. N., Gottschling, M., Gu, H., Söhner, S., Price, A. M., Marret, F., Pospelova, V., Smith, K. F., Carbonell-Moore, C., Nézan, E., Bilien, G., & Shin, H. H. (2020). Taxonomy and Molecular Phylogenetics of Ensiculiferaceae, fam. Nov. (Peridiniales, Dinophyceae), with Consideration of their Life-history. *Protist*, *171*(5), 125759. https://doi.org/10.1016/j.protis.2020.125759

Limoges, A., Ribeiro, S., Van Nieuwenhove, N., Jackson, R., Juggins, S., Crosta, X., & Weckström, K. (2023). Marine diatoms record Late Holocene regime shifts in the Pikialasorsuaq ecosystem. *Global Change Biology*, *29*(23), Article 23. https://doi.org/10.1111/gcb.16958

Limoges, A., Van Nieuwenhove, N., Head, M. J., Mertens, K. N., Pospelova, V., & Rochon, A. (2019). A review of rare and less well known extant marine organic-walled dinoflagellate cyst taxa of the orders Gonyaulacales and Suessiales from the Northern Hemisphere. *Marine Micropaleontology*, 101801. https://doi.org/10.1016/j.marmicro.2019.101801

Limoges, A., Weckström, K., Ribeiro, S., Georgiadis, E., Hansen, K. E., Martinez, P., Seidenkrantz, M.-S., Giraudeau, J., Crosta, X., & Massé, G. (2020). Learning from the past: Impact of the Arctic Oscillation on sea ice and marine productivity off northwest Greenland over the last 9,000 years. *Global Change Biology*, *26*(12), Article 12. https://doi.org/10.1111/gcb.15334

Lovejoy, C., Legendre, L., & Price, N. M. (2002). Prolonged diatom blooms and microbial food web dynamics: Experimental results from an Arctic polynya. *Aquatic Microbial Ecology*, *29*(3), Article 3. https://doi.org/10.3354/ame029267

Luostarinen, T., Weckström, K., Ehn, J., Kamula, M., Burson, A., Diaz, A., Massé, G., McGowan, S., Kuzyk, Z. Z., & Heikkilä, M. (2023). Seasonal and habitat-based variations in vertical export of biogenic sea-ice proxies in Hudson Bay. *Communications Earth & Environment*, *4*(1), 1–13. https://doi.org/10.1038/s43247-023-00719-3

Marchese, C., Albouy, C., Tremblay, J.-É., Dumont, D., D'Ortenzio, F., Vissault, S., & Bélanger, S. (2017). Changes in phytoplankton bloom phenology over the North Water (NOW) polynya: A response to changing environmental conditions. *Polar Biology*, *40*(9), Article 9. https://doi.org/10.1007/s00300-017-2095-2

Marret, F., Bradley, L., de Vernal, A., Hardy, W., Kim, S.-Y., Mudie, P., Penaud, A., Pospelova, V., Price, A. M., Radi, T., & Rochon, A. (2020). From bi-polar to regional distribution of modern dinoflagellate cysts, an overview of their biogeography. *Marine Micropaleontology*, *159*, 101753. https://doi.org/10.1016/j.marmicro.2019.101753

Melling, H., Gratton, Y., & Ingram, G. (2001). Ocean circulation within the North Water polynya of Baffin Bay. *Atmosphere-Ocean*, *39*(3), Article 3. https://doi.org/10.1080/07055900.2001.9649683

Meyers, P. A. (1997). Organic geochemical proxies of paleoceanographic, paleolimnologic, and paleoclimatic processes. *Organic Geochemistry*, *27*(5), Article 5. https://doi.org/10.1016/S0146-6380(97)00049-1

Michel, C., Hamilton, J., Hansen, E., Barber, D., Reigstad, M., Iacozza, J., Seuthe, L., & Niemi, A. (2015). Arctic Ocean outflow shelves in the changing Arctic: A review and perspectives. *Progress in Oceanography*, *139*, 66–88. https://doi.org/10.1016/j.pocean.2015.08.007

Mitra, A., Flynn, K. J., Tillmann, U., Raven, J. A., Caron, D., Stoecker, D. K., Not, F., Hansen, P. J., Hallegraeff, G., Sanders, R., Wilken, S., McManus, G., Johnson, M., Pitta, P., Våge, S., Berge, T., Calbet, A., Thingstad, F., Jeong, H. J., … Lundgren, V. (2016). Defining Planktonic Protist Functional Groups on Mechanisms for Energy and Nutrient Acquisition: Incorporation of Diverse Mixotrophic Strategies. *Protist*, *167*(2), 106–120. https://doi.org/10.1016/j.protis.2016.01.003

Montresor, M., Lovejoy, C., Orsini, L., Procaccini, G., & Roy, S. (2003). Bipolar distribution of the cyst-forming dinoflagellate *Polarella glacialis*. *Polar Biology*, *26*(3), Article 3. https://doi.org/10.1007/s00300-002-0473-9

Moore, G. W. K., Howell, S. E. L., Brady, M., Xu, X., & McNeil, K. (2021). Anomalous collapses of Nares Strait ice arches leads to enhanced export of Arctic sea ice. *Nature Communications*, *12*(1), Article 1. https://doi.org/10.1038/s41467-020-20314-w

Morales Maqueda, M. A. (2004). Polynya Dynamics: A Review of Observations and Modeling. *Reviews of Geophysics*, *42*(1), Article 1. https://doi.org/10.1029/2002RG000116

Mudie, P. J., & Rochon, A. (2001). Distribution of dinoflagellate cysts in the Canadian Arctic marine region. *Journal of Quaternary Science*, *16*(7), Article 7. https://doi.org/10.1002/jqs.658

Mudie, P. J., Rochon, A., & Levac, E. (2005). Decadal-scale sea ice changes in the Canadian Arctic and their impacts on humans during the past 4,000 years. *Environmental Archaeology*, *10*(2), Article 2. https://doi.org/10.1179/env.2005.10.2.113

Münchow, A., Falkner, K. K., & Melling, H. (2007). Spatial continuity of measured seawater and tracer fluxes through Nares Strait, a dynamically wide channel bordering the Canadian Archipelago. *Journal of Marine Research*, *65*(6), Article 6. https://doi.org/10.1357/002224007784219048

NOAA National Centers for Environmental information. (2024). Climate at a Glance: National Time Series. https://www.ncei.noaa.gov/access/monitoring/climate-at-a-glance/national/time-series

Parkinson, C. L., & DiGirolamo, N. E. (2021). Sea ice extents continue to set new records: Arctic, Antarctic, and global results. *Remote Sensing of Environment*, *267*, 112753. https://doi.org/10.1016/j.rse.2021.112753

Perdue, E. M., & Koprivnjak, J.-F. (2007). Using the C/N ratio to estimate terrigenous inputs of organic matter to aquatic environments. *Estuarine, Coastal and Shelf Science*, *73*(1). https://doi.org/10.1016/j.ecss.2006.12.021

Pospelova, V., Zonneveld, K. A. F., Heikkilä, M., Bringué, M., Price, A. M., Esenkulova, S., & Matsuoka, K. (2018). Seasonal, annual, and inter-annual Spiniferites cyst production: A review of sediment trap studies. *Palynology*, *42*(sup1). https://doi.org/10.1080/01916122.2018.1465738

Potvin, É., Kim, S.-Y., Yang, E. J., Head, M. J., Kim, H., Nam, S.-I., Yim, J. H., & Kang, S.-H. (2018). Islandinium minutum subsp. barbatum subsp. nov. (Dinoflagellata), a New Organic-Walled Dinoflagellate Cyst from the Western Arctic: Morphology, Phylogenetic Position Based on SSU rDNA and LSU rDNA, and Distribution. *Journal of Eukaryotic Microbiology*, *65*(6). https://doi.org/10.1111/jeu.12518

R Core Team. (2022). R: A language and environment for statistical computing. R Foundation for Statistical Computing. https://www.R-project.org

Radi, T., Bonnet, S., Cormier, M.-A., de Vernal, A., Durantou, L., Faubert, É., Head, M. J., Henry, M., Pospelova, V., Rochon, A., & Van Nieuwenhove, N. (2013). Operational taxonomy and (paleo-)autecology of round, brown, spiny dinoflagellate cysts from the Quaternary of high northern latitudes. *Marine Micropaleontology*, *98*, 41–57. https://doi.org/10.1016/j.marmicro.2012.11.001

Ribeiro, S., Limoges, A., Massé, G., Johansen, K. L., Colgan, W., Weckström, K., Jackson, R., Georgiadis, E., Mikkelsen, N., Kuijpers, A., Olsen, J., Olsen, S. M., Nissen, M., Andersen, T. J., Strunk, A., Wetterich, S., Syväranta, J., Henderson, A. C. G., Mackay,

H., … Davidson, T. A. (2021). Vulnerability of the North Water ecosystem to climate change. *Nature Communications*, *12*(1), 4475. https://doi.org/10.1038/s41467-021-24742-0

Rochon, A., Vernal, A. de, Turon, J.-L., Matthießen, J., & Head, M. J. (1999). Distribution of recent dinoflagellate cysts in surface sediments from the North Atlantic Ocean and adjacent seas in relation to sea-surface parameters. *American Association of Stratigraphic Palynologists Contribution Series*, *35*, 1–146.

RStudio Team. (2022). RStudio: Integrated development environment for R. RStudio, PBC. https://posit.co/products/open-source/rstudio/?sid=1

Rysgaard, S., Boone, W., Carlson, D., Sejr, M. K., Bendtsen, J., Juul-Pedersen, T., Lund, H., Meire, L., & Mortensen, J. (2020). An Updated View on Water Masses on the pan-West Greenland Continental Shelf and Their Link to Proglacial Fjords. *Journal of Geophysical Research: Oceans*, *125*(2). https://doi.org/10.1029/2019JC015564

Sharp, M., Burgess, D. O., Cawkwell, F., Copland, L., Davis, J. A., Dowdeswell, E. K., Dowdeswell, J. A., Gardner, A. S., Mair, D., Wang, L., Williamson, S. N., Wolken, G. J., & Wyatt, F. (2014). Remote sensing of recent glacier changes in the Canadian Arctic. In J. S. Kargel, G. J. Leonard, M. P. Bishop, A. Kääb, & B. H. Raup (Eds.), *Global Land Ice Measurements from Space* (pp. 205–228). Springer. https://doi.org/10.1007/978-3-540-79818-7_9

Sherr, E. B., & Sherr, B. F. (2007). Heterotrophic dinoflagellates: A significant component of microzooplankton biomass and major grazers of diatoms in the sea. *Marine Ecology Progress Series*, *352*, 187–197. https://doi.org/10.3354/meps07161

Simpson, G. L. (2018). Modelling Palaeoecological Time Series Using Generalised Additive Models. *Frontiers in Ecology and Evolution*, *6*. https://doi.org/10.3389/fevo.2018.00149

Simpson, G. L. (2022). gratia: Graceful ggplot-based graphics and other functions for GAMs fitted using mgcv. R package version 0.7.3. https://gavinsimpson.github.io/gratia

Solomina, O. N., Bradley, R. S., Hodgson, D. A., Ivy-Ochs, S., Jomelli, V., Mackintosh, A. N., Nesje, A., Owen, L. A., Wanner, H., Wiles, G. C., & Young, N. E. (2015). Holocene glacier fluctuations. *Quaternary Science Reviews*, *111*, 9–34. https://doi.org/10.1016/j.quascirev.2014.11.018

Stevenard, N., Montero-Serrano, J.-C., Eynaud, F., St-Onge, G., Zaragosi, S., & Copland, L. (2022). Lateglacial and Holocene sedimentary dynamics in northwestern Baffin Bay as recorded in sediment cores from Cape Norton Shaw Inlet (Nunavut, Canada). *Boreas*, *n/a*(n/a), Article n/a. https://doi.org/10.1111/bor.12575

Stroeve, J., & Notz, D. (2018). Changing state of Arctic sea ice across all seasons. *Environmental Research Letters*, *13*(10), 103001. https://doi.org/10.1088/1748-9326/aade56

Tang, C. C. L., Ross, C. K., Yao, T., Petrie, B., DeTracey, B. M., & Dunlap, E. (2004). The circulation, water masses and sea-ice of Baffin Bay. *Progress in Oceanography*, *63*(4), Article 4. https://doi.org/10.1016/j.pocean.2004.09.005

Tremblay, J.-É., Gratton, Y., Carmack, E. C., Payne, C. D., & Price, N. M. (2002). Impact of the large-scale Arctic circulation and the North Water Polynya on nutrient inventories in Baffin Bay. *Journal of Geophysical Research: Oceans*, *107*(C8), Article C8. https://doi.org/10.1029/2000JC000595

Tremblay, J.-E., Gratton, Y., Fauchot, J., & Price, N. M. (2002). Climatic and oceanic forcing of new, net, and diatom production in the North Water. *Deep Sea Research Part II: Topical Studies in Oceanography*, *49*(22), Article 22. https://doi.org/10.1016/S0967-0645(02)00171-6

Tremblay, J.-É., Hattori, H., Michel, C., Ringuette, M., Mei, Z.-P., Lovejoy, C., Fortier, L., Hobson, K. A., Amiel, D., & Cochran, K. (2006). Trophic structure and pathways of biogenic carbon flow in the eastern North Water Polynya. *Progress in Oceanography*, *71*(2), Article 2. https://doi.org/10.1016/j.pocean.2006.10.006

Van Nieuwenhove, N., Head, M. J., Limoges, A., Pospelova, V., Mertens, K. N., Matthiessen, J., De Schepper, S., de Vernal, A., Eynaud, F., Londeix, L., Marret, F., Penaud, A., Radi, T., & Rochon, A. (2020). An overview and brief description of common marine organic-walled dinoflagellate cyst taxa occurring in surface sediments of the Northern Hemisphere. *Marine Micropaleontology*, 101814. https://doi.org/10.1016/j.marmicro.2019.101814

Versteegh, G. J. M., & Blokker, P. (2004). Resistant macromolecules of extant and fossil microalgae. *Phycological Research*, *52*(4). https://doi.org/10.1111/j.1440-183.2004.00361.x

Vincent, R. F. (2019). A Study of the North Water Polynya Ice Arch using Four Decades of Satellite Data. *Scientific Reports*, *9*. https://doi.org/10.1038/s41598-019-56780-6

Wall, D., & Dale, B. (1966). "Living Fossils" in Western Atlantic Plankton. *Nature*, *211*(5053), Article 5053. https://doi.org/10.1038/2111025a0

Wood, S. N. (2017). *Generalized Additive Models: An Introduction with R, Second Edition* (2nd ed.). Chapman and Hall/CRC. https://doi.org/10.1201/9781315370279

Zonneveld, K. A. F., Marret, F., Versteegh, G. J. M., Bogus, K., Bonnet, S., Bouimetarhan, I., Crouch, E., de Vernal, A., Elshanawany, R., Edwards, L., Esper, O., Forke, S., Grøsfjeld, K., Henry, M., Holzwarth, U., Kielt, J.-F., Kim, S.-Y., Ladouceur, S., Ledu, D., … Young, M. (2013). Atlas of modern dinoflagellate cyst distribution based on 2405 data points. *Review of Palaeobotany and Palynology*, *191*, 1–197. https://doi.org/10.1016/j.revpalbo.2012.08.003

Zonneveld, K. A. F., Versteegh, G., & Kodrans-Nsiah, M. (2008). Preservation and organic chemistry of Late Cenozoic organic-walled dinoflagellate cysts: A review. *Marine Micropaleontology*, *68*(1), Article 1. https://doi.org/10.1016/j.marmicro.2008.01.015

1.11 SUPPLEMENTARY MATERIAL

Table 4. ^{137}Cs activity and standard error (SE) for sediment samples from 2.5BC and 2.7BC.

Core	Depth (cm)	137Cs (Bq/kg)	± (SE)
AMD19-2.5BC	0.5	4.93	0.85
AMD19-2.5BC	10.5	1.01	1.60
AMD19-2.5BC	11.5	4.14	0.88
AMD19-2.5BC	12.5	1.10	0.95
AMD19-2.5BC	13.5	1.58	0.76
AMD19-2.5BC	14.5	2.63	2.50
AMD19-2.5BC	29.5	-0.85	-1.69
AMD19-2.7BC	0.5	2.60	1.07
AMD19-2.7BC	6.5	4.87	0.92
AMD19-2.7BC	7.5	3.62	1.40
AMD19-2.7BC	9.5	4.56	0.92
AMD19-2.7BC	9.5	1.94	1.25
AMD19-2.7BC	40.75	-0.29	-0.75

Table 5. List of taxa and morphotypes observed in 2.7BC and 2.5BC.

Taxa/morphotype name	Trophic affinity	Biological affinity
Brigantedinium simplex	H	*Protoperidinium conicoides*
Brigantedinium cariacoense	H	*Protoperidinium avellana*
Brigantedinium spp.	H	*Protoperidinium* spp.
Round Brown	H	Unknown
Dubridinium spp.	H	Diplopsalid group
Dipopsalid	H	Diplopsalid group
Islandinium minutum subsp. *minutum*	H	*Islandinium minutum*
pale *Islandinium minutum* subsp. *minutum*	H	Protoperidiniaceae
cf. *Islandinium minutum* subsp. *minutum*	H	Protoperidiniaceae
Islandinium? *cezare*	H	Protoperidiniaceae
cf. *Islandinium brevispinosum*	H	Protoperidiniaceae
Islandinium minutum subsp. *barbatum*	H	Protoperidiniaceae
Echinidinium karaense	H	Diplopsalid or Protoperidinioid group
Echinidinium aculeatum	H	Diplopsalid or Protoperidinioid group
Echinidinium sp. 1	H	Diplopsalid or Protoperidinioid group
Echinidinium sp.	H	Diplopsalid or Protoperidinioid group
cf. *Echinidinium* sp. B	H	Diplopsalid or Protoperidinioid group
Spiny Brown Long processes	H	Unknown
Round Brown process-bearing cysts (Spiny Brown)	H	Unknown
Spiny Brown sp. A	H	Unknown
cyst of *Polykrikos* sp. of Kunz-Pirrung (1998)	H	Protoperidiniaceae
cf. cyst of *Polykrikos* sp. of Kunz-Pirrung (1998)	H	Protoperidiniaceae
Cyst of *Protoperidinium* spp.	H	Protoperidiniaceae
Cyst of *Protoperidinium americanum*	H	Protoperidiniaceae
cf. cyst of *Protoperidinium americanum*	H	Protoperidiniaceae
cyst of *Polarella glacialis*	M	*Polarella glacialis*
cf. *Biecheleria*	M	Unknown
Operculodinium centrocarpum sensu Wall & Dale 1966	M	*Protoceratium reticulatum*
Operculodinium centrocarpum Arctic morphotype	M	*Protoceratium reticulatum*
Operculodinium centrocarpum short processes	M	*Protoceratium reticulatum*

Operculodinium centrocarpum cezare morphotype	M	*Protoceratium reticulatum*
cyst of *Pentapharsodinium dalei*	M	*Pentapharsodinium dalei*
Spniferites elongatus	M	*Gonyaulax ovum*
Spiniferites ramosus	M	*Gonyaulax spinifera*
Spiniferites spp.	M	*Gonyaulax* spp.
Impagidinium pallidum	M	*Gonyaulax* spp.

Table 6. PC1 scores for 2.5BC and 2.7BC.

Taxa name	2.5 PC 1	2.7 PC1
Brigantedinium simplex	0.32668	0.2232
Brigantedinium cariacoense	-0.00889	-0.01638
Brigantedinium spp.	0.2378	0.2989
Round Brown	0.18897	-0.15371
Dubrindinium spp.	-0.00604	0.019662
Islandinium minutum subsp. *minutum*	-0.10874	-0.01929
pale *Islandinium minutum* subsp. *minutum*	-0.1146	-0.23854
cf. *Islandinium minutum* subsp. *minutum*	-0.04589	-0.02027
Islandinium? *cezare*	0.044124	-0.03778
cf. *Islandinium brevispinosum*	-0.18017	-0.14304
Islandinium minutum subsp. *barbatum*	-0.08409	-0.09408
Echinidinium karaense	-0.33198	0.023654
Echinidinium aculeatum	-0.06701	0.020112
Echinidinium sp. 1	-0.00825	-0.08351
Echinidinium sp.	0.009959	
cf. *Echinidinium* sp.B	-0.00503	0.00307
Spiny Brown Long processes	-0.08795	-0.04164
Round Brown process bearing cysts (Spiny Brown)	-0.01203	-0.21673
Spiny Brown sp. a	0.051863	2.38E-37
cyst *Polykrikos* sp. of Kunz-Pirrung (1998)	-0.03759	-0.01628
cf. cyst of *Polykrikos* sp. of Kunz-Pirrung (1998)	-0.14534	-0.08766
Protoperidinium spp.	-0.00432	3.86E-43
Protoperidinium americanum	0.021504	-0.01535
cyst of *Polarella glacialis*	0.41949	0.63134
cf. Biecheleria	0.019051	-0.02802
Operculodinium centrocarpum sensu Wall & Dale 1966	0.51046	0.37547
Operculodinium centrocarpum var. Arctic	0.019281	0.090266
Operculodinium centrocarpum short processes	0.098196	-0.00472
Operculodinium centrocarpum var. cezare	0.029237	-0.01758
cyst of *Pentapharsodinium dalei*	0.35714	0.32255
Spiniferites elongatus	0.086513	0.11514
Spiniferites ramosus	0.021504	0.00307
Spiniferites spp.	0.010137	0.11964
Impagidinium pallidum	0.017995	-0.03743
Diplopsalid	0.014144	

Table 7. *Halodinium* spp. counts from 2.7 and 2.5BC

2.7BC Age (Years CE)	2.7BC *Halodinium* spp.	2.5BC Age (Years CE)	2.5BC *Halodinium* spp.
2017.65	4	2018.625	13
2013.3	12	2014.725	15
2008.1	6	2010.675	12
2002.4	8	2005.975	15
1996.45	6	2000.45	11
1990.05	9	1994.4	7
1982.8	3	1989.125	22
1974.55	15	1984.675	15
1965.2	10	1979.85	15
1955.4	10	1975.075	10
1946.05	19	1969.75	14
1936.6	14	1964.275	21
1925.9	6	1958.3	13
1914.1	11	1951.425	9
1902.25	13	1943.975	12
1891.1	13	1935.125	16
1880.5	25	1924.875	18
1858.55	11	1901.325	8
1836.95	3	1877.9	12
1816.2	14	1857.225	15
1795.95	15	1836.25	22
1777.2	29	1815.2	15
1758.8	24	1795.475	12
1740.4	12	1776.875	22
1722	11	1758.275	24
1703.6	11	1739.675	16
1685.2	14	1721.075	14
1666.8	13	1702.475	8
1646.1	12	1683.875	6

CHAPITRE 2
VARIABILITÉ DES ZONES MARGINALES DE GLACE DANS LA POLYNIE DES EAUX DU NORD AU COURS DES 400 DERNIÈRES ANNÉES BASÉE SUR LES ASSEMBLAGES DE DIATOMÉES

2.1 RESUME EN FRANÇAIS

La polynie des eaux du Nord, zone très productive du nord de la baie de Baffin, est une étendue d'eau libre récurrente, bordée par des ponts de glace bien définis dans le détroit de Nares, le détroit de Jones et le détroit de Lancaster, ainsi que par une banquise côtière le long de ses marges ouest et est. Ces environnements de bordure de glace jouent un rôle essentiel dans le maintien de l'intense production primaire qui caractérise la région. Cette étude vise à utiliser les assemblages de diatomées préservés dans les sédiments pour déduire les variations de position et de stabilité de ces environnements, où la dynamique des ponts de glace et de la banquise côtière est déterminante. Un transect de sédiments de surface à travers la Polynie révèle des assemblages de diatomées distincts, associés à des conditions de glace et de surface marine contrastées. La partie ouest de la Polynie, influencée par la zone de glace marginale proche des côtes, présente des concentrations de diatomées plus élevées et une dominance de taxons pennés à croissance rapide, typiques des floraisons printanières précoces. À l'inverse, la partie est de la Polynie se caractérise par une plus grande contribution de taxons centriques qui prospèrent dans des conditions d'eau plus libre ou en sous-surface, plus tard dans la saison productive. L'analyse en profondeur de deux carottes sédimentaires (AMD19-2.5BC et AMD19-2.7BC) prélevées dans la partie ouest de la Polynie, couvrant les quelques 400 dernières années, indique une forte variabilité temporelle liée aux variations de la position de la limite des glaces. Entre 1600 à 1800 CE, les deux sites enregistrent une faible production de diatomées avec une plus grande abondance de diatomées centriques associés à la fin de floraison, telles que *Rhizosolenia* et *Thalassiosira*. Entre 1800 et 1900 CE, la carotte

AMD19-2.7BC montre une nette augmentation des concentrations totales de diatomées, dominées par des taxons pennés associés à la productivité printanière, typiques des environnements de la zone de glace marginale. De 1900 à 2019, la carotte AMD19-2.5BC présente les concentrations totales de diatomées les plus élevées et une augmentation des taxons pennés du début du printemps. Ces résultats indiquent une migration progressive vers le nord de la zone de glace marginale et soulignent le rôle important des environnements de bordure de glace, contrôlés par les ponts de glace et la dynamique de la banquise côtière, dans la modulation de la production de diatomées et de la composition des communautés dans la Polynie.

Cet article intitulé « *Variabilité des zones marginales de glace dans la polynie des eaux du Nord au cours des 400 dernières années basée sur les assemblages de diatomées* » est en cours de préparation pour être soumis à la revue *Paleogeography, Paleoclimatology, and Paleoecology.* En tant que première autrice, j'ai effectué la revue de la littérature, les analyses de tous les échantillons de carottes sédimentaires (analyses des diatomées et du $^{210}Pb/^{137}Cs$) et la rédaction du manuscrit. Audrey Limoges, deuxième autrice, a réalisé l'analyse des échantillons de sédiments de surface et a fourni des commentaires éditoriaux sur le manuscrit. André Rochon, dernier auteur, a fourni des commentaires et des corrections au manuscrit. Les résultats de ce chapitre ont été présentés à Geotop en 2025 sous forme d'affiche.

2.2 ABSTRACT

The highly productive North Water (NOW) Polynya in northern Baffin Bay is a recurrent area of open water bordered by well-defined ice bridges in Nares Strait, Jones Sound and Lancaster Sound, along with landfast sea ice along its western and eastern margins. These ice-edge environments play a key role in sustaining the intense primary production that characterizes the region. This study aims to use diatom assemblages preserved in the sediment to infer changes in the position and stability of the sea-ice edge environments, where the dynamics of the ice bridges and landfast sea ice play an important role. A transect of surface sediments across the NOW show distinct diatom assemblages associated with contrasting ice and sea-surface conditions. The western NOW, influenced by the Marginal Ice Zone (MIZ) near landfast ice, shows higher diatom concentrations and dominance of fast-growing pennate taxa typical of early spring blooms. In contrast, the eastern NOW is characterized by higher contributions of centric taxa that thrive under more open-water or subsurface conditions later in the productive season. Downcore analysis of two sediment cores (AMD19-2.5BC and AMD19-2.7BC) from the western NOW, covering the last ca. 400 years, indicates strong temporal variability linked to shifts in ice-edge position. From ca. 1600 to 1800 CE, both sites record low diatom production with higher abundance of late-bloom centric diatoms such as *Rhizosolenia* and *Thalassiosira*. Between 1800 and 1900 CE, core AMD19-2.7BC shows a marked increase in total diatom concentrations dominated by early-spring pennate taxa typical of MIZ environments. From 1900 CE to the present, core AMD19-2.5BC records the highest concentrations of total diatoms and an increase of early-spring pennate taxa. These results indicate a progressive northward migration of the MIZ and show the important role of ice-edge environments, controlled by ice bridges and landfast sea ice dynamics, in modulating diatom production and community composition in the NOW.

2.3 ICE EDGE VARIABILITY IN THE WESTERN NORTH WATER POLYNYA OVER THE LAST 400 YEARS BASED ON DIATOM ASSEMBLAGES

Kelsey A. Koerner[1], Audrey Limoges[2], and André Rochon[1]

Institutions :

1. Institut des sciences de la mer (ISMER), Université du Québec à Rimouski (UQAR), Geotop & Québec-Océan, Rimouski, QC, Canada
2. Department of Earth Sciences, University of New Brunswick (UNB), Fredericton, NB, Canada

2.4 INTRODUCTION

As transitional areas where open waters meet pack ice, Marginal Ice Zones (MIZ) are dynamic features of polar regions that have a key influence on biological productivity and the cycling of inorganic nutrients across local and regional scales (Ardyna et al., 2020). Although under-ice algal blooms occur within ice-covered areas (Arrigo & van Dijken., 2015; Leu et al., 2015), seasonally migrating MIZ are the location of brief but intense pulses of primary production, which develop in the spring as increasing solar radiation penetrates the surface mixed layer (Perrette et al., 2011; Ardyna et al., 2020). These blooms are often dominated by fast-growing microalgae, especially diatoms, but also other groups including pico- and nano- phytoplankton (e.g., Lizotte et al., 2020; Ribeiro et al. 2024), that rapidly consume the winter-accumulated nutrient inventory within days to weeks (Tremblay et al., 2006; Terrado et al., 2008; Tremblay & Gagnon, 2009). These springtime blooms contribute significantly to vertical transport of particulate organic matter to the benthos and typically act as an early-season carbon sink (Riedel et al., 2008, Krause et al., 2019), also accounting for much of the net annual primary production in the Arctic (Perrette et al., 2011). MIZ blooms also support early-season food webs by providing energy to secondary consumers like copepods (Madsen et al., 2008, Vilgrain et al. 2021) and have been linked to important trophic changes, including fluctuations in fish stocks in regions such as Baffin Bay (Pedro et

al., 2023). Over recent decades, the accelerating decline in Arctic sea ice has driven changes in the geometry and seasonal dynamics of MIZs (Rolph et al., 2020), resulting in changes to the timing and magnitude of early season primary production (Arrigo et al., 2008).

A prominent example of a productive ice-edge system is the North Water (NOW) polynya (*Pikialasorsuaq* in Greenlandic or *Sarvarjuaq* in Inuktitut) in northern Baffin Bay, which is an area characterized by early and persistent open water conditions surrounded by sea ice (Fig. 14A, B). Due in part to its early exposure to solar radiation, the NOW is one of the most biologically productive regions in the Arctic, supporting complex food webs and providing overwintering habitat for large mammals, such as narwals and belugas (Heide-Jørgensen et al., 2013; 2016). The northern boundary of the NOW is defined by a sharp, arc-shaped ice edge that forms across Smith Sound (Fig. 14B) and which plays a critical role in the formation of the polynya by restricting the southward export of sea ice from the Arctic Ocean into northern Baffin Bay (e.g., Vincent, 2019; Moore et al., 2021). Similar ice bridges form seasonally in Jones Sound and Lancaster Sound (Fig. 14B) where they contribute to the stabilisation of sea ice upstream of the polynya. Along the eastern and western sides of the NOW, sea-ice conditions are also influenced by contrasting ocean currents: the northward flowing relatively warm (>2 °C), saline (>34) West Greenland Current along the Greenland coast (Fig 14A; Tang et al., 2004; Rysgaard et al., 2019) and southward-flowing cold (>–1°C), relatively fresh (<34) waters along the Canadian side (Fig. 14A; Münchow et al., 2015). This asymmetry results in a more extensive and persistent landfast sea-ice edge projecting into the NOW from Ellesmere Island, on the western side (Fig. 14B-D), and leads to distinct biogeochemical gradients along longitudinal axes at the scale of Baffin Bay (Saint-Béat et al. 2020).

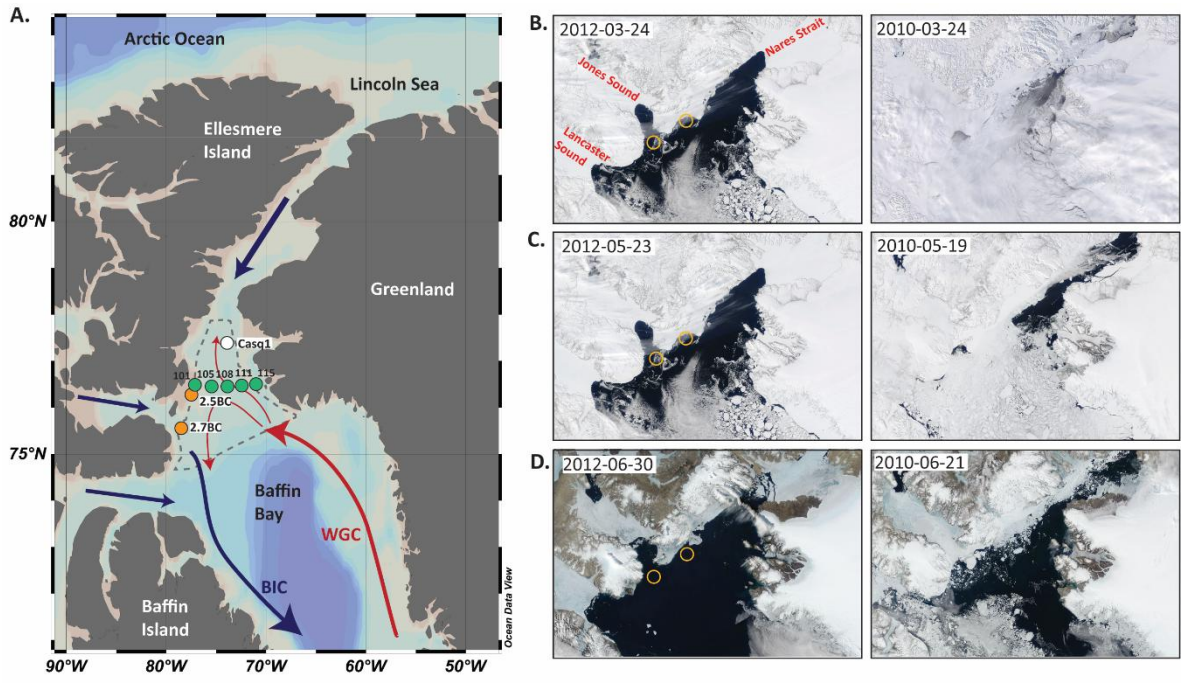

Figure 14. A) Map of northern Baffin Bay showing the locations of the two cores (orange circles), surface sediment (green dots) from this study, and the main oceanic currents that impact the region. WGC = West Greenland Current and BIC= Baffin Current. The grey dotted line represents the average springtime extent of the NOW. B) EOSDIS Satellite image of the average springtime extent of the NOW. B-D) EOSDIS Satellite images of the NOW during years with a stable ice bridge (left) and during years where the ice bridge failed (right).

The NOW is sensitive to climate warming and has experienced changes to its open water conditions in recent years (Vincent, 2019). Since the early 21st century, the Smith Sound ice arch has increasingly broken up earlier in the year or failed to form altogether due to rising air temperatures and other oceanographic processes (Kirillov et al., 2022; Moore et al., 2021). This has resulted in increased sea-ice and freshwater export from the Arctic Ocean into northern Baffin Bay (Vincent, 2019; Vincent, 2020). These southward-flowing ice flows tend to consolidate along the western NOW margin (Fig. 14B-D). As a result, the characteristic open water conditions within the polynya are significantly altered in years when ice bridge formation fails (Vincent, 2019). During years with strong ice bridge presence, the western landfast ice along the NOW is stronger near Smith Sound, whereas in the south at the exit of Jones Sound waters typically stays open. However, in years when the

ice bridge fails the western region of the NOW acts as a conveyor belt of sea ice exported out of the Arctic, resulting in a consistently ice filled area (Fig. 14B-D). The ice bridges themselves also act as an important control on the location of primary production as well as on the timing and intensity of phytoplankton blooms (Marchese et al., 2017; Tachon et al., 2025). However, the impact of a changing MIZ through time within the NOW has not yet been explored.

Algal phenology in the NOW remains poorly characterized, as only a few studies have specifically investigated its seasonal dynamics (Hargrave et al., 2002). However, a high throughput 18S RNA V4 amplicon sequencing analysis of surface waters across the NOW show that communities in the eastern portion are dominated by late-fall blooming dinoflagellates (Freyria et al., 2021), while the Si-rich Arctic outflow along the western NOW favors diatom productivity (Joli et al., 2018; Freyria et al., 2021). Distinct diatom species tend to dominate communities in Arctic sea ice (e.g., pennate taxa such as *Nitzschia*, *Navicula*, *Fragilariopsis;* Weckström et al., 2020), under ice (e.g., strand-forming centric *Melosira arctica;* Poulin et al., 2014), MIZ (e.g., *Fragilariopsis, Fossulaphycus;* von Quillfeldt, 1997; Weckström et al., 2020) and open-water (e.g., greater presence of centric taxa such as *Thalassiosira, Coscinodiscus* and *Chaetoceros;* Oksman et al., 2019). As such the variations in diatom assemblage composition provide valuable insight into climate-driven changes in sea-surface conditions, including sea ice. Following the termination of diatom blooms, often triggered by nutrient depletion, large sedimentation events of ungrazed cells and resting spores are frequently observed in the Arctic (Kiorboe et al., 1996; Booth et al., 2002; Toullec et al., 2021; Agafonova et al., 2022). The siliceous remains of diatoms can accumulate on the seafloor, preserving a record of past community structure and environmental conditions (Knudsen et al., 2008; Limoges et al., 2023).

Here, we consider the western MIZ of the NOW as not only a physical boundary between ice and open water, but as a dynamic, climate-sensitive feature whose variability holds ecological and cultural significance for surrounding Inuit communities. We first analyzed surface sediment samples to characterize recent diatom assemblages along a

transect across the NOW. We then used two short marine sediment cores to investigate variations in the western extent of the MIZ in the NOW over the last ca. 400 years. This interval encompasses two climatically contrasting periods: cooling in the Arctic that has been associated with the Little Ice Age (LIA), characterized by lower-than-average Arctic temperatures (Auger et al., 2019), and modern warming (MoW), during which Arctic temperatures have risen at approximately four times the global average (Rantanen et al., 2022). Together, these datasets allow a spatiotemporal comparison of the western NOW, integrating a longitudinal gradient in surface samples with temporal records from the western sector, to explore potential differences in MIZ dynamics through space and time. We show that diatoms are robust indicators of sea-ice variability, providing important information on past changes in the position of the MIZ within the NOW.

2.5 METHODS

2.5.1 Sediment sampling and Age-Model

Five surface sediment samples and two push cores were collected from box cores onboard the Canadian Coast Guard Ship Amundsen (Fig. 14A) during the 2019 ArcticNet sampling campaign. The surface sediment samples were immediately stored at -20°C until analysis and the sediment cores were stored at 4 °C until sub-sampling and microfossil analyses.

The cores were sub-sampled every 1 cm (2.7BC) and every 0.5 cm (2.5BC), with all samples stored at 4 °C until analysis. Age-models were developed using ^{210}Pb and ^{137}Cs measurements and the open-sourced Plum package (Fig. 15; Aquino-Martinez et al., 2018) in R (Version 0.5.0; Fig. 15) and were previously presented in Koerner et al. (2025).

2.5.2 Diatom assemblages

Sample preparation for diatom analyses followed the protocol presented in Limoges et al., (2020). Sediment samples were dried and weighed to approximately 0.2g per sample. Each sample was treated with a solution containing 870 mL of 30% hydrogen peroxide (H_2O_2) and 42g of dissolved sodium tetraphosphate ($Na_4P_2O_7 \cdot 10(H_2O)$) to dissolve the

organic material and disaggregate clumps. Samples were left for 1-3 days until the hydrogen peroxide reaction had ceased, then centrifuged and rinsed with distilled water until a neutral pH was reached. The samples were then treated with 10% hydrochloric acid (2.74 M; HCl) for a minimum of 3 hours to remove the carbonate material, then rinsed with distilled water and centrifuged to neutral pH. Samples were diluted to a final volume of 50mL.

For the surface sediment samples, an aliquot of 150µL of the diatom suspension was placed on a stub for scanning electron microscopy (Hitachi TM4000, UNB). The entire subsample was scanned for diatom analysis. Each sample was analyzed in duplicates. For the core samples, cover slips were placed in Petri dishes of known surface area and submerged in water. The diatom-rich suspension was homogenized, and 2-3 aliquots of 150 µL were evenly distributed in the petri dish. Samples were left undisturbed for 24 hours to allow complete settling, then dried, and mounted on slides using Naphrax©.

Diatoms were counted using an Olympus BX51 microscope at 100X magnification in oil immersion, with a minimum count of 300 valves per sample, with the exception of two samples: AMD19-2.7BC 14-15cm (n=147) and AMD19-2.5 28-28.5cm (n=265). Diatom specimens were counted following the counting rules described in Crosta & Koç (2007), whereby specimens were generally counted when more than 50% of the valve was observed. For *Rhizosolenia,* specimens were only counted when the spine-like proboscis was observed (Fig. 16). *Chaetoceros* resting spores were counted separately and excluded from the relative abundance calculations. Diatoms in the genus *Chaetoceros* are typically fast-growing and some can produce small, highly silicified resting spores that sink rapidly to the seafloor. *Chaetoceros* vegetative cells can be weakly silicified and thus typically poorly preserved in sediments, whereas their resting spores typically preserve better and can serve as reliable proxy for past primary production (Abelmann et al., 2006). For the core samples, diatoms are presented in concentrations expressed as valves per g of dry sediment.

2.5.3 Generalized Additive Models (GAMs)

Generalized Additive Models (GAMs) were fitted to the diatom fluxes to identify changes in total production in the downcore data (Wood, 2017; Simpson, 2018). All analyses were done in R (version 4.2.2; R Core Team, 2022) using the mgcv package (version 1.8-41; Wood, 2017) within RStudio (version 2022.07.2; RStudio Team, 2022). GAMs are non-parametric statistical tools used to model non-linear time series and are suited to stratigraphic datasets characterized by heteroscedasticity and uneven temporal resolution, such as those arising from variable sedimentation rates. To account for heteroscedasticity and difference in temporal resolution, observational weights were applied as recommended by Simpson (2018). The gratia package (version 0.7.3; Simpson, 2022) was used to compute the first derivative of the fitted smooth terms and objectively identify intervals of significant diatom flux change. Simultaneous confidence intervals were identified from these derivatives and enabled robust identification of statistically significant trends. We identified the change at the start of a period of significant change defined where the confidence interval of the first derivative did not include zero, indicating a departure from temporal stability. The GAMs were applied to the total diatom fluxes for both core 2.5 and 2.7.

2.6 RESULTS

2.6.1 Core chronologies

Cores 2.5BC and 2.7BC show high surface ^{210}Pb activity (157 Bq/kg and 185 Bq/kg respectively), which decrease exponentially to background levels of 20 Bq/kg and 27 Bq/kg around 20 cm (Fig. 15). Based on these profiles, both cores are estimated to span the last ca. 360 years with a temporal resolution ranging from 8 to 60 years per sample.

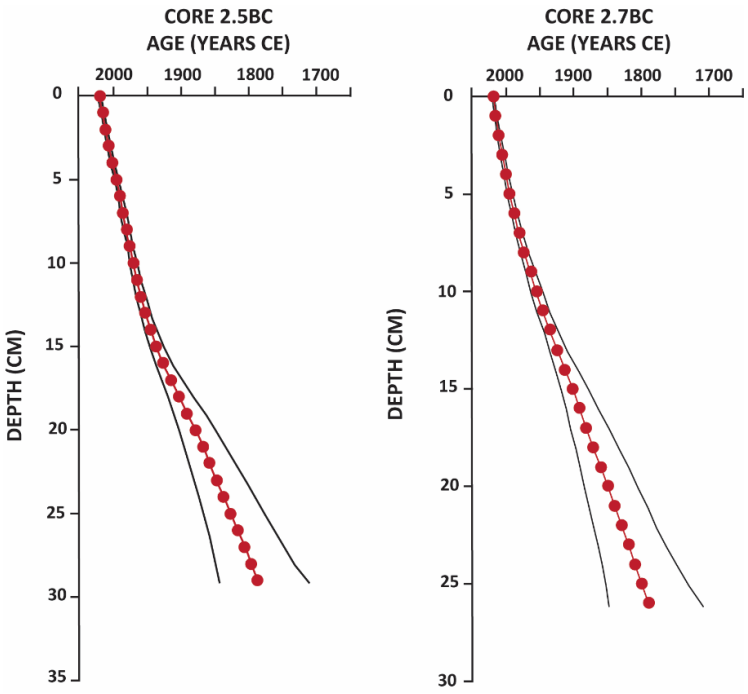

Figure 15. Age-depth models based on ^{210}Pb activity for 2.5BC (left) and 2.7BC (right). The red line represents the modelled ages and the black lines represent the associated error with each age.

2.6.2 Diatom assemblages and concentrations

Surface sediment transect

Total diatom concentrations range between 36 x 10^7 and 120 x 10^7 valves/g. Marked differences are observed along the surface sediment transect, both in diatom abundance and assemblage composition (Fig. 17). The westernmost station (101) shows the highest total diatom and *Chaetoceros* resting spore concentrations, with the highest contribution from the marginal ice zone (MIZ) taxa *Fossulaphycus arcticus*, *Fragilariopsis cylindrus*, *Fragilariopsis oceanica, Fragilariopsis reginae-jahniae* (hereafter referred to as the MIZ group) and lowest proportion of centric diatoms such as *Thalassisosira* spp. (Fig. 17). Progressing eastward, MIZ group abundances gradually decline while centric taxa increase. Station 111, despite high diatom concentrations, shows the lowest MIZ group abundance, and a marked increase in *Thalassiosira* spp., *Coscinodiscus* spp., and *Porosira glacialis* (Fig. 17). At the easternmost station (115), the MIZ group increases again, and notably, this site

records the highest contribution of *Rhizosolenia hebetata* and the sub-ice species *Melosira arctica* (Fig. 17).

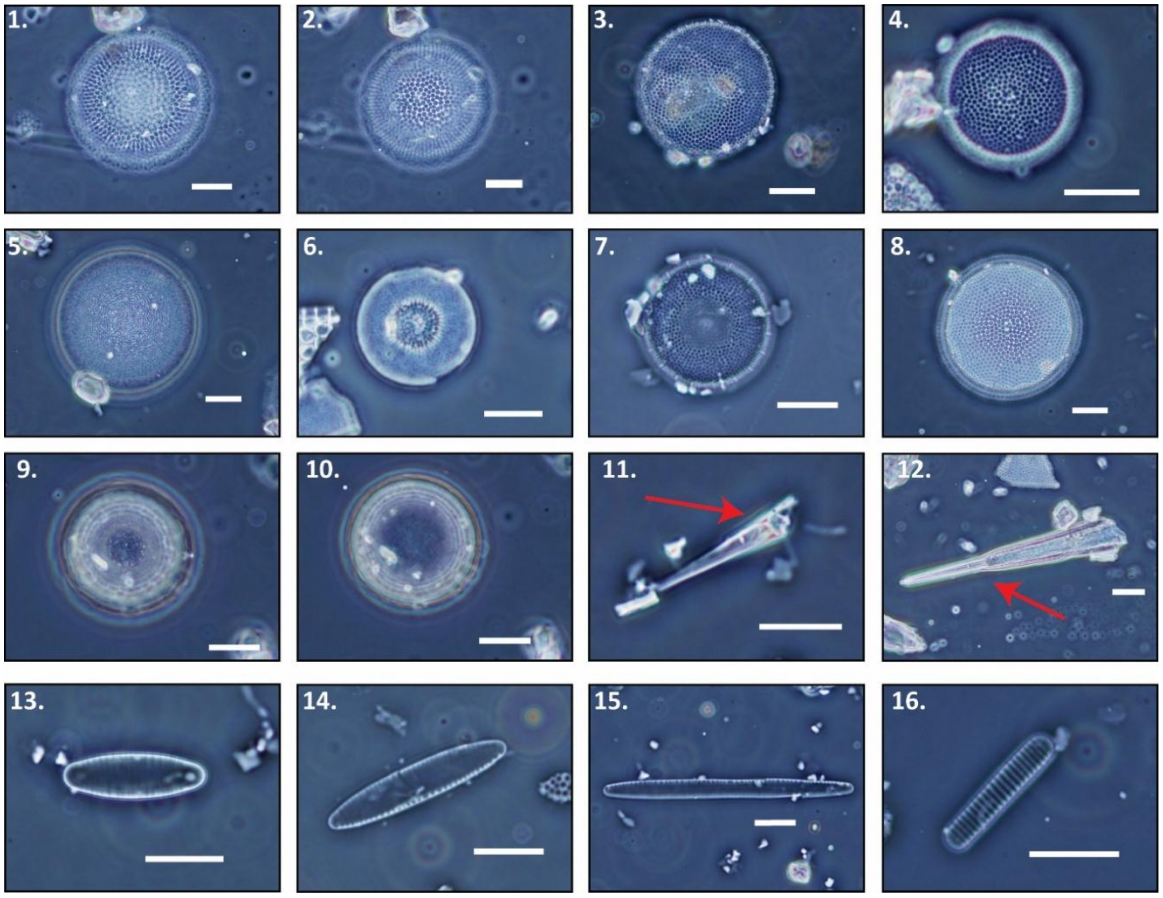

Figure 16. Micrographs of the main diatom taxa observed in AMD19-2.5BC and -2.7BC. 1-2) *Thalassiosira antarctica* var. *borealis* secondary valve (type coarse), 3) *Thalassiosira antarctica* var. *borealis* primary valve, 4) *Thalassiosira antarctica* var. *borealis* secondary valve (type fine), 5) *Porosira glacialis*, 6) *Bacterosira bathyomphala* resting sopre, 7) *Bacterosira bathyomphala* vegetative cell, 8) *Actinocyclus curvatulus*, 9-10) *Melosira arctica*, 11) *Rhizosolenia hebetata* f. *semispina*, 12) *Rhizosolenia hebetata* var. *hebetata*, 13) *Fossulaphycus arcticus*, 14) *Fragilariopsis oceanica*, 15) *Fragilariopsis reginae-jahniae*, and 16) *Fragilariopsis cynlindrus*. The red arrow shows the spine-like proboscis on *Rhizosolenia*. White bar represents 10 µm.

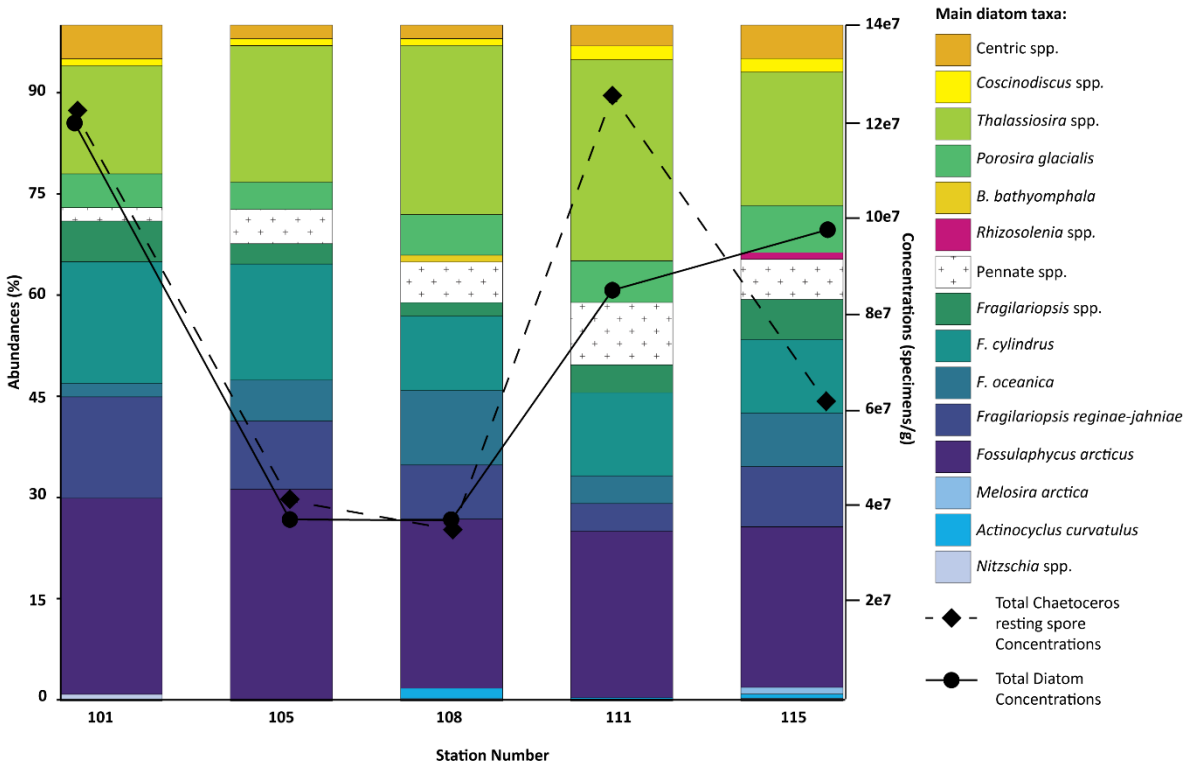

Figure 17. Relative abundances, total diatom concentrations and *Chaetoceros* resting spore concentrations for the NOW surface sediment transect.

Cores 2.5BC and 2.7BC

A total of 28 taxa were identified between both cores. The dominant taxa (>2%) in cores 2.5BC and 2.7 BC were *Fossulaphycus arcticus* (7 to 42%; 7 to 35%), *Thalassiosira antarctica* var. *borealis* resting spores (12 to 27%; 5 to 39%), *Porosira glacialis* (2 to 16%; 0 to 15%), *Fragilariopsis cylindrus* (2 to 7%; 0 to 12%), *Fragilariopsis oceanica* (2 to 20%; 2 to 14%), *Fragilariopsis reginae-jahniae* (2 to 11%; 3 to 13%), *Bacterosira bathyomphala* (0 to 6%; 0 to 4%) *Rhizosolenia* spp. (composed of *Rhizosolenia hebetata* f. *semispina*, (0 to 6%; 0 to 5%) and *Rhizosolenia hebetata* var. *hebetata* (0 to 3.5%; 0 to 5%)), *Melosira arctica* (0 to 3%; 0 to 3%), and *Actinocyclus curvatulus* (0 to 2%; 0 to 5%) (Figs. 18 & 19). Diatom concentrations ranged from 3.8 x 10^7 valves/g to 3.6 x 10^8 valves/g for core 2.5BC and 2.7 x 10^7 valves/g to 7.7 x 10^7 valves/g for core 2.7BC and *Chaetoceros* resting spore concentrations ranged from 9.86 x 10^6 spores/g to 1.1 x 10^8 spores/g for 2.5BC and 8.32 x 10^6 spores/g and 4.93 x 10^8 spores/g for 2.7BC (Figs. 18 & 19).

From 1680 to 1800 CE, diatom assemblages in both cores are dominated by *Thalassiosira antarctica* var. *borealis*, *Bacterosira bathyomphala*, *Rhizosolenia* spp., and the sea ice-associated species *Actinocyclus curvatulus* and *Melosira arctica* (Figs. 18 & 19). This interval is also marked by the lowest concentrations of both total diatoms and *Chaetoceros* resting spores in the entire sedimentary records (Figs. 18 & 19).

From 1800 to 1900 CE, core 2.7BC shows a marked change in diatom assemblage composition, characterized by a 7-fold increase in both total diatom concentrations and *Chaetoceros* resting spores (Fig. 19). This is accompanied by a notable rise in the relative abundance of the MIZ group. The GAMs show the start of a period of significant change around 1800 CE and 1900 CE (Fig. 19). In contrast, core 2.5BC shows relatively stable diatom concentrations and assemblage composition during the same period (Fig. 18).

In core 2.5BC, from 1900 to 2019 CE, there is a stepwise increase in total diatom and *Chaetoceros* resting spore concentrations and an increase in the relative abundances of *Porosira glacialis*, *Bacterosira bathyomphala*, *Fragilariopsis cylindrus*, *Fragilariopsis oceanica*, and *Fossulaphycus arcticus* (Fig. 18). These changes are also accompanied by the beginning of a period of significant change identified by the GAMs for 2.5BC (Fig. 18). In 2.7BC, diatom and *Chaetoceros* resting spore concentrations return to previous levels. The assemblage shows a marked increase in the relative abundance of *Thalassiosira antarctica* var. *borealis* (resting spore), *Porosira glacialis*, and *Melosira arctica* (Fig. 19). Overall, total diatom valve and *Chaetoceros* resting spore concentrations remain relatively stable throughout the record, except between 1800 and 1900 CE, when both reach pronounced peaks of up to 8 $x10^8$ valves/g and 5 x 10^8 spores/g, respectively.

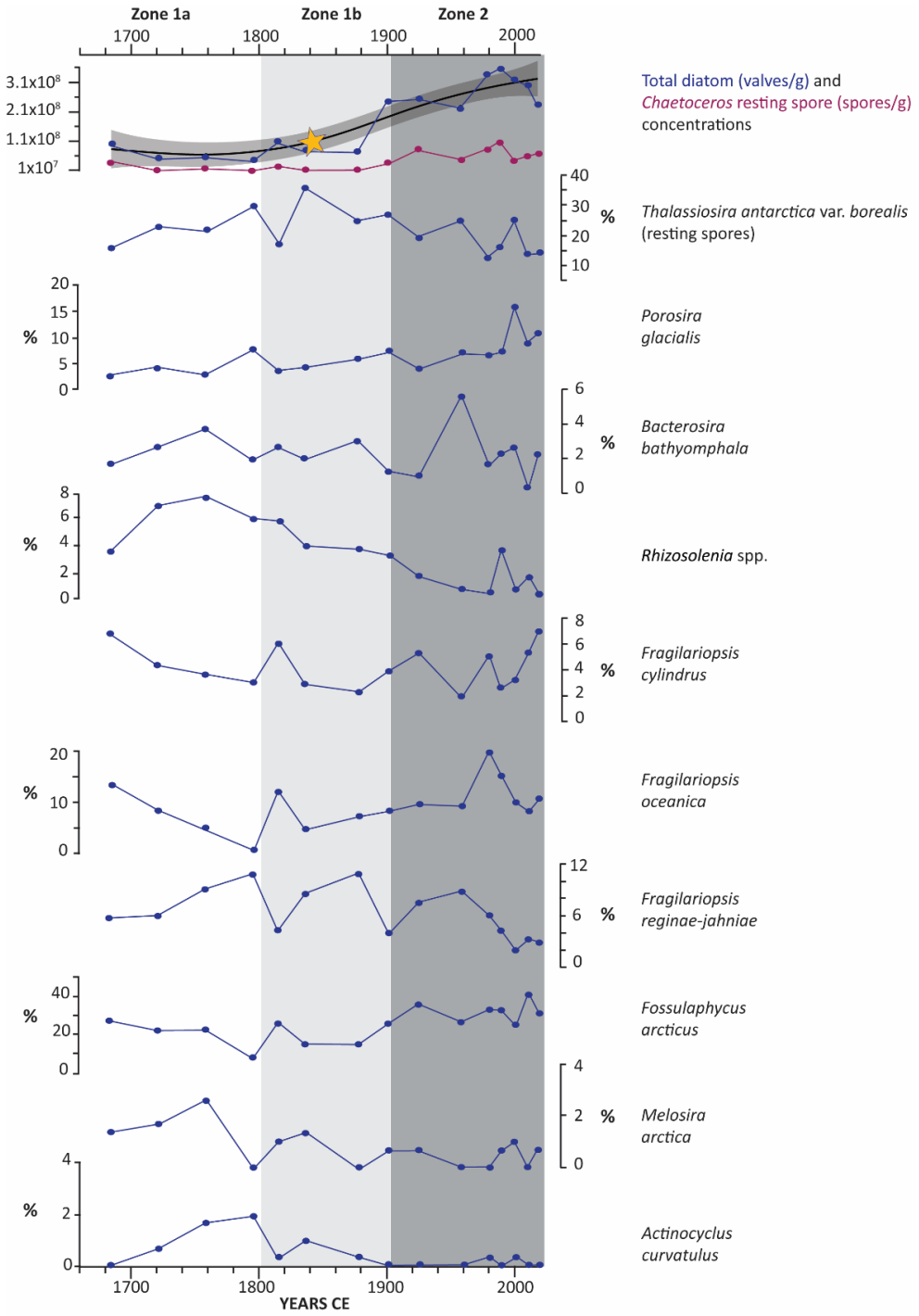

Figure 18. Relative abundances and concentrations of core 2.5BC diatoms and *Chaetoceros* resting spores. The gray curve represents the GAM-derived best-fit smooth and associated uncertainty, and the star shows the point of statistically significant change identified from the first derivative of the GAMs. The gray boxes represent the environmental zones visually interpreted from the diatom assemblages.

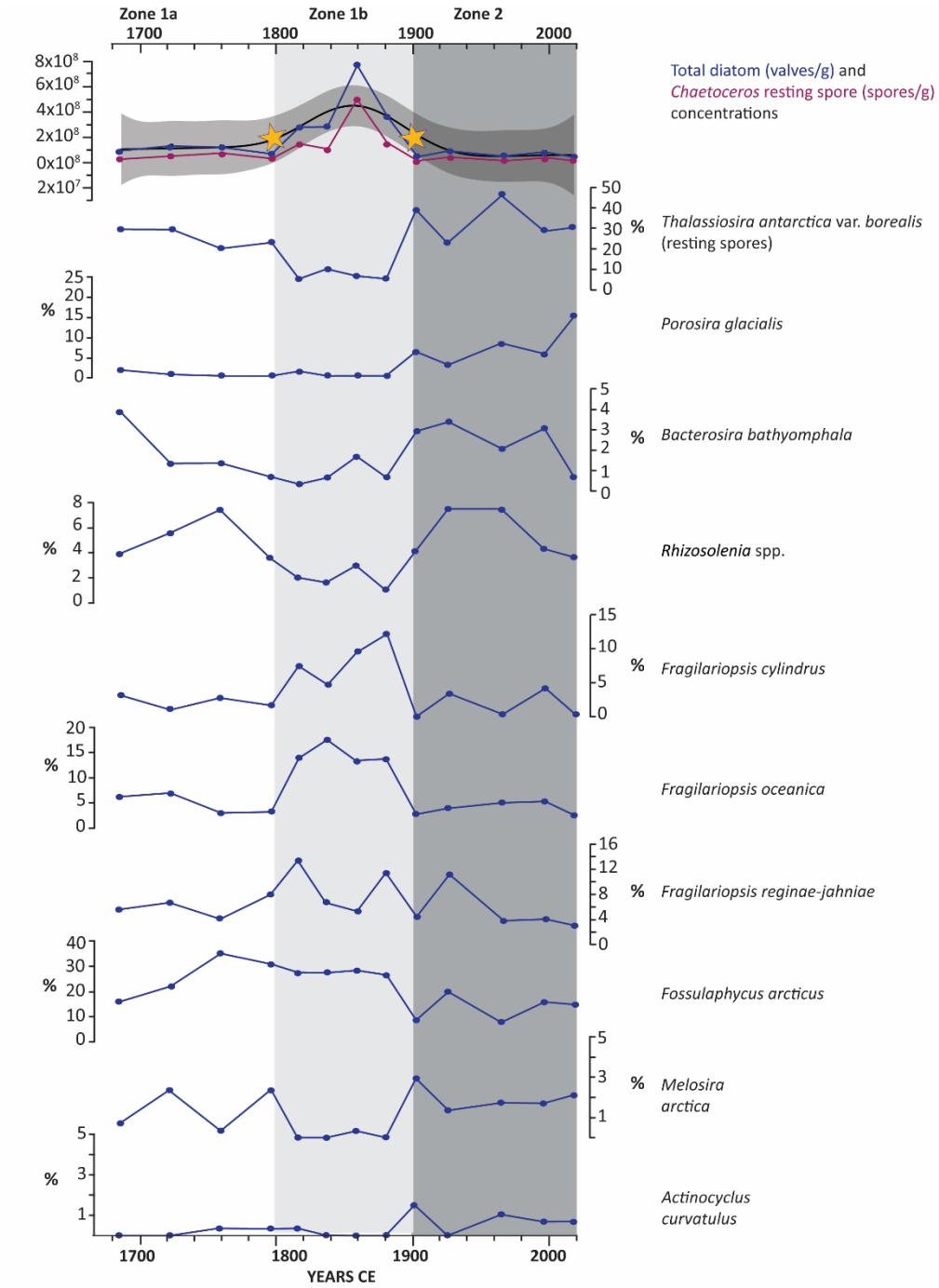

Figure 19. Relative abundances and concentrations of core 2.7BC diatoms and *Chaetoceros* resting spores. The gray curve represents the GAM-derived best-fit smooth and associated uncertainty, and the star shows the point of statistically significant change identified from the first derivative of the GAMs. The gray boxes represent the environmental zones visually interpreted from the diatom assemblages.

2.7 DISCUSSION

Diatoms reflect differing sea ice environments across the NOW

Both diatom concentrations and species composition changes reflect differences in hydrological conditions and sea-ice dynamics along the NOW transect. The western NOW, characterized by relatively higher sea-ice concentrations and fresher, more Si-rich outflows (Tremblay et al., 2002; Fig. 14) is dominated by the MIZ diatom group, which includes taxa that are well adapted to quickly exploit available nutrients in surface waters (Tremblay et al., 2006). Typically, these small(er) pennate taxa are fast blooming and contribute significantly to the net primary production in the NOW (Lovejoy et al., 2002). High diatom production is reflected in the surface sediment transect by the highest overall concentrations of diatom and *Chaetoceros* resting spores in the western region (Fig. 17). The eastern NOW is typically characterized by both earlier open water due to the upwelling of the relatively warm WGC (Tang et al. 2004) and less sea ice export and Si-rich waters than the western region (Tang et al., 2004; Münchow et al., 2015). As such, the diatom assemblages in the east are characterized by higher proportions of open-water taxa, such as late(r) bloomers *Rhizosolenia* spp. (Fig. 17), but are characterized by high diatom concentrations comparable to those in the western NOW.

Spatiotemporal Variability Between 2.5 and 2.7BC

Diatom concentrations in core 2.5BC are up to 2 factors higher than those observed in the central portion of the NOW (Limoges et al., 2023; Fig. 18), and in other regions of Baffin Bay, such as Upernavik (Limoges et al., 2020). This pattern is consistent with modern observations of primary production, which indicate that diatoms make up an important portion of the primary production in the NOW (e.g., Lovejoy et al., 2002), particularly in the western sector. There, elevated productivity near the sea-ice edge is sustained by Si-rich outflows (e.g., Freyria et al., 2021). This spatial pattern is also reflected in the surface

sediment samples, where diatom concentrations are higher in the western region compared to the east.

Despite their close geographical proximity, 2.5BC and 2.7BC show notable differences in diatom assemblage composition and concentrations over the last ca. 400 years. 2.7BC shows its highest diatom concentrations between ca. 1800 and 1900 CE (Fig. 19), whereas 2.5BC shows a sustained increase beginning around 1900 CE and continuing to the present (Fig. 18). Major changes in diatom assemblage composition coincide with these changes in concentration, primarily reflecting variations in the dominance of the MIZ group (Fig. 20). In core 2.7BC, MIZ taxa peak between ca. 1800 and 1900 CE, whereas in 2.5BC, their highest abundances occur from 1900 to 2019 CE. Regional surface sediment data sets from Baffin Bay show that peak diatom concentrations typically follow the position of the marginal ice edge, favoring MIZ taxa (Krawczyk et al., 2021; Tachon et al., 2025). These modern observations are consistent with the sedimentary archives presented in this study, suggesting that variations in diatom concentrations and assemblage composition are largely driven by changes in sea-ice dynamics in the NOW.

2.7.1 Zone 1a (1680 to 1800 CE): More persistent western sea-ice edge

Both 2.5BC and 2.7BC show similar diatom assemblage composition and concentrations during the period 1680 to 1800 CE, with the lowest total concentrations of diatoms and *Chaetoceros* resting spores, indicating lower primary production during this interval (Figs. 18 & 19). Notably, 2.5BC shows the highest contributions from two taxa associated with pack ice: *Actinocyclus curvatulus* and *Melosira arctica* (Poulin et al., 2014; Hegseth & von Quillfeldt, 2023; Fig. 20). This assemblage points to more persistent sea-ice conditions in the western NOW sector that have supported the development of productive ice-algal communities despite low overall diatom production (Figs. 18 & 19).

This interval also shows the highest relative abundances of *Rhizosolenia* spp., a genus associated with enhanced summer subsurface nutrient availability (Figs. 18 & 19; Oksman et al., 2019), suggesting a more stratified water column during summer months (Limoges et al. 2023). Resting spores of *Thalassiosira antarctica* var. *borealis* are also an important

contribution to the assemblages during this interval; this species has been linked to cooler than present day summer conditions, that could point to increased sea ice concentration and later sea ice break up (Oksman et al., 2019). Other sediment archives in northern Baffin Bay have inferred that sea-ice concentration gradually increases during the late Holocene in the western NOW due in part to reduced atmospheric temperatures from the neoglacial cooling period (Harning et al., 2025).

The period from 1680 to 1900 CE is typically associated with cooling across North America and Europe and is referred to as the Little Ice Age. During that period, glacial records in the Baffin Bay region indicate marine-terminating glaciers reaching their maximum extents (Carrivick et al., 2023). Furthermore, changes in microfossils (dinoflagellate cysts and diatoms), biomarkers (IP_{25} and HBI III) and other geochemical proxies (TOC) in marine sediment cores from the central NOW suggest a contracted, but still productive NOW during this interval (Jackson et al., 2021; Koerner et al., 2021; Ribeiro et al., 2021; Limoges et al., 2023; Koerner et al., 2025). Our results from the western NOW support this interpretation and suggest a longer-lasting seasonal sea-ice cover in the western NOW region.

2.7.2 Zone 1b (1800 to 1900 CE): Persistent southern marginal ice zone

Between 1800 to 1900 CE, core 2.7BC shows a fourfold increase in total diatom and *Chaetoceros* resting spore concentrations, accompanied by a pronounced shift in assemblage composition (Fig. 19) toward dominance by the MIZ group. Similar patterns have been reported in sediment cores located to the north and east (Knudsen et al. 2008), where an increase in sea-ice associated taxa during the late LIA was interpreted as evidence for increased sea-ice presence in the region. At site 2.7BC, the concurrent increase in total diatom concentrations and the dominance of early spring-blooming taxa suggests a shift either to greater sea ice influence or closer proximity to the MIZ at site 2.7BC.

In contrast, core 2.5BC shows no significant change in either diatom concentrations or assemblage composition during this interval (Fig. 18), indicating that the signal observed at 2.7BC reflects a localized response, likely related to ice-edge position. The period from 1800

to 1900 CE, marks the transition from the late LIA to the onset of modern warming in Baffin Bay (Grove, 2001). The strong increase in early-spring-blooming taxa at 2.7BC implies conditions favourable for spring blooms, possibly driven by a more offshore ice margin proximal to core 2.7BC. By comparison, sea-ice cover at 2.5BC may have remained thicker or more compact, thereby limiting spring bloom development.

2.7.3 Zone 2 (1900 to 2019 CE): Northward migration of marginal ice zone in the western NOW

At the start of the 20th century, total diatom and *Chaetoceros* resting spore concentrations decline at site 2.7BC, whereas site 2.5BC shows a two-step increase from 1900 to 2019 CE (Fig. 19). Despite these contrasting trends in concentrations, both cores show a shift in diatom assemblage composition characterized by an increased contribution of late(r)-blooming taxa, including *Rhizosolenia* spp., *Thalassiosira antarctica* var. *borealis* (resting spores), and *Porosira glacialis* (Figs. 18 & 19). A similar step-wise increase in total diatom concentrations is shown at the nearby Casq1 site (Fig. 14), driven by an increase in early spring-time taxa such as the *Fragilariopsis* genera (Limoges et al., 2023), in phase with a transition to a more unstable NOW associated with modern warming (Ribeiro et al. 2020). Our records align with this interpretation, as the growing contribution of these larger, later-blooming taxa suggests enhanced nutrient availability later in the growing season, potentially associated with cooler, more stratified waters via glacial melt in the late summer season (Figs. 18-20). Supporting this interpretation, *in situ* hydrographic data analyzed between 2006 and 2024 show freshening and increased nutrient availability in the Nares Strait waters (Barut et al., 2025). We note, however, that this interval only encompasses two data points for site 2.5BC and one for 2.7BC site.

Since the start of the 21st century, the western NOW region near site 2.5BC has been characterized by a pronounced sea-ice edge extending from Ellesmere Island into southern Smith Sound (Fig 14B-D). This persistent ice margin supports a strong early spring bloom, leading to increased export of cryopelagic taxa and diatom valves to the seafloor at the

location of core 2.5BC (Fig. 18). A similar shift in species composition is observed in Casq1, with a marked increase in cryopelagic taxa and diatom concentrations over the last ca. 100 years (Limoges et al., 2023; Fig. 18). The southern ice bridge in Nares Strait typically forms near the entrance to Smith Sound (Moore et al., 2021; Fig. 14B) and likely contributes to elevated primary production in regions adjacent to the ice bridges (Tachon et al., 2025). Both 2.5BC and Casq1 are located near this southern ice bridge during years of its formation (Moore et al. 2021), showing the role of ice-edge dynamics in promoting early spring-time production.

2.7.4 Importance of the MIZ to early primary production

Recent satellite-derived observations show a pan-Arctic increase in primary production linked to declining sea-ice extent and a longer open-water season, which enhances light availability and intensify productivity in the seasonally shifting MIZ (Ardyna et al., 2020). In early spring, the MIZ promotes intense primary production as meltwater-driven stratification stabilizes the surface layer and retains phytoplankton within the euphotic zone, while winter-replenished nutrients are available in surface waters (Barber et al., 2015). Additionally, the MIZ is more affected by storms and wave action, which in nutrient depleted seasons such as fall, can result in mixing that entrains and transports deep nutrients to the surface, also enhancing primary production. As a result, the MIZ plays an important role in facilitating phytoplankton blooms across-seasons and contributes significantly to net primary production (Perrette et al., 2011), often supporting communities dominated by small, lipid-rich pennate taxa that form an important food source for higher trophic levels (Vilgrain et al. 2021).

While these processes are well documented in modern observations, their longer-term variability remains poorly constrained. Our study reconstructs past changes in the position of the MIZ in northwestern Baffin Bay, providing a palaeoceanographic perspective on ice-edge dynamics. Our records point to a northward migration of the MIZ, consistent with regional trends previously suggested by Kalenitchenko et al., 2019. Our data also show a northward migration of peak diatom and *Chaetoceros* resting spore concentrations that aligns well with

these modern observations (Figs. 18 & 19). This reconstructed migration aligns with modern satellite data showing that primary production "hotspots" in northern Baffin Bay track the position of the sea ice edge in Nares Strait (Tachon et al., 2025). Similar trends have also been observed to the north in Kane Basin, with primary production shifting into the 21st century (Kvorning et al., 2025). Collectively, these results highlight the importance of the MIZ for early Arctic seasonal primary production and thus the ecosystem functioning in the region (i.e, grazing dynamics). As climate warming continues to alter Arctic sea-ice distribution and properties, our sedimentary records suggest that early primary producers, particularly MIZ-associated diatom assemblages, are likely to undergo reorganization.

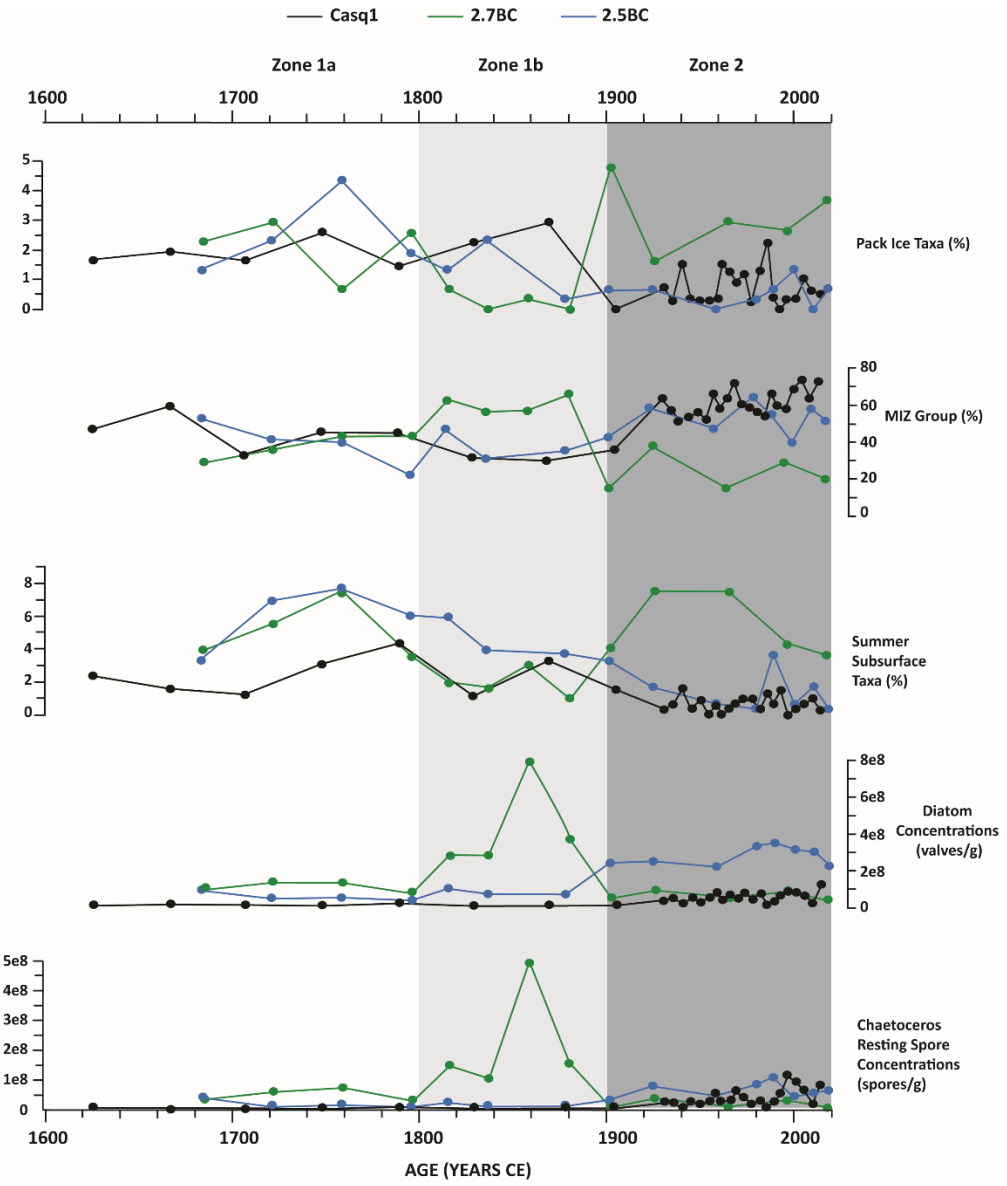

Figure 20. Relative abundances of Pack Ice Taxa (*Actinocyclus curvatulus* and *Melosira arctica*), MIZ Group (*Fossulaphycus arcticus, Fragilariopsis oceanica, Fragilariopsis reginae-jahniae, Fragilariopsis cynlindrus*), Summer subsurface Taxa (*Rhizosolenia* spp.), Total diatom concentrations, and *Chaetoceros* resting spore concentrations for the two cores from this study AMD19-2.7BC (green) and AMD19-2.5BC (blue) and Casq1 (black; Limoges et al., 2023). The gray boxes represent the environmental zones visually inferred from Core 2.5 and 2.7BC abundances.

2.8 CONCLUSIONS

Sub-fossil diatom assemblages from two marine sediment cores retrieved from northwestern Baffin Bay indicate a northward migration of the MIZ over the past ~400 years. Our results from surface sediment samples show that smaller pennate taxa typical of the MIZ are most abundant in the western region of the NOW, where sea ice influence is stronger. This is in contrast to the eastern portion of the NOW, which shows higher abundance of open-water centric taxa such as *Thalassiosira* and *Rhizosolenia*. Our results also show spatiotemporal differences between cores 2.5 and 2.7 BC mainly driven by changes in the abundances of the MIZ taxa, total diatom concentrations and total *Chaetoceros* resting spore concentrations over the last ca. 400 years. This points to the importance of localized forcings such as sea ice on primary production in the western NOW. As the Arctic continues to warm and the geometry of the MIZ evolve, the spatiotemporal variability of early spring production and its cascading effects on Arctic ecosystem dynamics, remain difficult to predict but important to monitor.

2.9 REFERENCES

Abelmann, A., Gersonde, R., Cortese, G., Kuhn, G., & Smetacek, V. (2006). Extensive phytoplankton blooms in the Atlantic sector of the glacial Southern Ocean. *Paleoceanography*, *21*(1). https://doi.org/10.1029/2005PA001199

Agafonova, E., Novichkova, E., Novigatsky, A., Kravchishina, M., Klyuvitkin, A., & Bulokhov, A. (2023). Diatom and Dinocyst Production, Composition and Flux from the Annual Cycle Sediment Trap Study in the Barents Sea. *Geosciences*, *13*(1). https://doi.org/10.3390/geosciences13010001

Aquino-López, M. A., Blaauw, M., Christen, J. A., & Sanderson, N. K. (2018). Bayesian Analysis of ^{210}Pb Dating. *Journal of Agricultural, Biological and Environmental Statistics*, *23*(3). https://doi.org/10.1007/s13253-018-0328-7

Ardyna, M., & Arrigo, K. R. (2020). Phytoplankton dynamics in a changing Arctic Ocean. *Nature Climate Change*, *10*(10), Article 10. https://doi.org/10.1038/s41558-020-0905-y

Arrigo, K. R., Dijken, G. van, & Pabi, S. (2008). Impact of a shrinking Arctic ice cover on marine primary production. *Geophysical Research Letters*, *35*(19), Article 19. https://doi.org/10.1029/2008GL035028

Arrigo, K. R., & van Dijken, G. L. (2015). Continued increases in Arctic Ocean primary production. *Progress in Oceanography*, *136*, 60–70. https://doi.org/10.1016/j.pocean.2015.05.002

Auger, J. D., Mayewski, P. A., Maasch, K. A., Schuenemann, K. C., Carleton, A. M., Birkel, S. D., & Saros, J. E. (2019). 2000 years of North Atlantic-Arctic climate. *Quaternary Science Reviews*, *216*, 1–17. https://doi.org/10.1016/j.quascirev.2019.05.020

Barber, D. G., Hop, H., Mundy, C. J., Else, B., Dmitrenko, I. A., Tremblay, J.-E., Ehn, J. K., Assmy, P., Daase, M., Candlish, L. M., & Rysgaard, S. (2015). Selected physical, biological and biogeochemical implications of a rapidly changing Arctic Marginal Ice Zone. *Progress in Oceanography, Overarching Perspectives of Contemporary and Future Ecosystems in the Arctic Ocean*, *139*, 122–150. https://doi.org/10.1016/j.pocean.2015.09.003

Barut, G., Tremblay, J.-É., Burgers, T., Schiffrine, N., Michel, C., & Ardyna, M. (2025). Water Mass Assemblages and Nutrient Dynamics in Nares Strait: A Multiyear Perspective. *Journal of Geophysical Research: Oceans*, *130*(12), e2025JC023074. https://doi.org/10.1029/2025JC023074

Booth, B. C., Larouche, P., Bélanger, S., Klein, B., Amiel, D., & Mei, Z.-P. (2002). Dynamics of *Chaetoceros socialis* blooms in the North Water. *Deep Sea Research Part II: Topical Studies in Oceanography, The International North Water Polynya Study*, *49*(22), 5003–5025. https://doi.org/10.1016/S0967-0645(02)00175-3

Carrivick, J. L., Boston, C. M., Sutherland, J. L., Pearce, D., Armstrong, H., Bjørk, A., Kjeldsen, K. K., Abermann, J., Oien, R. P., Grimes, M., James, W. H. M., & Smith, M. W. (2023). Mass Loss of Glaciers and Ice Caps Across Greenland Since the Little Ice Age. *Geophysical Research Letters*, *50*(10), e2023GL103950. https://doi.org/10.1029/2023GL103950

Crosta, X., & Koç, N. (2007). Chapter Eight Diatoms: From Micropaleontology to Isotope Geochemistry. In *Developments in Marine Geology* (Vol. 1, pp. 327–369). Elsevier. https://doi.org/10.1016/S1572-5480(07)01013-5

Freyria, N. J., Joli, N., & Lovejoy, C. (2021). A decadal perspective on north water microbial eukaryotes as Arctic Ocean sentinels. *Scientific Reports*, *11*(1), Article 1. https://doi.org/10.1038/s41598-021-87906-4

Grove, J. M. (2001). The Initiation of the "Little Ice Age" in Regions Round the North Atlantic. *Climatic Change*, *48*(1), 53–82. https://doi.org/10.1023/A:1005662822136

Hargrave, B. T., Walsh, I. D., & Murray, D. W. (2002). Seasonal and spatial patterns in mass and organic matter sedimentation in the North Water. *Deep Sea Research Part II: Topical Studies in Oceanography*, *49*(22), 5227–5244. https://doi.org/10.1016/S0967-0645(02)00187-X

Harning, D. J., Jennings, A. E., Holman, B., Kelleher, R. V., Feng, S., Brooks, N. K. S., Andrews, J. T., Marchitto, T., & Sepúlveda, J. (2025). Spatiotemporal Variability in the Holocene Extent of Pikialasorsuaq (North Water Polynya), Baffin Bay. *Paleoceanography and Paleoclimatology*, *40*(8), e2025PA005153. https://doi.org/10.1029/2025PA005153

Hegseth, E. N., & von Quillfeldt, C. (2022). The Sub-Ice Algal Communities of the Barents Sea Pack Ice: Temporal and Spatial Distribution of Biomass and Species. *Journal of Marine Science and Engineering*, *10*(2), Article 2. https://doi.org/10.3390/jmse10020164

Heide-Jørgensen, M. P., Burt, L. M., Hansen, R. G., Nielsen, N. H., Rasmussen, M., Fossette, S., & Stern, H. (2013). The Significance of the North Water Polynya to Arctic Top Predators. *AMBIO*, *42*(5), Article 5. https://doi.org/10.1007/s13280-012-0357-3

Heide-Jørgensen, M. P., Sinding, M.-H. S., Nielsen, N. H., Rosing-Asvid, A., & Hansen, R. G. (2016). Large numbers of marine mammals winter in the North Water polynya. *Polar Biology*, *39*(9), Article 9. https://doi.org/10.1007/s00300-015-1885-7

Jackson, R., Kvorning, A. B., Limoges, A., Georgiadis, E., Olsen, S. M., Tallberg, P., Andersen, T. J., Mikkelsen, N., Giraudeau, J., Massé, G., Wacker, L., & Ribeiro, S. (2021). Holocene polynya dynamics and their interaction with oceanic heat transport in northernmost Baffin Bay. *Scientific Reports*, *11*(1), 10095. https://doi.org/10.1038/s41598-021-88517-9

Joli, N., Gosselin, M., Ardyna, M., Babin, M., Onda, D. F., Tremblay, J.-É., & Lovejoy, C. (2018). Need for focus on microbial species following ice melt and changing freshwater regimes in a Janus Arctic Gateway. *Scientific Reports*, *8*(1), Article 1. https://doi.org/10.1038/s41598-018-27705-6

Kalenitchenko, D., Joli, N., Potvin, M., Tremblay, J.-É., & Lovejoy, C. (2019). Biodiversity and Species Change in the Arctic Ocean: A View Through the Lens of Nares Strait. *Frontiers in Marine Science*, *6*. https://doi.org/10.3389/fmars.2019.00479

Kirillov, S., Dmitrenko, I., Babb, D. G., Ehn, J. K., Koldunov, N., Rysgaard, S., Jensen, D., & Barber, D. G. (2022). The role of oceanic heat flux in reducing thermodynamic ice growth in Nares Strait and promoting earlier collapse of the ice bridge. *Ocean Science*, *18*(5), Article 5. https://doi.org/10.5194/os-18-1535-2022

Kiorboe, T., Hansen, J., Alldredge, A., Jackson, G., Passow, U., Dam, H., Drapeau, D., Waite, A., & Garcia, C. (1996). Sedimentation of phytoplankton during a diatom bloom: Rates and mechanisms. *Journal of Marine Research*, *54*(6). https://elischolar.library.yale.edu/journal_of_marine_research/2212

Knudsen, K. L., Stabell, B., Seidenkrantz, M.-S., Eiríksson, J., & Blake, W. (2008). Deglacial and Holocene conditions in northernmost Baffin Bay: Sediments, foraminifera, diatoms and stable isotopes. *Boreas*, *37*(3), Article 3. https://doi.org/10.1111/j.1502-3885.2008.00035.x

Koerner, K. A., Limoges, A., Pike-Connolly, E., Van Nieuwenhove, N., & Rochon, A. (2025). Early impacts of Arctic amplification in the western North Water Polynya: A 400-year perspective. *Marine Micropaleontology*, *197–198*, 102470. https://doi.org/10.1016/j.marmicro.2025.102470

Koerner, K., Limoges, A., Van Nieuwenhove, N., Richerol, T., Massé, G., & Ribeiro, S. (2021). Late Holocene sea-surface changes in the North Water polynya reveal freshening of northern Baffin Bay in the 21st century. *Global and Planetary Change*, 103642. https://doi.org/10.1016/j.gloplacha.2021.103642

Krause, J. W., Schulz, I. K., Rowe, K. A., Dobbins, W., Winding, M. H. S., Sejr, M. K., Duarte, C. M., & Agustí, S. (2019). Silicic acid limitation drives bloom termination and potential carbon sequestration in an Arctic bloom. *Scientific Reports*, *9*(1), 8149. https://doi.org/10.1038/s41598-019-44587-4

Krawczyk, D. W., Kryk, A., Juggins, S., Burmeister, A., Pearce, C., Seidenkrantz, M.-S., Moros, M., Høyer, J. L., Kuijpers, A., & Witkowski, A. (2021). Spatio-temporal changes in ocean conditions and primary production in Baffin Bay and the Labrador Sea. *Palaeogeography, Palaeoclimatology, Palaeoecology*, *563*, 110175. https://doi.org/10.1016/j.palaeo.2020.110175

Kvorning, A. B., Sicre, M.-A., Luetzenburg, G., Schmidt, S., Andersen, T. J., Klein, V., Georgiadis, E., Limoges, A., Giraudeau, J., Bjørk, A. A., Larsen, N. K., & Ribeiro, S. (2025). Cryosphere and ocean variability in Kane Basin since the 18th century: Insights from two marine multi-proxy records. *EGUsphere*, 1–34. https://doi.org/10.5194/egusphere-2025-2641

Leu, E., Mundy, C. J., Assmy, P., Campbell, K., Gabrielsen, T. M., Gosselin, M., Juul-Pedersen, T., & Gradinger, R. (2015). Arctic spring awakening – Steering principles behind the phenology of vernal ice algal blooms. *Progress in Oceanography*, *139*, 151–170. https://doi.org/10.1016/j.pocean.2015.07.012

Lizotte, M., Levasseur, M., Galindo, V., Gourdal, M., Gosselin, M., Tremblay, J.-É., Blais, M., Charette, J., & Hussherr, R. (2020). Phytoplankton and dimethylsulfide dynamics at two contrasting Arctic ice edges. *Biogeosciences*, *17*(6), 1557–1581. https://doi.org/10.5194/bg-17-1557-2020

Limoges, A., Ribeiro, S., Van Nieuwenhove, N., Jackson, R., Juggins, S., Crosta, X., & Weckström, K. (2023). Marine diatoms record Late Holocene regime shifts in the Pikialasorsuaq ecosystem. *Global Change Biology*, *29*(23), Article 23. https://doi.org/10.1111/gcb.16958

Limoges, A., Weckström, K., Ribeiro, S., Georgiadis, E., Hansen, K. E., Martinez, P., Seidenkrantz, M.-S., Giraudeau, J., Crosta, X., & Massé, G. (2020). Learning from the past: Impact of the Arctic Oscillation on sea ice and marine productivity off northwest Greenland over the last 9,000 years. *Global Change Biology*, *26*(12), Article 12. https://doi.org/10.1111/gcb.15334

Lovejoy, C., Legendre, L., & Price, N. M. (2002). Prolonged diatom blooms and microbial food web dynamics: Experimental results from an Arctic polynya. *Aquatic Microbial Ecology*, *29*(3), Article 3. https://doi.org/10.3354/ame029267

Madsen, S. J., Nielsen, T. G., Tervo, O. M., & Söderkvist, J. (2008). Importance of feeding for egg production in Calanus finmarchicus and C. glacialis during the Arctic spring. *Marine Ecology Progress Series*, *353*, 177–190. https://doi.org/10.3354/meps07129

Moore, G. W. K., Howell, S. E. L., Brady, M., Xu, X., & McNeil, K. (2021). Anomalous collapses of Nares Strait ice arches leads to enhanced export of Arctic sea ice. *Nature Communications*, *12*(1), Article 1. https://doi.org/10.1038/s41467-020-20314-w

Münchow, A., Falkner, K. K., & Melling, H. (2015). Baffin Island and West Greenland Current Systems in northern Baffin Bay. *Progress in Oceanography*, *132*, 305–317. https://doi.org/10.1016/j.pocean.2014.04.001

Oksman, M., Juggins, S., Miettinen, A., Witkowski, A., & Weckström, K. (2019). The biogeography and ecology of common diatom species in the northern North Atlantic, and their implications for paleoceanographic reconstructions. *Marine Micropaleontology*, *148*, 1–28. https://doi.org/10.1016/j.marmicro.2019.02.002

Pedro, S., Lemire, M., Hoover, C., Saint-Béat, B., Janjua, M., Herbig, J., Geoffroy, M., Yunda-Guarin, G., Moisan, M.-A., Boissinot, J., Tremblay, J.-É., Little, M., Chan, L., Babin, M., Kenny, T.-A., & Maps, F. (2023). Structure and function of the western Baffin Bay coastal and shelf ecosystem. *Elementa: Science of the Anthropocene*, *11*(1). https://doi.org/10.1525/elementa.2022.00015

Perrette, M., Yool, A., Quartly, G. D., & Popova, E. E. (2011). Near-ubiquity of ice-edge blooms in the Arctic. *Biogeosciences*, *8*(2), 515–524. https://doi.org/10.5194/bg-8-515-2011

Poulin, M., Underwood, G. J. C., & Michel, C. (2014). Sub-ice colonial Melosira arctica in Arctic first-year ice. *Diatom Research*, *29*(2), 213–221. https://doi.org/10.1080/0269249X.2013.877085

Rantanen, M., Karpechko, A. Y., Lipponen, A., Nordling, K., Hyvärinen, O., Ruosteenoja, K., Vihma, T., & Laaksonen, A. (2022). The Arctic has warmed nearly four times faster than the globe since 1979. *Communications Earth & Environment*, *3*(1), 168. https://doi.org/10.1038/s43247-022-00498-3

R Core Team. (2022). R: A language and environment for statistical computing. R Foundation for Statistical Computing. https://www.R-project.org

Ribeiro, C. G., Lopes dos Santos, A., Trefault, N., Marie, D., Lovejoy, C., & Vaulot, D. (2024). Arctic phytoplankton microdiversity across the marginal ice zone: Subspecies vulnerability to sea-ice loss. *Elementa: Science of the Anthropocene*, *12*(1), 00109. https://doi.org/10.1525/elementa.2023.00109

Ribeiro, S., Limoges, A., Massé, G., Johansen, K. L., Colgan, W., Weckström, K., Jackson, R., Georgiadis, E., Mikkelsen, N., Kuijpers, A., Olsen, J., Olsen, S. M., Nissen, M., Andersen, T. J., Strunk, A., Wetterich, S., Syväranta, J., Henderson, A. C. G., Mackay, H., … Davidson, T. A. (2021). Vulnerability of the North Water ecosystem to climate change. *Nature Communications*, *12*(1), 4475. https://doi.org/10.1038/s41467-021-24742-0

Riedel, A., Michel, C., Gosselin, M., & LeBlanc, B. (2008). Winter–spring dynamics in sea-ice carbon cycling in the coastal Arctic Ocean. *Journal of Marine Systems*, *74*(3), 918–932. https://doi.org/10.1016/j.jmarsys.2008.01.003

Rolph, R. J., Feltham, D. L., & Schröder, D. (2020). Changes of the Arctic marginal ice zone during the satellite era. *The Cryosphere*, *14*(6), 1971–1984. https://doi.org/10.5194/tc-14-1971-2020

RStudio Team. (2022). RStudio: Integrated development environment for R. RStudio, PBC. https://posit.co/products/open-source/rstudio/?sid=1

Rysgaard, S., Boone, W., Carlson, D., Sejr, M. K., Bendtsen, J., Juul-Pedersen, T., Lund, H., Meire, L., & Mortensen, J. (2020). An Updated View on Water Masses on the pan-West Greenland Continental Shelf and Their Link to Proglacial Fjords. *Journal of Geophysical Research: Oceans*, *125*(2), Article 2. https://doi.org/10.1029/2019JC015564

Saint-Béat, B., Fath, B. D., Aubry, C., Colombet, J., Dinasquet, J., Fortier, L., Galindo, V., Grondin, P.-L., Joux, F., Lalande, C., LeBlanc, M., Raimbault, P., Sime-Ngando, T., Tremblay, J.-E., Vaulot, D., Maps, F., & Babin, M. (2020). Contrasting pelagic ecosystem functioning in eastern and western Baffin Bay revealed by trophic network modeling. *Elementa: Science of the Anthropocene*, *8*, 1. https://doi.org/10.1525/elementa.397

Simpson, G. L. (2018). Modelling Palaeoecological Time Series Using Generalised Additive Models. Frontiers in Ecology and Evolution, 6. https://doi.org/10.3389/fevo.2018.00149

Simpson, G. L. (2022). gratia: Graceful ggplot-based graphics and other functions for GAMs fitted using mgcv. R package version 0.7.3. https://gavinsimpson.github.io/gratia

Tachon, F., Nieto, K., Massicotte, P., Archambault, P., Latil, M., Bélanger, S., Babin, M., Attard, K., & Ardyna, M. (2025). *Sea-ice arches structure Arctic primary production hotspots at the Last Ice Area gateway*. Research Square. https://doi.org/10.21203/rs.3.rs-7827911/v1

Tang, C. C. L., Ross, C. K., Yao, T., Petrie, B., DeTracey, B. M., & Dunlap, E. (2004). The circulation, water masses and sea-ice of Baffin Bay. *Progress in Oceanography*, *63*(4), Article 4. https://doi.org/10.1016/j.pocean.2004.09.005

Terrado, R., Lovejoy, C., Massana, R., & Vincent, W. F. (2008). Microbial food web responses to light and nutrients beneath the coastal Arctic Ocean sea ice during the winter–spring transition. *Journal of Marine Systems*, *74*(3), 964–977. https://doi.org/10.1016/j.jmarsys.2007.11.001

Toullec, J., Moriceau, B., Vincent, D., Guidi, L., Lafond, A., & Babin, M. (2021). Processes controlling aggregate formation and distribution during the Arctic phytoplankton spring bloom in Baffin Bay. *Elementa: Science of the Anthropocene*, *9*(1), 00001. https://doi.org/10.1525/elementa.2021.00001

Tremblay, J.-É., & Gagnon, J. (2009). The effects of irradiance and nutrient supply on the productivity of Arctic waters: A perspective on climate change. In J. C. J. Nihoul & A. G. Kostianoy (Eds.), *Influence of Climate Change on the Changing Arctic and Sub-Arctic Conditions* (pp. 73–93). Springer Netherlands. https://doi.org/10.1007/978-1-4020-9460-6_7

Tremblay, J.-É., Gratton, Y., Carmack, E. C., Payne, C. D., & Price, N. M. (2002). Impact of the large-scale Arctic circulation and the North Water Polynya on nutrient inventories in Baffin Bay. *Journal of Geophysical Research: Oceans*, *107*(C8), Article C8. https://doi.org/10.1029/2000JC000595

Tremblay, J.-É., Michel, C., Hobson, K. A., Gosselin, M., & Price, N. M. (2006). Bloom dynamics in early opening waters of the Arctic Ocean. *Limnology and Oceanography*, *51*(2), 900–912. https://doi.org/10.4319/lo.2006.51.2.0900

Vilgrain, L., Maps, F., Picheral, M., Babin, M., Aubry, C., Irisson, J.-O., & Ayata, S.-D. (2021). Trait-based approach using in situ copepod images reveals contrasting ecological patterns across an Arctic ice melt zone. *Limnology and Oceanography*, *66*(4), 1155–1167. https://doi.org/10.1002/lno.11672

Vincent, R. F. (2019). A Study of the North Water Polynya Ice Arch using Four Decades of Satellite Data. *Scientific Reports*, *9*. https://doi.org/10.1038/s41598-019-56780-6

Vincent, R. F. (2020). An Examination of the Non-Formation of the North Water Polynya Ice Arch. *Remote Sensing*, *12*(17), Article 17. https://doi.org/10.3390/rs12172712

von Quillfeldt, C. H. (1997). Distribution of diatoms in the Northeast Water Polynya, Greenland. *Journal of Marine Systems*, *10*(1), Article 1. https://doi.org/10.1016/S0924-7963(96)00056-5

Weckström, K., Roche, B. R., Miettinen, A., Krawczyk, D., Limoges, A., Juggins, S., Ribeiro, S., & Heikkilä, M. (2020). Improving the paleoceanographic proxy tool kit – On the biogeography and ecology of the sea ice-associated species Fragilariopsis oceanica, Fragilariopsis reginae-jahniae and Fossula arctica in the northern North Atlantic. *Marine Micropaleontology*, *157*, 101860. https://doi.org/10.1016/j.marmicro.2020.101860

Wood, S. N. (2017). Generalized Additive Models: An Introduction with R, Second Edition (2nd ed.). Chapman and Hall/CRC. https://doi.org/10.1201/9781315370279

CHAPITRE 3
DIFFÉRENTES TRAJECTOIRES DES EAUX DOUCES VERS LE NORD-OUEST DE LA BAIE DE BAFFIN AU COURS DES 1200 DERNIÈRES ANNÉES, RECONSTITUÉES À L'AIDE DE PROXIES SÉDIMENTAIRES ET BIOGÉNIQUES

3.1 RÉSUMÉ EN FRANÇAIS

Le réchauffement de l'Arctique a accéléré la fonte des glaces et des glaciers, augmentant ainsi les apports d'eau douce dans le milieu marin. La polynie des Eaux du Nord, située au nord de la baie de Baffin, est particulièrement sensible à ces apports d'eau douce, de par sa proximité avec les glaciers canadiens et groenlandais et sa situation géographique le long des voies d'écoulement de l'océan Arctique via les détroits de Nares, de Jones et de Lancaster. Nous avons étudié l'influence des apports polaires et glaciaires sur les conditions passées des eaux de mer de surface à partir d'une carotte sédimentaire prélevée à 40 km au sud-est de l'île Devon, couvrant les quelques 1200 dernières années. Les analyses ont porté sur la minéralogie globale quantitative, la granulométrie et les assemblages de kystes de dinoflagellés afin d'identifier les sources d'eau douce et leurs impacts. Nos résultats mettent en évidence trois intervalles distincts : 1) 750–1600 CE caractérisé par des sédiments mal triés et riches en sable provenant de sources distales et par de faibles concentrations de kystes de dinoflagellés (dinokystes), indiquant un transport de sédiments plus distal ; 2) 1600–1900 CE., avec une augmentation des débris transportés par les glaces et une dominance des taxons d'eau froide (*Islandinium minutum* subsp. *minutum*, *Islandinium* ? *cezare* et *Echinidinium karaense*), suggérant une activité glaciaire accrue et une bordure de glace persistante ; et 3) 1920–2019 CE., montrant un apport accru de sédiments proximaux et des contributions plus importantes de taxons mixotrophes (*Operculodinium centrocarpum* et les kystes de *Pentapharsodinium dalei*), indiquant des eaux douces plus stratifiées et d'origine atlantique, probablement issues de la calotte glaciaire de Devon. Nos données montrent des apports variables de sources sédimentaires distales et proximales qui sont contemporains des changements dans les assemblages de kystes de dinoflagellés, montrant une augmentation

progressive des apports glaciaires proximaux dans le nord de la baie de Baffin, signe d'un réchauffement arctique accru.

Cet article « *Différentes trajectoires des eaux douces vers le nord-ouest de la baie de Baffin au cours des 1 200 dernières années, reconstituées à l'aide de proxies sédimentaires et biogéniques* » est en cours de préparation pour être soumis à la revue *JGR Biogeosciences*. J'ai effectué la revue de la littérature, les analyses de tous les échantillons (modèle d'âge, dinokystes, granulométrie, qXRD et MSCL), les analyses statistiques et la rédaction du manuscrit. Audrey Limoges, deuxième autrice, a apporté des modifications et des commentaires à l'ensemble du manuscrit. Jean-Carlos, troisième auteur, a réalisé les analyses qXRD dans powdR et SedUnMix et a également participé à la révision du manuscrit. André Rochon, dernier auteur, a apporté des modifications et des commentaires au manuscrit.

3.2 ABSTRACT

Arctic warming has accelerated sea ice and glacier melt, increasing freshwater input into the marine environment. The North Water Polynya (NOW), in northern Baffin Bay, is sensitive to such input due to its proximity to Canadian and Greenland glaciers and its connection to Arctic Ocean outflow via Nares Strait, Jones Sound and Lancaster Sound. We investigated the influence of polar and glacial outflows on past sea-surface conditions using a sediment core collected 40 km southeast of Devon Island, spanning the last ca. 1200 years. Analyses of quantitative bulk mineralogy, grain size, and dinoflagellate cyst assemblages allowed us to identify freshwater sources and assess their impacts on surface waters. Our results highlight three distinct intervals: 1) 750–1600 CE, characterized by poorly-sorted, sand-rich sediments and low dinoflagellate cyst (dinocyst) conditions, indicating distal sediment transport; 2) 1600–1900 CE, with elevated ice-rafted debris and dominance of cold-water taxa (*Islandinium minutum* subsp. *minutum*, *Islandinium*? *cezare*, and *Echinidinium karaense*), suggesting enhanced glacial activity and a persistent ice edge; and 3) 1920-2019 CE, showing increased proximal sediment input and higher contributions of mixotrophic taxa (*Operculodinium centrocarpum* and the cysts of *Pentapharsodinium dalei*), indicative of increased influence of both Devon Ice Cap melt waters and Atlantic-derived waters. Our records show varying input of distal and proximal sediment sources that are coeval with changes in dinoflagellate cyst assemblages, providing a paleoceanographic record of accelerated Arctic warming and its influence on surface water conditions in the NOW.

3.3 UNDERSTANDING DIFFERING FRESHWATER OUTFLOW PATHWAYS INTO NORTHWESTERN BAFFIN BAY OVER THE LAST CA. 1200 YEARS USING SEDIMENTARY AND BIOGENIC PROXIES

Kelsey A. Koerner[1], Audrey Limoges[2], Jean-Carlos Montero-Serrano[1], and André Rochon[1]

Institutions :

1. Institut des sciences de la mer (ISMER), Université du Québec à Rimouski (UQAR), Geotop & Québec-Océan, Rimouski, QC, Canada
2. Department of Earth Sciences, University of New Brunswick (UNB), Fredericton, NB, Canada

3.4 INTRODUCTION

The Canadian Arctic Archipelago (CAA) is host to over 300 marine-terminating glaciers, accounting for up to 14% of the Earth's glacier and ice cap area (Radić & Hock, 2010; Sharp et al., 2011). Many of these glaciers have experienced substantial retreat and mass loss since the mid-20th century, largely attributable to enhanced surface melting in recent decades associated with anthropogenic climate change (Noël et al., 2018; Cook et al., 2019). This has led to increased glacial discharge into local fjord systems and, more broadly, into Baffin Bay, particularly during the summer melt season (Bhatia et al., 2021; Hopwood et al., 2018, Williams et al., 2021). As the Arctic is projected to continue to warm in the coming decades, both land and marine-terminating glaciers in the CAA are likely to continue melting (Wychen et al., 2020), further contributing freshwater and nutrient input to the marine ecosystem.

Both land and marine terminating glaciers influence marine systems through the export of meltwater and sediment. Land-terminating glaciers deliver meltwater, nutrients and particulate matter through riverine outflow. Marine-terminating glaciers introduce similar materials through subglacial discharge and glacimarine processes, such as calving and sediment plumes. These inputs can influence primary productivity and alter coastal biogeochemical cycles (e.g., Hopwood et al., 2020). For example, enhanced primary production near marine-terminating glaciers (Meire et al., 2017; Hoshiba et al., 2024) has

been linked to important delivery of macro- and micro-nutrients to the marine environment during both the early spring (Vonnahme et al., 2021) and summer melt/runoff season (Meire et al., 2017; Kanna et al., 2018; Bhatia et al. 2013), a period when nutrients typically become limiting following the plankton bloom (Arrigo et al., 2017). This localized input results in brief increases in primary production near marine terminating glaciers (Hawkings, 2021), resulting in increased food availability for grazers, such as copepods and fish stocks (Losapio et al., 2025). At broader spatial scales, the input of metal nutrients (e.g., Fe, Mn) via meltwater and glacial sediments can further enhance productivity (Bhatia et al., 2013; Bhatia et al., 2021), particularly in regions like northern Baffin Bay where these elements are otherwise present at low concentrations (Tremblay et al., 2015; Colombo et al., 2020).

Glacial discharge typically influences the stratification and mixing of the water column through two main mechanisms: 1) surface meltwater that transports atmospherically deposited debris and nutrients, forming a stratified surface layer (Hodson, 2005); and 2) buoyant subsurface flows containing bedrock-derived material, which, due to density differences with the overlying seawaters, eventually upwells at locations distal to the marine terminus (Straneo and Cenedese, 2015). Surface meltwater from glaciers drains during early spring and summer into regions proximal to the glacier terminus but may not always be nutrient rich (Halbach et al., 2019). In contrast, subsurface meltwater flows between the bedrock and base of the glacier, transporting debris and nutrients sourced from the underlying bedrock, with nutrient concentrations varying according to bedrock composition (Halbach et al., 2019). These buoyant plumes are released at depth, rising through the water column and often upwelling tens to hundreds of kilometers from the glacial terminus (Hopwood et al., 2020).

Northern Baffin Bay is influenced by glacial outflow from the CAA and northern Greenland, where glacial outflow merge with southward-flowing Arctic waters before converging in the region (Tang et al., 2004). Nutrient inventories in northern Baffin Bay are largely dictated by the interactions of these main oceanic currents (Tremblay et al., 2002; Münchow et al., 2015), supplemented by inputs derived from glacial discharge in

surrounding catchments (Bhatia et al., 2013; 2021). The region hosts the North Water (NOW) polynya, an area of important biological productivity (Bryndum-Buchholz et al., 2024), where nutrient supply plays a key role in regulating the timing and magnitude of primary production (Joli et al., 2018). However, the influence of glacial outflow on primary production in northern Baffin Bay is poorly constrained, particularly over long timescales and across the wide spatial extent of the region.

Due to the contrasting bedrock compositions of the CAA and Greenland (Fig. 21), the mineralogy of marine seafloor sediments can be used as a proxy for tracing sediment transport pathways driven by oceanic currents. Several studies in northern Baffin Bay have demonstrated the utility of sediment minerology for identifying and characterizing the provenance of detrital particles (Andrews et al., 2018; 2019). Moreover, Holocene-scale reconstructions of oceanic transport pathways has been conducted in eastern Baffin Bay (Caron et al., 2020) and northern Nares Strait (Okuma et al., 2023; Stevenard et al., 2022; Jennings et al., 2019; Georgiadis et al., 2018).

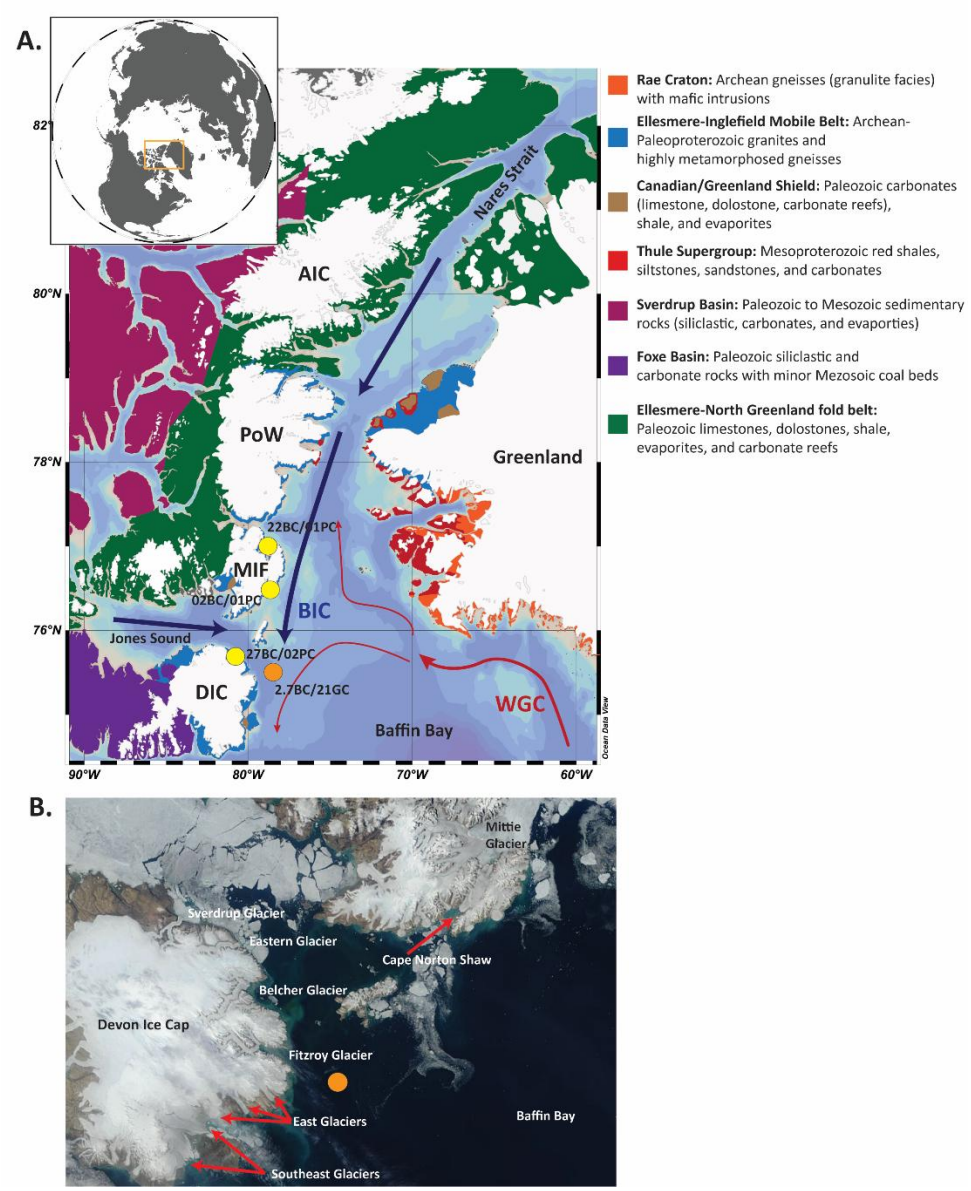

Figure 21. A) Map of northern Baffin Bay showing the bedrock geology, modified from Braquart et al. (2025) and Stevenard et al. (2021). The location of cores 2.7BC/21GC are shown by the orange circle (this study), the other sediment archives discussed in this paper are shown by a yellow circle 22BC/01PC (Bracquart et al., 2021), 02BC/01PC (Stevenard et al., 2021), 27BC/02PC (Brossard, 2021). The main oceanographic currents are shown where WGC = West Greenland Current and BIC= Baffin Current. The red lines represent relatively warm and saline (sub)-surface waters and the blue lines represent cool and fresher surface waters. B) Satellite image of Devon Ice Cap, Manson Ice Field, and Jones Sound highlighting sediment-laden meltwater discharge from the glaciers (light blue-green), and the position of the study core in orange. AIC = Agassiz Ice Cap, PoW = Prince of Wales Ice Field, MIF = Manson Ice Field, DIC = Devon Ice Cap.

Here, we test the hypothesis that variations in the sediment provenance can be used to identify the sources of freshwater export into northern Baffin Bay and evaluate their influence on sea-surface conditions in the western NOW. To this purpose, we analyzed sedimentological and mineralogical properties together with dinoflagellate cyst (dinocyst) assemblages from sediment cores collected approximately 40 km southeast of two marine-terminating glaciers (Belcher and Fitzroy) of the Devon Ice Cap, located on Devon Island (Fig. 21). These analyses aimed to (1) reconstruct the sediment sources and associated changes in freshwater export pathways into northern Baffin Bay, and (2) document variations in sea-surface conditions and explore potential co-variations between glacial influence and surface ocean dynamics through time. We build on a previously published study (Koerner et al., 2025) by extending the analysis of the sedimentary record further back in time (i.e., covering the last ca. 1200 years) and by increasing the sample resolution, allowing us to capture distinct shifts in Arctic climate conditions: the Medieval Climate Anomaly (MCA; 950 to 1250 CE; Mann et al., 2009), the Little Ice Age (LIA; 1400 to 1700 CE; Mann et al., 2009), and the Modern Warming (MoW; ~1920 to present; Wood & Overland, 2010), periods associated with well-documented fluctuations in glacial extent and retreat (Cook et al., 2019).

3.5 Regional Setting

Northwestern Baffin Bay is at the confluence of Arctic-sourced waters flowing southward and Atlantic-sourced waters entering from the south via the West Greenland Current (WGC; Tang et al., 2004). The southward-flowing Baffin Current, composed of modified Pacific and Arctic waters (Jones 2001; Münchow et al., 2007; Fig. 21), originates from outflows through Nares Strait and Jones Sound. It is relatively cool (> -1 °C) and fresh (<34) and receives important freshwater input from glacial outflow along the coasts of the CAA and Greenland (Fig. 21). In contrast, the WGC carries warmer (> 2 °C), more saline (~34) Atlantic-sourced waters along the coast of Greenland, ranging at depths from 700 to 200 m, becoming shallower as it flows northward in Baffin Bay. The WGC typically upwells in northern Baffin Bay and circulates in a cyclonic pattern before turning southward along the western margin of Baffin Bay (Rysgaard et al., 2020; Fig. 21). In addition to these main

currents, localized freshwater inputs from glacial runoff along both the Canadian and Greenland coasts further influence surface conditions in the region (Fig. 21).

Northern Baffin Bay is also host to the North Water (NOW) polynya, or *Pikialasorsuaq* in Greenlandic (Eegeesiak et al., 2017) and *Sarvarjuaq* in Inuktitut (North Qikiqtaaluk), which is an area of ice-free conditions in a region where ice is normally expected (Morales Maqueda, 2004). The NOW is the largest recurrent polynya in the Arctic, and an area of enhanced primary production and ecological activity (e.g., Barber and Massom, 2007). The polynya typically forms in early March and stays open until the rest of Baffin Bay becomes ice-free in the summer. The open waters of the NOW strongly associated with the consolidation of ice bridges in Nares Strait, preventing ice flow from the Arctic into the region (Moore et al., 2021). Additional factors that aid in maintaining open water conditions in the polynyas are northerly winds that push newly formed ice out of the region, along with the upwelling of the WGC along the eastern region of the NOW. Over the last ca. 30 years, the ice bridges in Nares Strait are becoming less stable and more variable, resulting in changes to the NOW dynamics (Vincent, 2019; Moore et al., 2021). Ice bridges that form in Jones Sound also aid in preventing ice flow out of Jones Sound into northwestern Baffin Bay (Bi et al., 2019).

The regional bedrock geology of northern Baffin Bay is dominated by five Paleoproterozoic-aged geologic groups, composed mostly of siliclastic rocks with minor carbonate contributions (Fig. 21). The most extensive is the Ellesmere-North Greenland fold belt, which consists predominately of limestones, dolostones, shale, evaporites and carbonate reefs. This group forms most of the bedrock in Nares Strait and western Jones Sound (Harrison et al., 2011; Fig. 21). The Ellesmere-Inglefield Mobile Belt surrounds the Prince of Wales Ice Field, Manson Ice Field, and the Devon Ice Cap, and consists of Archean granites and gneisses (Andrews et al., 2019). In the western region of Devon Island, the Foxe Basin group, consists of Paleozoic siliciclastic-carbonate rocks with some minor coal-bearing beds (Harrison & St-Onge, 2023). Along the western coast of Greenland lie two additional groups: the Thule Supergroup, composed of red sedimentary rocks with some carbonates

(Harrison et al., 2011) and the Rae Craton, which consists of Archean gneisses with mafic intrusions (Harrison et al., 2011).

The Devon Ice Cap is approximately 14,000 km^2 and is bordered by marine-terminating glaciers along the northern, eastern, and southern shores of Devon Island (Fig. 21B). This ice cap has been the focus of studies aiming to understand glacial discharge and ice dynamics (e.g., Wychen et al., 2017). Over the last ca. 20-30 years, observations have revealed a general receding trend, though with spatially variable dynamics across the ice cap (Wychen et al., 2020). More recent work has examined nutrient export from the northern margin of the Devon Ice Cap into Jones Sound and their impact on marine primary production (Bhatia et al., 2021; Williams et al., 2021) showing that nutrient-rich glacial plumes flow into Jones Sound, and eventually into Baffin Bay, providing an important contribution of nutrients to the surrounding water column. In addition, Brossard (2021) analyzed marine sediment cores from Belcher Inlet to investigate glacier dynamics throughout the Holocene and showed that the Belcher Glacier dynamics are influenced by atmospheric climate trends. Building on this foundation, our study offers new insight by examining how freshwater and sediment export from the well-studied Devon Ice Cap may influence more distal marine environments, particularly in northern Baffin Bay.

3.6 METHODS

3.6.1 Core Collection

Sediment cores AMD19-2.7BC and AMD1902-21GC (hereafter referred to as 2.7BC and 21GC; Table 8) were collected in 2019 onboard the CCGS Amundsen using a box core and gravity corer, respectively. Both cores were retrieved from the same location on the continental shelf as part of ArcticNet Arctic Mapping Seafloor and Dissemination Project. Coring locations were selected based on high-resolution sub-bottom and swath bathymetric data to target continuous Holocene sedimentary sequences and avoid areas affected by mass wasting or disturbance. 2.7BC was sub-sampled at every 1-cm intervals, whereas 21GC was sub-sampled at 0.5 to 1-cm intervals. All subsamples were stored at 4 °C until analysis.

Table 8. Sediment cores used in this study, with their geographic locations, total lengths, and the water depths at which they were retrieved.

Core	Latitude	Longitude	Length (cm)	Water Depth (m)
AMD19-2.7BC	75.482°	-78.675	40	521
AMD1902-21GC	75.482°	-78.676	223.5	522

3.6.2 X-Ray Imaging and Multi-Sensor Core Logger Analysis (MSCL)

Split sections of 2.7BC and 21GC were scanned with a GEOTEK X-Ray Computed Tomography (X-CT) system at the marine geology lab from the *Institut des sciences de la mer* (ISMER; Rimouski, Canada). X-CT imaging was used to reveal different sedimentary structures, and to identify large particles within the core (St-Onge et al., 2007). Both whole and split core sections were also analysed using the GEOTEK Multi Sensor Core to measure low-field volumetric magnetic susceptibility (k_{LF}), and the split sections were then analysed for their diffuse spectral reflectance measurements using a Minolta CM-2600d spectrophotometer to characterize sediment color (L*, a*, b*; Fig. 30) in CIE color space. Measurements of k_{LF} and sediment color were conducted at 0.5-cm intervals for 2.7BC and 1-cm intervals for 21GC.

3.6.3 Composite Age Model: Cores 2.7BC and 21GC

2.7BC and 21GC were analyzed for their ^{210}Pb activity by alpha spectrometry (Ghaleb, 2009; Fig. 28). For 2.7BC, measurements were done at every 1 cm for the first 20 cm and every 5 cm for the remainder of the core. For 21GC, measurements were done at every 1 cm for the first 20 cm. A spike of ^{209}Po was added to each sediment sample, which was then digested using a series of acids: nitric and hydrochloric acid (HNO_3 and HCl), hydrofluoric acid (HF), boric acid (H_3BO_4), hydrogen peroxide (H_2O_2), and a secondary HCl treatment. The resulting solutions were plated onto silver disks to collect ^{210}Po. Alpha emissions were subsequently counted using an EGG-Ortec Type 576Atm alpha spectrometer at Geotop Research Center (Montreal, Canada).

Material suitable for radiocarbon (^{14}C) dating in both cores was limited as both benthic and planktonic foraminifera were virtually absent. Therefore, five shells and shell fragments recovered near the base of the core were selected for ^{14}C dating (Table 9). Samples were pre-treated (leaching) at the Radiocarbon Dating Laboratory at Université Laval and subsequently analyzed at the Keck Carbon Cycle Accelerator Mass Spectrometry Facility at the University of California, Irvine (USA).

Table 9. Depths, ages, and type of dated material for AMD1902-21GC.

Sample depth (cm)	Lab ID	Material	^{14}C age (years BP)	Error (years BP)	$\delta^{13}C$ ‰
129.5	UCIAMS-269905	shell fragments	2825	45	n/a
153.5	UCIAMS-269903	shell fragments	2670	15	0.8
186.5	UCIAMS-269904	shell (*Macoma* sp.)	2985	15	0.5
188.5	UCIAMS-269908	shell (*Macoma* sp.)	2995	15	1
194.5	UCIAMS-269902	shell fragments	3035	15	n/a

A composite record was constructed by correlating physical parameters from both cores, including core descriptions and colour data (k_{LF}, L*, a*, b*; Fig. 30). Based on this comparison, it was inferred that 21GC had lost ~6 cm from its surface, likely due to disturbance of the sediment-water interface when the core tip penetrated the seafloor. To construct a continuous sedimentary record, samples from 2.7BC and 21GC were combined into a single composite sequence, referred to as 2.7CS. The box corer (2.7BC), which is designed for collecting minimally disturbed surface sediments, provided the uppermost 5 cm of the sequence. The remaining portion, from 6 to 80 cm depth, was derived from gravity 21GC.

An age-model was constructed by integrating both ^{210}Pb and radiocarbon data using the R packages rPlum (version 3.5.2; Aquino-López et al., 2018) with the Marine20 calibration curve (Heaton, 2020). Following the recommendations of Pieńkowski et al. (2022) we applied an age reservoir correction (ΔR) of 0, with an associated error margin of

±50. This choice reflects the fact that the study is influenced by both the Baffin Current and WGC, each associated with different ΔR values (Pearce et al., 2023) and that the relative influence of these currents varies through time and space within northern Baffin Bay. In line with Pieńkowski et al. (2022), and given the absence of a robust, time-varying ΔR estimate for the region, we therefore opted not to apply a specific ΔR correction.

3.6.4 Quantitative X-Ray diffraction mineralogy and sediment sources

Quantitative X-ray diffraction (qXRD) analysis of the <2 mm bulk sediment fraction was employed to infer sediment provenance and track changes in source material throughout the Late Holocene. The qXRD analysis were performed at every 2 cm at ISMER, using the protocol developed by Eberl (2003) and described in Caron et al. (2020). For this, ~1 g of each sample was mixed with 0.25 g of corundum and then ground in a McCrone micronizing mill with 5 mL of ethanol to produce a homogenous powder. The resulting slurry was dried in a fume hood. To minimize agglomeration of fine particles, 0.5 mL of Vertrel was added. The final powder was sieved to <500 µm, side-loaded into sample holders, and analyzed using a PANalytical X'Pert Powder diffractometer. The samples were scanned between 5° and 65° two-theta with a step of 0.02° two-theta, and a count time of 2s per step. The quantification was established by converting the intensity data into mineral weight percentage (wt.%) using the R package powdR (Butler and Hillier, 2021). The calculated wt% were then normalized to a sum of 100%.

To quantitatively evaluate downcore variations in bulk sediment provenance, we applied the nonlinear unmixing tool SedUnMix, an Excel-based macro developed by Andrews and Eberl, (2012) and Andrews et al. (2015). The analysis was performed using normalized data for principal minerals that together represented more than 70% of the total mineral content in the sediment samples. Based on regional surface geology (Harrison et al., 2011) and recent sediment provenance studies in northern Baffin Bay (e.g., Jennings et al., 2019; Caron et al., 2020; Stevenard et al., 2022; Bracquart et al., 2025), we suggest that Late Holocene sediments near eastern Devon Island represent a mixture of two dominant source regions: 1) Ellesmere-Inglefield Mobile Belt, which dominates the bedrock of eastern Devon

Island, is characterized by sediments rich in plagioclase and feldspar (Stevenard et al., 2022; Bracquart et al., 2025); and 2) Ellesmere-North Greenland Fold Belt (hereafter referred to as the Ellesmere Island carbonates) is characterized by the prevalence of detrital carbonates, primarily calcite and dolomite.

3.6.5 Grain size analysis and IRD Counts

Grain size analyses (<2 mm fraction) were performed at 1-cm intervals at ISMER using a Malvern-Panalytical Mastersizer 3000 particle-size analyzer following the protocol outlined in Belzile & Montero-Serrano (2022). Following this, samples were diluted with ~20 mL of a 1% sodium hexametaphosphate (Calgon) solution to aid dispersion, sieved at <2 mm, and disaggregated using an in-house rotator for 12 hours prior to analysis. Following the analysis, the raw data was then treated using the GRADISTAT package version 9.1 developed by Blott & Pye (2001) to determine the grain size composition (clay, silt, and sand). Additionally, the abundance of ice-rafted debris (IRD) was assessed by counting clasts larger than 2 mm in X-CT scans of the cores, using continuous 2-cm intervals, following the procedure described by Grobe (1987).

3.6.6 Dinoflagellate Cysts

Sediment samples for dinocyst analysis were prepared following the protocol described in Koerner et al. (2025). Sediment samples were wet-sieved using 100 µm and 10 µm nylon mesh sieves, then treated with room-temperature 10% HCl for 24 hours to remove carbonate material. Samples were then treated with room-temperature HF (40%) for 1-7 days to dissolve silicates. A second 10% HCl treatment was applied, followed by a second sieving to remove any organic aggregates. The remaining residue was then mounted in glycerin jelly on microscope slides for analysis.

Dinocyst samples were counted on Nikon Eclipse 80i (at ISMER) and Olympus BX43 (at UNB) microscopes. Samples from the 2.7BC were previously presented in Koerner et al., 2025. Here, we increased the resolution by analyzing 4 additional samples in 2.7BC, and analyzed an additional 18 samples downcore in 21GC, with a resolution of 1-4 cm in the

core. A minimum of 300 cysts were counted per slide, and dinocyst taxonomy follows Rochon et al., (1999), Radi et al., (2013), Potvin et al., (2018), Limoges et al., (2020), Van Nieuwenhove et al., (2020). When the cysts preservation or orientation on the slide did not permit species-level identification, smooth round brown cysts were counted as "round brown", and process-bearing round brown cysts were counted as "spiny brown". We show the dinocyst relative abundances (%), dinocyst concentrations (cysts/g), and the presumed mixotrophic to heterotrophic (M/H) ratio of dinoflagellate cysts. We excluded the cyst of *Polarella glacialis* from this ratio due to its specific sea ice associated ecological niche (Montresor et al., 2003).

3.6.7 Statistical Analyses: PCA Analyses and Generalized Additive Models (GAMs)

To identify statistically significant changes in the species composition, we conducted principal component analysis on the log-transformed abundance data using the program PAST4 (version 4.09; Hammer and Harper, 2001). GAMs were applied to the downcore PCA scores (Wood, 2017; Simpson, 2018), using R (version 4.2.2; R Core Team, 2022) and and the mgcv package (mgcv package (version 1.8-41; Wood, 2017) within RStudio (version 2022.07.2; RStudio Team, 2022). GAMs identify areas of significant change on time-series data and can accommodate heteroscedasticity (e.g., changing sedimentation rates). To account for heteroscedasticity in AMD1902-21GC, observational weights were applied as recommended by Simpson (2018). The gratia package (version 0.7.3; Simpson, 2022) was used to compute the first derivative of the fitted smooth terms and their 95% confidence intervals. Points of start of significant changes are identified when the confidence intervals of the first derivative does not include zero. GAMs were applied to the PC1 and PC2 axes for AMD1902-21GC.

3.7 RESULTS

3.7.1 Age model

Both 2.7BC and 21GC show an exponential decay in ^{210}Pb activity profiles, reaching background levels (~29 Bq kg^{-1}) around 20 cm depth (Fig. 28), consistent with other studies in the region (Cormier et al., 2016; Jackson et al., 2021). The composite record derived from

these cores spans from ~1200 years BP to -69 years BP (750 to 2019 CE; Fig. 22), with sedimentation rates ranging between 0.15 and 0.3 cm per year (Fig. 22). We note a marked change in sedimentation rate between 2.7BC and 21 GC (Fig. 22) at 7.5 cm, likely attributable to 1) differential sediment compression during sampling and 2) the absence of datable material between 20 cm (the limit of the ^{210}Pb profile) and 129 cm (the first available radiocarbon age). This gap in chronological constraints contributes to large uncertainty in the age-model for 2.7CS (Fig. 22). Given these limitations, we report ages in this paper as approximate indicators and rely primarily on composite depths for our interpretations. We also avoided presenting dinocyst results as fluxes to prevent any bias associated with the composite sequence. Despite these uncertainties, the resulting chronology aligns reasonably well with other regional records from northern Baffin Bay (Cormier et al., 2016; St-Onge & St-Onge 2014). For example, St-Onge & St-Onge (2014) show that the upper ~100 cm of their record covers the last ca. 1000 years. In this study, we focus on the upper ~85 cm of the composite sequence, which encompasses the last ca. 1200 years, including the MCA, LIA, and MoW intervals.

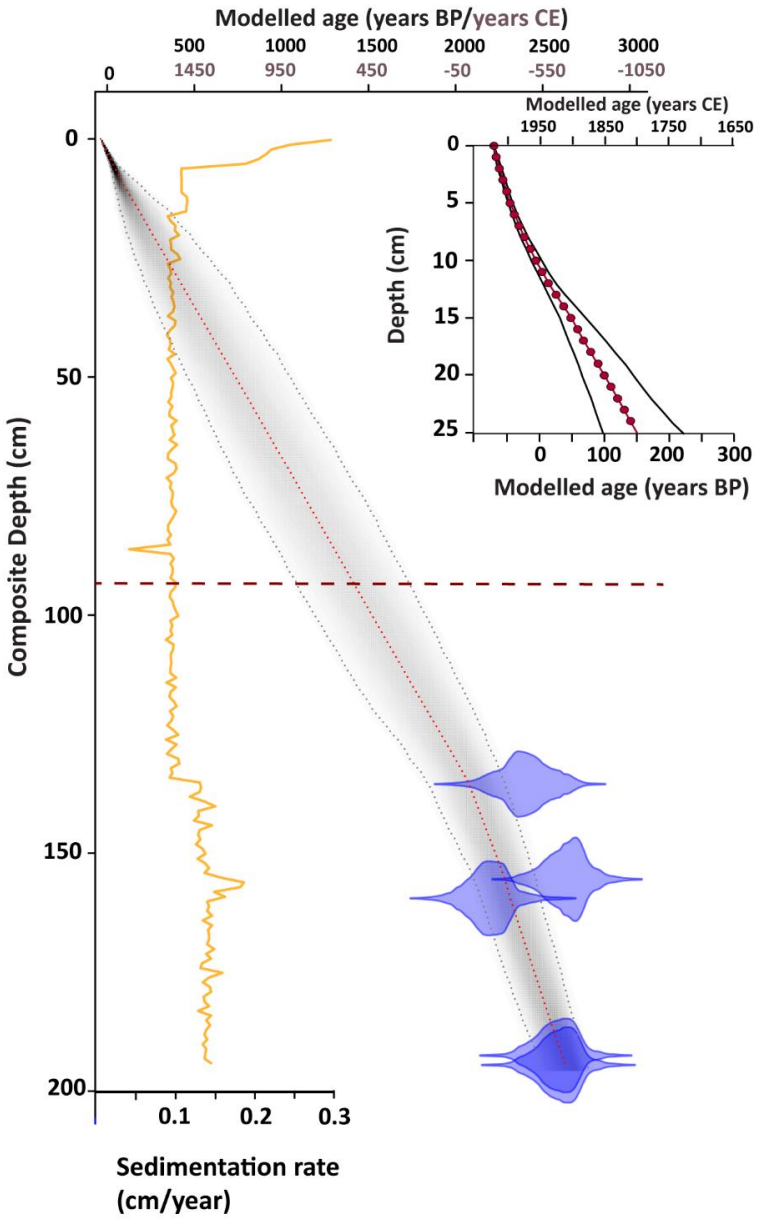

Figure 22. Composite age-model for 2.7BC (top right) and 21GC (left). The red lines represent the modelled ages, while the black lines indicate the associated uncertainties. The blue violin plots show the distribution and uncertainties of the calibrated ages derived from dated carbonate material. The dotted red line shows the depth of analysis presented in this study.

3.7.2 Mineralogical characteristics

The bulk sediment mineralogy of 2.7BC and 21GC shows that the cores are dominated by plagioclase and potassium feldspars (Pl+Kfs; 25 to 29%), quartz (Qz; 16 to 21%), chlorite and biotite (Chl+Bt; 10 to 14%), illite and muscovite (Ill + Ms; 10 to 16%), smectite (Sme; 1 to 9%), calcite and dolomite (Cal + Dol; 4 to 9%), kaolinite (Kln; 2 to 4%), amphibole (Am; 0 to 3%), pyroxene (Px; 0 to 2%), Fe-bearing minerals (0.6 to 1%) (Fig. 23 & 29).

Sediment source modeling analyses suggest that the sediments in the studied cores consist of a mixture derived primarily from the Ellesmere-Inglefield Mobile Belt (60–73%), which is located along the east coast of Devon Island (Fig. 21) and secondarily from the Ellesmere Island carbonates located in western Jones Sound and Nares Strait contributing 20–40% (Figs. 21 & 23). The proportion of material from the Ellesmere-Inglefield Mobile Belt generally increases from around 800 to 2019 CE, peaking near 1450 CE (Fig. 23). In contrast, the contribution from the detrital carbonate sources decreases over the same interval, with the highest input observed between approximately 800 and 1300 CE (Fig. 23).

3.7.3 Grain size distribution

Sediment throughout both cores was described as medium silt, with the grain size distribution throughout the core dominated by silt (82 to 92%), followed by sand (4 to 11%), and clay (4 to 8%) (Fig. 23). Sand content is highest between 800 to 1100 CE, then steadily declines, reaching its lowest values around ca. 1850 CE. Silt content increases between 800 to 1300 CE, followed by a decrease from 1300 to 1600 CE, and then remains stable until ca. 2019 CE. Clay shows relatively low contribution between 800 to 1300 CE, with a sharp increase between 1350 to 1600 CE. This is followed by relatively stable contribution toward the top of the core. Additionally, IRD counts were generally low, ranging from 0 to 5, but with notably high values observed between 1600 and 1900 CE (Fig. 23).

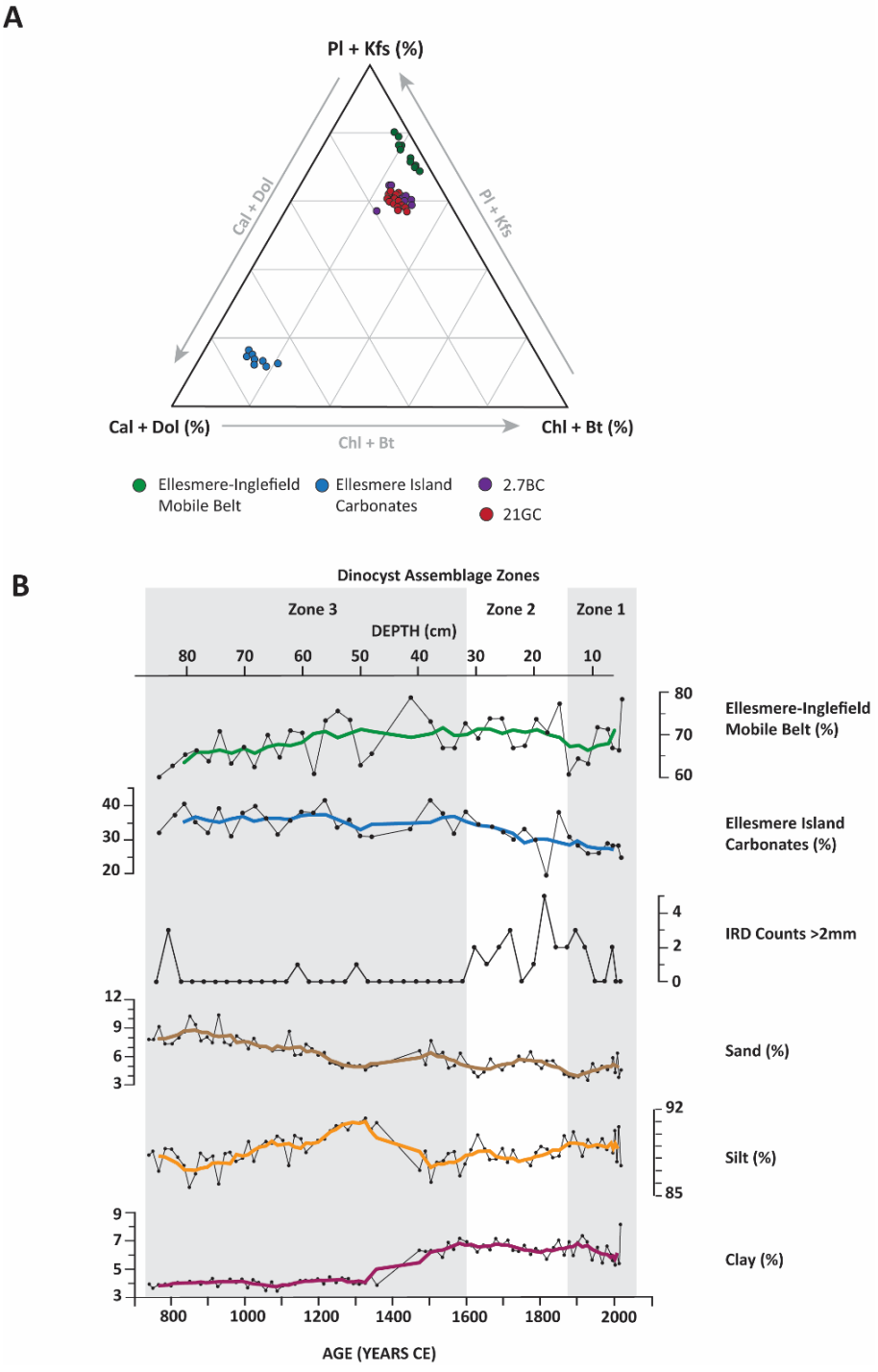

Figure 23. A) Ternary diagram showing the mineralogical composition of 2.7CS. B) The percent (%) contribution of mineral sources from the Ellesmere-Inglefield Mobile Belt and Ellesmere Island Carbonates, along with IRD counts, and grain size fractions (sand, silt and clay). The colored thick lines represent 5-point moving averages for each dataset.

3.7.4 Dinoflagellate cysts

Thirty-three taxa, species and morpho-species of dinocysts were identified and counted in 2.7CS (Fig. 24). The dominant (>2%) taxa in the assemblages are: *Islandinium minutum* subsp. *minutum* (44 to 70%), Round brown process-bearing cysts (hereafter referred to as spiny brown; 4 to 24%), *Brigantedinium* spp. (2 to 16%; including *Brigantedinium simplex* and *B. cariacoense*), Round Brown (2 to 14%), cf. *Islandinium brevispinosum* (0.3 to 12%), cyst of *Polarella glacialis* (0 to 7%), *Operculodinium centrocarpum* (0 to 6%), cyst of *Pentapharsodinium dalei* (0 to 5%), *Spiniferites elongatus* (0 to 2.6%), and *Spiniferites* spp. (0 to 1 %) (Fig. 24). Total dinocyst concentrations ranged between 9,800 and 33,000 cysts/g of dry sediment throughout the entire core (Fig. 25). The total variance for the first two PC axes was 36.7%. The PC1 axis showed 21.4% variance, and the PC2 showed 15.3% variance. Based on the visual changes in dinocyst relative abundances, total dinocyst concentrations, and the PCA values, three dinocyst assemblage zones were inferred. The GAMs show significant points of change around 1850 CE.

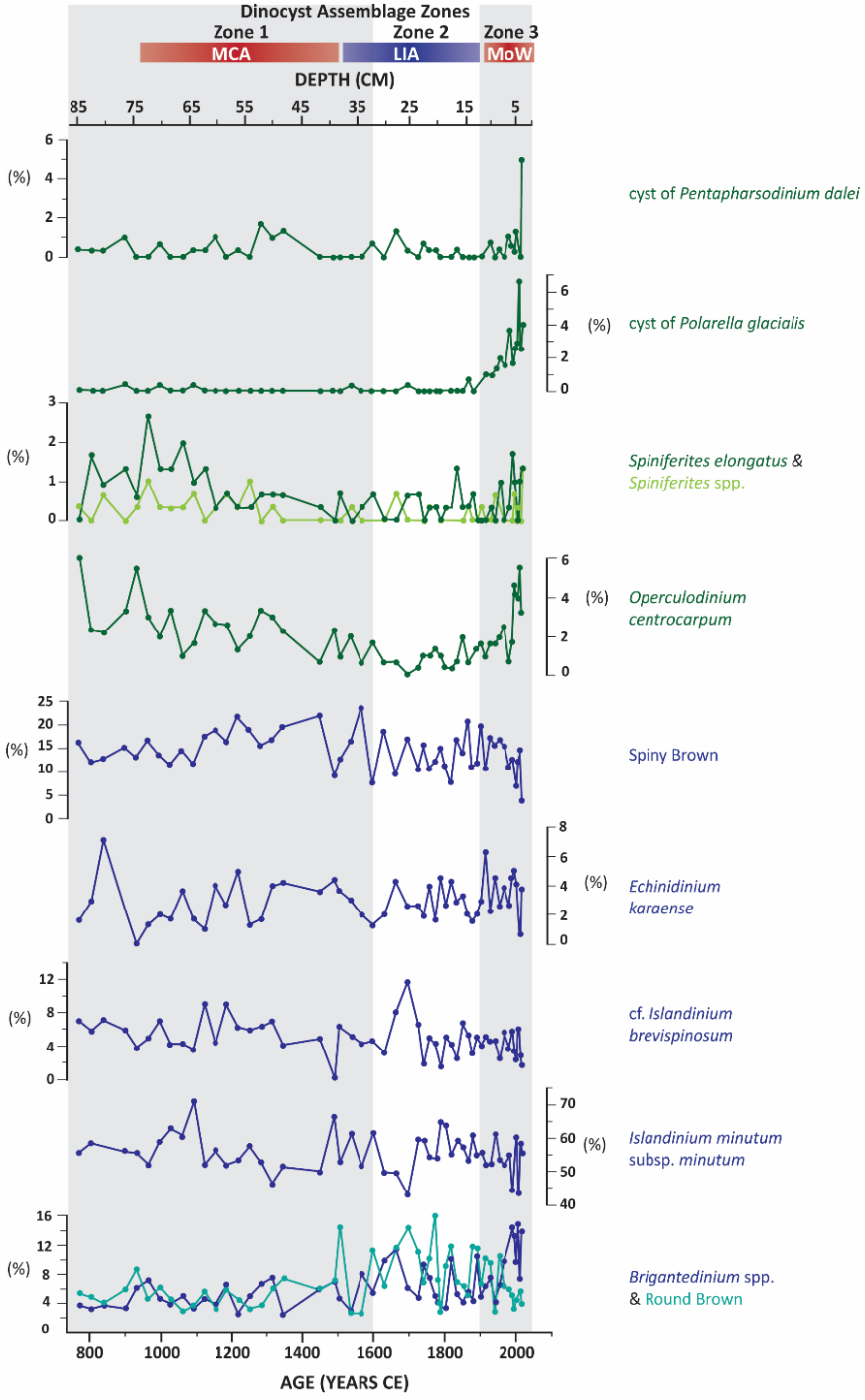

Figure 24. Relative abundances of the main (>2%) dinocyst taxa observed in composite 2.7CS. The grey bars represent the dinocyst assemblage zones based on dinocyst assemblage composition, concentrations, and PCA analyses. The taxa with green lines represent the presumed mixotrophic taxa and the taxa with the blue lines are the heterotrophic taxa.

Dinocyst assemblage zone 1

From 750 to 1600 CE, dinocyst concentrations remain low, ranging between 10,000 and 22,000 cysts/g (Fig. 25). The PC1 axis shows predominately positive values during this interval whereas the PC2 shows predominately negative values (Fig. 25), further reflected by an elevated, but decreasing, M/H ratio between 0.04 and 0.10. The dinocyst assemblages are dominated by *Islandinium minutum* subsp. *minutum*, and Spiny Brown with accompanying relative abundances of *Operculodinium centrocarpum* and *Spiniferites elongatus* that are the highest for the entire record (Fig. 24).

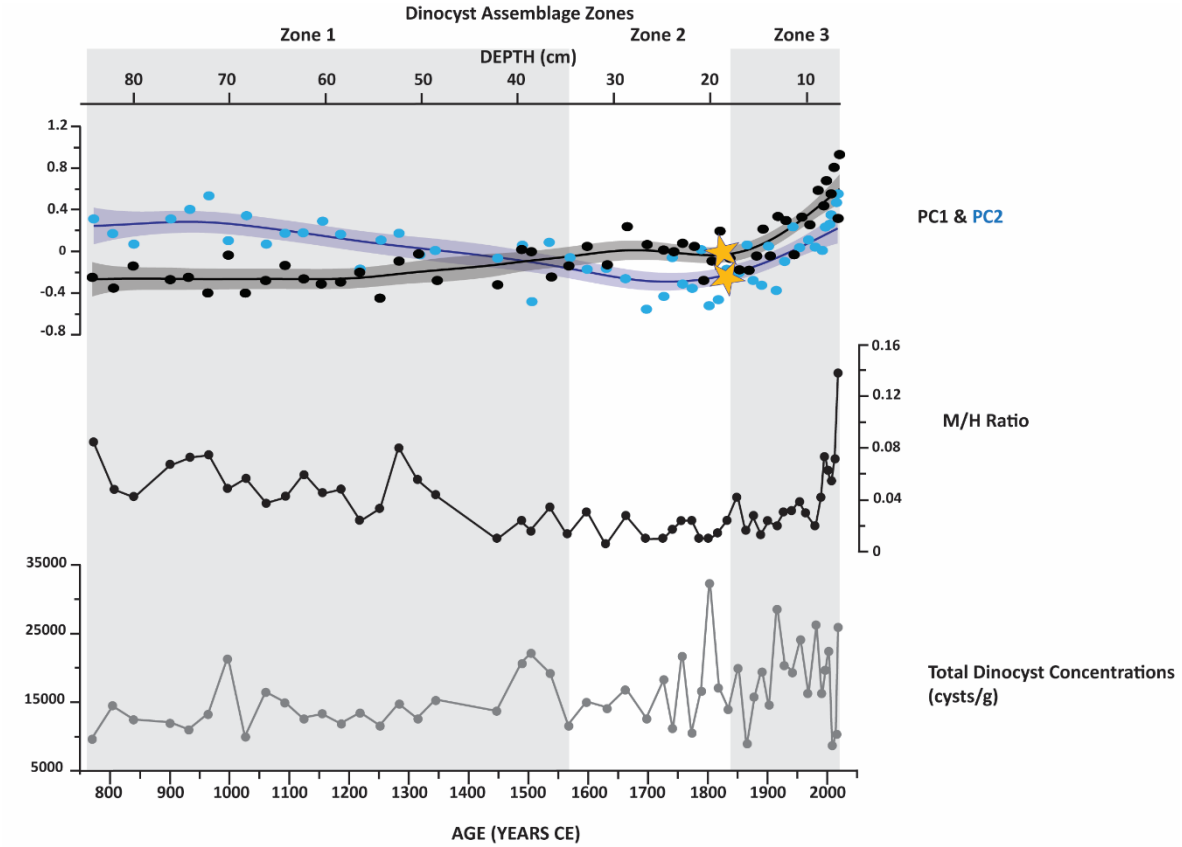

Figure 25. The PCA 1 and 2 axes derived from the log-transformed relative abundances with the GAM curves and identified points of significant change (yellow stars), the mixotroph (M) to heterotroph (H) ratio, and the total dinocyst concentrations for composite 2.7CS. The gray boxes represent the dinocyst assemblage zones.

Dinocyst assemblage zone 2

The period from 1600 to 1920 CE is marked by total dinocyst concentrations that fluctuate between 10,000 to 35,000 cysts/g and the lowest M/H ratios for the entire core (Fig. 25). Both the PC1 and PC2 axes fluctuate between positive and negative values close to 0. The main dinocyst taxa dominating this interval are the typical cold-water species *Islandinium minutum* subsp. *minutum* (Head et al., 2001), with the highest contributions of Round Brown dinocysts and accompanying contributions of *Echinidinium karaense* and cf. *Islandinium brevispinosum* (Fig. 24).

Dinocyst assemblage zone 3

From 1920 to 2019 CE, total dinocyst concentrations continue to vary between 10,000 to 30,000 cysts/g, with concentrations generally slightly higher than during the previous ca. 1000 years. Both PC axes show a shift from negative to positive values. This interval is also marked by a sharp increase in the M/H ratio, driven by increased abundances of mixotrophic taxa such as *Operculodinium centrocarpum, Spiniferites elongatus,* and *Spiniferites* spp. (Fig. 24). Notably, there is a substantial increase in the cyst of *Polarella glacialis*, the only known dinoflagellate to complete its entire life cycle in sea ice (Montresor et al., 2003; Fig. 24), and *Brigantedinium* spp. Although represented by only one data point, an increase in the cyst of *Pentapharsodinium dalei* is also observed near the top of the core.

3.8 DISCUSSION

Despite the low-resolution age-model for 2.7CS, the biogenic and sedimentary proxies show coherent, synchronous changes in three distinct intervals, broadly corresponding to the timing of the MCA, LIA, and MoW.

3.8.1 Increased ice-rafted sediment transport into northwestern Baffin Bay (85 to 32.5cm; ~750 to 1600 CE)

2.7CS records the highest contributions of sand-sized grains and poorest sediment sorting between ca. 800 to 1300 CE (Fig. 23B), coinciding with peak relative abundances of

distally-sourced Ellesmere Island carbonates (Fig. 23). The coarser grain-size distribution suggests enhanced sediment-laden sea-ice transport (Letaïef et al., 2021), a mechanism capable of delivering far-travelled material such as the Ellesmere Island carbonates from western Jones Sound and Nares Strait into northern Baffin Bay (Fig. 26).

Atmospheric reconstructions indicate that from ~700 to 800 CE, the Arctic was predominantly characterized by a negative Arctic Oscillation phase, which strengthened surface winds within the CAA and increased sea-ice export through gateways such as Nares Strait (Darby et al., 2012; Georgiadis et al., 2020). Increased sea-ice export during this interval would have facilitated the long-distance transport of coarse, carbonate-rich sediment into the region. Even though the onset of predominantly negative Arctic Oscillation conditions predates the start of the 2.7CS record, the sedimentological trends suggest that favorable export conditions persisted or were re-established during 750–1600 CE (Fig. 26).

Independent sediment archives from Belcher Glacier and Cape Norton Shaw, located west of our study site, show that glacial extent reached a minimum between 750 to 1600 CE, with both systems retreating to nearshore or possibly land-terminating positions (Brossard 2021; Stevenard et al., 2021; Fig. 26). While meltwater plumes primarily transport fine-grained sediment, near-coastal glacier retreat would have increased the availability of coarse material for subsequent entrainment and redistribution by sea ice and icebergs (Fig. 26; Ó Cofaigh et al., 2013). Similar increases in coarse-grained sediment during the MCA are reported from sites closer to these glaciers (Brossard 2021; Stevenard et al., 2021), reinforcing the interpretation of enhanced sediment delivery to northern Baffin Bay during this interval.

Dinocyst assemblages between 750 to 1600 CE are characterized by low total concentrations and a dominance of heterotrophic taxa, with mixotrophic contributions mainly from *Operculodinium centrocarpum* (Figs. 24 & 25). In Baffin Bay, *Operculodinium centrocarpum* has been linked with the presence Atlantic-derived waters (Rochon et al. 1999; de Vernal et al., 2020), suggesting enhanced WGC influence during this interval. Increased Atlantic-sourced water advection, combined with warmer atmospheric conditions during the

MCA (Cook et al., 2019), may have contributed to glacier retreat in the CAA and modulated regional sediment transport processes. The presence of the cyst of *Pentapharsodinium dalei,* a species linked to stratified, freshwater spring conditions (Heikkilä et al., 2014), further supports the influence of meltwater inputs and a freshened surface layer (Jones, 2001).

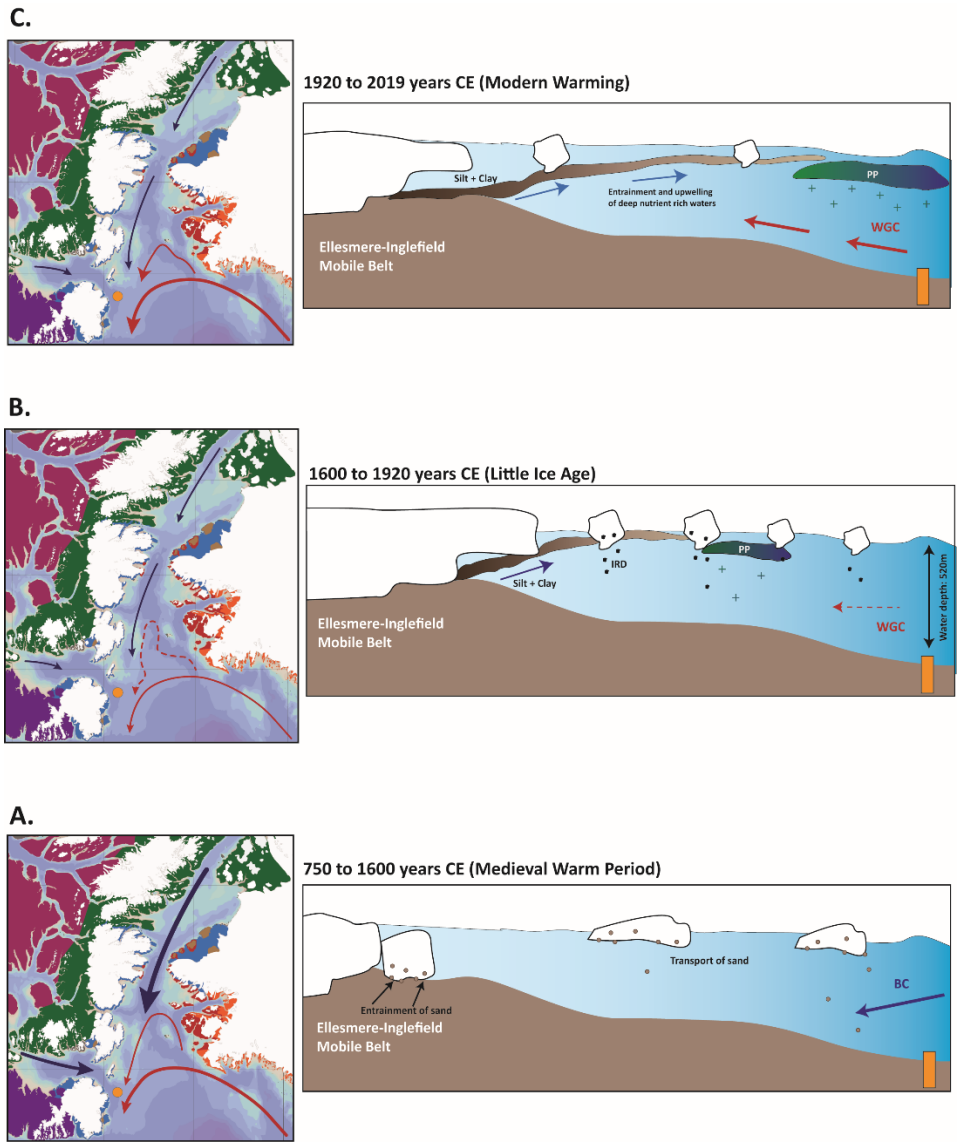

Figure 26. Simplified schematic of the three main climatic periods of the Holocene, their associated depositional regimes and hypothesized influence on sea-surface conditions and dinocyst production. A) Medieval Warm Period: characterized by retreated glacial termini, influence of the WGC in northwestern Baffin Bay, and enhanced input from more distal sediment sources with deposits characterized by coarser and more poorly-sorted materials. As a result, primary production (represented by the "+" symbol) remains relatively low during this interval and constricted proximal to the glacier. B) Little Ice Age: characterized by an advanced glacier front, intensified glacial activity and increased delivery of sediment through subglacial plumes and IRD. Influence of the WGC is diminished (represented by red-dashed lines). C) Modern Warming: increased glacial runoff via subglacial plumes which possibly entrain the deeper-nutrient rich waters (such as the WGC), stimulating primary production.

3.8.2 Extended glacial margin and a more contracted NOW (32 to 10 cm; ~1600 to 1920 CE)

Sediment source modeling shows an increased contribution from the Ellesmere-Inglefield Mobile Belt between 1600 to 1920 CE, coinciding with the highest IRD content in the entire core (Fig. 23). This interval also shows a transition toward finer-grained, clay-rich and better-sorted sediments, suggesting important influx of fine material (Fig. 23). These sedimentary signals point to intensified glacier activity in the region. Increased IRD and higher Ellesmere Island Mobile Belt contributions are consistent with expanded or more persistent marine-terminating glacier margins in eastern Devon Island and a more expansive sea-ice edge along the western NOW (Fig. 26; Moore et al., 2021). The increase in fine-grained, well-sorted sediments is consistent with elevated meltwater discharge, as glacier-fed plumes generate large volumes of suspended "rock flour" that can be transported tens to hundreds of kilometers from their source (Hopwood et al., 2020; Fig. 26). Reconstructions near Mittie Glacier (Bracquart et al., 2025) and Cape Norton Shaw (Stevenard et al., 2021) similarly document maximum glacier extent during this interval, with episodic surge-like behaviour and higher contributions from Ellesmere-Inglefield Mobile Belt material (Fig. 27), supporting the hypothesis of a more expansive sea ice edge.

During the same interval, dinocyst assemblages are dominated by heterotrophic taxa, particularly species indicative of cold, ice-influenced surface waters (Head et al. 2001). These assemblages reflect cooler oceanographic conditions in northern Baffin Bay during 1600–1920 CE and aligns with records from the western (Harning et al., 2025; Cormier et al., 2016; Levac et al., 2001) and central NOW (Limoges et al., 2023; Ribeiro et al., 2021; Jackson et al., 2021; Koerner et al., 2021), which infer a contraction of the NOW and increased sea-ice concentration along its western margin. Such conditions are consistent with cooler atmospheric temperatures and the persistence of stable ice bridges in Nares Strait, promoting an extended northern ice edge (Harning et al., 2025).

Glacier reconstructions in the CAA (Brossard, 2021; Stevenard et al., 2021; Braquart et al., 2025) and Greenland (Briner et al., 2016; Lecavalier et al., 2017; Kjær et al., 2022)

document widespread glacier advances during the late Holocene neoglacial cooling. Reduced solar insolation likely contributed to sustained cooling (Briner et al., 2016), favoring glacier growth and readvance. The elevated IRD values in our record (Fig. 23), combined with the dominance of cold-water dinocyst taxa (Fig. 24), likely reflect intensified glacier activity and enhanced delivery of glacially-derived material to northern Baffin Bay, particularly from the more proximal location of eastern Devon Island (Fig. 26).

3.8.3 Enhanced local glacial meltwater influence and ecosystem reorganization (10 to 0 cm; ~1920 to 2019 CE)

Across the CAA, it is well-established that since the mid-20th century, most marine-terminating glaciers have undergone rapid retreat, primarily driven by rising atmospheric temperatures (Howell et al., 2019). Our records are consistent with this trend, showing the highest contribution of silt- and clay-sized sediments in the core, along with an increased contribution of sediment from the Ellesmere-Inglefield Mobile Belt, indicating stronger influence of localized sedimentary inputs such as transport via glacial meltwater plumes on the depositional system (Fig. 23; 26). Similarly, marine sediments from Belcher Inlet record increased local sediment input (Brossard, 2021), attributed to modern atmospheric Arctic warming.

This warming intensifies subglacial runoff, which entrains fine-grained particles at the glacier bed and delivers them to the marine environment via meltwater plumes. Observations at Belcher Glacier have documented that such plumes can upwell nutrient-rich waters, stimulating primary production up to 25 km from the glacier front and extending into Jones Sound and northern Baffin Bay (Williams et al., 2021). Our records suggest that increased subglacial discharge may influence sedimentation and nutrient redistribution beyond the immediate coastal zone, potentially through upwelling that delivers nutrient-rich waters from the coast into the wider depositional area (Fig. 26).

Dinocyst assemblages in the uppermost portion of our record show a marked increase in mixotrophic taxa, particularly *Operculodinium centrocarpum*, the cyst of *Polarella*

glacialis, and the cyst of *Pentapharsodinium dalei* (Fig. 24). Increased abundance of *Operculodinium centrocarpum* have been interpreted as indicative of stronger WGC influence in northwestern Baffin Bay (Koerner et al., 2025). Our sedimentary data also suggest increased subglacial discharge, which may be modulated in part by oceanic heat delivery, although recent analyses indicate that atmospheric forcing remains the primary driver of glacier retreat across the CAA (Cook et al., 2019).

Changes in Atlantification and glacial meltwater discharge have important implications for marine ecosystems, including increased nutrient fluxes to distal areas and enhanced water column stratification (Hopwood et al., 2020). Nutrient delivery during the melt season (June to September) has been shown to promote conditions favorable for elevated primary production in Greenland fjords (Meire et al., 2017). We hypothesize that ongoing fluctuations in glacial discharge associated with climate warming and thus changes in nutrient availability may affect bloom timing and succession in the NOW, potentially triggering cascading ecosystem responses with yet-unknown consequences.

The early 20th century portion in 2.7CS is marked by concurrent changes in all proxies, including higher total dinocyst concentrations, fining sediments, and increased contributions from mixotrophic dinocyst taxa (Figs. 23-25). Dinocyst PCA axes 1 and 2 shift from negative to positive values, reflecting compositional changes in the assemblages (Fig. 25). Through the 21st century, dinocyst assemblages become increasingly mixotrophic, suggesting that the NOW is entering a new transitionary state associated with ongoing climate warming as suggested by previous studies based on dinocysts (Koerner et al., 2021), diatoms (Limoges et al., 2023), and foraminiferal assemblages (Jackson et al., 2021).

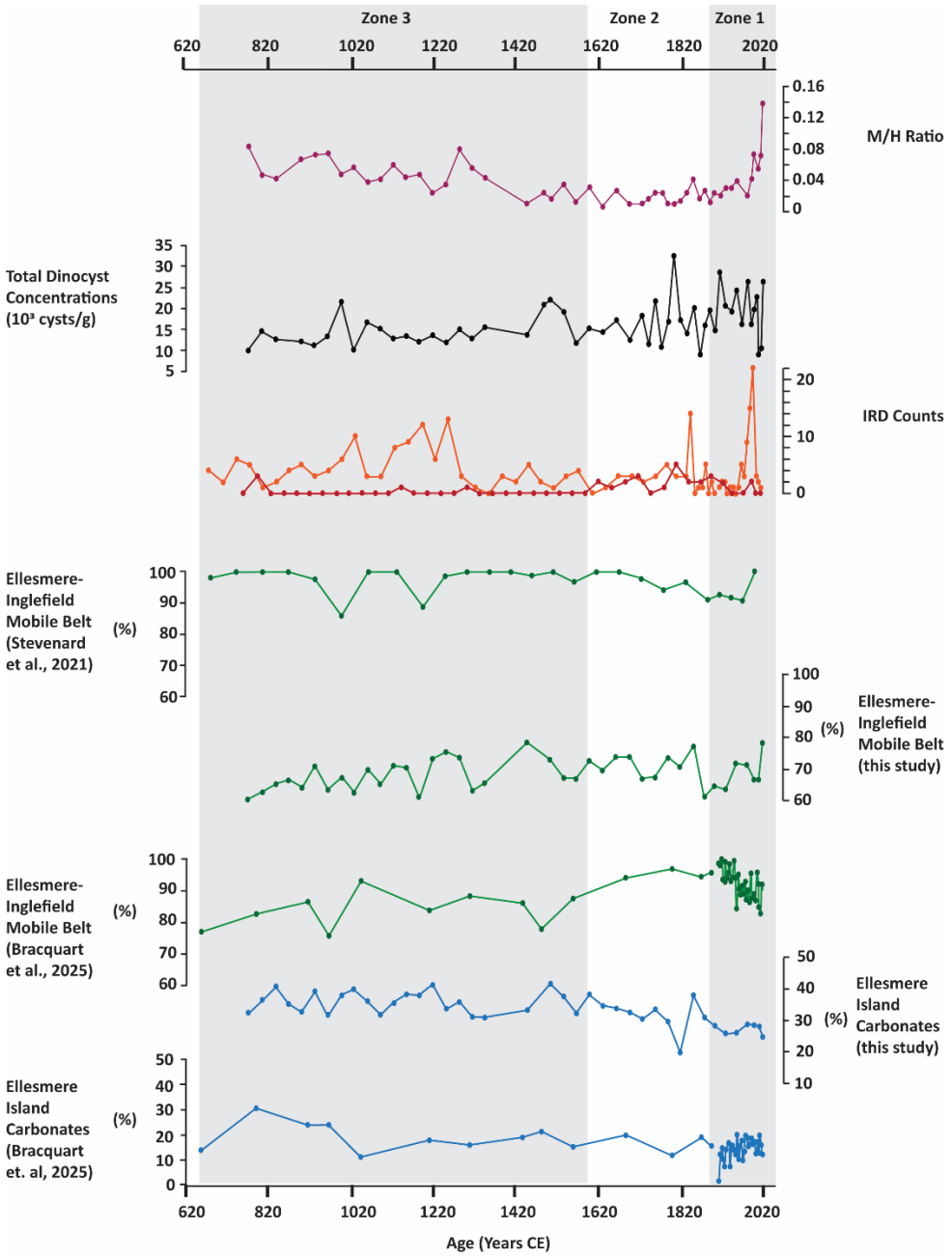

Figure 27. Mineralogy from 22BC and 01 PC (Braquart et al., 2025), and 02BC/01PC (Stevenard et al., 2021), along with the mineralogy from this study. IRD counts from this study (red) and from Bracquart et al., 2025 (orange). The total dinocyst concentrations and Mixotrophic (M) to Heterotrophic (H) ratio from this study are also presented. The grey bars represent the dinoflagellate cyst assemblage zones.

3.8.4 Constraints on reconstructing freshwater sources and its implications on the NOW ecosystem productivity

A unique feature of northern Baffin Bay is its location at the confluence of Arctic Ocean outflow, glacial meltwater, and Atlantic-derived waters (Rysgaard et al., 2020). Each of these water sources is characterized by distinct physical properties and nutrient signatures (Tang et al., 2004), which support different primary producer communities (Joli et al., 2018). Interpreting past changes in primary production is further complicated by the NOW's early seasonal opening, which extends light availability and influences the timing and magnitude of phytoplankton blooms.

Many studies have used biogenic proxies to investigate changes in sea-surface conditions, bottom water conditions, and polynya dynamics over the Holocene (e.g., Jackson et al. 2021; Koerner et al., 2021; Ribeiro et al., 2021). However, distinguishing between inputs of cool, fresh waters derived from glacial melt versus Arctic Ocean outflow remains difficult to resolve in marine sediment cores, despite the clear importance of each on shaping seasonal primary production patterns. Modern observations indicate that the nutrient characteristics of the Baffin Current differ substantially from those of glacial meltwater (Williams et al., 2021), with phytoplankton communities responding differently to each source. Thus, reconstructing variations in glacial input provides valuable context for interpreting the response of primary producers and thus ecosystem dynamics to changes in glacial input within the NOW.

Here we explored sediment provenance in one sediment core from the western region of the NOW. A robust age model could not be developed due to the scarcity of dateable material, and our record spans the last ca. 1200 years, which only represents a small fraction of the Holocene. Despite these limitations, our results suggest that sediment provenance can serve as a semi-qualtitative indicator of freshwater outputs (i.e., proximal glacial input versus more distal input). Future work would benefit from analyses of multiple sediment cores along a proximal-to-distal transect glacially influenced fjord, ideally with well-constrained age

models, to better understand the influence of glacial freshwater input on sedimentation patterns and primary production across the NOW.

3.9 CONCLUSIONS

As the Arctic warms and glaciers continue to recede, understanding the contribution of glacial runoff to the marine environments is increasingly important. Here, we examined sedimentary and biogenic records from a marine sediment core located ~40 km offshore in northerwestern Baffin Bay to assess the influence of glacial meltwater outflow, Arctic outflow and Atlantic-derived waters on depositional processes and surface-water conditions. By integrating biogenic (e.g., dinocysts) and sedimentological proxies (grain size and mineralogy), we demonstrate that sediment provenance can be used as a qualitative indicator of changing export pathways and freshwater influences in the western NOW. Our results show that:

- From 85 to 32.5 cm (broadly aligning with the MCA), increased contributions of distally sourced sediment suggest enhanced sea-ice mediated transport associated with Arctic outflow. Dinocyst concentrations were low, with assemblages composed of a mix of mixotrophic and heterotrophic taxa, suggesting cooler and more ice loaded surface waters.
- From 32 to 10 cm (broadly aligning with the LIA), high abundance of cold-water heterotrophic dinocysts points to relatively cooler sea-surface conditions. This biogenic signal coincides with elevated IRD counts and an increased contribution from proximal bedrock sources, indicating more localized glacial influence via cool freshwater runoff.
- From 10 to 0 cm (broadly aligning with MoW), total dinocyst concentrations increased, with a higher proportion of mixotrophic taxa, and greater sediment input of fine-grained sediment from proximal bedrock sources on eastern Devon Island. These trends reflect increased instability in the NOW, pointing to a transitionary period associated with modern warming.

These patterns suggest that both Arctic-derived and glacial freshwater inputs influenced northwestern Baffin Bay over the last 1200 years, with important implications for sedimentation and nutrient availability. Continued monitoring and improved spatial coverage of sediment cores will be essential to better understand how Arctic marine ecosystems will respond to ongoing warming in the future.

3.10 ACKNOWLEDGMENTS

We would like to thank the captain, officers, crew, and scientists onboard the CCGS Amundsen during the 2019 (Leg 3) ArcticNet expedition for the recovery of the sediment cores used in this study. We also thank Quentin Beauvais (ISMER-UQAR) for his help with X-CT scans and Multi-Sensor Core Logger analysis; Claude Belzile (ISMER-UQAR) for his advice with the grain size analyses; Antonin Prijac and Nicole Sanderson (Geotop-UQAM) for their advice on the ^{210}Pb measurements. This research was funded by the FRQNT Doctoral Scholarship Bourse pour la Francophonie Canadienne to K.Koerner, ArcticNet (a Network of Centres of Excellence Canada), Amundsen Science, Geotop, Québec-Océan, the Natural Sciences and Engineering Research Council of Canada (NSERC) through Discovery grants to A. Rochon, A. Limoges, and J.-C. Montero-Serrano.

Declaration of competing interest

All authors declare that there are no conflicts of interest regarding the publication of this paper.

Data Availability Statement

All analytical data presented will be available electronically in the PANGAEA database (https://www.pangaea.de/).

CRediT authorship contribution statement

Conceptualization: KK, AR, AL, JCMS, Methodology: KK, AR, AL, JCMS, Formal Analysis: KK, JCMS, Investigation: KK, Data Curation: KK, AR, AL, JCMS, Writing

Original Draft: KK, Writing – Review and Editing, KK, AR, AL, JCMS, Visualisation: KK, Supervision: AR, AL, JCMS, Funding Acquisition: KK, AR, AL, JCMS

3.11 REFERENCES

Andrews, J. T. (2019). Baffin Bay/Nares Strait surface (seafloor) sediment mineralogy: Further investigations and methods to elucidate spatial variations in provenance. *Canadian Journal of Earth Sciences*, *56*(8), Article 8. https://doi.org/10.1139/cjes-2018-0207

Andrews, J. T., & Eberl, D. D. (2012). Determination of sediment provenance by unmixing the mineralogy of source-area sediments: The "SedUnMix" program. *Marine Geology*, *291–294*, 24–33. https://doi.org/10.1016/j.margeo.2011.10.007

Andrews, J. T., Klein, A. J., Jenner, K. A., Jennings, A. E., & Campbell, C. (2018). The variability of Baffin Bay seafloor sediment mineralogy: The identification of discrete glacial sediment sources and application to Late Quaternary downcore analysis. *Canadian Journal of Earth Sciences*. https://doi.org/10.1139/cjes-2017-0223

Andrews, J. T., Bjork, A. A., Eberl, D. D., Jennings, A. E., & Verplanck, E. P. (2015). Significant differences in late Quaternary bedrock erosion and transport: East versus West Greenland ~70°N – evidence from the mineralogy of offshore glacial marine sediments. *Journal of Quaternary Science*, *30*(5), 452–463. https://doi.org/10.1002/jqs.2787

Aquino-López, M. A., Blaauw, M., Christen, J. A., & Sanderson, N. K. (2018). Bayesian Analysis of ^{210}Pb Dating. *Journal of Agricultural, Biological and Environmental Statistics*, *23*(3), Article 3. https://doi.org/10.1007/s13253-018-0328-7

Arrigo, K. R., van Dijken, G. L., Castelao, R. M., Luo, H., Rennermalm, Å. K., Tedesco, M., Mote, T. L., Oliver, H., & Yager, P. L. (2017). Melting glaciers stimulate large summer phytoplankton blooms in southwest Greenland waters. *Geophysical Research Letters*, *44*(12), 6278–6285. https://doi.org/10.1002/2017GL073583

Barber, D. G., & Massom, R. A. (2007). Chapter 1 The Role of Sea Ice in Arctic and Antarctic Polynyas. In W. O. Smith & D. G. Barber (Eds.), *Elsevier Oceanography Series* (Vol. 74, pp. 1–54). Elsevier. https://doi.org/10.1016/S0422-9894(06)74001-6

Belzile, C., & Montero-Serrano, J.-C. (2022). Quantifying simulated fine sand fraction in muddy sediment using laser diffraction. *Canadian Journal of Earth Sciences*, *59*(7), 455–461. https://doi.org/10.1139/cjes-2022-0011

Bhatia, M. P., Kujawinski, E. B., Das, S. B., Breier, C. F., Henderson, P. B., & Charette, M. A. (2013). Greenland meltwater as a significant and potentially bioavailable source of iron to the ocean. *Nature Geoscience*, *6*(4), Article 4. https://doi.org/10.1038/ngeo1746

Bhatia, M. P., Waterman, S., Burgess, D. O., Williams, P. L., Bundy, R. M., Mellett, T., Roberts, M., & Bertrand, E. M. (2021). Glaciers and Nutrients in the Canadian Arctic Archipelago Marine System. *Global Biogeochemical Cycles*, *35*(8), e2021GB006976. https://doi.org/10.1029/2021GB006976

Bi, H., Zhang, Z., Wang, Y., Xu, X., Liang, Y., Huang, J., Liu, Y., & Fu, M. (2019). Baffin Bay sea ice inflow and outflow: 1978–1979 to 2016–2017. *The Cryosphere*, *13*(3), 1025–1042. https://doi.org/10.5194/tc-13-1025-2019

Blott, S. J., & Pye, K. (2001). GRADISTAT: A grain size distribution and statistics package for the analysis of unconsolidated sediments. *Earth Surface Processes and Landforms*, *26*(11), 1237–1248. https://doi.org/10.1002/esp.261

Bracquart, E., Montero-Serrano, J.-C., Lajeunesse, P., St-Onge, G., & Copland, L. (n.d.). The Holocene sedimentary record of Mittie Glacier dynamics in Smith Bay, Ellesmere Island (eastern Canadian Arctic Archipelago). *Journal of Quaternary Science*, *n/a*(n/a). https://doi.org/10.1002/jqs.70005

Briner, J. P., McKay, N. P., Axford, Y., Bennike, O., Bradley, R. S., de Vernal, A., Fisher, D., Francus, P., Fréchette, B., Gajewski, K., Jennings, A., Kaufman, D. S., Miller, G., Rouston, C., & Wagner, B. (2016). Holocene climate change in Arctic Canada and Greenland. *Quaternary Science Reviews*, *147*, 340–364. https://doi.org/10.1016/j.quascirev.2016.02.010

Brossard, Jade. (2021). Dynamique sédimentaire holocène dans le détroit de jones reconstituée à partir des carottes sédimentaires recueillies dans la baie de belcher (calotte glaciaire de Devon, Nunavut, Canada) [Mémoire]. https://semaphore.uqar.ca/id/eprint/1959

Bryndum-Buchholz, A., Herbig, J. L., Darnis, G., Geoffroy, M., & Eddy, T. D. (2024). Ecosystem structure and function of the North Water Polynya. *Arctic Science*, *10*(3), Article 3. https://doi.org/10.1139/as-2023-0050

Butler, B. M., & Hillier, S. (2021). powdR: An R package for quantitative mineralogy using full pattern summation of X-ray powder diffraction data. *Computers & Geosciences*, *147*, 104662. https://doi.org/10.1016/j.cageo.2020.104662

Caron, M., Montero-Serrano, J.-C., St-Onge, G., & Rochon, A. (2020). Quantifying Provenance and Transport Pathways of Holocene Sediments From the Northwestern

Greenland Margin. *Paleoceanography and Paleoclimatology*, *35*(5), Article 5. https://doi.org/10.1029/2019PA003809

Colombo, M., Jackson, S. L., Cullen, J. T., & Orians, K. J. (2020). Dissolved iron and manganese in the Canadian Arctic Ocean: On the biogeochemical processes controlling their distributions. *Geochimica et Cosmochimica Acta*, *277*, 150–174. https://doi.org/10.1016/j.gca.2020.03.012

Cook, A. J., Copland, L., Noël, B. P. Y., Stokes, C. R., Bentley, M. J., Sharp, M. J., Bingham, R. G., & van den Broeke, M. R. (2019). Atmospheric forcing of rapid marine-terminating glacier retreat in the Canadian Arctic Archipelago. *Science Advances*, *5*(3), eaau8507. https://doi.org/10.1126/sciadv.aau8507

Cormier, M.-A., Rochon, A., de Vernal, A., & Gélinas, Y. (2016). Multi-proxy study of primary production and paleoceanographical conditions in northern Baffin Bay during the last centuries. *Marine Micropaleontology*, *127*, 1–10. https://doi.org/10.1016/j.marmicro.2016.07.001

Darby, D. A., Ortiz, J. D., Grosch, C. E., & Lund, S. P. (2012). 1,500-year cycle in the Arctic Oscillation identified in Holocene Arctic sea-ice drift. *Nature Geoscience; London*, *5*(12), Article 12. http://dx.doi.org.proxy.hil.unb.ca/10.1038/ngeo1629

de Vernal, A., Radi, T., Zaragosi, S., Van Nieuwenhove, N., Rochon, A., Allan, E., De Schepper, S., Eynaud, F., Head, M. J., Limoges, A., Londeix, L., Marret, F., Matthiessen, J., Penaud, A., Pospelova, V., Price, A., & Richerol, T. (2020). Distribution of common modern dinoflagellate cyst taxa in surface sediments of the Northern Hemisphere in relation to environmental parameters: The new n=1968 database. *Marine Micropaleontology*, *159*, 101796. https://doi.org/10.1016/j.marmicro.2019.101796

Eberl, D. D. (2003). User Guide to RockJock—A Program for Determining Quantitative Mineralogy from X-Ray Diffraction Data. In *Open-File Report* (Nos. 2003–78). U.S. Geological Survey. https://doi.org/10.3133/ofr200378

Eegeesiak, O., Aariak, E., & V. Kleist, K. (2017). *People of the Ice Bridge: The future of the Pikialasorsuaq* (Report of the Pikialasorsuaq Commission, p. 119). Inuit Circumpolar Council Canada.

Georgiadis, E., Giraudeau, J., Jennings, A., Limoges, A., Jackson, R., Ribeiro, S., & Massé, G. (2020). Local and regional controls on Holocene sea ice dynamics and oceanography in Nares Strait, Northwest Greenland. *Marine Geology*, *422*, 106115. https://doi.org/10.1016/j.margeo.2020.106115

Georgiadis, E., Giraudeau, J., Martinez, P., Lajeunesse, P., St-Onge, G., Schmidt, S., & Massé, G. (2018). Deglacial to postglacial history of Nares Strait, Northwest Greenland: A marine perspective from Kane Basin. *Climate of the Past*, *14*(12), Article 12. https://doi.org/10.5194/cp-14-1991-2018

Ghaleb, B. (2009). Overview of the methods for the measurement and interpretation of short-lived radioisotopes and their limits. *IOP Conference Series: Earth and Environmental Science*, *5*(1), 012007. https://doi.org/10.1088/1755-1307/5/1/012007

Grobe, H. (1987). A simple method for the determination of ice-rafted debris in sediment cores. *Polarforschung*, *57*(3), 123–126.

Halbach, L., Vihtakari, M., Duarte, P., Everett, A., Granskog, M. A., Hop, H., Kauko, H. M., Kristiansen, S., Myhre, P. I., Pavlov, A. K., Pramanik, A., Tatarek, A., Torsvik, T., Wiktor, J. M., Wold, A., Wulff, A., Steen, H., & Assmy, P. (2019). Tidewater Glaciers and Bedrock Characteristics Control the Phytoplankton Growth Environment in a Fjord in the Arctic. *Frontiers in Marine Science*, *6*. https://doi.org/10.3389/fmars.2019.00254

Hammer, Ø., Harper, D. A. T., & Ryan, P. D. (n.d.). *PAST: Paleontological Statistics Software Package for Education and Data Analysis. 9.*

Harning, D. J., Jennings, A. E., Holman, B., Kelleher, R. V., Feng, S., Brooks, N. K. S., Andrews, J. T., Marchitto, T., & Sepúlveda, J. (2025). Spatiotemporal Variability in the Holocene Extent of Pikialasorsuaq (North Water Polynya), Baffin Bay. *Paleoceanography and Paleoclimatology*, *40*(8), e2025PA005153. https://doi.org/10.1029/2025PA005153

Harrison, C., & St-Onge, M. R. (2022). Geological history and supercontinent cycles of the Arctic. *GSA Bulletin*, *135*(1–2), 162–189. https://doi.org/10.1130/B36398.1

Harrison, J. C., Brent, T. A., & Oakey, G. N. (2011). Baffin Fan and its inverted rift system of Arctic eastern Canada: Stratigraphy, tectonics and petroleum resource potential. In A. M. Spencer, A. F. Embry, D. L. Gautier, A. V. Stoupakova, & K. Sørensen (Eds.), *Arctic Petroleum Geology* (Vol. 35, p. 0). Geological Society of London. https://doi.org/10.1144/M35.40

Hawkings, J. R. (2021). Trickle and Treat? The Critical Role of Marine-Terminating Glaciers as Icy Macronutrient Pumps in Polar Regions. *Journal of Geophysical Research: Biogeosciences*, *126*(10), e2021JG006598. https://doi.org/10.1029/2021JG006598

Head, M. J., Harland, R., & Matthiessen, J. (2001). Cold marine indicators of the late Quaternary: The new dinoflagellate cyst genus Islandinium and related morphotypes. *Journal of Quaternary Science*, *16*(7), Article 7. https://doi.org/10.1002/jqs.657

Heaton, T. J., Köhler, P., Butzin, M., Bard, E., Reimer, R. W., Austin, W. E. N., Ramsey, C. B., Grootes, P. M., Hughen, K. A., Kromer, B., Reimer, P. J., Adkins, J., Burke, A., Cook, M. S., Olsen, J., & Skinner, L. C. (2020). Marine20—The Marine Radiocarbon Age Calibration Curve (0–55,000 cal BP). *Radiocarbon*, *62*(4), 779–820. https://doi.org/10.1017/RDC.2020.68

Heikkilä, M., Pospelova, V., Hochheim, K. P., Kuzyk, Z. Z. A., Stern, G. A., Barber, D. G., & Macdonald, R. W. (2014). Surface sediment dinoflagellate cysts from the Hudson Bay system and their relation to freshwater and nutrient cycling. *Marine Micropaleontology*, *106*, 79–109. https://doi.org/10.1016/j.marmicro.2013.12.002

Hodson, A. J., Mumford, P. N., Kohler, J., & Wynn, P. M. (2005). The High Arctic glacial ecosystem: New insights from nutrient budgets. *Biogeochemistry*, *72*(2), 233–256. https://doi.org/10.1007/s10533-004-0362-0

Hopwood, M. J., Carroll, D., Browning, T. J., Meire, L., Mortensen, J., Krisch, S., & Achterberg, E. P. (2018). Non-linear response of summertime marine productivity to increased meltwater discharge around Greenland. *Nature Communications*, *9*(1), Article 1. https://doi.org/10.1038/s41467-018-05488-8

Hopwood, M. J., Carroll, D., Dunse, T., Hodson, A., Holding, J. M., Iriarte, J. L., Ribeiro, S., Achterberg, E. P., Cantoni, C., Carlson, D. F., Chierici, M., Clarke, J. S., Cozzi, S., Fransson, A., Juul-Pedersen, T., Winding, M. H. S., & Meire, L. (2020). Review article: How does glacier discharge affect marine biogeochemistry and primary production in the Arctic? *The Cryosphere*, *14*(4), 1347–1383. https://doi.org/10.5194/tc-14-1347-2020

Hoshiba, Y., Matsumura, Y., Kanna, N., Ohashi, Y., & Sugiyama, S. (2024). Impacts of glacial discharge on the primary production in a Greenlandic fjord. *Scientific Reports*, *14*(1), Article 1. https://doi.org/10.1038/s41598-024-64529-z

Howell, S. E. L., & Brady, M. (2019). The Dynamic Response of Sea Ice to Warming in the Canadian Arctic Archipelago. *Geophysical Research Letters*, *46*(22), 13119–13125. https://doi.org/10.1029/2019GL085116

Jackson, R., Kvorning, A. B., Limoges, A., Georgiadis, E., Olsen, S. M., Tallberg, P., Andersen, T. J., Mikkelsen, N., Giraudeau, J., Massé, G., Wacker, L., & Ribeiro, S. (2021). Holocene polynya dynamics and their interaction with oceanic heat transport in northernmost Baffin Bay. *Scientific Reports*, *11*(1), 10095. https://doi.org/10.1038/s41598-021-88517-9

Jennings, A. E., Andrews, J. T., Oliver, B., Walczak, M., & Mix, A. (2019). Retreat of the Smith Sound Ice Stream in the Early Holocene. *Boreas*, *48*(4), Article 4. https://doi.org/10.1111/bor.12391

Joli, N., Gosselin, M., Ardyna, M., Babin, M., Onda, D. F., Tremblay, J.-É., & Lovejoy, C. (2018). Need for focus on microbial species following ice melt and changing freshwater regimes in a Janus Arctic Gateway. *Scientific Reports*, *8*(1), Article 1. https://doi.org/10.1038/s41598-018-27705-6

Jones, E. P. (2001). Circulation in the Arctic Ocean. *Polar Research*, *20*(2), Article 2. https://doi.org/10.1111/j.1751-8369.2001.tb00049.x

Kanna, N., Sugiyama, S., Ohashi, Y., Sakakibara, D., Fukamachi, Y., & Nomura, D. (2018). Upwelling of Macronutrients and Dissolved Inorganic Carbon by a Subglacial Freshwater Driven Plume in Bowdoin Fjord, Northwestern Greenland. *Journal of Geophysical Research: Biogeosciences*, *123*(5), 1666–1682. https://doi.org/10.1029/2017JG004248

Kjær, K. H., Winther Pedersen, M., De Sanctis, B., De Cahsan, B., Korneliussen, T. S., Michelsen, C. S., Sand, K. K., Jelavić, S., Ruter, A. H., Schmidt, A. M. A., Kjeldsen, K. K., Tesakov, A. S., Snowball, I., Gosse, J. C., Alsos, I. G., Wang, Y., Dockter, C., Rasmussen, M., Jørgensen, M. E., … Willerslev, E. (2022). A 2-million-year-old ecosystem in Greenland uncovered by environmental DNA. *Nature*, *612*(7939), 283–291. https://doi.org/10.1038/s41586-022-05453-y

Koerner, K. A., Limoges, A., Pike-Connolly, E., Van Nieuwenhove, N., & Rochon, A. (2025). Early impacts of Arctic amplification in the western North Water Polynya: A 400-year perspective. *Marine Micropaleontology*, *197–198*, 102470. https://doi.org/10.1016/j.marmicro.2025.102470

Koerner, K., Limoges, A., Van Nieuwenhove, N., Richerol, T., Massé, G., & Ribeiro, S. (2021). Late Holocene sea-surface changes in the North Water polynya reveal freshening of northern Baffin Bay in the 21st century. *Global and Planetary Change*, 103642. https://doi.org/10.1016/j.gloplacha.2021.103642

Lecavalier, B. S., Fisher, D. A., Milne, G. A., Vinther, B. M., Tarasov, L., Huybrechts, P., Lacelle, D., Main, B., Zheng, J., Bourgeois, J., & Dyke, A. S. (2017). High Arctic Holocene temperature record from the Agassiz ice cap and Greenland ice sheet evolution. *Proceedings of the National Academy of Sciences*, *114*(23), Article 23. https://doi.org/10.1073/pnas.1616287114

Letaïef, S., Montero-Serrano, J.-C., & St-Onge, G. (2021). Sedimentary Processes Within the Canadian Arctic Archipelago: Relationships Among Sedimentological, Geochemical, and Magnetic Sediment Properties. *Geochemistry, Geophysics, Geosystems*, *22*(7), e2021GC009719. https://doi.org/10.1029/2021GC009719

Levac, E., Vernal, A. D., & Jr, W. B. (2001). Sea-surface conditions in northernmost Baffin Bay during the Holocene: Palynological evidence. *Journal of Quaternary Science*, *16*(4), Article 4. https://doi.org/10.1002/jqs.614

Limoges, A., Ribeiro, S., Van Nieuwenhove, N., Jackson, R., Juggins, S., Crosta, X., & Weckström, K. (2023). Marine diatoms record Late Holocene regime shifts in the Pikialasorsuaq ecosystem. *Global Change Biology*, *29*(23), Article 23. https://doi.org/10.1111/gcb.16958

Limoges, A., Van Nieuwenhove, N., Head, M. J., Mertens, K. N., Pospelova, V., & Rochon, A. (2020). A review of rare and less well known extant marine organic-walled dinoflagellate cyst taxa of the orders Gonyaulacales and Suessiales from the Northern Hemisphere. *Marine Micropaleontology*, 101801. https://doi.org/10.1016/j.marmicro.2019.101801

Losapio, G., Lee, J. R., Fraser, C. I., Gillespie, M. A. K., Kerr, N. R., Zawierucha, K., Hamilton, T. L., Hotaling, S., Kaufmann, R., Kim, O.-S., Klopsch, C., Liu, Y., Lukashanets, D., Robinson, S. A., & Brown, L. E. (2025). Impacts of deglaciation on biodiversity and ecosystem function. *Nature Reviews Biodiversity*, *1*(6), 371–385. https://doi.org/10.1038/s44358-025-00049-6

Mann, M. E., Zhang, Z., Rutherford, S., Bradley, R. S., Hughes, M. K., Shindell, D., Ammann, C., Faluvegi, G., & Ni, F. (2009). Global Signatures and Dynamical Origins of the Little Ice Age and Medieval Climate Anomaly. *Science*, *326*(5957), 1256–1260. https://doi.org/10.1126/science.1177303

Meire, L., Mortensen, J., Meire, P., Juul-Pedersen, T., Sejr, M. K., Rysgaard, S., Nygaard, R., Huybrechts, P., & Meysman, F. J. R. (2017). Marine-terminating glaciers sustain high productivity in Greenland fjords. *Global Change Biology*, *23*(12), Article 12. https://doi.org/10.1111/gcb.13801

Montresor, M., Lovejoy, C., Orsini, L., Procaccini, G., & Roy, S. (2003). Bipolar distribution of the cyst-forming dinoflagellate *Polarella glacialis*. *Polar Biology*, *26*(3), Article 3. https://doi.org/10.1007/s00300-002-0473-9

Moore, G. W. K., Howell, S. E. L., Brady, M., Xu, X., & McNeil, K. (2021). Anomalous collapses of Nares Strait ice arches leads to enhanced export of Arctic sea ice. *Nature Communications*, *12*(1), Article 1. https://doi.org/10.1038/s41467-020-20314-w

Morales Maqueda, M. A. (2004). Polynya Dynamics: A Review of Observations and Modeling. *Reviews of Geophysics*, *42*(1), Article 1. https://doi.org/10.1029/2002RG000116

Münchow, A., Falkner, K. K., & Melling, H. (2007). Spatial continuity of measured seawater and tracer fluxes through Nares Strait, a dynamically wide channel bordering the Canadian Archipelago. *Journal of Marine Research*, *65*(6), Article 6. https://doi.org/10.1357/002224007784219048

Münchow, A., Falkner, K. K., & Melling, H. (2015). Baffin Island and West Greenland Current Systems in northern Baffin Bay. *Progress in Oceanography*, *132*, 305–317. https://doi.org/10.1016/j.pocean.2014.04.001

Noël, B., van de Berg, W. J., Lhermitte, S., Wouters, B., Schaffer, N., & van den Broeke, M. R. (2018). Six Decades of Glacial Mass Loss in the Canadian Arctic Archipelago. *Journal of Geophysical Research: Earth Surface*, *123*(6), 1430–1449. https://doi.org/10.1029/2017JF004304

Ó Cofaigh, C., Andrews, J. T., Jennings, A. E., Dowdeswell, J. A., Hogan, K. A., Kilfeather, A. A., & Sheldon, C. (2013). Glacimarine lithofacies, provenance and depositional processes on a West Greenland trough-mouth fan. *Journal of Quaternary Science*, *28*(1), 13–26. https://doi.org/10.1002/jqs.2569

Okuma, E., Hingst, J., Weiser, J., Madaj, L., Titschack, J., Vogt, C., Kienast, M., Hillaire-Marcel, C., Hebbeln, D., & Kasemann, S. A. (2023). Deglacial and Holocene sediment dynamics and provenances off Lancaster Sound: Implications for paleoenvironmental conditions in northern Baffin Bay. *Quaternary Science Reviews*, *309*, 108101. https://doi.org/10.1016/j.quascirev.2023.108101

Pearce, C., Özdemir, K. S., Forchhammer Mathiasen, R., Detlef, H., & Olsen, J. (2023). The marine reservoir age of Greenland coastal waters. *Geochronology*, *5*(2), Article 2. https://doi.org/10.5194/gchron-5-451-2023

Pieńkowski, A. J., Coulthard, R. D., & Furze, M. F. A. (2022). Revised marine reservoir offset (ΔR) values for molluscs and marine mammals from Arctic North America. *Boreas*, *n/a*(n/a), Article n/a. https://doi.org/10.1111/bor.12606

Potvin, É., Kim, S.-Y., Yang, E. J., Head, M. J., Kim, H., Nam, S.-I., Yim, J. H., & Kang, S.-H. (2018). Islandinium minutum subsp. barbatum subsp. nov. (Dinoflagellata), a New Organic-Walled Dinoflagellate Cyst from the Western Arctic: Morphology, Phylogenetic Position Based on SSU rDNA and LSU rDNA, and Distribution. *Journal of Eukaryotic Microbiology*, *65*(6), Article 6. https://doi.org/10.1111/jeu.12518

Radi, T., Bonnet, S., Cormier, M.-A., de Vernal, A., Durantou, L., Faubert, É., Head, M. J., Henry, M., Pospelova, V., Rochon, A., & Van Nieuwenhove, N. (2013). Operational taxonomy and (paleo-)autecology of round, brown, spiny dinoflagellate cysts from the Quaternary of high northern latitudes. *Marine Micropaleontology*, *98*, 41–57. https://doi.org/10.1016/j.marmicro.2012.11.001

R Core Team. (2022). R: A language and environment for statistical computing. R Foundation for Statistical Computing. https://www.R-project.org

Radić, V., & Hock, R. (2010). Regional and global volumes of glaciers derived from statistical upscaling of glacier inventory data. *Journal of Geophysical Research: Earth Surface*, *115*(F1). https://doi.org/10.1029/2009JF001373

Ribeiro, S., Limoges, A., Massé, G., Johansen, K. L., Colgan, W., Weckström, K., Jackson, R., Georgiadis, E., Mikkelsen, N., Kuijpers, A., Olsen, J., Olsen, S. M., Nissen, M., Andersen, T. J., Strunk, A., Wetterich, S., Syväranta, J., Henderson, A. C. G., Mackay, H., … Davidson, T. A. (2021). Vulnerability of the North Water ecosystem to climate change. *Nature Communications*, *12*(1), 4475. https://doi.org/10.1038/s41467-021-24742-0

Rochon, A., Vernal, A. de, Turon, J.-L., Matthießen, J., & Head, M. J. (1999). Distribution of recent dinoflagellate cysts in surface sediments from the North Atlantic Ocean and adjacent seas in relation to sea-surface parameters. *American Association of Stratigraphic Palynologists Contribution Series*, *35*, 1–146.

RStudio Team. (2022). RStudio: Integrated development environment for R. RStudio, PBC. https://posit.co/products/open-source/rstudio/?sid=1

Rysgaard, S., Boone, W., Carlson, D., Sejr, M. K., Bendtsen, J., Juul-Pedersen, T., Lund, H., Meire, L., & Mortensen, J. (2020). An Updated View on Water Masses on the pan-West Greenland Continental Shelf and Their Link to Proglacial Fjords. *Journal of Geophysical Research: Oceans*, *125*(2), Article 2. https://doi.org/10.1029/2019JC015564

Sharp, M., Burgess, D. O., Cawkwell, F., Copland, L., Davis, J. A., Dowdeswell, E. K., Dowdeswell, J. A., Gardner, A. S., Mair, D., Wang, L., Williamson, S. N., Wolken, G. J., & Wyatt, F. (2014). Remote sensing of recent glacier changes in the Canadian Arctic. In J. S. Kargel, G. J. Leonard, M. P. Bishop, A. Kääb, & B. H. Raup (Eds.), *Global Land Ice Measurements from Space* (pp. 205–228). Springer. https://doi.org/10.1007/978-3-540-79818-7_9

Simpson, G. L. (2018). Modelling Palaeoecological Time Series Using Generalised Additive Models. Frontiers in Ecology and Evolution, 6. https://doi.org/10.3389/fevo.2018.00149

Simpson, G. L. (2022). gratia: Graceful ggplot-based graphics and other functions for GAMs fitted using mgcv. R package version 0.7.3. https://gavinsimpson.github.io/gratia

Stevenard, N., Montero-Serrano, J.-C., Eynaud, F., St-Onge, G., Zaragosi, S., & Copland, L. (2022). Lateglacial and Holocene sedimentary dynamics in northwestern Baffin Bay as

recorded in sediment cores from Cape Norton Shaw Inlet (Nunavut, Canada). *Boreas*. https://doi.org/10.1111/bor.12575

St-Onge, G., Mulder, T., Francus, P., & Long, B. (2007). Chapter Two Continuous Physical Properties of Cored Marine Sediments. In *Developments in Marine Geology* (Vol. 1, pp. 63–98). Elsevier. https://doi.org/10.1016/S1572-5480(07)01007-X

St-Onge, M.-P., & St-Onge, G. (2014). Environmental changes in Baffin Bay during the Holocene based on the physical and magnetic properties of sediment cores. *Journal of Quaternary Science*, *29*(1). https://doi.org/10.1002/jqs.2674

Straneo, F., & Cenedese, C. (2015). The Dynamics of Greenland's Glacial Fjords and Their Role in Climate. *Annual Review of Marine Science*, *7*(Volume 7, 2015), 89–112. https://doi.org/10.1146/annurev-marine-010213-135133

Tang, C. C. L., Ross, C. K., Yao, T., Petrie, B., DeTracey, B. M., & Dunlap, E. (2004). The circulation, water masses and sea-ice of Baffin Bay. *Progress in Oceanography*, *63*(4). https://doi.org/10.1016/j.pocean.2004.09.005

Tremblay, J.-É., Anderson, L. G., Matrai, P., Coupel, P., Bélanger, S., Michel, C., & Reigstad, M. (2015). Global and regional drivers of nutrient supply, primary production and CO2 drawdown in the changing Arctic Ocean. *Progress in Oceanography*, *139*, 171–196. https://doi.org/10.1016/j.pocean.2015.08.009

Tremblay, J.-É., Gratton, Y., Carmack, E. C., Payne, C. D., & Price, N. M. (2002). Impact of the large-scale Arctic circulation and the North Water Polynya on nutrient inventories in Baffin Bay. *Journal of Geophysical Research: Oceans*, *107*(C8), Article C8. https://doi.org/10.1029/2000JC000595

Van Nieuwenhove, N., Head, M. J., Limoges, A., Pospelova, V., Mertens, K. N., Matthiessen, J., De Schepper, S., de Vernal, A., Eynaud, F., Londeix, L., Marret, F., Penaud, A., Radi, T., & Rochon, A. (2020). An overview and brief description of common marine organic-walled dinoflagellate cyst taxa occurring in surface sediments of the Northern Hemisphere. *Marine Micropaleontology*, 101814. https://doi.org/10.1016/j.marmicro.2019.101814

Vincent, R. F. (2019). A Study of the North Water Polynya Ice Arch using Four Decades of Satellite Data. *Scientific Reports*, *9*. https://doi.org/10.1038/s41598-019-56780-6

Vonnahme, T. R., Persson, E., Dietrich, U., Hejdukova, E., Dybwad, C., Elster, J., Chierici, M., & Gradinger, R. (2021). Early spring subglacial discharge plumes fuel under-ice primary production at a Svalbard tidewater glacier. *The Cryosphere*, *15*(4), 2083–2107. https://doi.org/10.5194/tc-15-2083-2021

Williams, P. L., Burgess, D. O., Waterman, S., Roberts, M., Bertrand, E. M., & Bhatia, M. P. (2021). Nutrient and Carbon Export From a Tidewater Glacier to the Coastal Ocean in the Canadian Arctic Archipelago. *Journal of Geophysical Research: Biogeosciences*, *126*(9), e2021JG006289. https://doi.org/10.1029/2021JG006289

Wood, S. N. (2017). Generalized Additive Models: An Introduction with R, Second Edition (2nd ed.). Chapman and Hall/CRC. https://doi.org/10.1201/9781315370279

Wood, K. R., & Overland, J. E. (2010). Early 20th century Arctic warming in retrospect. *International Journal of Climatology*, *30*(9), 1269–1279. https://doi.org/10.1002/joc.1973

Wychen, W. V., Burgess, D., Kochtitzky, W., Nikolic, N., Copland, L., & Gray, L. (2020). RADARSAT-2 Derived Glacier Velocities and Dynamic Discharge Estimates for the Canadian High Arctic: 2015–2020. *Canadian Journal of Remote Sensing*, *46*(6), Article 6. https://doi.org/10.1080/07038992.2020.1859359

Wychen, W. V., Davis, J., Copland, L., Burgess, D. O., Gray, L., Sharp, M., Dowdeswell, J. A., & Benham, T. J. (2017). Variability in ice motion and dynamic discharge from Devon Ice Cap, Nunavut, Canada. *Journal of Glaciology*, *63*(239), 436–449. https://doi.org/10.1017/jog.2017.2

3.12 SUPPLEMENTARY MATERIAL

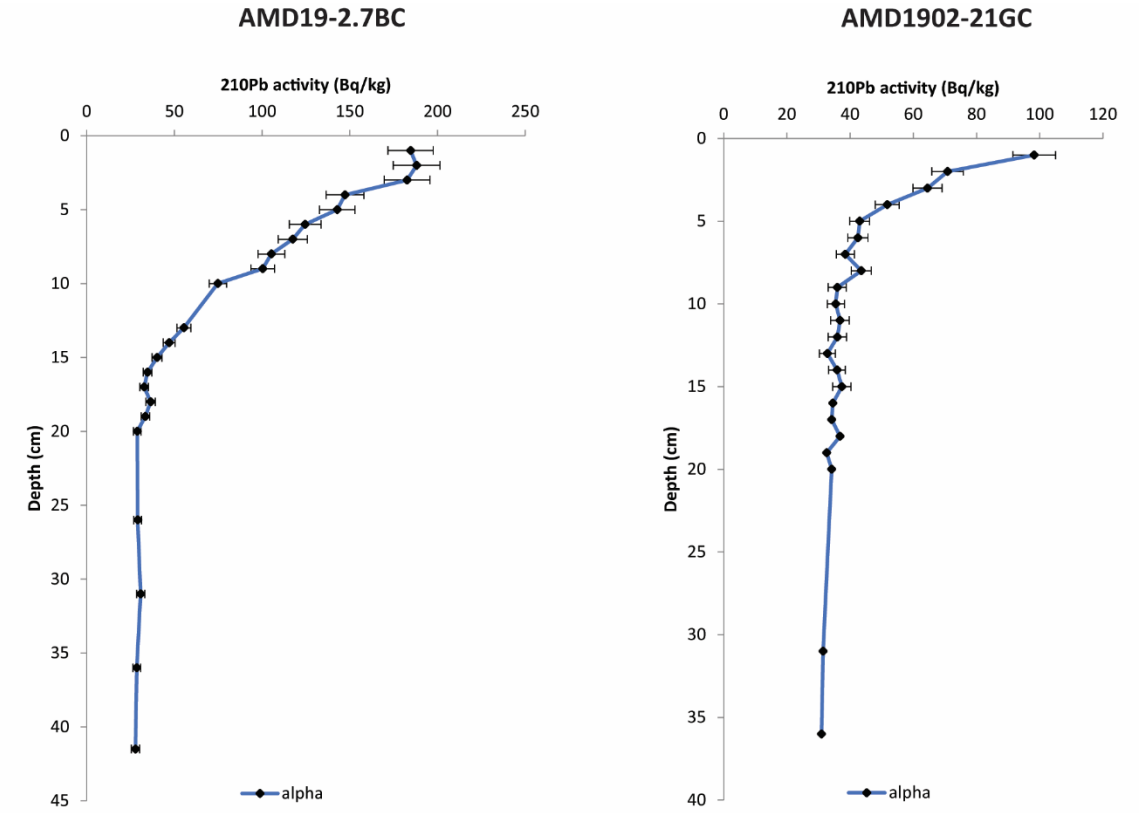

Figure 28. ^{210}Pb activity profiles for AMD19-2.7BC (left) and AMD1902-21GC (right)

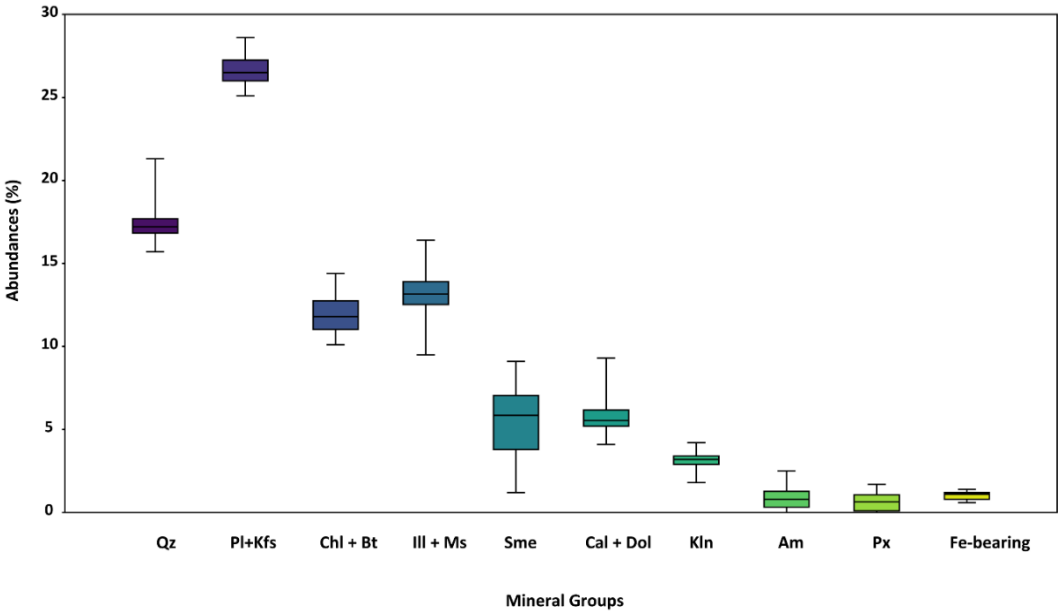

Figure 29. Box plot of mineralogy in AMD19-2.7BC and AMD1902-21GC

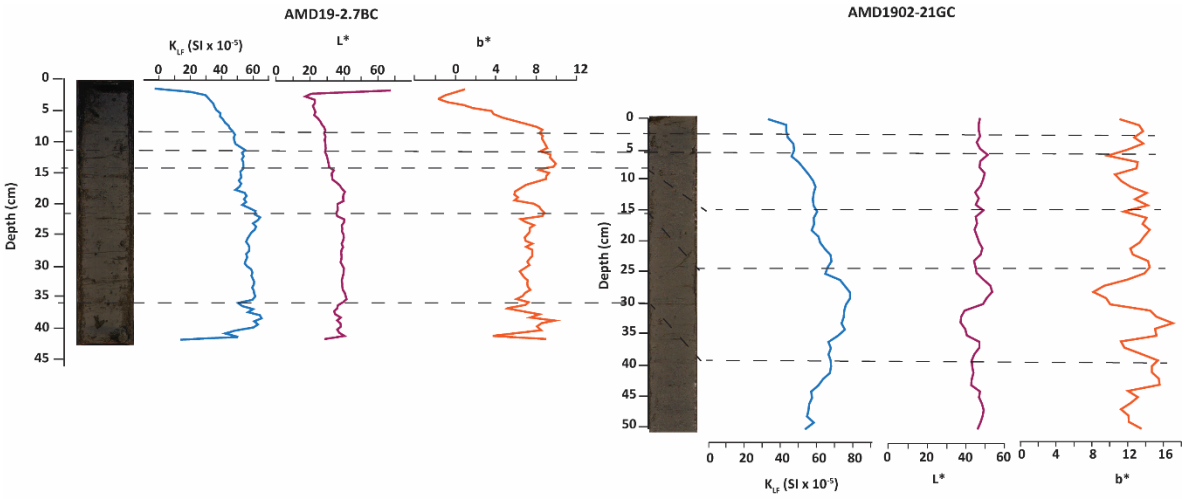

Figure 30. Correlation between AMD19-2.7BC (left) and AM1902-21GC (right).

CONCLUSION GÉNÉRALE

The overall aim of this thesis was to assess how 21st century ice-bridge failures and other climate-driven cryosphere changes have affected sea-surface conditions in northwestern Baffin Bay during the Late Holocene. In recent years, ice-bridge failures have been linked to increased export of Arctic sea ice and freshwater into the region, with potential consequences for surface stratification and ecosystem productivity. To investigate these changes, we applied a multi-proxy approach combining biogenic (dinocysts and diatoms), geochemical (TOC, TN, $\delta^{15}N$, $\delta^{13}C$) proxies along with sedimentological tools (grain size, qXRD) on three sediment cores collected along the western NOW in northern Baffin Bay. The western NOW is an ideal location for assessing freshwater-driven environmental variability because it is influenced by freshwater inputs from three main sources: 1) the Arctic Ocean, 2) proximal glacial melt from the Devon Ice Cap, and 2) distal glacial melt from Ellesmere Island and the GIS. Collectively, the three papers that form this thesis establish a baseline of modern distribution of our biogenic proxies (e.g., dinocyst and diatoms; Fig. 31), provide new insights into how sea-surface conditions in the western NOW have evolved with respect to recent climate change, and how these recent changes compare to variability over the last ca. 400-1200 years (Fig. 32).

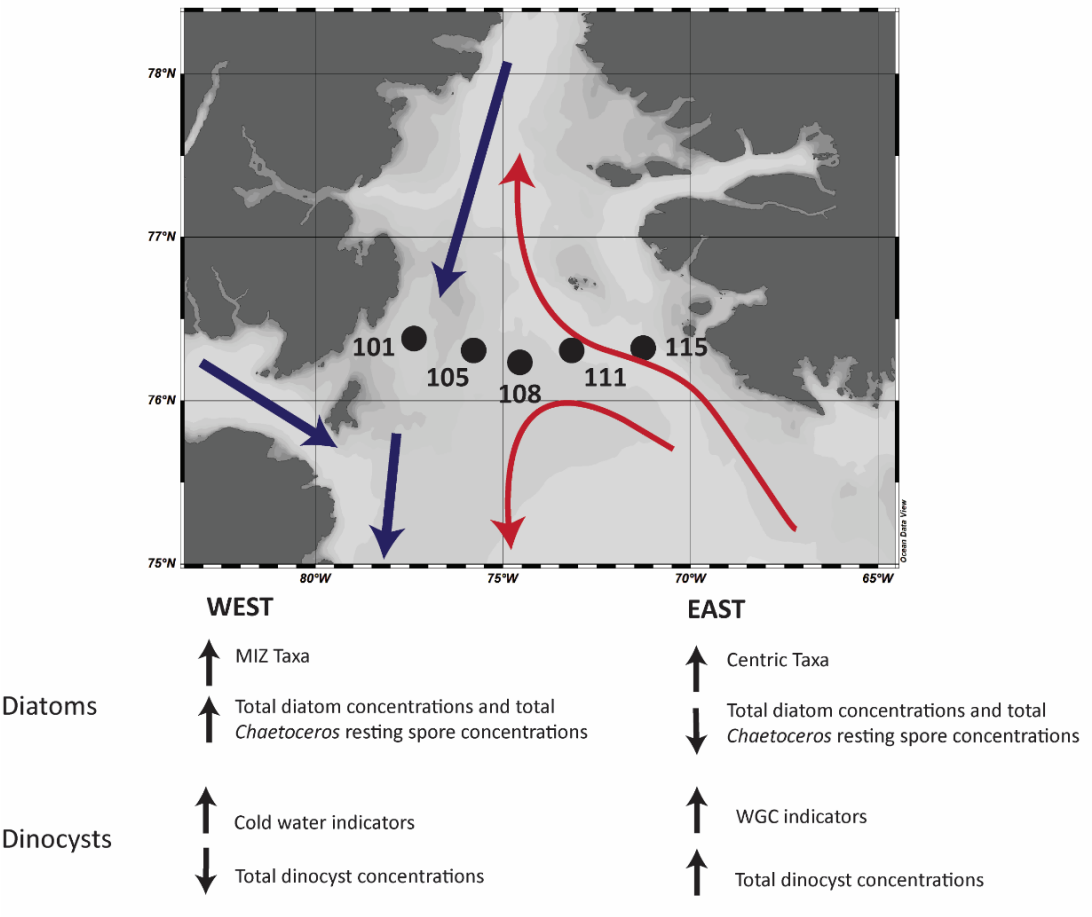

Figure 31. Summary schematic showing the assemblage and concentration differences of dinocysts and diatoms in the western and eastern NOW.

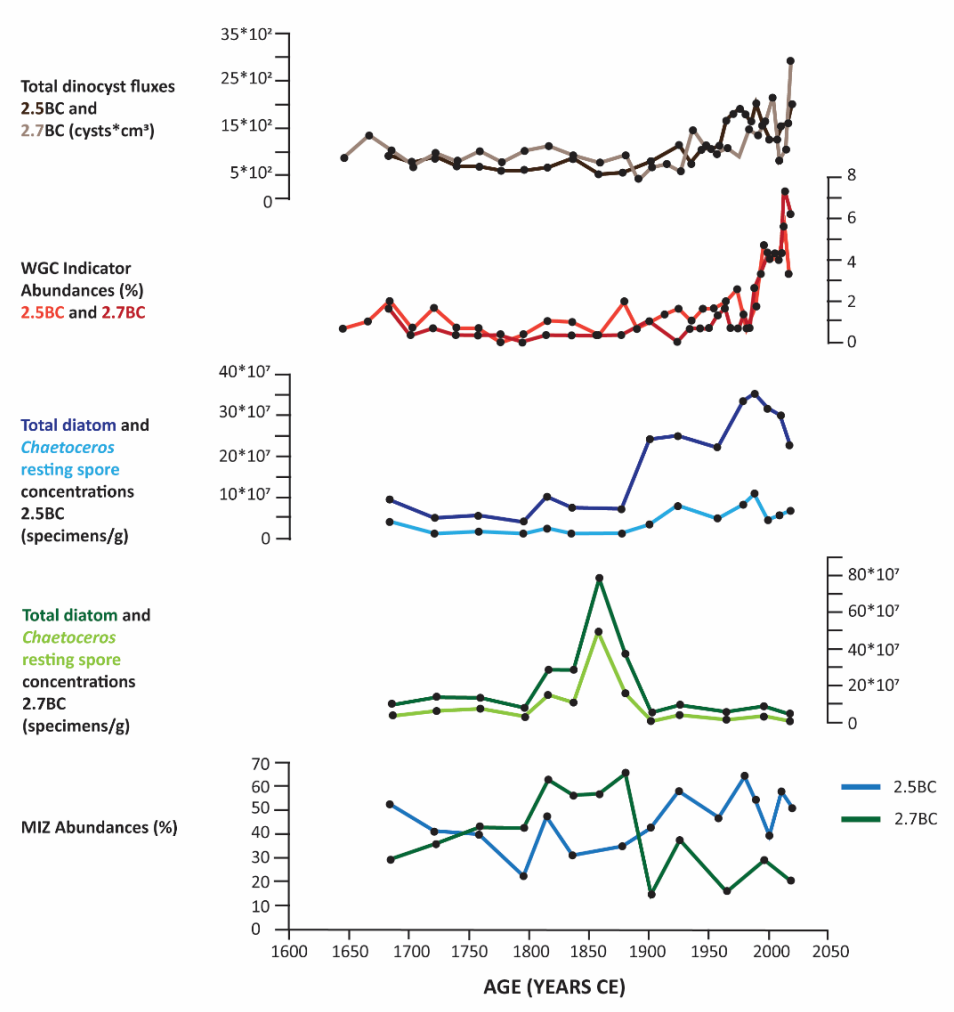

Figure 32. Summary figure of AMD19-2.5 and -2.7BC showing the main downcore changes in dinocyst and diatom assemblage composition and concentrations.

Objective 1- Use dinoflagellate cysts and geochemistry (TOC, TN, $\delta^{15}N$, $\delta^{13}C$) as a proxy for changes in sea-surface conditions and organic matter provenance respectively to assess changes in the NOW conditions and primary production

The first paper presented in this thesis had two main objectives. The first was to assess if dinoflagellate cyst assemblages preserved in surface sediments reflect distinct hydrographic conditions across the NOW and more broadly in Baffin Bay. The second objective was to investigate downcore changes in dinocyst assemblages and geochemistry

(TOC, TN, $\delta^{15}N$, $\delta^{13}C$) to reconstruct variations in sea-surface conditions and organic matter sources over the last ca. 400 years. This paper showed that dinoflagellate cyst assemblages in surface sediments reliably capture the spatial hydrologic gradients of both the NOW and Baffin Bay, thereby providing the baseline framework necessary for interpreting the downcore records. The downcore results show that over a relatively short timescale of ca. 400 years, the NOW shows an earlier and more pronounced response to Arctic Amplification than previously documented. Both sediment cores show a statistically significant shift in dinocyst assemblage composition and increased total dinocyst fluxes at the beginning of the 20th century, which predates the start of the Nares Strait ice bridge northern migration in the 1990's and recurrent failures in the 21st century (Vincent, 2019; Moore et al., 2021). An unexpected result was a signal of increasing influence of the WGC in the most recent sediment. This indicates that, although northern processes, such as the Nares Strait ice bridge failures, are impacting the NOW, southern processes—particularly the northward penetration of Atlantic-derived waters—are simultaneously exerting an important influence. Monitoring and understanding the influence of these northerly and southerly forcings remain important for anticipating the impact of climate change on the NOW and surrounding regions.

Objective 2: Use sub-fossil diatoms as an indicator of changes in sea ice dynamics and sea-surface conditions to assess changes in the marginal ice zone in the western NOW

Given their more direct relationship with sea ice, the second paper focused on using diatoms as a proxy of sea-ice dynamics in the western NOW over the last ca. 400 years. Similar to the previous chapter, surface sediment samples across a longitudinal transect in the NOW were first analyzed to assess whether diatoms reflected gradients in sea-surface conditions, including sea ice. Results from the transect showed marked spatial differences in both concentrations and assemblage composition. The western sector was dominated by higher overall diatom concentrations and higher contribution of small pennate taxa typical of marginal ice zone assemblages. Although the eastern portion of the NOW also exhibited high concentrations of diatoms, a higher proportion of centric taxa contributed to the assemblages. We then analyzed two push cores for their diatom assemblage composition and

concentrations. Most notable from this study was the spatial differences in timing and magnitude of diatom concentrations and assemblage composition between both sediment cores that are approximately 100 km apart from each other. The southerly 2.7BC reached peak concentrations and abundances of typical marginal ice zone taxa between 1800 and 1900 CE, likely reflecting a stable and extended ice edge during the LIA. 2.5BC showed peak concentrations and abundances between 1900 to present, likely influenced in part by the modern configuration of the Nares Strait ice bridges. Our results indicate that diatoms can be used to better understand spatiotemporal changes in the marginal ice zone. Other pan-Arctic research has indicated that changes in the geometry of sea ice plays an important role in the early spring primary production (Ardyna et al., 2020). Our study highlights local spatiotemporal changes in the MIZ characterizing the western NOW, showing a northward migration of the ice edge that is consistent with modern day observations (Vincent, 2019), likely influencing the location of early-spring time bloomers in northern Baffin Bay.

Objective 3: Assess the use of sediment provenance and grain size analysis as an additional tool to provide information on freshwater transport pathways into northern Baffin Bay

The final chapter of this thesis investigates the use of sedimentary proxies (i.e., grain size analysis) and sediment provenance inferred from mineralogy to better characterize freshwater transport pathways into northern Baffin Bay. Our results showed that changes in sedimentary data were coeval with changes in dinocyst abundances and concentrations, where grain size and sediment provenance provided additional information to characterize transport pathways into Baffin Bay. This paper contextualizes both localized inputs from glaciers of the Devon Ice Cap and more distal inputs delivered through western Jones Sound and Nares Strait, showing their respective influence on sea-surface conditions in the NOW. Overall, our results suggest that provenance-based sedimentary proxies hold promise as supplementary tools for distinguishing between multiple freshwater outflow sources in northern Baffin Bay, providing a good starting point for understanding long-term changes in freshwater transport.

Perspectives, caveats, and future work

Collectively, the three papers in this thesis highlight the responsiveness and thus sensitivity of the NOW to climate-induced changes, where the western NOW seems to be particularly vulnerable due to its location along the Arctic outflow pathway. All three chapters show the impact of modern warming on the western NOW, where the response to Arctic Amplification occurs earlier than previously observed and with no observable analogue over the last 400 to 1200 years. All three chapters indicate changes in proxies around the start of the 20th century, shown by increased dinocyst fluxes and mixotrophic composition (Chapter One), increased diatom concentrations at the northernmost site (Chapter Two), and increased localized glacial influence (Chapter Three). Consequently, our records indicate that the modern sea-surface conditions in the NOW represent a transitional environmental regime with no comparable analogue to the last ca. 1200 years.

This thesis also uniquely highlights the importance of assessing how biogenic proxies represent hydrological conditions on a more localized scale. The surface sediments analyzed in Chapters One and Two provided important context on how dinocyst and diatom assemblages in the surface sediment reflect different ocean currents and sea ice dynamics on across the NOW. There is already a large database of surface sediment dinocyst assemblages linked to sea-surface conditions (de Vernal et al., 2020; Thöle et al., 2023) that provides important information on dinocyst ecology. However, due in part to some samples being collected before the start of the 21st century, these datasets can miss modern-warming influence on a localized scale on dinocyst assemblage composition. For example, in the Northern Hemisphere dataset *Operculodinium centrocarpum* is often referred to as a cosmopolitan taxon (de Vernal et al., 2020; Marret et al., 2020), and in other studies representative of Atlantic waters (Rochon et al., 1999). Our records show that *Operculodinium centrocarpum* has distinct relationship with Atlantic-derived currents and but also earlier open water conditions in Baffin Bay. Similar surface sediment datasets have been analyzed for diatoms in Baffin Bay (Krawcyzk et al, 2017; Oksman et al. 2019; Weckström et al., 2020) and northeastern Greenland (Limoges et al., 2018) which provide a

good starting point for environmental interpretation. The transect studied here helped to better define how diatoms represented different sea-surface conditions and particularly sea ice dynamics (i.e., pack ice, marginal ice zone, and open water conditions) across the NOW.

This thesis also presents some caveats. The absence of reliable downcore dates in the core presented in Chapter Three reduced the robustness of our age model and constrained our ability to confidently interpret the climatic periods represented in our records. Producing robust age-models is a common problem in the Arctic, where carbonate material is typically not well preserved in the sediment. To this end, future studies could aim to use other dating methods such as paleomagnetism, that has successfully been used in the Arctic (Barletta et al., 2010) to date sediment cores and shows potential in resolving localized ΔR fluctuations (Girard et al., 2024) and also focus on previously well-dated cores looking at a suite of proxies for a more robust paleo-environmental interpretation.

The biogenic proxies presented here (dinocysts, diatoms, and geochemical signatures in the sediment) also represent only a fragmentary record in the sediment. Only 15-20% of dinoflagellate species produce resting cysts, which only gives a snapshot of information on the overall population. Similarly, diatoms silica dissolution in the Arctic can result in factionary records and their fragility during slide preparation can result in fragmentation of frustules. This thesis highlights the value of multi-proxy work in providing a more robust analysis. Future work could aim at taking this multi-proxy approach a step further by looking at other proxies such as biomarkers (e.g., IP25 and HBIs) and sedimentary ancient DNA to give more information of past sea ice dynamics and community composition respectively.

Furthermore, in the case of dinocysts and diatoms, it is important to note that specific taxa cannot be indicative of one singular environmental parameter (i.e., freshwater input) and in most cases, species ecology is not completely known. The presence of individual species is influenced by more than one parameter such as: light availability, temperature, salinity, sea ice presence, and different nutrient availabilities in the water column. The surface sediment transects presented in Chapter One and Chapter Two of this thesis aims to better understand and nuance the environmental influences on dinocysts and diatom assemblages

within the NOW. However, sea-surface conditions are based on limited *in situ* or satellite data and the surface sediment samples are not well time-constrained. Furthermore, environmental conditions are based on long-term averages and are unable to resolve phenological differences in phytoplankton. Deploying sediment traps and analyzing community composition would help to better understand phenology of phytoplankton and better link dinoflagellates and diatoms to distinct water properties. Furthermore, the analyses of sediment traps could provide ecological context to other Non-Pollen Palynomorphs (NPP)'s routinely counted in palynological slides such as the ciliates (see Annex One) that could be used as an additional environmental interpretation.

ANNEXE 1

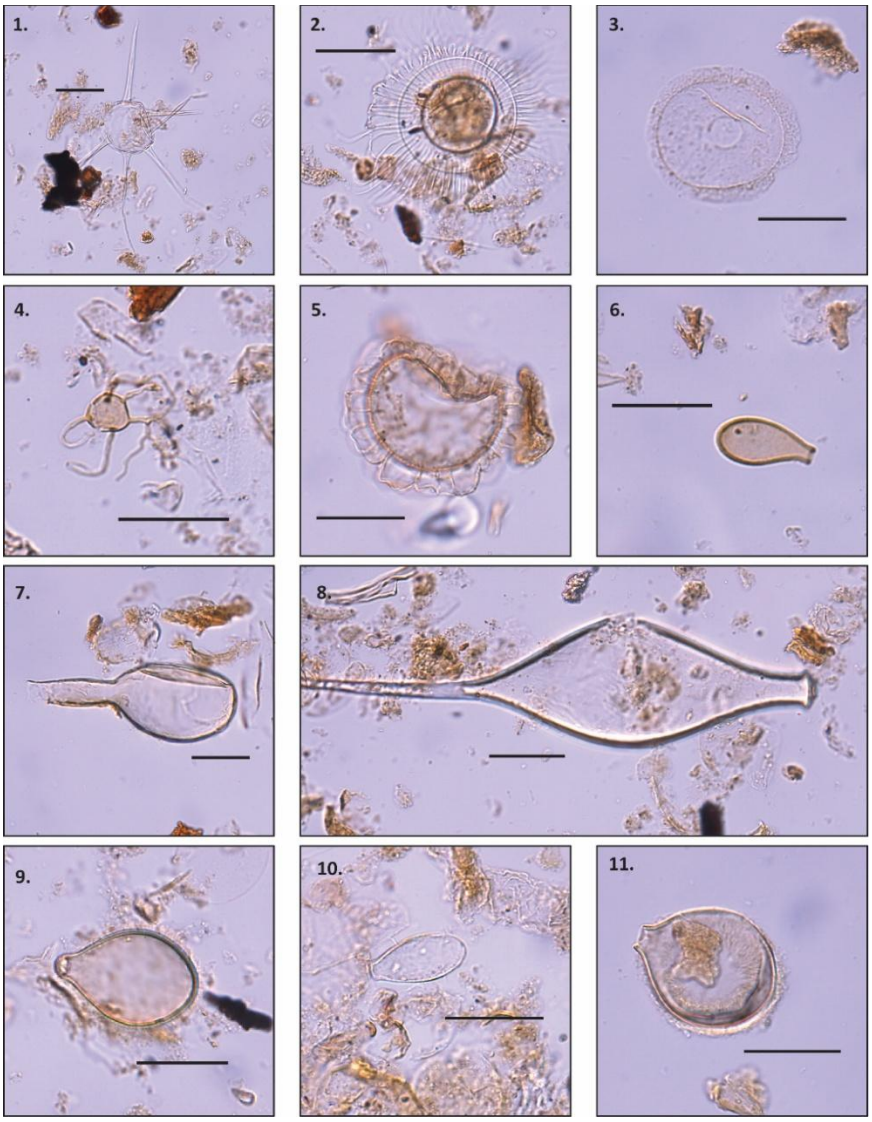

Figure 33. Micrographs of selected non-pollen palynomorphs counted in AMD19-2.5BC, -2.7BC and AMD1902-21GC. 1.) *Hexasterias problematica*, 2.) *Radiosperma corbiferum*, 3.) *Halodinium* spp., 4.) Acritarch "tentacles", 5.) Tintinnid type A, 6.) Tintinnid type X., 7.) Tintinnid type J, 8.) Tintinnid type L, 9.) Tintinnid type C., 10.) Tintinnid type Y., and 11) Tintinnid type D. The black bars represent 20 μm.

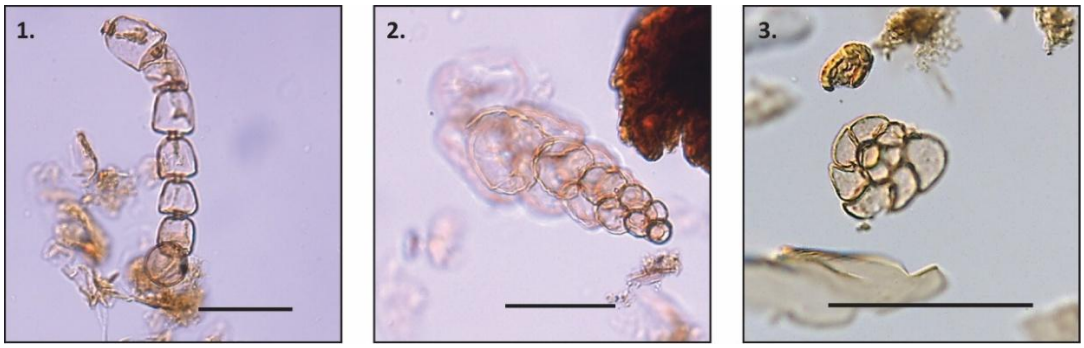

Figure 34. Foraminiferal linings counted in AMD19-2.5BC, -2.7BC and AMD1902-21GC. 1.) Uniserial, 2.) Triserial, 3.) Planispiral. The black bars represent 20 µm.

RÉFÉRENCES BIBLIOGRAPHIQUES

Alves, E. Q., Macario, K., Ascough, P., & Bronk Ramsey, C. (2018). The Worldwide Marine Radiocarbon Reservoir Effect: Definitions, Mechanisms, and Prospects. *Reviews of Geophysics*, *56*(1), 278–305. https://doi.org/10.1002/2017RG000588

Anderson, L. G., & Macdonald, R. W. (2015). Observing the Arctic Ocean carbon cycle in a changing environment. *Polar Research*. https://doi.org/10.3402/polar.v34.26891

Andrews, J. T. (2019). Baffin Bay/Nares Strait surface (seafloor) sediment mineralogy: Further investigations and methods to elucidate spatial variations in provenance. *Canadian Journal of Earth Sciences*, *56*(8), Article 8. https://doi.org/10.1139/cjes-2018-0207

Andrews, J. T., Klein, A. J., Jenner, K. A., Jennings, A. E., & Campbell, C. (2018). The variability of Baffin Bay seafloor sediment mineralogy: The identification of discrete glacial sediment sources and application to Late Quaternary downcore analysis. *Canadian Journal of Earth Sciences*. https://doi.org/10.1139/cjes-2017-0223

Appleby, P. G. (2001). Chronostratigraphic Techniques in Recent Sediments. In W. M. Last & J. P. Smol (Eds.), *Tracking Environmental Change Using Lake Sediments: Basin Analysis, Coring, and Chronological Techniques* (pp. 171–203). Springer Netherlands. https://doi.org/10.1007/0-306-47669-X_9

Ardyna, M., Babin, M., Gosselin, M., Devred, E., Rainville, L., & Tremblay, J.-É. (2014). Recent Arctic Ocean sea ice loss triggers novel fall phytoplankton blooms. *Geophysical Research Letters*, *41*(17). https://doi.org/10.1002/2014GL061047

Ardyna, M., Mundy, C. J., Mayot, N., Matthes, L. C., Oziel, L., Horvat, C., Leu, E., Assmy, P., Hill, V., Matrai, P. A., Gale, M., Melnikov, I. A., & Arrigo, K. R. (2020). Under-Ice Phytoplankton Blooms: Shedding Light on the "Invisible" Part of Arctic Primary Production. *Frontiers in Marine Science*, *7*. https://doi.org/10.3389/fmars.2020.608032

Arias-Ortiz, A., Masqué, P., Garcia-Orellana, J., Serrano, O., Mazarrasa, I., Marbà, N., Lovelock, C. E., Lavery, P. S., & Duarte, C. M. (2018). Reviews and syntheses: ^{210}Pb-derived sediment and carbon accumulation rates in vegetated coastal ecosystems – setting the record straight. *Biogeosciences*, *15*(22), 6791–6818. https://doi.org/10.5194/bg-15-6791-2018

Arrigo, K. R., Dijken, G. van, & Pabi, S. (2008). Impact of a shrinking Arctic ice cover on marine primary production. *Geophysical Research Letters*, *35*(19), Article 19. https://doi.org/10.1029/2008GL035028

Arrigo, K. R., & van Dijken, G. L. (2015). Continued increases in Arctic Ocean primary production. *Progress in Oceanography*, *136*, 60–70. https://doi.org/10.1016/j.pocean.2015.05.002

Babb, D. G., Galley, R. J., Kirillov, S., Landy, J. C., Howell, S. E. L., Stroeve, J. C., Meier, W., Ehn, J. K., & Barber, D. G. (2023). The Stepwise Reduction of Multiyear Sea Ice Area in the Arctic Ocean Since 1980. *Journal of Geophysical Research: Oceans*, *128*(10), e2023JC020157. https://doi.org/10.1029/2023JC020157

Bâcle, J., Carmack, E. C., & Ingram, R. G. (2002). Water column structure and circulation under the North Water during spring transition: April–July 1998. *Deep Sea Research Part II: Topical Studies in Oceanography*, *49*(22), Article 22. https://doi.org/10.1016/S0967-0645(02)00170-4

Bailey, J. N.-L., Macdonald, R. W., Sanei, H., Outridge, P. M., Johannessen, S. C., Hochheim, K., Barber, D., & Stern, G. A. (2013). Change at the margin of the North Water Polynya, Baffin Bay, inferred from organic matter records in dated sediment cores. *Marine Geology*, *341*, 1–13. https://doi.org/10.1016/j.margeo.2013.04.017

Barletta, F., St-Onge, G., Channell, J. E. T., & Rochon, A. (2010). Dating of Holocene western Canadian Arctic sediments by matching paleomagnetic secular variation to a geomagnetic field model. *Quaternary Science Reviews*, *29*(17), 2315–2324. https://doi.org/10.1016/j.quascirev.2010.05.035

Bélanger, S., Babin, M., & Tremblay, J.-É. (2013). Increasing cloudiness in Arctic damps the increase in phytoplankton primary production due to sea ice receding. *Biogeosciences*, *10*(6), Article 6. https://doi.org/10.5194/bg-10-4087-2013

Bhatia, M. P., Kujawinski, E. B., Das, S. B., Breier, C. F., Henderson, P. B., & Charette, M. A. (2013). Greenland meltwater as a significant and potentially bioavailable source of iron to the ocean. *Nature Geoscience*, *6*(4). https://doi.org/10.1038/ngeo1746

Bhatia, M. P., Waterman, S., Burgess, D. O., Williams, P. L., Bundy, R. M., Mellett, T., Roberts, M., & Bertrand, E. M. (2021). Glaciers and Nutrients in the Canadian Arctic Archipelago Marine System. *Global Biogeochemical Cycles*, *35*(8), e2021GB006976. https://doi.org/10.1029/2021GB006976

Blais, M., Ardyna, M., Gosselin, M., Dumont, D., Bélanger, S., Tremblay, J.-É., Gratton, Y., Marchese, C., & Poulin, M. (2017). Contrasting interannual changes in phytoplankton

productivity and community structure in the coastal Canadian Arctic Ocean. *Limnology and Oceanography*, *62*(6), Article 6. https://doi.org/10.1002/lno.10581

Blott, S. J., & Pye, K. (2006). Particle size distribution analysis of sand-sized particles by laser diffraction: An experimental investigation of instrument sensitivity and the effects of particle shape. *Sedimentology*, *53*(3), 671–685. https://doi.org/10.1111/j.1365-3091.2006.00786.x

Bourke, R. H., & Paquette, R. G. (1991). Formation of Baffin Bay Bottom and Deep Waters. In P. C. Chu & J. C. Gascard (Eds.), *Elsevier Oceanography Series* (Vol. 57, pp. 135–155). Elsevier. https://doi.org/10.1016/S0422-9894(08)70065-5

Bracquart, E., Montero-Serrano, J.-C., Lajeunesse, P., St-Onge, G., & Copland, L. (n.d.). The Holocene sedimentary record of Mittie Glacier dynamics in Smith Bay, Ellesmere Island (eastern Canadian Arctic Archipelago). *Journal of Quaternary Science*, *n/a*(n/a). https://doi.org/10.1002/jqs.70005

Carmack, E. C., Yamamoto-Kawai, M., Haine, T. W. N., Bacon, S., Bluhm, B. A., Lique, C., Melling, H., Polyakov, I. V., Straneo, F., Timmermans, M.-L., & Williams, W. J. (2016). Freshwater and its role in the Arctic Marine System: Sources, disposition, storage, export, and physical and biogeochemical consequences in the Arctic and global oceans. *Journal of Geophysical Research: Biogeosciences*, *121*(3), 675–717. https://doi.org/10.1002/2015JG003140

Caron, M., Montero-Serrano, J.-C., St-Onge, G., & Rochon, A. (2020). Quantifying Provenance and Transport Pathways of Holocene Sediments From the Northwestern Greenland Margin. *Paleoceanography and Paleoclimatology*, *35*(5), Article 5. https://doi.org/10.1029/2019PA003809

Caron, M., St-Onge, G., Montero-Serrano, J.-C., Rochon, A., Georgiadis, E., Giraudeau, J., & Massé, G. (2019). Holocene chronostratigraphy of northeastern Baffin Bay based on radiocarbon and palaeomagnetic data. *Boreas*, *48*(1), Article 1. https://doi.org/10.1111/bor.12346

Carr, J. R., Stokes, C. R., & Vieli, A. (2017). Threefold increase in marine-terminating outlet glacier retreat rates across the Atlantic Arctic: 1992–2010. *Annals of Glaciology*, *58*(74), 72–91. https://doi.org/10.1017/aog.2017.3

Casciotti, K. L. (2016). Nitrogen and Oxygen Isotopic Studies of the Marine Nitrogen Cycle. *Annual Review of Marine Science*, *8*(1), Article 1. https://doi.org/10.1146/annurev-marine-010213-135052

Cook, A. J., Copland, L., Noël, B. P. Y., Stokes, C. R., Bentley, M. J., Sharp, M. J., Bingham, R. G., & van den Broeke, M. R. (2019). Atmospheric forcing of rapid marine-

terminating glacier retreat in the Canadian Arctic Archipelago. *Science Advances*, *5*(3), eaau8507. https://doi.org/10.1126/sciadv.aau8507

Cormier, M.-A., Rochon, A., de Vernal, A., & Gélinas, Y. (2016). Multi-proxy study of primary production and paleoceanographical conditions in northern Baffin Bay during the last centuries. *Marine Micropaleontology*, *127*, 1–10. https://doi.org/10.1016/j.marmicro.2016.07.001

Crosta, X. (2011). Marine diatoms in polar and sub-polar environments and their application to Late Pleistocene paleoclimate reconstruction. *IOP Conference Series: Earth and Environmental Science*, *14*, 012006. https://doi.org/10.1088/1755-1315/14/1/012006

Crosta, X., & Koç, N. (2007). Chapter Eight Diatoms: From Micropaleontology to Isotope Geochemistry. In *Developments in Marine Geology* (Vol. 1, pp. 327–369). Elsevier. https://doi.org/10.1016/S1572-5480(07)01013-5

Darby, D. A., Ortiz, J. D., Grosch, C. E., & Lund, S. P. (2012). 1,500-year cycle in the Arctic Oscillation identified in Holocene Arctic sea-ice drift. *Nature Geoscience; London*, *5*(12), Article 12. http://dx.doi.org.proxy.hil.unb.ca/10.1038/ngeo1629

Davidson, T. A., Wetterich, S., Johansen, K. L., Grønnow, B., Windirsch, T., Jeppesen, E., Syväranta, J., Olsen, J., González-Bergonzoni, I., Strunk, A., Larsen, N. K., Meyer, H., Søndergaard, J., Dietz, R., Eulears, I., & Mosbech, A. (2018). The history of seabird colonies and the North Water ecosystem: Contributions from palaeoecological and archaeological evidence. *Ambio*, *47*(2), Article 2. https://doi.org/10.1007/s13280-018-1031-1

de Vernal, A., Radi, T., Zaragosi, S., Van Nieuwenhove, N., Rochon, A., Allan, E., De Schepper, S., Eynaud, F., Head, M. J., Limoges, A., Londeix, L., Marret, F., Matthiessen, J., Penaud, A., Pospelova, V., Price, A., & Richerol, T. (2020). Distribution of common modern dinoflagellate cyst taxa in surface sediments of the Northern Hemisphere in relation to environmental parameters: The new n=1968 database. *Marine Micropaleontology*, *159*, 101796. https://doi.org/10.1016/j.marmicro.2019.101796

Deming, J. W., Fortier, L., & Fukuchi, M. (2002). The International North Water Polynya Study (NOW): A brief overview. *Deep Sea Research Part II: Topical Studies in Oceanography*, *49*(22), Article 22. https://doi.org/10.1016/S0967-0645(02)00168-6

Dodd, P. A., Rabe, B., Hansen, E., Falck, E., Mackensen, A., Rohling, E., Stedmon, C., & Kristiansen, S. (2012). The freshwater composition of the Fram Strait outflow derived from a decade of tracer measurements. *Journal of Geophysical Research: Oceans*, *117*(C11). https://doi.org/10.1029/2012JC008011

Dumont, D., Gratton, Y., & Arbetter, T. E. (2009). Modeling the Dynamics of the North Water Polynya Ice Bridge. *Journal of Physical Oceanography*, *39*(6), Article 6. https://doi.org/10.1175/2008JPO3965.1

Dunbar, M., & Dunbar, M. J. (1972). 21.—The History of the North Water. *Proceedings of the Royal Society of Edinburgh, Section B: Biological Sciences*, *72*(1), Article 1. https://doi.org/10.1017/S0080455X00001788

Eberl, D. D. (2003). User Guide to RockJock—A Program for Determining Quantitative Mineralogy from X-Ray Diffraction Data. In *Open-File Report* (Nos. 2003–78). U.S. Geological Survey. https://doi.org/10.3133/ofr200378

Eegeesiak, O., Aariak, E., & V. Kleist, K. (2017). *People of the Ice Bridge: The future of the Pikialasorsuaq* (Report of the Pikialasorsuaq Commission, p. 119). Inuit Circumpolar Council Canada.

Fox, A., & Walker, B. D. (2022). Sources and Cycling of Particulate Organic Matter in Baffin Bay: A Multi-Isotope δ13C, δ15N, and Δ14C Approach. *Frontiers in Marine Science*, *9*. https://doi.org/10.3389/fmars.2022.846025

Freyria, N. J., Joli, N., & Lovejoy, C. (2021). A decadal perspective on north water microbial eukaryotes as Arctic Ocean sentinels. *Scientific Reports*, *11*(1), Article 1. https://doi.org/10.1038/s41598-021-87906-4

Georgiadis, E., Giraudeau, J., Jennings, A., Limoges, A., Jackson, R., Ribeiro, S., & Massé, G. (2020). Local and regional controls on Holocene sea ice dynamics and oceanography in Nares Strait, Northwest Greenland. *Marine Geology*, *422*, 106115. https://doi.org/10.1016/j.margeo.2020.106115

Georgiadis, E., Giraudeau, J., Martinez, P., Lajeunesse, P., St-Onge, G., Schmidt, S., & Massé, G. (2018). Deglacial to postglacial history of Nares Strait, Northwest Greenland: A marine perspective from Kane Basin. *Climate of the Past*, *14*(12), Article 12. https://doi.org/10.5194/cp-14-1991-2018

Girard, J., Reilly, B. T., St-Onge, G., Lagroix, F., Montero-Serrano, J.-C., Stoner, J. S., & Jennings, A. E. (2024). Paleomagnetic Secular Variations in North Greenland Around 81°N Over the Last 6,000 Years. *Geochemistry, Geophysics, Geosystems*, *25*(10), e2024GC011620. https://doi.org/10.1029/2024GC011620

Gotfredsen, A. B., Appelt, M., & Hastrup, K. (2018). Walrus history around the North Water: Human–animal relations in a long-term perspective. *Ambio*, *47*(2), Article 2. https://doi.org/10.1007/s13280-018-1027-x

Halbach, L., Vihtakari, M., Duarte, P., Everett, A., Granskog, M. A., Hop, H., Kauko, H. M., Kristiansen, S., Myhre, P. I., Pavlov, A. K., Pramanik, A., Tatarek, A., Torsvik, T., Wiktor, J. M., Wold, A., Wulff, A., Steen, H., & Assmy, P. (2019). Tidewater Glaciers and Bedrock Characteristics Control the Phytoplankton Growth Environment in a Fjord in the Arctic. *Frontiers in Marine Science*, *6*. https://doi.org/10.3389/fmars.2019.00254

Hamel, D., Vernal, A. de, Gosselin, M., & Hillaire-Marcel, C. (2002). Organic-walled microfossils and geochemical tracers: Sedimentary indicators of productivity changes in the North Water and northern Baffin Bay during the last centuries. *Deep Sea Research Part II: Topical Studies in Oceanography*, *49*(22), Article 22. https://doi.org/10.1016/S0967-0645(02)00190-X

Hanna, E., Huybrechts, P., Steffen, K., Cappelen, J., Huff, R., Shuman, C., Irvine-Fynn, T., Wise, S., & Griffiths, M. (2008). *Increased Runoff from Melt from the Greenland Ice Sheet: A Response to Global Warming*. https://doi.org/10.1175/2007JCLI1964.1

Hargrave, B. T., Walsh, I. D., & Murray, D. W. (2002). Seasonal and spatial patterns in mass and organic matter sedimentation in the North Water. Deep Sea Research Part II: Topical Studies in Oceanography, The International North Water Polynya Study, 49(22), 5227–5244. https://doi.org/10.1016/S0967-0645(02)00187-X

Harning, D. J., Jennings, A. E., Holman, B., Kelleher, R. V., Feng, S., Brooks, N. K. S., Andrews, J. T., Marchitto, T., & Sepúlveda, J. (2025). Spatiotemporal Variability in the Holocene Extent of Pikialasorsuaq (North Water Polynya), Baffin Bay. *Paleoceanography and Paleoclimatology*, *40*(8), e2025PA005153. https://doi.org/10.1029/2025PA005153

Hastrup, K., Mosbech, A., & Grønnow, B. (2018). Introducing the North Water: Histories of exploration, ice dynamics, living resources, and human settlement in the Thule Region. *Ambio*, *47*(2), Article 2. https://doi.org/10.1007/s13280-018-1030-2

Head, M. J. (1996). Modern dinoflagellate cysts and their biological affinities. *Palynology: principles and applications*, *3*, 1197-1248.

Heaton, T. J., Köhler, P., Butzin, M., Bard, E., Reimer, R. W., Austin, W. E. N., Ramsey, C. B., Grootes, P. M., Hughen, K. A., Kromer, B., Reimer, P. J., Adkins, J., Burke, A., Cook, M. S., Olsen, J., & Skinner, L. C. (2020). Marine20—The Marine Radiocarbon Age Calibration Curve (0–55,000 cal BP). *Radiocarbon*, *62*(4), 779–820. https://doi.org/10.1017/RDC.2020.68

Heide-Jørgensen, M. P., Burt, L. M., Hansen, R. G., Nielsen, N. H., Rasmussen, M., Fossette, S., & Stern, H. (2013). The Significance of the North Water Polynya to Arctic Top Predators. *AMBIO*, *42*(5), Article 5. https://doi.org/10.1007/s13280-012-0357-3

Heide-Jørgensen, M. P., Sinding, M.-H. S., Nielsen, N. H., Rosing-Asvid, A., & Hansen, R. G. (2016). Large numbers of marine mammals winter in the North Water polynya. *Polar Biology*, *39*(9), Article 9. https://doi.org/10.1007/s00300-015-1885-7

Hughen, K. A. (2007). Chapter Five Radiocarbon Dating of Deep-Sea Sediments. In *Developments in Marine Geology* (Vol. 1, pp. 185–210). Elsevier. https://doi.org/10.1016/S1572-5480(07)01010-X

Jackson, R., Kvorning, A. B., Limoges, A., Georgiadis, E., Olsen, S. M., Tallberg, P., Andersen, T. J., Mikkelsen, N., Giraudeau, J., Massé, G., Wacker, L., & Ribeiro, S. (2021). Holocene polynya dynamics and their interaction with oceanic heat transport in northernmost Baffin Bay. *Scientific Reports*, *11*(1), 10095. https://doi.org/10.1038/s41598-021-88517-9

Jennings, A. E., Andrews, J. T., Oliver, B., Walczak, M., & Mix, A. (2019). Retreat of the Smith Sound Ice Stream in the Early Holocene. *Boreas*, *48*(4), Article 4. https://doi.org/10.1111/bor.12391

Jeppesen, E., Appelt, M., Hastrup, K., Grønnow, B., Mosbech, A., Smol, J. P., & Davidson, T. A. (2018). Living in an oasis: Rapid transformations, resilience, and resistance in the North Water Area societies and ecosystems. *Ambio*, *47*(2), Article 2. https://doi.org/10.1007/s13280-018-1034-y

Joli, N., Gosselin, M., Ardyna, M., Babin, M., Onda, D. F., Tremblay, J.-É., & Lovejoy, C. (2018). Need for focus on microbial species following ice melt and changing freshwater regimes in a Janus Arctic Gateway. *Scientific Reports*, *8*(1), Article 1. https://doi.org/10.1038/s41598-018-27705-6

Jones, E. P. (2001). Circulation in the Arctic Ocean. *Polar Research*, *20*(2), Article 2. https://doi.org/10.1111/j.1751-8369.2001.tb00049.x

Kirillov, S., Dmitrenko, I., Babb, D. G., Ehn, J. K., Koldunov, N., Rysgaard, S., Jensen, D., & Barber, D. G. (2022). The role of oceanic heat flux in reducing thermodynamic ice growth in Nares Strait and promoting earlier collapse of the ice bridge. *Ocean Science*, *18*(5), Article 5. https://doi.org/10.5194/os-18-1535-2022

Knudsen, K. L., Stabell, B., Seidenkrantz, M.-S., Eiríksson, J., & Blake, W. (2008). Deglacial and Holocene conditions in northernmost Baffin Bay: Sediments, foraminifera, diatoms and stable isotopes. *Boreas*, *37*(3), Article 3. https://doi.org/10.1111/j.1502-3885.2008.00035.x

Koerner, K., Limoges, A., Van Nieuwenhove, N., Richerol, T., Massé, G., & Ribeiro, S. (2021). Late Holocene sea-surface changes in the North Water polynya reveal

freshening of northern Baffin Bay in the 21st century. *Global and Planetary Change*, 103642. https://doi.org/10.1016/j.gloplacha.2021.103642

Kravitz, J. H. (1976). Textural and mineralogical characteristics of the surficial sediments of Kane Basin. *Journal of Sedimentary Research*, *46*(3), Article 3. https://doi.org/10.1306/212F7036-2B24-11D7-8648000102C1865D

Krawczyk, D. W., Witkowski, A., Moros, M., Lloyd, J. M., Høyer, J. L., Miettinen, A., & Kuijpers, A. (2017). Quantitative reconstruction of Holocene sea ice and sea surface temperature off West Greenland from the first regional diatom data set. *Paleoceanography*, *32*(1), Article 1. https://doi.org/10.1002/2016PA003003

Krawczyk, D., Witkowski, A., Moros, M., Lloyd, J., Kuijpers, A., & Kierzek, A. (2010). Late-Holocene diatom-inferred reconstruction of temperature variations of the West Greenland Current from Disko Bugt, central West Greenland. *The Holocene*, *20*(5), Article 5. https://doi.org/10.1177/0959683610371993

Kuzyk, Z. Z. A., Macdonald, R. W., Tremblay, J.-É., & Stern, G. A. (2010). Elemental and stable isotopic constraints on river influence and patterns of nitrogen cycling and biological productivity in Hudson Bay. *Continental Shelf Research*, *30*(2), Article 2. https://doi.org/10.1016/j.csr.2009.10.014

Kwok, R., Pedersen, L. T., Gudmandsen, P., & Pang, S. S. (2010). Large sea ice outflow into the Nares Strait in 2007. *Geophysical Research Letters*, *37*(3), Article 3. https://doi.org/10.1029/2009GL041872

Libby, W. F. (1946). Atmospheric Helium Three and Radiocarbon from Cosmic Radiation. *Physical Review*, *69*(11–12), 671–672. https://doi.org/10.1103/PhysRev.69.671.2

Limoges, A., Ribeiro, S., Van Nieuwenhove, N., Jackson, R., Juggins, S., Crosta, X., & Weckström, K. (2023). Marine diatoms record Late Holocene regime shifts in the Pikialasorsuaq ecosystem. *Global Change Biology*, *29*(23), Article 23. https://doi.org/10.1111/gcb.16958

Limoges, A., Ribeiro, S., Weckström, K., Heikkilä, M., Zamelczyk, K., Andersen, T. J., Tallberg, P., Massé, G., Rysgaard, S., Nørgaard-Pedersen, N., & Seidenkrantz, M.-S. (2018). Linking the Modern Distribution of Biogenic Proxies in High Arctic Greenland Shelf Sediments to Sea Ice, Primary Production, and Arctic-Atlantic Inflow. *Journal of Geophysical Research: Biogeosciences*, *123*(3), Article 3. https://doi.org/10.1002/2017JG003840

Limoges, A., Weckström, K., Ribeiro, S., Georgiadis, E., Hansen, K. E., Martinez, P., Seidenkrantz, M.-S., Giraudeau, J., Crosta, X., & Massé, G. (2020). Learning from the past: Impact of the Arctic Oscillation on sea ice and marine productivity off northwest

Greenland over the last 9,000 years. *Global Change Biology*, *26*(12), Article 12. https://doi.org/10.1111/gcb.15334

López-Blanco, E., Jackowicz-Korczynski, M., Mastepanov, M., Skov, K., Westergaard-Nielsen, A., Williams, M., & Christensen, T. R. (2020). Multi-year data-model evaluation reveals the importance of nutrient availability over climate in arctic ecosystem C dynamics. *Environmental Research Letters*, *15*(9), 094007. https://doi.org/10.1088/1748-9326/ab865b

Lovejoy, C., Legendre, L., & Price, N. M. (2002). Prolonged diatom blooms and microbial food web dynamics: Experimental results from an Arctic polynya. *Aquatic Microbial Ecology*, *29*(3), Article 3. https://doi.org/10.3354/ame029267

Mackensen, A., & Schmiedl, G. (2019). Stable carbon isotopes in paleoceanography: Atmosphere, oceans, and sediments. *Earth-Science Reviews*, *197*, 102893. https://doi.org/10.1016/j.earscirev.2019.102893

Marchese, C., Albouy, C., Tremblay, J.-É., Dumont, D., D'Ortenzio, F., Vissault, S., & Bélanger, S. (2017). Changes in phytoplankton bloom phenology over the North Water (NOW) polynya: A response to changing environmental conditions. *Polar Biology*, *40*(9), Article 9. https://doi.org/10.1007/s00300-017-2095-2

Marret, F., Bradley, L., de Vernal, A., Hardy, W., Kim, S.-Y., Mudie, P., Penaud, A., Pospelova, V., Price, A. M., Radi, T., & Rochon, A. (2020). From bi-polar to regional distribution of modern dinoflagellate cysts, an overview of their biogeography. *Marine Micropaleontology*, *159*, 101753. https://doi.org/10.1016/j.marmicro.2019.101753

Matthews, K. M., Kim, C.-K., & Martin, P. (2007). Determination of 210Po in environmental materials: A review of analytical methodology. *Applied Radiation and Isotopes*, *65*(3), Article 3. https://doi.org/10.1016/j.apradiso.2006.09.005

März, C., Meinhardt, A.-K., Schnetger, B., & Brumsack, H.-J. (2015). Silica diagenesis and benthic fluxes in the Arctic Ocean. *Marine Chemistry*, *171*, 1–9. https://doi.org/10.1016/j.marchem.2015.02.003

Mei, Z.-P., Legendre, L., Tremblay, J.-É., Miller, L. A., Gratton, Y., Lovejoy, C., Yager, P. L., & Gosselin, M. (2005). Carbon to nitrogen (C:N) stoichiometry of the spring–summer phytoplankton bloom in the North Water Polynya (NOW). *Deep Sea Research Part I: Oceanographic Research Papers*, *52*(12), Article 12. https://doi.org/10.1016/j.dsr.2005.07.001

Melling, H., Gratton, Y., & Ingram, G. (2001). Ocean circulation within the North Water polynya of Baffin Bay. *Atmosphere-Ocean*, *39*(3), Article 3. https://doi.org/10.1080/07055900.2001.9649683

Meyers, P. A. (1997). Organic geochemical proxies of paleoceanographic, paleolimnologic, and paleoclimatic processes. *Organic Geochemistry*, *27*(5), Article 5. https://doi.org/10.1016/S0146-6380(97)00049-1

Montero-Serrano, J.C., and Brossard, J. (2019). Collecting sedimentary sequences and plankton samples in the continental margins from the eastern Canadian Arctic Archipelago. ArcticNet Leg 2b Cruise Report - CCGS Amundsen expedition (25 July to 15 August 2019). ArcticNet, 22 p.

Moore, G. W. K., Howell, S. E. L., Brady, M., Xu, X., & McNeil, K. (2021). Anomalous collapses of Nares Strait ice arches leads to enhanced export of Arctic sea ice. *Nature Communications*, *12*(1), Article 1. https://doi.org/10.1038/s41467-020-20314-w

Moore, G. W. K., & McNeil, K. (2018). The Early Collapse of the 2017 Lincoln Sea Ice Arch in Response to Anomalous Sea Ice and Wind Forcing. *Geophysical Research Letters*, *45*(16), Article 16. https://doi.org/10.1029/2018GL078428

Morales Maqueda, M. A. (2004). Polynya Dynamics: A Review of Observations and Modeling. *Reviews of Geophysics*, *42*(1), Article 1. https://doi.org/10.1029/2002RG000116

Mortimer, C. A., Sharp, M., & Wychen, W. V. (2018). Influence of recent warming and ice dynamics on glacier surface elevations in the Canadian High Arctic, 1995–2014. *Journal of Glaciology*, *64*(245), Article 245. https://doi.org/10.1017/jog.2018.37

Mudie, P. J., Rochon, A., & Levac, E. (2005). Decadal-scale sea ice changes in the Canadian Arctic and their impacts on humans during the past 4,000 years. *Environmental Archaeology*, *10*(2), Article 2. https://doi.org/10.1179/env.2005.10.2.113

Müller, P. J., & Suess, E. (1979). Productivity, sedimentation rate, and sedimentary organic matter in the oceans—I. Organic carbon preservation. *Deep Sea Research Part A. Oceanographic Research Papers*, *26*(12), Article 12. https://doi.org/10.1016/0198-0149(79)90003-7

Münchow, A., Falkner, K. K., & Melling, H. (2007). Spatial continuity of measured seawater and tracer fluxes through Nares Strait, a dynamically wide channel bordering the Canadian Archipelago. *Journal of Marine Research*, *65*(6), Article 6. https://doi.org/10.1357/002224007784219048

Münchow, A., Falkner, K. K., & Melling, H. (2015). Baffin Island and West Greenland Current Systems in northern Baffin Bay. *Progress in Oceanography*, *132*, 305–317. https://doi.org/10.1016/j.pocean.2014.04.001

Nicolaus, M., Katlein, C., Maslanik, J., & Hendricks, S. (2012). Changes in Arctic sea ice result in increasing light transmittance and absorption. *Geophysical Research Letters*, *39*(24). https://doi.org/10.1029/2012GL053738

Noël, B., van de Berg, W. J., Lhermitte, S., Wouters, B., Schaffer, N., & van den Broeke, M. R. (2018). Six Decades of Glacial Mass Loss in the Canadian Arctic Archipelago. *Journal of Geophysical Research: Earth Surface*, *123*(6), 1430–1449. https://doi.org/10.1029/2017JF004304

Notz, D., Dörr, J., Bailey, D. A., Blockley, E., Bushuk, M., Debernard, J. B., Dekker, E., DeRepentigny, P., Docquier, D., Fučkar, N. S., Fyfe, J. C., Jahn, A., Holland, M., Hunke, E., Iovino, D., Khosravi, N., Massonnet, F., Madec, G., O'Farrell, S., … Vancoppenolle, M. (2020). Arctic Sea Ice in CMIP6. *Geophysical Research Letters*, *n/a*(n/a), Article n/a. https://doi.org/10.1029/2019GL086749

Oksman, M., Juggins, S., Miettinen, A., Witkowski, A., & Weckström, K. (2019). The biogeography and ecology of common diatom species in the northern North Atlantic, and their implications for paleoceanographic reconstructions. *Marine Micropaleontology*, *148*, 1–28. https://doi.org/10.1016/j.marmicro.2019.02.002

Otosaka, I. N., Horwath, M., Mottram, R., & Nowicki, S. (2023). Mass Balances of the Antarctic and Greenland Ice Sheets Monitored from Space. *Surveys in Geophysics*, *44*(5), 1615–1652. https://doi.org/10.1007/s10712-023-09795-8

Parkinson, C. L., & DiGirolamo, N. E. (2021). Sea ice extents continue to set new records: Arctic, Antarctic, and global results. *Remote Sensing of Environment*, *267*, 112753. https://doi.org/10.1016/j.rse.2021.112753

Pearce, C., Özdemir, K. S., Forchhammer Mathiasen, R., Detlef, H., & Olsen, J. (2023). The marine reservoir age of Greenland coastal waters. *Geochronology*, *5*(2), Article 2. https://doi.org/10.5194/gchron-5-451-2023

Pennington, W., Tutin, T. G., Cambray, R. S., & Fisher, E. M. (1973). Observations on Lake Sediments using Fallout 137 Cs as a Tracer. *Nature*, *242*(5396), Article 5396. https://doi.org/10.1038/242324a0

Perdue, E. M., & Koprivnjak, J.-F. (2007). Using the C/N ratio to estimate terrigenous inputs of organic matter to aquatic environments. *Estuarine, Coastal and Shelf Science*, *73*(1), Article 1. https://doi.org/10.1016/j.ecss.2006.12.021

Perner, K., Moros, M., Jennings, A., Lloyd, J., & Knudsen, K. (2013). Holocene palaeoceanographic evolution off West Greenland. *The Holocene*, *23*(3), Article 3. https://doi.org/10.1177/0959683612460785

Pineault, S., Tremblay, J.-É., Gosselin, M., Thomas, H., & Shadwick, E. (2013). The isotopic signature of particulate organic C and N in bottom ice: Key influencing factors and applications for tracing the fate of ice-algae in the Arctic Ocean. *Journal of Geophysical Research: Oceans*, *118*(1), Article 1. https://doi.org/10.1029/2012JC008331

Proshutinsky, A., Krishfield, R., Toole, J. M., Timmermans, M.-L., Williams, W., Zimmermann, S., Yamamoto-Kawai, M., Armitage, T. W. K., Dukhovskoy, D., Golubeva, E., Manucharyan, G. E., Platov, G., Watanabe, E., Kikuchi, T., Nishino, S., Itoh, M., Kang, S.-H., Cho, K.-H., Tateyama, K., & Zhao, J. (2019). Analysis of the Beaufort Gyre Freshwater Content in 2003–2018. *Journal of Geophysical Research: Oceans*, *124*(12), 9658–9689. https://doi.org/10.1029/2019JC015281

Rantanen, M., Karpechko, A. Y., Lipponen, A., Nordling, K., Hyvärinen, O., Ruosteenoja, K., Vihma, T., & Laaksonen, A. (2022). The Arctic has warmed nearly four times faster than the globe since 1979. *Communications Earth & Environment*, *3*(1), Article 1. https://doi.org/10.1038/s43247-022-00498-3

Rau, G. H., Sweeney, R. E., & Kaplan, I. R. (1982). Plankton 13C: 12C ratio changes with latitude: differences between northern and southern oceans. *Deep Sea Research Part A. Oceanographic Research Papers*, *29*(8), Article 8. https://doi.org/10.1016/0198-0149(82)90026-7

Rau, G. H., Takahashi, T., Des Marais, D. J., Repeta, D. J., & Martin, J. H. (1992). The relationship between δ13C of organic matter and [CO2(aq)] in ocean surface water: Data from a JGOFS site in the northeast Atlantic Ocean and a model. *Geochimica et Cosmochimica Acta*, *56*(3), Article 3. https://doi.org/10.1016/0016-7037(92)90073-R

Ribeiro, S., Limoges, A., Massé, G., Johansen, K. L., Colgan, W., Weckström, K., Jackson, R., Georgiadis, E., Mikkelsen, N., Kuijpers, A., Olsen, J., Olsen, S. M., Nissen, M., Andersen, T. J., Strunk, A., Wetterich, S., Syväranta, J., Henderson, A. C. G., Mackay, H., … Davidson, T. A. (2021). Vulnerability of the North Water ecosystem to climate change. *Nature Communications*, *12*(1), 4475. https://doi.org/10.1038/s41467-021-24742-0

Ritchie, J. C., & McHenry, J. R. (1990). Application of Radioactive Fallout Cesium-137 for Measuring Soil Erosion and Sediment Accumulation Rates and Patterns: A Review. *Journal of Environmental Quality*, *19*(2), Article 2. https://doi.org/10.2134/jeq1990.00472425001900020006x

Rochon, A., Vernal, A. de, Turon, J.-L., Matthießen, J., & Head, M. J. (1999). Distribution of recent dinoflagellate cysts in surface sediments from the North Atlantic Ocean and adjacent seas in relation to sea-surface parameters. *American Association of Stratigraphic Palynologists Contribution Series*, *35*, 1–146.

Rudels, B. (2012). Arctic Ocean circulation and variability—Advection and external forcing encounter constraints and local processes. *Ocean Science; Katlenburg-Lindau*, *8*(2), Article 2.

Rudels, B., Anderson, L. G., & Jones, E. P. (1996). Formation and evolution of the surface mixed layer and halocline of the Arctic Ocean. *Journal of Geophysical Research: Oceans*, *101*(C4), Article C4. https://doi.org/10.1029/96JC00143

Rysgaard, S., Boone, W., Carlson, D., Sejr, M. K., Bendtsen, J., Juul-Pedersen, T., Lund, H., Meire, L., & Mortensen, J. (2020). An Updated View on Water Masses on the pan-West Greenland Continental Shelf and Their Link to Proglacial Fjords. *Journal of Geophysical Research: Oceans*, *125*(2), Article 2. https://doi.org/10.1029/2019JC015564

Sampei, M., Sasaki, H., Hattori, H., Fukuchi, M., & Hargrave, B. T. (2004). Fate of sinking particles, especially fecal pellets, within the epipelagic zone in the North Water (NOW) polynya of northern Baffin Bay. *Marine Ecology Progress Series*, *278*, 17–25. https://doi.org/10.3354/meps278017

Sarnthein, M., Winn, K., Duplessy, J.-C., & Fontugne, M. R. (1988). Global variations of surface ocean productivity in low and mid latitudes: Influence on CO2 reservoirs of the deep ocean and atmosphere during the last 21,000 years. *Paleoceanography*, *3*(3), Article 3. https://doi.org/10.1029/PA003i003p00361

Schubert, C. J., & Calvert, S. E. (2001). Nitrogen and carbon isotopic composition of marine and terrestrial organic matter in Arctic Ocean sediments: Implications for nutrient utilization and organic matter composition. *Deep Sea Research Part I: Oceanographic Research Papers*, *48*(3), Article 3. https://doi.org/10.1016/S0967-0637(00)00069-8

Serreze, M. C., & Barry, R. G. (2011). Processes and impacts of Arctic amplification: A research synthesis. *Global and Planetary Change*, *77*(1), 85–96. https://doi.org/10.1016/j.gloplacha.2011.03.004

Sha, L., Jiang, H., Seidenkrantz, M.-S., Li, D., Andresen, C. S., Knudsen, K. L., Liu, Y., & Zhao, M. (2017). A record of Holocene sea-ice variability off West Greenland and its potential forcing factors. *Palaeogeography, Palaeoclimatology, Palaeoecology*, *475*, 115–124. https://doi.org/10.1016/j.palaeo.2017.03.022

Skinner, L. C., & Bard, E. (2022). Radiocarbon as a Dating Tool and Tracer in Paleoceanography. *Reviews of Geophysics*, *60*(1), e2020RG000720. https://doi.org/10.1029/2020RG000720

Slater, D. A., & Straneo, F. (2022). Submarine melting of glaciers in Greenland amplified by atmospheric warming. *Nature Geoscience*, *15*(10), 794–799. https://doi.org/10.1038/s41561-022-01035-9

Stevenard, N., Montero-Serrano, J.-C., Eynaud, F., St-Onge, G., Zaragosi, S., & Copland, L. (2022). Lateglacial and Holocene sedimentary dynamics in northwestern Baffin Bay as recorded in sediment cores from Cape Norton Shaw Inlet (Nunavut, Canada). *Boreas*, *n/a*(n/a), Article n/a. https://doi.org/10.1111/bor.12575

St-Onge, M.-P., & St-Onge, G. (2014). Environmental changes in Baffin Bay during the Holocene based on the physical and magnetic properties of sediment cores. *Journal of Quaternary Science*, *29*(1), Article 1. https://doi.org/10.1002/jqs.2674

Stroeve, J., & Notz, D. (2018). Changing state of Arctic sea ice across all seasons. *Environmental Research Letters*, *13*(10), 103001. https://doi.org/10.1088/1748-9326/aade56

Swarzenski, P. W. (2013). 210Pb Dating. In W. J. Rink & J. Thompson (Eds.), *Encyclopedia of Scientific Dating Methods* (pp. 1–11). Springer Netherlands. https://doi.org/10.1007/978-94-007-6326-5_236-1

Swift, J. H., Jones, E. P., Aagaard, K., Carmack, E. C., Hingston, M., MacDonald, R. W., McLaughlin, F. A., & Perkin, R. G. (1997). Waters of the Makarov and Canada basins. *Deep Sea Research Part II: Topical Studies in Oceanography*, *44*(8), Article 8. https://doi.org/10.1016/S0967-0645(97)00055-6

Tang, C. C. L., Ross, C. K., Yao, T., Petrie, B., DeTracey, B. M., & Dunlap, E. (2004). The circulation, water masses and sea-ice of Baffin Bay. *Progress in Oceanography*, *63*(4), Article 4. https://doi.org/10.1016/j.pocean.2004.09.005

Thöle, L. M., Nooteboom, P. D., Hou, S., Wang, R., Nie, S., Michel, E., Sauermilch, I., Marret, F., Sangiorgi, F., & Bijl, P. K. (2023). An expanded database of Southern Hemisphere surface sediment dinoflagellate cyst assemblages and their oceanographic affinities. *Journal of Micropalaeontology*, *42*(1), Article 1. https://doi.org/10.5194/jm-42-35-2023

Torres-Valdés, S., Tsubouchi, T., Bacon, S., Naveira-Garabato, A. C., Sanders, R., McLaughlin, F. A., Petrie, B., Kattner, G., Azetsu-Scott, K., & Whitledge, T. E. (2013). Export of nutrients from the Arctic Ocean. *Journal of Geophysical Research: Oceans*, *118*(4), Article 4. https://doi.org/10.1002/jgrc.20063

Tremblay, J.-É., Anderson, L. G., Matrai, P., Coupel, P., Bélanger, S., Michel, C., & Reigstad, M. (2015). Global and regional drivers of nutrient supply, primary production

and CO2 drawdown in the changing Arctic Ocean. *Progress in Oceanography*, *139*, 171–196. https://doi.org/10.1016/j.pocean.2015.08.009

Tremblay, J.-É., Gratton, Y., Carmack, E. C., Payne, C. D., & Price, N. M. (2002). Impact of the large-scale Arctic circulation and the North Water Polynya on nutrient inventories in Baffin Bay. *Journal of Geophysical Research: Oceans*, *107*(C8), Article C8. https://doi.org/10.1029/2000JC000595

Tremblay, J.-É., Hattori, H., Michel, C., Ringuette, M., Mei, Z.-P., Lovejoy, C., Fortier, L., Hobson, K. A., Amiel, D., & Cochran, K. (2006). Trophic structure and pathways of biogenic carbon flow in the eastern North Water Polynya. *Progress in Oceanography*, *71*(2), Article 2. https://doi.org/10.1016/j.pocean.2006.10.006

Tremblay, J.-É., Robert, D., Varela, D. E., Lovejoy, C., Darnis, G., Nelson, R. J., & Sastri, A. R. (2012). Current state and trends in Canadian Arctic marine ecosystems: I. Primary production. *Climatic Change*, *115*(1), 161–178. https://doi.org/10.1007/s10584-012-0496-3

Van Nieuwenhove, N., Head, M. J., Limoges, A., Pospelova, V., Mertens, K. N., Matthiessen, J., De Schepper, S., de Vernal, A., Eynaud, F., Londeix, L., Marret, F., Penaud, A., Radi, T., & Rochon, A. (2020). An overview and brief description of common marine organic-walled dinoflagellate cyst taxa occurring in surface sediments of the Northern Hemisphere. *Marine Micropaleontology*, 101814. https://doi.org/10.1016/j.marmicro.2019.101814

Varela, D. E., Crawford, D. W., Wrohan, I. A., Wyatt, S. N., & Carmack, E. C. (2013). Pelagic primary productivity and upper ocean nutrient dynamics across Subarctic and Arctic Seas. *Journal of Geophysical Research: Oceans*, *118*(12), 7132–7152. https://doi.org/10.1002/2013JC009211

Versteegh, G. J. M., Blokker, P., Bogus, K. A., Harding, I. C., Lewis, J., Oltmanns, S., Rochon, A., & Zonneveld, K. A. F. (2012). Infra red spectroscopy, flash pyrolysis, thermally assisted hydrolysis and methylation (THM) in the presence of tetramethylammonium hydroxide (TMAH) of cultured and sediment-derived Lingulodinium polyedrum (Dinoflagellata) cyst walls. *Organic Geochemistry*, *43*, 92–102. https://doi.org/10.1016/j.orggeochem.2011.10.007

Vincent, R. F. (2019). A Study of the North Water Polynya Ice Arch using Four Decades of Satellite Data. *Scientific Reports*, *9*. https://doi.org/10.1038/s41598-019-56780-6

Wadham, J. L., Hawkings, J., Telling, J., Chandler, D., Alcock, J., O'Donnell, E., Kaur, P., Bagshaw, E., Tranter, M., Tedstone, A., & Nienow, P. (2016). Sources, cycling and export of nitrogen on the Greenland Ice Sheet. *Biogeosciences*, *13*(22), Article 22. https://doi.org/10.5194/bg-13-6339-2016

Wang, H., Legg, S., & Hallberg, R. (2018). *The Effect of Arctic Freshwater Pathways on North Atlantic Convection and the Atlantic Meridional Overturning Circulation*. https://doi.org/10.1175/JCLI-D-17-0629.1

Wang, J., Baskaran, M., & Niedermiller, J. (2017). Mobility of 137Cs in freshwater lakes: A mass balance and diffusion study of Lake St. Clair, Southeast Michigan, USA. *Geochimica et Cosmochimica Acta*, *218*, 323–342. https://doi.org/10.1016/j.gca.2017.09.017

Weckström, K., Roche, B. R., Miettinen, A., Krawczyk, D., Limoges, A., Juggins, S., Ribeiro, S., & Heikkilä, M. (2020). Improving the paleoceanographic proxy tool kit – On the biogeography and ecology of the sea ice-associated species Fragilariopsis oceanica, Fragilariopsis reginae-jahniae and Fossula arctica in the northern North Atlantic. *Marine Micropaleontology*, *157*, 101860. https://doi.org/10.1016/j.marmicro.2020.101860

Williams, P. L., Burgess, D. O., Waterman, S., Roberts, M., Bertrand, E. M., & Bhatia, M. P. (2021). Nutrient and Carbon Export From a Tidewater Glacier to the Coastal Ocean in the Canadian Arctic Archipelago. *Journal of Geophysical Research: Biogeosciences*, *126*(9), e2021JG006289. https://doi.org/10.1029/2021JG006289

Wouters, B., & Sasgen, I. (2022). *Increasing Freshwater Fluxes from the Greenland Ice Sheet Observed from Space | Oceanography*. Retrieved November 7, 2025, from https://tos.org/oceanography/article/increasing-freshwater-fluxes-from-the-greenland-ice-sheet-observed-from-space

Wychen, W. V., Burgess, D., Kochtitzky, W., Nikolic, N., Copland, L., & Gray, L. (2020). RADARSAT-2 Derived Glacier Velocities and Dynamic Discharge Estimates for the Canadian High Arctic: 2015–2020. *Canadian Journal of Remote Sensing*, *46*(6), Article 6. https://doi.org/10.1080/07038992.2020.1859359

Zhuang, Y., Jin, H., Cai, W.-J., Li, H., Jin, M., Qi, D., & Chen, J. (2021). Freshening leads to a three-decade trend of declining nutrients in the western Arctic Ocean. *Environmental Research Letters*, *16*(5), 054047. https://doi.org/10.1088/1748-9326/abf58b

Zonneveld, K. A. F., Versteegh, G., & Kodrans-Nsiah, M. (2008). Preservation and organic chemistry of Late Cenozoic organic-walled dinoflagellate cysts: A review. *Marine Micropaleontology*, *68*(1).